ALTERED MICRORNA REGULATORY NETWORKS IN INDIVIDUALS WITH SCHIZOPHRENIA

by

MICHAEL P. MOREAU

A dissertation submitted to the

Graduate School-New Brunswick

Rutgers, The State University of New Jersey

and

The Graduate School of Biomedical Sciences

University of Medicine and Dentistry of New Jersey

In partial fulfillment of the requirements

For the degree of

Doctor of Philosophy

Graduate Program in Microbiology and Molecular Genetics

Written under the direction of

Dr. Linda Brzustowicz

And Approved by

_____

_____

_____

_____

New Brunswick, New Jersey

October, 2009

ABSTRACT OF THE DISSERTATION

Altered microRNA Regulatory Networks in Individuals with Schizophrenia

By MICHAEL P. MOREAU

Dissertation Director:

Dr. Linda Brzustowicz

MicroRNAs (miRNAs) are small, endogenous non-coding RNA molecules that interact with messenger RNAs to direct their post-transcriptional repression. Like messenger RNAs, miRNAs exhibit distinct spatiotemporal expression signatures. The human brain, marked by tremendous structural and functional complexity, has an especially diverse miRNA expression profile. Altered expression or function of miRNAs has been linked to several neuropsychiatric disorders, including Alzheimer's disease, Tourette's syndrome, and Schizophrenia.

Schizophrenia is a debilitating psychiatric disorder that affects 0.5-1% of the world's population. Family and twin studies suggest a strong genetic component to the disease, but efforts to isolate causal variants have been hampered by genetic heterogeneity, as well as interacting environmental factors. The underlying goal of this dissertation research is to investigate altered miRNA regulatory networks in individuals with schizophrenia spectrum disorders.

The work presented herein begins with a miRNA expression atlas of the developing human brain. Tissue samples representing fetal, early postnatal, and adult time points (n = 48 total) were analyzed using microarrays, and 312 miRNAs were classified according to their temporal expression patterns. This work goes on to describe the development of a multiplexed, bead-based SNP genotyping assay which was applied in a family-based genetic association study of the miRNA processing gene DGCR8. Comprehensive miRNA expression analysis of post-mortem brain tissue samples from subjects with schizophrenia, subjects with bipolar disorder, and psychiatrically healthy controls (n = 35 each group) revealed significant under-expression of several miRNAs in individuals with major psychosis, substantiating a proposed defect in miRNA processing. A pattern-based algorithm called miRSNiPer was developed, and used to predict SNPs that alter miRNA binding sites. A panel of 48 putative "miRSNPs" were genotyped in 25 extended pedigrees, and a SNP in the 3'UTR of H3F3B showed evidence of association (PPLD = 17%) to schizophrenia and schizoaffective disorder. Finally, the miRSNiPer algorithm was used to identify enriched genes and pathways among the targets of mis-expressed miRNAs.

DEDICATION

This dissertation is dedicated to the following people:

First and foremost my mother, Debra Moreau, whose unconditional love and guidance shaped me into the person that I am today.

My father, Patrick Moreau, who taught me the meaning of courage and perseverance.

The Petroskey family, Wayne, Barbara, Wayne Jr., and Sharon, for their enduring love and support throughout the years.

And my wife Sandy Moreau, my true love and inspiration in life.

Thank you to all

ACKNOWLEDGEMENTS

Over the past several years, many people have either directly contributed to the work described herein, or have otherwise shaped my intellectual and scientific development. I would like to begin by thanking all of the participating individuals and families who gave their time and effort for the advancement of science. Samples were generously provided by the following organizations: the NICHD Brain and Tissue Bank for Developmental Disorders, the Stanley Medical Research Institute, and the NIMH Human Genetics Initiative schizophrenia collection.

I would like to thank the following collaborators for their technical and/or scientific contributions: Dr. Anne Bassett for her assistance in ascertainment and phenotypic characterization of the Canadian pedigrees; Nicole Flaherty and Brian Polizzi from Perkin Elmer Life and Analytical Sciences for their assistance in adopting laboratory automation protocols; Kelly Howard and Mary Baltazar from Applied Biosystems for their assistance with molecular profiling applications; Dr. Steve Buyske, Dr. Rebecka Jornsten, and Richard David-Rus, for conducting statistical analyses of gene expression data; and Dr. Veronica Vieland for developing and supporting the statistical methodologies used for family-based genetic association analysis.

I would like to extend my heartfelt gratitude to the many past and present members of the Brzustowicz lab who I have had the pleasure of working with over the years; Neda Gharani, Naomi McGregor, and Slava Saviouk, for many helpful lessons and discussions; my fellow graduate students Abby Hare, Carmen Ramirez, and Pilar Garavito, for sharing their experiences and offering encouragement; Jaime Messenger and Jared Hayter, not only for assisting with countless logistical and technical matters, but for always ensuring

that I was adequately caffeinated to tackle my daily tasks; Anthony Marcketta, Dan Lee, and Marco Azaro, for their assistance in bioinformatics and computational tasks. Marco's talent and intelligence have made him an integral member of the lab, and much of this work would not have been possible without his vital contributions.

I owe much of my success in the lab to two people, who taught me to blend scientific intuition with an organized, systematic approach. When I first started in the lab as an undergraduate, Ray Zimmerman took me under his wing and taught me the fundamentals of experimental design and execution. Thank you, Ray, for those early lessons, as well as the many productive discussions and brainstorming sessions in more recent times. In my junior year as an undergraduate, I stood at a crossroads, contemplating which career path to pursue. Shannon Bruse, more than anyone else, is responsible for my decision to pursue a career in scientific research. Shannon not only helped me to realize my potential in the lab, but he instilled in me the idea that science could be exciting and fun. Shannon continues to be a friend and close collaborator on much of the work presented herein.

Finally, I would like to thank the members of my dissertation committee, Dr. Tara Matise, Dr. Richard Padgett, Dr. Jim Millonig, and Dr. Linda Brzustowicz for their support and guidance through this process. I owe a tremendous debt of gratitude to my thesis advisor and mentor, Dr. Linda Brzustowicz. Linda put a tremendous amount of faith in me, allowing me to branch off into new and unfamiliar areas of research. She kept me focused and on task, but allowed independence and creativity in my scientific pursuits. I owe Dr. Brzustowicz for the many opportunities that have come my way as a graduate student, and for those that are still to come.

The work presented in chapter 3 was previously published in *Biotechniques 45:559-571 (November 2008).* Dr. Shannon Bruse was the primary author of this paper. This work represents a collaborative project with contributions from all listed coauthors. The thesis author made original and meaningful contributions to the fundamental experimental design and protocol development. The majority of the data presented represents the laboratory work of the thesis author and Dr. Shannon Bruse.

TABLE OF CONTENTS

LIST OF TABLES

LIST OF FIGURES

Chapter 1: Introduction

Less than a decade ago, the scientific community viewed the newly completed consensus build of the human genome as sparse islands of protein coding sequence interspersed in a sea of "junk" DNA. The number of protein coding genes failed to correlate with organismal complexity, leaving researchers to seek alternative explanations for the rich phenotypic diversity among human beings. The pilot phase of the Encyclopedia of DNA Elements (ENCODE) project [1] and the revelation of genome-wide pervasive transcription triggered a paradigm shift. Definitions of genes as the structural entities of genomes that confer phenotypic variation have expanded beyond the boundaries of mRNA encoding units, and several classes of functional small non-coding RNAs (sncRNAs) have emerged. Stochastic (random and probabilistic) programs have supplanted the traditional, deterministic models of transcriptional regulation, with sncRNAs acting to subtly modulate gene regulatory networks.

MicroRNAs are the best characterized members of the sncRNA family, which are predicted to negatively regulate between 74% and 92% of mRNAs [2]. Altered expression or function of microRNAs has been linked to numerous complex genetic diseases, including cancer, cardiovascular disease, and neurological conditions. The capacity of microRNAs to fine tune or buffer transcriptional programs may mask the phenotypic effects of primary mutations in regulatory elements, making it difficult to pinpoint such mutations using conventional molecular and statistical genetics approaches. A re-envisioned two-hit hypothesis of complex disease etiology posits that primary genetic mutations are manifested upon the loss of microRNA regulation, and therefore microRNA expression profiles combine with genetic polymorphisms to form complex

disease phenocodes. The following describes a multifaceted research project seeking to expose a disease phenocode underlying the pathophysiology of schizophrenia spectrum disorders.

miRNA Genomics and Biogenesis Pathways

The term RNA interference (RNAi) was coined to describe a potent mechanism of post-transcriptional gene repression mediated by double-stranded RNAs [3]. However, the serendipitous discovery of the first microRNA gene actually occurred years earlier in a genetic screen for developmental defects in *C. elegans* [4]. Originally thought to be nematode-specific, cloning of the *let-7* heterochronic gene in multiple species uncovered a wide-spread regulatory mechanism based on homologous RNA-RNA interactions. These newly discovered developmental regulators were termed small temporal RNAs (stRNAs) [5] but as more of these small molecules emerged and appeared to influence a range of biological processes, they became collectively known as microRNAs (miRNAs). While mammals lack many of the RNAi pathways present in plants and lower animals, miRNAs comprise a growing class of endogenous regulatory molecules. By binding to partially complementary regions at the 3' end of messenger RNAs, these ~21 nucleotide single-stranded molecules induce degradation, deadenylation, or translational attenuation of targeted mRNA transcripts.

Mammalian miRNA biogenesis was formerly believed to be a linear, universal process, but individual miRNAs now appear to exploit distinct regulatory options at various stages of maturation. Generally, miRNA genes are transcribed by RNA polymerase II to form capped, polyadenylated primary miRNA transcripts (pri-miRNAs) [6, 7]. However, a cluster of primate-specific miRNAs on chromosome 19 is instead

transcribed by RNA polymerase III [8]. RNA editing of certain miRNAs leads to deamination of adenosine residues to inosine, altering miRNA sequence and sometimes target binding properties [9]. Human pri-miRNAs contain one or more hairpins, which are endonucleolytically cleaved by a microprocessor complex consisting of the RNase III enzyme Drosha and a cofactor known as DiGeorge syndrome critical region gene 8 (DGCR8) [10]. DGCR8 confers RNA binding affinity to the complex, recognizing the double-stranded stem and adjacent unpaired flanking regions, and it also acts as a molecular spacer to select the exact cleavage site [11, 12]. Polymorphisms within the DGCR8 recognition motif may block Drosha activity [13]. Several miRNA-specific regulatory mechanisms exist at this initial processing step. Besides the small microprocessor complex comprised of only Drosha and DGCR8, a larger complex containing the RNA helicases p68 and p72 along with other ribonucleoproteins acts on a subset of miRNAs [14]. Certain intron-derived miRNAs called mirtrons circumvent Drosha cleavage altogether, and are instead processed by the ordinary mRNA splicing machinery [15]. Adding yet another layer of complexity, a self-regulating mechanism exists in which Drosha alone cleaves two hairpin structures in the 5'UTR of the Dgcr8 mRNA, promoting its rapid degradation [16].

Drosha cleavage in the nucleus releases a ~70 nucleotide hairpin precursor miRNA (pre-miRNA), which is then exported to the cytoplasm by the Exportin-5-Ran-GTP pathway [17]. Cytoplasmic pre-miRNAs are trimmed, unwound, and loaded into an effector complex called RISC (RNA-induced silencing complex). Cytoplasmic processing of miRNAs and assembly of RISC is mediated by the RISC loading complex (RLC) [18]. The Tar RNA binding protein (TRBP) and protein activator of PKR (PACT)

facilitate the activity of a second RNase III enzyme called Dicer, which cleaves pre-miRNAs to the mature ~21 base pair length [19]. This processing step appears to be essential, as knocking out Dicer eliminates production of mature miRNAs in several model systems. Following cleavage, Dicer, TRBP and PACT dissociate from the short miRNA duplex, which must then be unwound prior to incorporation into RISC. The miRNA guide strand ultimately templates RISC target binding, while the passenger strand is degraded. The universal helicase responsible for unwinding the mature length miRNA duplex is still unknown. Guide strand selection is contingent upon thermodynamic properties of the duplex, with preferential loading of the miRNA strand with less stable base pairing at the 5'end [20]. Besides forming the catalytic core of the RISC complex, the argonaute (Ago) proteins sometimes nick the 3' arm of prospective passenger strands prior to Dicer cleavage. This improves the efficiency of Dicer in processing hairpins with a high degree of sequence complementarity [21]. While little is known about miRNA turnover pathways, loss of endogenous Ago2 is associated with reduced mature miRNA expression, possibly because of the capacity to bind to and stabilize these short molecules [22]. In sum, miRNA biosynthesis does not proceed in a generalized, linear manner, and divergent processing mechanisms provide multiple opportunities for posttranscriptional regulation of miRNA expression.

Early attempts to characterize the genomic localization of vertebrate miRNA genes revealed considerable variability. Their coding sequences are often intergenic but are sometimes within introns of protein-coding genes, in either the sense or antisense orientation [23]. miRBase, the central online repository of miRNA sequences, annotations and target predictions [24], currently lists 9169 mature miRNA products from

103 species, including 706 human miRNAs. The first breakthrough in large-scale miRNA identification occurred when cDNA libraries of endogenous 19-25 nucleotide RNAs were constructed [25]. Cloned species were mapped to genomic hairpins and confirmed by Northern blotting. This technique successfully identified hundreds of novel miRNAs in diverse cell lines and mouse-derived tissue types. However, this approach lacked the sensitivity to detect miRNAs expressed at a low level or in highly specific cell types. This problem was overcome, in part, by using bioinformatic approaches to predict additional candidate miRNAs. The earliest computational methods, such as MiRscan and miRseeker, used phylogenetic conservation and observed structural features of miRNA precursors to predict homologs of already known miRNAs [26, 27]. The number of primate-specific miRNAs greatly expanded when Bentwich and colleagues developed the first integrative prediction strategy. Genomic hairpins were predicted and scored for thermodynamic stability, then embedded miRNAs were verified using high-throughput microarray expression analysis in several tissues [28]. The miRDeep algorithm is a reversal of this approach, which starts with quantitative sequencing reads from next generation platforms and scores the position and frequency of fragments derived from putative secondary structures [29].

miRNA genes are scattered throughout the human genome with the exception of the Y chromosome. Nearly half of miRNAs are found in clusters, and are transcribed as polycistronic primary transcripts [30]. Clustered miRNAs often have similar sequences, and may have arisen through a gene duplication event. When unrelated miRNAs are present within the same cluster, transcriptional co-regulation often produces overlapping patterns of expression [31]. It is plausible but not yet proven that such miRNAs are

functionally related by virtue of targeting common genes, or targeting different genes in a given biological pathway. While intronic miRNAs may be transcribed coincidentally with their "host" genes, the nature of intergenic primary miRNA transcripts has only recently been investigated. Thorough analysis of transcription start sites, CpG islands, and polyadenylation signals suggests that most pri-miRNAs are 1-4 kb in length, while a few may be as long as 10 kb [32]. Systematic investigation of transcription factor binding sites and regulatory motifs that influence miRNA processing have only just begun.

Mechanisms of Gene Repression and Target Site Recognition by miRNAs

Initial experiments have produced a widely accepted and largely empirical framework describing miRNA-mRNA interactions that can be summarized as follows. Plant miRNAs regulate transcripts with single, highly complementary target sites mainly through internal slicing. Animal miRNAs target transcripts through imperfect base-pairing to multiple sites in the 3' untranslated region (3'UTR). Watson-Crick base-pairing of the so-called "seed" region that comprises nucleotides 2-7 of the mature miRNA is crucial for targeting, as these positions may be pre-organized by bound Ago proteins to favor efficient pairing [33]. 3'end pairing, although less important, may supplement or compensate for weaker seed interactions. Central bulges and mismatches in positions 9-12 enable repression through translational attenuation or deadenylation, while rare cases of central complementarity can lead to internal cleavage of mRNAs. Target site multiplicity is thought to enhance the degree of repression by animal miRNAs, each of which can have hundreds or thousands of targets due to relaxed base-pairing constraints. While the number of confidently identified and experimentally

validated targets has risen to about 400 in humans, computational approaches still drive miRNA target prediction.

While many key principles of miRNA targeting have emerged in recent years, several challenges remain. Due to the small size of miRNAs, there is great potential for over-prediction of targets based on chance sequence matches. Bioinformatic prediction algorithms must be sensitive and selective so as to minimize false positives. The search for target sites is often relegated to the 3'UTR of genes, and 5' dominant ("seed") complementarity is heavily prioritized. The importance of exact base pairing of the seed region gained experimental support from reporter constructs fused to pseudo-3'UTRs harboring predicted target sites [34]. However, additional targeting motifs, such as 3' compensatory sites, can bypass the seed-pairing rule and demonstrate similar binding efficacy [35]. *In vitro* reporter assays are confounded by the artificiality of miRNA over-expression as well as the lack of endogenous cofactors. The use of sensor constructs in an endogenous context has shown that seed pairing is not sufficient to reliably predict miRNA-target interactions [36]. Combinatorial repression of a given transcript by co-expressed miRNAs is contingent upon 3'UTR length, the number of target sites, and the distance between binding sites [37]. Additional context determinants may include AU-rich nucleotide composition near target sites, the distance of sites from the stop codon, and the distance of sites from the center of long 3'UTRs [38].

"Signature-based" prediction algorithms strive for a balance of sensitivity and noise reduction by integrating novel classes of miRNA binding motifs, known context determinants, as well as evolutionary conservation. For example, the target-finding algorithm PicTar detects sites with perfect seed matches as well as imperfect nuclei

bearing a 3' compensatory motif, and then applies a free energy filter to assess binding thermodynamics [39]. PicTar also exploits cross-species comparisons among divergent *Drosophila* lineages to further distinguish accurate site predictions from noise. Unfortunately, one cannot use evolutionary conservation to aid in target predictions for human-specific miRNAs, such as the large cluster of miRNAs on chromosome 19. *Rna22* utilizes an alternative "pattern-based" approach to target prediction. A motif discovery algorithm called Teiresias is trained on all mature, non-redundant miRNA sequences in the RNA families database of alignments and covariance models (Rfam). Teiresias identifies variable length sequence motifs that comprise a minimum of 4 nucleotides, and have at least 30% of their positions specified. Reverse complements of these elementary patterns are mapped onto a sequence of interest, and patterns that cluster around a specific location define a "target island," which represents a putative miRNA binding site. miRNAs are associated with target sites using adjustable parameters such as the minimum required number of complementary base-pairs and the maximum allowed number of unpaired bases in the seed region.

Enrichment of miRNAs at structurally and functionally distinct RNA granules suggests their possible involvement in targeted mRNA transport for local protein synthesis. Neuronal RNA granules were once described merely as intermediates in mRNA transport, nothing more than a transient accumulation of synapse-bound RNPs. It is now known that compositionally and functionally diverse classes of RNA granules (reviewed in [40]) are intimately involved in the regulation of local RNA translation and degradation. Rather than being homogeneous entities, RNA granules are subdivided into transport RNPs, stress granules, and P-bodies. Dynamic RNP complexes exhibiting rapid

anterograde and retrograde microtubule-associated motility were observed in cultured cortical neurons using the membrane permeable nucleic acid stain SYTO 14 [41]. Subsequent biochemical analysis revealed that these RNPs contained numerous ribosomal proteins and elongation factors, suggesting they may be competent to initiate translation upon reaching their final cellular destination. Exposure of mammalian cells to heat or oxidative stress causes the recruitment of housekeeping mRNAs to stress granules, where they are temporarily stored as stalled translational complexes while the cell up-regulates production of chaperones and other damage control proteins [42].

As a distinct RNA granule containing decapping enzymes, exonucleases, and elements of the nonsense-mediated decay pathway, processing bodies (P-bodies) provided the first allusion of spatially restricted mRNA degradation [43]. While these P-bodies lack critical translation elongation factors [44], [45], recent evidence suggests that instead of being committed to degradation, mRNAs can oscillate between P-bodies and polysomes to reinitiate translation in a stimulus-dependent manner [46]. Though they are structurally distinct elements, stress granules and P-bodies utilize common constituents to repress translation of resident mRNA. Co-localization with both polyribosomes and RNA granules implicates the fragile-X mental retardation protein in the duel role of mRNA localization and translational repression [47]. Rather than serving a catalytic function, recent models depict FMRP as an integral component of the miRNA-containing RNA induced silencing complex, seemingly acting as a downstream effector of dicer that helps to assemble miRNAs onto targeted transcripts [48]. It is yet to be determined whether miRNAs act only to suppress translation of mRNAs while *en route* to their final cellular destination, or if they play an active role in localization.

Biological Functions of miRNAs

Like mRNAs, miRNA expression profiles vary dramatically between tissue types, but are highly concordant for identical tissues in different individuals [49]. Early expression studies that used Northern blot analysis or filter arrays, as well as subsequent microarray studies, uncovered many tissue-specific miRNAs. Examples include miR-1 in the heart and muscle, miR-9, -124, -125, and -128 in the brain, miR-122a in liver, miR-133a and miR-206 in muscle, and miR-142 and -150 in spleen [50-52]. Interestingly, hierarchical clustering also showed that related tissues, such as heart and skeletal muscle, had a higher degree of overlap in miRNA expression signatures. Distinct temporal expression profiles have been observed in pluripotent versus differentiated cells, and in tissues of developing and mature rodents [53]. Taken together, these observations implicate miRNAs as critical regulatory components that influence adoption and maintenance of cell fate, and help to define tissue-specific gene regulatory networks.

Strikingly, the miRNA profile of the brain was found to be the most divergent of all tissue types, likely due to the tremendous structural and functional complexity of this organ. Approximately 70% of known miRNAs are expressed in the nervous system, often with a high degree of spatial and temporal specificity [51]. A survey of miRNA expression patterns in various organ and tissue types identified numerous brain-specific and brain-enriched miRNAs, many of which were up-regulated in embryonal carcinoma cells induced to adopt a neural cell fate [52]. miRNA profiling of the developing and adult mouse brain revealed a “chronological wave” of expression [54]. The appearance of sequentially expressed classes of miRNAs may correlate with the onset of neurodevelopmental processes, such as neuronal proliferation, migration, neurite growth,

and synaptogenesis. However, the correlation between miRNA expression patterns and neurodevelopmental milestones fails to establish a causal relationship.

Perhaps the best way to assess the global developmental impact of miRNAs is to examine Dicer knockout animals that fail to process pre-miRNA hairpins into mature, biologically active miRNAs. Knocking out Dicer1 results in embryonic lethality in mice, seemingly caused by defects in cell proliferation and maintenance of stem cell populations [55]. Generation of conditional alleles that bypass the early requirement for dicer showed that miRNA processing was essential for limb morphogenesis but dispensable for axis formation and patterning [56]. In a landmark study, Giraldez et. al. examined maternal zygotic zebrafish dicer knockouts, and found that global elimination of miRNAs produced gross morphological abnormalities, especially in the nervous system. However, gene expression analysis revealed normal patterns of expression with respect to dorsal-ventral and anterior-posterior bodily axes. Marker labeling confirmed that all major neuronal cell types were present and properly localized. Remarkably, the severe morphogenetic abnormalities in maternal zygotic knockout animals were almost entirely rescued by injecting miR-430 family mature miRNAs [57]. In sum, Dicer knockout studies seem to portray somewhat contradictory roles for miRNAs. While miRNAs act as potent regulators of embryonic morphogenesis, abolishing hundreds of regulatory genes and derepressing thousands of targets had remarkably subtle phenotypic effects on cell differentiation and patterning. With a few notable exceptions, miRNAs may act primarily to fine-tune transcriptional programs in a cell- or tissue-specific manner, rather than serving a wide-spread obligatory function. An important caveat regarding these studies is the unknown extent to which Dicer ablation directly disrupts

cellular functions and contributes to observed phenotypes, as well as an organism's ability to circumvent single gene knockouts.

miRNAs in the Brain

The mammalian brain is comprised of diverse populations of neurons with precise synaptic circuitry. These neurons must respond to functional and developmental stimuli by rapidly altering gene expression patterns. Accordingly, RNA-mediated gene repression may play a role in neurogenesis, neural differentiation, and synaptic plasticity, as well as in neurological and psychiatric diseases. In a landmark study, expression changes of specific miRNAs occurred upon induction of mouse embryonic stem cell neural differentiation [58]. Two miRNAs, miR-124a and miR-9, were implicated in the decision of neural precursors to adopt a neuronal or glial fate. Transfecting these duplexes into progenitor cells decreased the number of cells expressing glial markers (GFAP) while increasing the number of neurons. This stem cell model has been expanded to include additional miRNAs as well as a global checkpoint, whereby cells target RISCs for selective degradation in order to recalibrate miRNA expression patterns at critical cell lineage control nodes [59].

Following differentiation, miRNAs continue to play important biological roles in developing and mature neurons. Axonal pathfinding is the process by which complex neural circuitry is established, and growth cones found at the tips of neuronal processes act as the principal navigators. These growth cones must integrate attractive turning cues from netrins and repulsive cues from semaphorins that trigger growth cone collapse. A critical facet of a neuron's ability to respond to local guidance cues is the compartmentalized capacity for local protein synthesis [60]. Functional RISCs

containing AGO3, AGO4, Dicer, and FMRP have been observed in developing axons of cultured rat cells [61]. Furthermore, the 3'UTR of *rhoA*, the downstream effector in the semaphorin signaling cascade, contains numerous miRNA target sites and is associated with components of the miRNA-dependent silencing machinery [62]. As the brain grows, blood vessel arborization and secretion of extracellular matrix is accompanied by the massive loss of neurons and glia. Members of the miR-2 family are implicated in suppressing apoptosis by targeting pro-apoptotic factors in *Drosophila* embryos [63]. Dicer knockout studies in zebrafish and mouse have shown that miRNAs act in shaping gross level anatomical structure through regulated apoptosis [56, 57], so a role in appropriately culling neurons in the developing brain seems plausible. Many miRNAs are expressed at a high level in the fully mature adult human brain. Enduring synaptic plasticity requires local protein synthesis [64, 65], exposing a potential role for miRNAs as regulators of molecular memory and learning [66, 67].

In recent years, miRNAs have been implicated in a number of pathological conditions of the central nervous system. miR-133b mediates differentiation of dopaminergic neurons derived from midbrain cultures, alluding to a potential role in Parkinson's disease. Dopaminergic neurons of mice with conditional deletion of Dicer undergo progressive degeneration, and expression of miR-133b is undetectable in the midbrain of patients with Parkinson's disease [68]. Significantly decreased expression of miR-107 was observed in patients with Alzheimer's disease. Multiple predicted target sites of miR-107 fall in the 3'UTR of beta-site amyloid precursor protein-cleaving enzyme 1 (BACE1), thus linking miRNA misexpression to the formation of pathogenic amyloid plaques [69]. Lastly, alterations in miRNA levels have been detected in the prefrontal

cortex and temporal lobe of individuals with schizophrenia [70, 71]. Since the pathophysiology of schizophrenia is still largely unknown, alterations in miRNA regulatory networks may provide valuable insights into underlying disease etiology.

miRNAs in Schizophrenia

Schizophrenia is a severely debilitating psychiatric disorder characterized by disturbed thought, perception, emotion, and behavior. Schizophrenia is a spectrum disorder related to schizoaffective disorder, schizotypal personality disorder, and paranoid personality disorder. Epidemiological studies of schizophrenia suggest a world-wide prevalence of 0.5-1%, which is uniform across many cultures [72]. The clinical symptoms of schizophrenia are broken down into positive, negative, and cognitive symptom clusters. The positive symptoms are active manifestations of abnormal behavior, including the hallmark symptoms of delusions and hallucinations. The negative symptoms are marked by an absence or lack of normal behavior, and may include apathy, alogia, anhedonia, flattened affect, and social withdrawal. Finally, the cognitive symptoms include severe disruptions in speech, attention and concentration, psychomotor function, learning and memory [73]. Schizophrenia affects males and females about equally, though the average age of onset for men is 20-28, compared to 26-32 for women [74]. The primary diagnostic instruments for schizophrenia are the *Tenth Revision of the International Classification of Diseases* (ICD-10) and the *Diagnostic and Statistical Manual, Fourth Edition* (DSM-IV). Both achieve a systematic and objective assessment of psychiatric impairment, but the DSM-IV requires the duration of illness to exceed 6 months in order to distinguish schizophrenia from schizophreniform disorder.

Both genetic and environmental factors are believed to contribute to the etiology of schizophrenia. The disorder occurs more frequently in relatives of patients than in the general population. Concordance rates are 41-65% in monozygotic twin pairs and 0-28% in dizygotic pairs, with heritability estimates of 80-85% [75]. Proposed environmental factors include prenatal events such as maternal influenza or rubella, smoking during pregnancy, and obstetric complications. Other environmental influences may include cannabis use, emotional stressors, and socioeconomic factors like poverty and urban living [reviewed in [76]]. Neuroanatomical studies have identified structural and functional brain abnormalities in individuals with schizophrenia [77], including enlarged ventricles and reduced tissue volume in adjacent areas [78], as well as dendritic spine defects. Perturbations in neurotransmission and synaptic connectivity are believed to play a prominent role in disease etiology. The longstanding dopamine hypothesis states that excess dopamine signaling in the prefrontal cortex leads to schizophrenia. Two pharmacological observations that support this model are the ability of dopamine agonists (amphetamines) to trigger psychosis, and the use of dopamine antagonists to effectively alleviate psychotic symptoms. More recently, hypoactive glutamate transmission at the N-methyl-D-aspartate receptor (NMDAR) has been implicated as a causative factor in schizophrenia. Noncompetitive NMDAR antagonists, such as phencyclidine (PCP) and ketamine, mimic a fuller range of symptoms than do dopamine agonists [79]. These NMDAR antagonists also produce an increase in dopamine in the prefrontal cortex, arguing that the primary defect is in glutamate signaling and that defects in dopamine signaling are secondary [80].

Many genome-wide linkage scans for schizophrenia susceptibility loci have been performed to date. These studies have revealed significant or suggestive evidence for linkage in several chromosomal regions, including 1q21–22, 1q42, 5q21–q33, 6p24–22, 6q16–25, 8p21–22, 10p15–p11, 13q32–34, and 22q11–12 [81-93]. While certain regions have been investigated in multiple studies, positive linkage findings have not been replicated in a majority of studies for any chromosomal region. This lack of consistency is likely due to genetic heterogeneity and the innate complexity of schizophrenia, which may require a combination of mutations at various loci to result in phenotypic manifestation. Despite these obstacles, rank-based genome scan meta-analysis was applied to data from 32 schizophrenia genome-wide scans [94], revealing a degree of consistency among various studies not previously recognized. Linkage studies provide an unbiased method of locating broad regions of susceptibility, but association studies, on the other hand, typically rely on selection of candidate genes beneath linkage peaks. Since genetic association studies are informed by the "biological plausibility" of candidate genes, functional non-coding RNA genes beneath linkage peaks may be ignored.

Genetic models of schizophrenia must consider not only primary mutations that alter the function or expression of protein-coding genes, but also sncRNAs that may modulate these effects. A thorough dissection of dicer knockout studies led Hornstein and Shomron to put forth an intriguing hypothesis stating that miRNAs act to canalize developmental pathways [95]. Canalization is a design principle wherein developmental pathways are stabilized to increase phenotypic reproducibility. There are two ways in which miRNAs can confer robustness to genetic pathways in the face of imperfect

transcriptional regulation. First, one can envision a transcriptional program where expression of a set of genes is repressed, with concurrent upregulation of miRNAs that target these same genes. In such a scheme, miRNAs would act to quell the deleterious effects of leaky transcription, thereby sharpening developmental switches or cell fate transitions. Alternatively, one may consider a transcriptional paradigm in which miRNAs and their targets are co-expressed at intermediate levels. In this scenario, miRNAs may act to buffer genetic noise and suppress fluctuations in gene expression due to stochastic effects at suboptimal promoters.

In canalizing complex developmental programs, miRNAs could allow increased mutational variance without phenotypic consequences. By buffering transcriptional programs, miRNAs could offset the deleterious effects of aberrantly expressed transcription factors or mutations in *cis*-regulatory elements. Thus, cryptic mutations could silently accumulate in the population, with phenotypic manifestation occurring only upon the loss of canalization. If miRNAs act to conceal underlying genetic variation, it may be possible to infer biological function or pathway organization based on cell or tissue-specific miRNA expression profiles. By extension, it may be possible to dissect the molecular etiology of complex genetic diseases based on abnormal miRNA expression patterns.

Rationale for Thesis Experiments: Uncovering the Schizophrenia Phenocode

The concept of disease "phenocodes" was introduced by Gennadi Glinsky as a new mechanistic dimension by which non-coding RNAs could influence complex genetic traits. Glinsky performed sequence homology profiling on several distinct classes of sncRNAs, including transintrons, expressed distal intergenic sequences, and piRNAs.

Surprisingly, he discovered sequence and structural elements in common with ~85% of human miRNAs, sparking the theory that sncRNAs are trans-acting RNA intermediaries that interfere with the bioactivity of miRNAs [96]. Glinsky went on to examine the most significantly associated intergenic SNPs from genome-wide association studies (GWAS) of 15 complex genetic disorders. Again, he performed sequence homology profiling of the DNA sequence flanking these functionally ambiguous SNPs. Surprisingly, this SNP-guided strategy revealed 18 miRNAs with high degrees of sequence homology which, in turn, have a propensity to target genes of the nuclear import pathway [97]. Thus, Glinsky proposed a unified disease phenocode comprised of SNPs in *trans*-acting sncRNAs, a set of miRNAs that are functionally inhibited, and a set of protein-coding genes that escape miRNA-based repression.

In genetic studies of schizophrenia, non-replication of association findings from candidate gene studies is the norm. Furthermore, multiple testing corrections limit findings with genome-wide significance from GWAS, and studies employing a case-control design are hampered by the effects of population stratification and genetic heterogeneity. Therefore, efforts to elucidate a schizophrenia disease phenocode should not rely on existing genetic association data as a starting point. Instead, the following chapters will describe a multifaceted investigation of miRNAs in major psychosis that utilizes brain-derived expression signatures as the cornerstone of an evolving phenocode model.

In hopes of better understanding the neurobiological roles of specific miRNAs, chapter 2 presents the first ever miRNA expression atlas of the developing human brain. Chapter 3 describes the development of a bead-based multiplexed SNP genotyping assay,

and this method was applied in a genetic association study of the miRNA processing gene DGCR8, which is described in chapter 4. Chapter 5 describes a large-scale post-mortem expression study, where expression levels of 435 miRNAs were measured in brain tissue samples originating from individuals with schizophrenia, individuals with bipolar disorder, and psychiatrically healthy control subjects. Chapter 6 presents a novel, pattern-based miRNA target prediction algorithm called miRSNiPer, which was utilized in a genetic association study of polymorphic miRNA target sites. If miRNAs do indeed suppress the effects of regulatory mutations to increase phenotypic reproducibility, then genes targeted by misexpressed miRNAs present attractive candidates for thorough mutation analysis in future studies.

Chapter 2: A microRNA Expression Atlas of the Developing Human Brain

ABSTRACT

MicroRNAs are a recently identified class of endogenous molecules believed to regulate multiple neurobiological processes. Expression studies have revealed distinct temporal expression patterns in animal model systems, but expression profiling of the developing human brain has never been attempted. We performed microarray-based expression analysis of all annotated mature miRNAs (miRBase 10.0) as well as 373 novel, predicted miRNAs. Expression levels were measured in 48 post-mortem brain tissue samples, representing gestational ages 14-24 weeks, as well as early postnatal and adult time points. Expression levels of 312 miRNAs changed significantly between at least two of the broad age categories, defined as fetal, young, and adult. We have constructed a miRNA expression atlas of the developing human brain, and we propose a classification scheme to guide future studies of neurobiological function.

INTRODUCTION

MicroRNAs (miRNAs) form a growing class of endogenous non-coding RNA molecules that modulate gene expression post-transcriptionally. Like transcription factors, an increase in the number of miRNAs strongly correlates with greater organismal complexity [98]. miRNAs form elaborate and sophisticated regulatory networks, where a given miRNA can influence the stability or translatability of hundreds of mRNA targets [2], and numerous miRNAs can act in concert to repress a common target. While transcription factors act as "switches" to initiate broad developmental transitions, miRNAs may act downstream to fine-tune genetic regulatory programs. An influential model posits that highly expressed miRNAs act to quell the deleterious effects of leaky transcription, while moderately expressed miRNAs buffer fluctuations in expression at weak or suboptimal promoters [95].

Generation of cellular diversity during mammalian brain development requires precise coordination of gene regulatory networks, with integral involvement of miRNAs. Lineage-specific expression signatures of cultured astrocytes and neurons [59] implicate miRNAs in neural cell fate specification. Neurobiological functions have been attributed to specific miRNAs. For example, miR-124 promotes neuronal differentiation [99], and miR-134 is involved in dendritic branching [100]. Global ablation of miRNAs is achieved in model systems by knocking out the essential miRNA processing enzyme, Dicer. In zebrafish, maternal zygotic Dicer knockout embryos undergo axis formation and body patterning, but exhibit profound defects in brain morphogenesis [57]. Likewise, selective inactivation of Dicer produces morphogenetic CNS abnormalities in

conditional knockout mice, including microcephaly and reduced elaboration of dendritic branches [101]. While neuronal progenitors remain viable in the absence of miRNAs, cytoarchitectural abnormalities arise from failures to differentiate and propagate newborn neurons [102]. Dysregulation of miRNAs has been implicated in the etiology of schizophrenia [71, 103-105], as well as age-related neurodegenerative disorders [106-108].

Early expression studies uncovered a subset of brain-specific or brain-enriched miRNAs [52]. Molecular profiling studies in rodents showed that miRNAs are dynamically regulated during brain development [51], with a "chronological wave" of sequentially expressed miRNA classes [54]. Since these landmark studies, hundreds of additional miRNAs have been discovered, including many that are specific to humans. In the present study, we have performed comprehensive miRNA expression analysis in human postmortem brain samples representing fetal, early postnatal, and adult time points. We measured the expression of nearly all currently known miRNAs, as well as 373 novel, putative miRNAs. Classifying miRNAs based on temporal expression profiles may provide insight into their regulation and potential neurobiological functions.

MATERIALS AND METHODS

Sample selection and preparation

Frozen brain tissue samples were obtained from the NICHD Brain and Tissue Bank for Developmental Disorders. The tissue bank, housed at the University of Maryland and supported by the National Institute of Child Health and Human Development, is a repository of over 60,000 specimens. More than 400 prenatal control samples are available, ranging in gestational age from 8 weeks to 39 weeks, and additional control

samples are available from children and adults. Brain sectioning procedures began by first transecting the medulla at its juncture with the distal pons and then separating the cerebral hemispheres. The left hemisphere was further dissected by sectioning posterior to the cerebral peduncles to separate the midbrain/pons/cerebellum. The remaining cerebrum was sectioned coronally at approximately 1 cm intervals, gently rinsed, blotted dry, and placed in a freezing bath. Frozen tissue samples were individually stored at -80° C in plastic bags.

A total of 48 frozen cerebral tissue samples were obtained. Fetal samples originated from subjects ranging in gestational age from 14 weeks to 24 weeks. Additionally, tissue samples were obtained to represent early postnatal time points. The majority of tissue samples originated from African American individuals, and samples from each developmental time point were well-matched with respect to post-mortem interval. Three samples were excluded from microarray expression analysis, two due to poor RNA integrity measures and one due to uncertain sample identification. This information is summarized in **Table 2.1**. The adult time point is represented by two commercially available total RNA products. FirstChoice Human Brain Total RNA (Ambion) is a high-quality RNA sample derived from an 81 year old adult male, and FirstChoice Human Brain Reference RNA is pooled from several donors. FirstChoice Human Brain Reference RNA was extensively characterized in the MicroArray Quality Control (MAQC) Project initiated by the U.S. Food and Drug Administration.

All tissue samples were thawed for a minimum of 16 hours at -20°C in RNAlater-ICE (Ambion). RNAlater-ICE was decanted and tissue samples were gently rinsed in saline solution. Tissue homogenization and RNA extraction procedures were performed using

the *mir*Vana PARIS kit (Ambion). Six volumes of provided cell disruption buffer were added to 200-500 mg sections of frozen tissue, and a PowerGen35 handheld homogenizer was used for tissue disruption. After adding one volume of denaturing solution, 750 μl aliquots of lysate were stored for subsequent RNA isolation. Total RNA extractions were performed according to the manufacturer's protocol, and yield and purity were determined using a NanoDrop ND-1000 spectrophotometer.

Microarray preparation and data acquisition

Dual-channel microarray expression analysis was performed using the NCode Human miRNA Microarray V3 (Invitrogen). On each array, a single Cy3 labeled total RNA sample was competitively hybridized against a Cy5 labeled control pool. This control pool was a mixture of all RNA samples, where each developmental time point was equally represented, and each individual sample was equally represented within a given time point. For each channel, 1 μg of total RNA was labeled with the *Label* IT® miRNA Labeling Kit, Version 2 (Mirus Bio) according to manufacturer's protocol. Samples were hybridized to the array at 37˚C overnight using the hybridization buffer included with the labeling kit.

Image analysis was performed on a GenePix 4000B microarray scanner. A marked difference in pixel intensity was observed between Sanger miRNAs and the novel features exclusively present on the NCode V3 arrays, with many of the latter approaching saturation. Photomultiplier tube (PMT) settings were adjusted so as to balance signal intensity in the red and green channels, and maximize pixel intensity without saturation at 10% power. Arrays were then rescanned at 100% power without PMT adjustment. Automatic feature identification was performed using Genepix 4.0 software, and all

images were then inspected by eye and atypical features were manually flagged. Images were exported and further processed using the Acuity 4.0 software package. Data filtering parameters were established to include only features with (1) at least 70% of pixels greater than 2 standard deviations above background in either the red or green channel, (2) regression R^2 greater than 0.5 to ensure feature uniformity, (3) less than 20% of pixels saturated in both the red and the green channels, and (4) no flags upon visual inspection. Normalization was performed with the LOWESS (locally weighted regression) method, and expression log ratios were exported for statistical analysis.

Analysis of microarray data

Missing values were present in the dataset due to the aforementioned data filtering criteria. The causes of data flags were irretrievable, making it impossible to extract meaning from missing values. Rather than inferring the type of flag (saturation versus absence of signal) by comparing across datasets, an alternative approach was used to merge the 10% and 100% scan data. Normalization had rendered the 10% and 100% scans comparable with a simple statistical model. The 100% scan values for each spot followed a linear regression model on 10% scan data, with the slope of the regression model found to be statistically equal to 1, and with an intercept of 0.18 (a constant shift between log ratio values in the 100% and 10% scan data). For spots where only the 10% scan data value was recorded, this value was used in the analysis. For spots where only the 100% scan data value was recorded, this value with 0.18 subtracted was used (rendering the 10% and 100% scan values directly comparable). For spots where both 10% and 100% scan values were recorded, the analysis was based on the average of the 10% and 100% scan value with 0.18 subtracted. The rationale was that by taking an

average this would further suppress scanning noise in the data. As a final step in quality filtering, only genes with non-missing values for at least 75% of the provided samples of each sample type (defined as fetal, young, and adult) were included in subsequent analyses. 464 genes (48%) passed this filter.

Prior to running significance analysis the following distribution assumption checks were performed. The within-sample type variance was computed for each gene. It was found that an equal variance assumption for the different sample types was well supported by the data. Thus, F-tests and regression models can be used to analyze the data. A graphical examination of the error distribution using normal Quantile-Quantile plots revealed that the error distribution was long-tailed. To perform testing we thus used a re-sampling based approach to compute p-values. A model was fit to each gene where a separate mean expression level was estimated for each of the three sample types. The residuals from this fit were stored in a data matrix. We then used re-sampling techniques to generate a data set for which the null hypothesis of no sample type differences is true. This is done by randomly assigning residuals to each of the sample types, letting these re-sampled residuals take on the role of real data. Because of the random assignment the null hypothesis is true for re-sampled data. The benefit of this approach is that we do not need to assume a normal error distribution when we test significance.

We analyzed 464 genes using backward F-test model selection. We provide a brief description of the technique here. We start by modeling all genes with the so-called “full model”. The full model is a model which allows for a unique mean expression level for each of the three sample types (fetal, young, adult). The second step of the analysis is to simplify the full model. There are three models that constitute a simplification of the full

model; (1) a model where the young and adult samples have the same mean expression, but the fetal samples have a different mean expression ($F \neq Y = A$); (2) a model where the fetal and young mean expression coincides, and the adult mean expression differs ($F = Y \neq A$); (3) a model where the fetal and adult mean expression coincides, and the young mean expression differs ($F = A \neq Y$). We compare these 3 models in terms of fit for each gene, and pick the best model with the smallest error sum of squares. The third step of the analysis is to compare the best model (one of models 1, 2 and 3) to the "null model" where the mean expression values for fetal, young and adult samples coincide.

In standard backward F-test model selection we do the following; we fit the full model as above, and then fit models 1, 2, and 3 to the data. We perform an F-test comparing the full model to the best of models 1, 2 and 3. If this F-test leads to a rejection (the p-value is below some cutoff, e.g. 1%) we keep the full model to describe our gene. If, on the other hand, the F-test leads to a non-rejection, we select the best of models 1, 2 and 3 to describe the gene. We then perform an F-test comparing the best of models 1, 2 and 3 to the null model. If the p-value of this test is below the cutoff 1%, we keep the best of models 1, 2 and 3. If the p-value of this test is above the cutoff 1%, we keep the null model to describe our gene.

Just like in standard significance analysis we have to adjust for multiple testing. Here, we use simulation based FDR estimation similar to the SAM procedure. That is, we perform the model selection for each gene as outlined above. We obtain p-values for testing the full model versus the best of models 1, 2 and 3 for each gene, and we obtain p-values for testing the best of models 1, 2 and 3 against the null model for each gene. To estimate the FDR for a given p-value cutoff, we simulate data for which the null model is

true (see description above). We then perform model selection as described above, and obtain 2 sets of p-values for each gene in each simulated data set. For each p-value cutoff under consideration we compare the p-values obtained from the real data to the p-value cutoff and count the number of genes for which the null model is not selected. These are the detected genes at this p-value cutoff. On each of the simulated data sets we also count the number of genes for which the null model is not selected. By construction these are all false detections. We estimate the FDR of our procedure by the ratio (mean number of false detections across simulated data sets / number of detections on the real data set). We try different p-value cutoffs until our estimated FDR is controlled at some pre-chosen level (e.g. 1%). In this analysis we used 2500 simulated data sets to estimate the FDR. To control the FDR at 1%, it was found that the p-value cutoff should equal 0.001901.

Expression analysis of distinct RNA fractions

Distinct RNA fractions were prepared from total RNA (First Choice Human Brain, Ambion), which were either depleted of or enriched for small RNAs using the *mir*Vana (Ambion) glass-fiber filter based protocol. Fractions enriched for small RNA or depleted of small RNA were independently labeled and hybridized to NCode V3 arrays as previously described. For all spotted features, we calculated the difference in background subtracted median fluorescence between the large and small RNA fractions.

Preparation and analysis of TaqMan miRNA arrays

Sample pools for each unique developmental age were constructed by combining equal amounts of extracted total RNA (**Table 2.1**). Reverse transcription reactions were performed using 600 ng total RNA input, and reagents from the TaqMan miRNA Reverse

Transcription Kit and Megaplex Primer Pools (Applied Biosystems). Reactions were performed (without preamplification) according to the Megaplex Pools protocol (Applied Biosystems), and thermal cycling was performed in a PTC-200 DNA Engine (MJ Research). Real-time PCR reactions were performed using the TaqMan Human miRNA Array set v2.0 in a 7900HT real-time PCR system (Applied Biosystems). A single array set was run for each sample pool. Relative expression analysis was performed using the SDS 2.3 software. Using the $2^{-\Delta\Delta Ct}$ method [109], expression levels of all miRNAs were measured relative to a stably expressed endogenous control gene, mammalian U6 snRNA. Fold changes for each unique developmental time point were calculated relative to an adult calibrator sample (FirstChoice Human Brain Reference RNA, Ambion). Intergroup fold changes were also calculated by averaging ΔCt values for fetal, early postnatal, and adult samples.

Table 2.1: Brain tissue samples for developmental miRNA expression profiling. Basic demographic variables (age, sex, race) are indicated, as well as post-mortem interval.

UMB#	GA weeks	Years	Days	Pool	Sex	Race	PMI (hrs)
4912	14			1	female	African American	1
4799	14			1	male	African American	3
4794	14			1	male	African American	1
4934	16			2	male	African American	2
4573	16			2	female	African American	1
1388	16			2	male	African American	1
396	16			2	male	African American	1
249	17			3	male	African American	1
12	17			3	male	African American	1
43	17			3	female	African American	1
57	18			4	female	African American	1
42	18			4	female	African American	1
33	18			4	female	African American	1
31	18			4	male	African American	1
14	18			4	female	African American	3
4825	18			4	male	African American	1
4823	18			4	male	African American	4
113	18			4	female	African American	1
201	18			4	male	African American	1
278	18			4	male	African American	1
279	18			4	female	African American	1
1521	18			4	female	African American	1
280	18			4	female	African American	2
291	18			4	male	African American	12
391	18			4	male	Caucasian	1
392	19			5	male	African American	1
4609	19			5	female	African American	2
261	19			5	male	African American	1
250	19			5	male	African American	1
66	19			5	female	African American	3
9	19			5	female	African American	2
46	19			5	female	Caucasian	12
4889	19			5	male	African American	2
4715	20			6	male	African American	4
4654	20			6	unknown	African American	2
45	20			6	male	African American	2
*311	24				female	Caucasian	1
779		0	5	7	male	African American	5
*633		0	60		male	African American	21
1055		0	96	7	male	Caucasian	12
*1742		0	89		female	African American	24
1296		0	98	7	male	African American	16
1453		1	78	8	male	African American	19
1063		1	123	8	male	African American	21
1488		1	137	8	male	African American	21
1499		4	170	9	female	Asian	21
4670		4	273	9	male	Caucasian	17
1185		4	258	9	male	Caucasian	17

*samples excluded from expression analysis
UMB# - Sample identifier, NICHD Brain and Tissues Bank for Developmental Disorders
GA – gestational age
Pool – indicates sample pooling for TaqMan arrays
PMI – post-mortem interval

RESULTS

MicroRNA expression analysis was performed using the NCode Human miRNA microarray (Invitrogen), which contains 710 probes for validated human miRNAs from miRBase release 10.0, as well as 373 Invitrogen novel human miRNAs. We immediately observed striking differences in signal intensity between novel and validated miRNAs present on the array, and thus we maximized data capture by scanning all microarrays at 10% and 100% power and subsequently merging these data sets. The data was easily seen to be of very high quality, and after normalization, the 100% scan values for each spot followed a linear regression model on 10% scan data in the entire range of observed log ratios. The multiple R-squared of this regression model was 93% (meaning there was a very tight correlation between the 100% and 10% scan data). Merging the datasets reduced the number of missing value spots by 50% compared with the 10% and 100% datasets analyzed separately. We chose to only analyze genes for which a substantial number of samples have recorded (non-missing) values. Only genes with non-missing values for at least 75% of the provided samples of each sample type (fetal, young, adult) were included in subsequent analyses. Since competitive hybridization against a control pool was performed on each array (see methods), these filtering criteria should not be expected to eliminate detection of miRNAs that are uniquely expressed in certain age groups, and indeed, missingness is highly correlated across all time points. Filtering reduced the set of genes to be analyzed from 965 to 464. The gene set consisted of the following groups; (1) After merging there were a total of 26 genes for which only 10% scan data was available, and among these 26 only 16 genes passed the filtering test; (2) There were 273 genes for which only 100% scan data was available, and none of these

genes passed the filtering test; (3) There were 666 genes for which both 10% and 100% data were available, and among these 448 passed the filter. By merging the 10% and 100% scan, the gene set that passed the filter contained 100 additional genes that would have otherwise been excluded from the analysis, and 96 of these were novel miRNAs. Thus, merging scan data provided substantial gains in data quality (by averaging of the two scan values) and quantity.

Traditionally, miRNA microarrays have required the use of total RNA fractions enriched for small RNA in order to ensure robust and specific detection of miRNAs. To avoid potentially biasing expression profiles due to size fractionation, we labeled and hybridized total RNA extracts. We compared alternate labeling methods (enzymatic and chemical) as well as alternate hybridization temperatures (data not shown). While the labeling method did not significantly affect the number of false positives, hybridization temperature clearly did. We chose to pursue a lower hybridization temperature than that recommended by the manufacturer, which resulted in more false positives but far fewer false negatives as determined by experiments using synthetic pools of miRNAs (data not shown). Due to modest improvements in sensitivity, a chemical labeling method was adopted for our study. Since this method uniformly labels nucleic acids, we questioned whether strikingly robust detection of many novel miRNAs present on the NCode V3 array indicated hybridization of miRNA precursors or other large non-coding RNA species, rather than mature miRNAs. To test this possibility, we measured miRNA expression in small and large RNA size fractions. The expectation is that little specific signal (derived from mature miRNAs) should be seen in the large RNA fraction. We compared background subtracted median fluorescence values from small and large RNA

fractions (**Figure 2.1**). Filter based methods of depletion/enrichment are likely to be imperfect, but even with an imperfect depletion, one still expects to observe much higher relative signal in the small RNA fraction. Indeed, only a handful of traditional (Sanger) miRNAs violated this assumption. However, a much greater proportion of the novel, putative miRNAs showed greater signal of detection in the large RNA fraction. These species were not excluded from the statistical analysis, but they were flagged as potentially belonging to other classes of non-coding RNA (**Table 2.2**).

Figure 2.1: Expression analysis of size fractionated RNA samples. Total RNA samples were either enriched for or depleted of small RNAs. 1 μg each of enriched and depleted samples were labeled and hybridized to glass slide arrays. The background subtracted median fluorescence (MFI) was calculated, and the MFI of depleted samples was subtracted from the MFI of enriched samples. A) represents detectable Sanger miRNAs, B) represents detectable novel miRNAs.

A

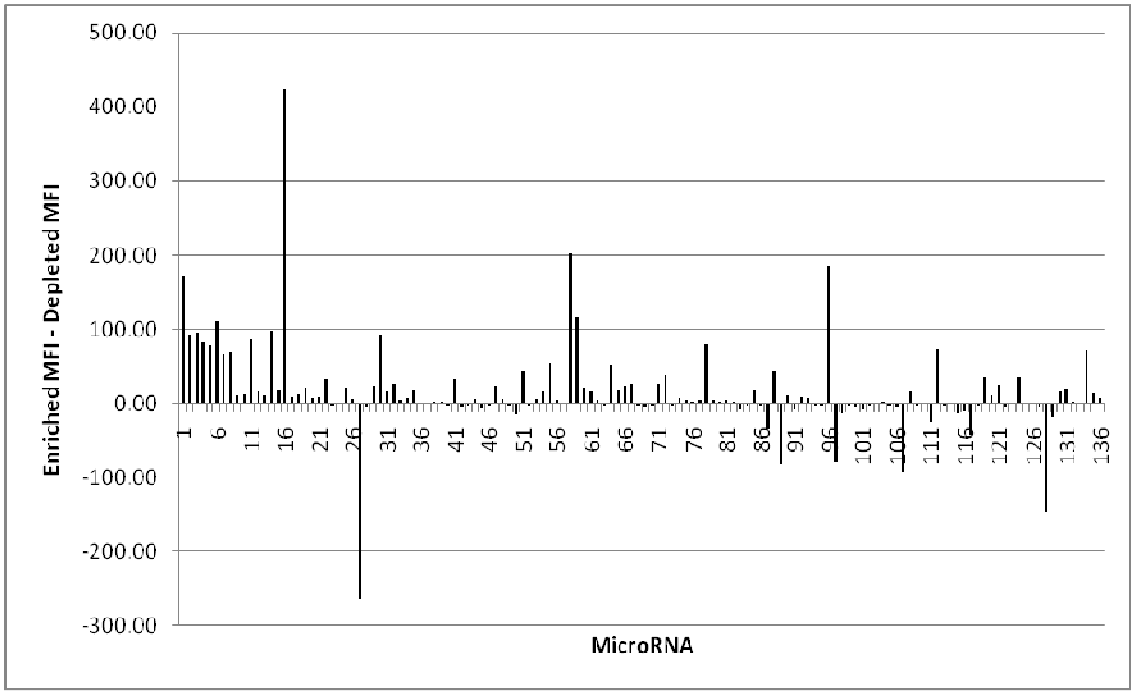

B

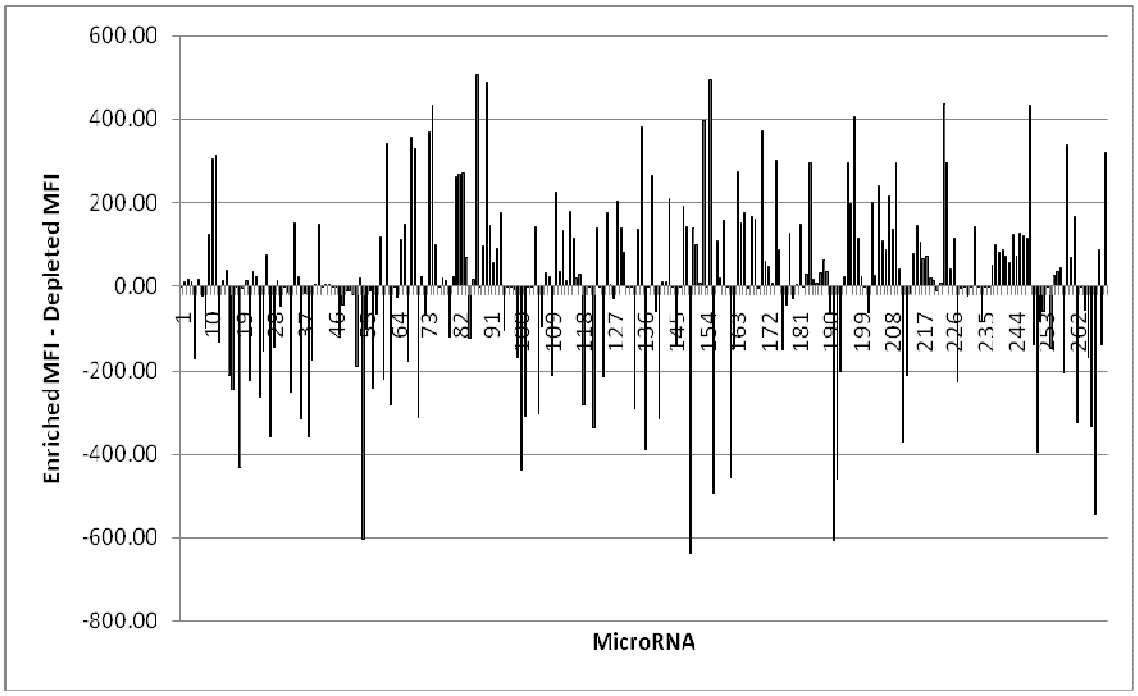

In our data set consisting of 464 genes, 312 were found to be significant based on an F-test with p-values calculated from re-sampling, suggesting that their mean expression levels differs between at least two of the sample types, defined as fetal, young and adult. Developmental expression patterns for these 312 miRNAs were analyzed using correlation-based hierarchical clustering (**Figure 2.2**). Samples from developmentally proximal time points had more similar miRNA expression signatures, suggesting that a global miRNA expression profile can act as a marker of developmental stage. A landmark expression study revealed a "chronological wave" of miRNA expression in the developing mouse brain, where expression levels gradually transitioned from the fetal to adult state [54]. In contrast, our analysis revealed a subset of miRNAs with distinct early postnatal expression levels, which were non-intermediate along the fetal to adult spectrum. Of the 312 significant genes; (a) 81 genes correspond to the case where

F≠Y=A, i.e., the fetal mean expression is significantly different from young and adult; (b) 101 genes correspond to the case where F=Y≠A; (c) 60 genes correspond to the case where F=A≠Y; and (d) 70 genes correspond to the case where all mean expression levels differ (F≠Y≠A).

Figure 2.2: Hierarchical clustering of all significant miRNAs. Hierarchical clustering was performed on 312 differentially expressed miRNAs using a correlation metric. Included miRNAs have significantly different expression levels in at least one pair-wise comparison between the general sample types fetal, young and adult. The sample types are indicated in the colored bar (blue-fetal, red-young, green-adult).

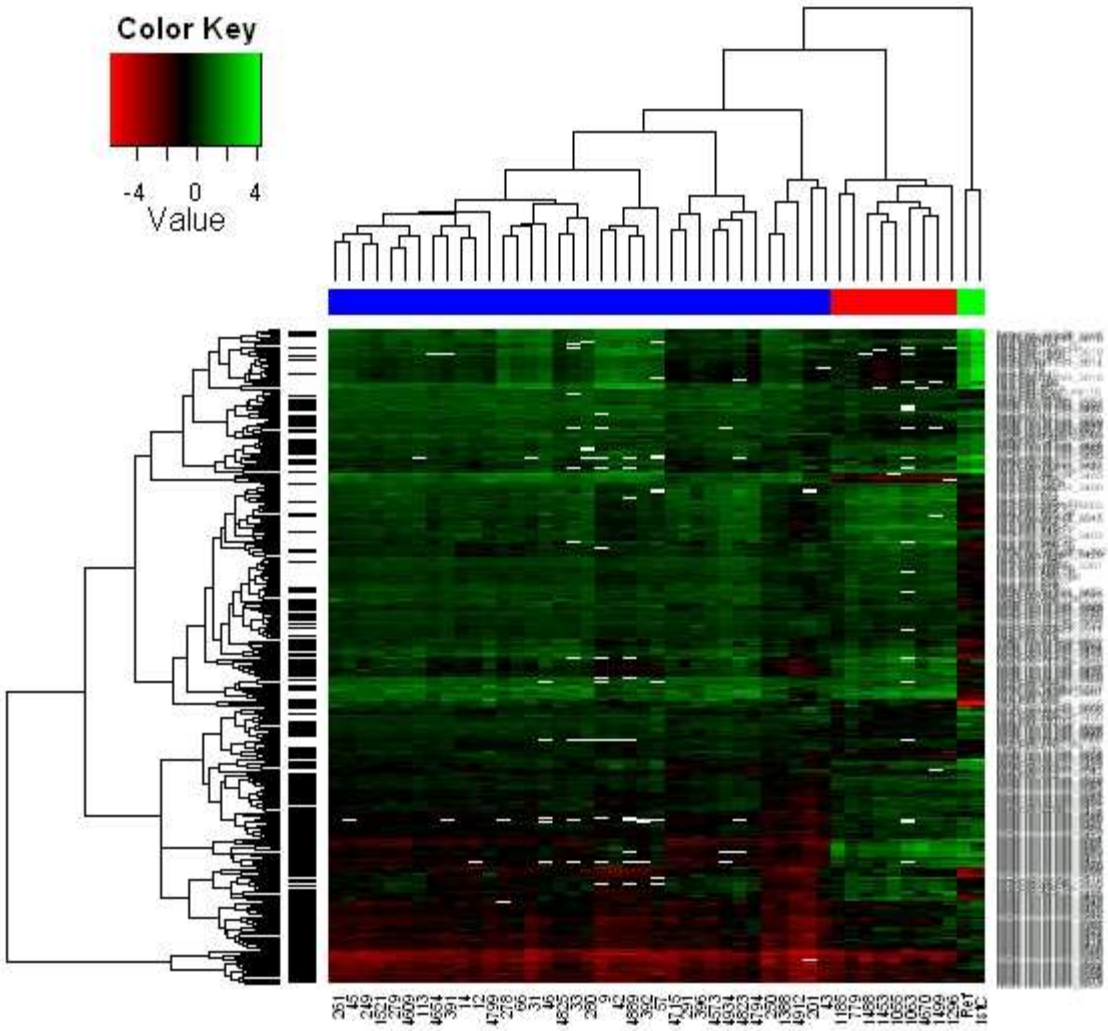

Model classes were refined to take into account the direction of expression differences between sample types, resulting in 13 unique model classes. The miRNAs belonging to all non-null model classes are listed in **table 2.2**. Model classes 1 and 2 are models for which the young and adult mean expression levels coincide, and the fetal mean expression differs. A substantially greater number of miRNAs belong to the class where fetal expression levels are lower than that of young and adult samples (60 miRNAs versus 14 that show higher relative expression). Model classes 1 and 7, marked by lowest expression at fetal time points, appear to be particularly enriched for novel miRNAs (**Figure 2.3**). Re-sampling via permutation of age category labels confirmed that this enrichment for novel miRNAs is significant, $p = 0.0015$ for class 1, $p = 0.0393$ for class 7. For model classes where the fetal and young mean expression levels coincide and adult expression differs, there is a more balanced split between down-regulation and up-regulation (model classes 3 and 4 with 41 and 60 genes, respectively). The same is also true when fetal and adult expression levels coincide, with the young being different (model classes 5 and 6 with 33 and 27 genes, respectively).

Table 2.2: Classifying miRNAs based on developmental expression profiles. Using statistical modeling, miRNAs were classified based on all possible expression relationships between fetal, young, and adult samples.

Class 1: F<Y=A	Class 2: F>Y=A	Class 3: F=Y<A	Class 4: F=Y>A	Class 5: F=A<Y
hsa-miR-138	1539-mut2-mir-200c	hsa-let-7e	1529-shuf-has-mir-93	hsa-miR-187*
hsa-miR-382	hsa-miR-17	hsa-let-7f	1532-rev-mir-150	hsa-miR-220b
IVGN-novel-miR_3301	hsa-miR-185	hsa-miR-103	1541-shuf-mir-200c	hsa-miR-30c-1*
IVGN-novel-miR_3311	hsa-miR-516b	hsa-miR-107	hsa-miR-125a-3p	hsa-miR-425
IVGN-novel-miR_3313	hsa-miR-654-5p	hsa-miR-125a-5p	hsa-miR-142-5p	hsa-miR-491-5p
IVGN-novel-miR_3314	IVGN-novel-miR_3408	hsa-miR-181c	hsa-miR-150*	hsa-miR-612
IVGN-novel-miR_3318	IVGN-novel-miR_3456	hsa-miR-24	hsa-miR-193b*	hsa-miR-617
IVGN-novel-miR_3321	IVGN-novel-miR_3493	hsa-miR-26a	hsa-miR-198	hsa-miR-628-3p
IVGN-novel-miR_3326	IVGN-novel-miR_3558	hsa-miR-29a	hsa-miR-214	hsa-miR-665
IVGN-novel-miR_3327	IVGN-novel-miR_3644	hsa-miR-30d	hsa-miR-23a*	hsa-miR-744
IVGN-novel-miR_3346 X	IVGN-novel-miR_3646	hsa-miR-373	hsa-miR-296-3p	hsa-miR-92b*
IVGN-novel-miR_3351	IVGN-novel-miR_3652	hsa-miR-491-3p	hsa-miR-298	IVGN-novel-miR_3309
IVGN-novel-miR_3356	IVGN-novel-miR_3654	hsa-miR-497	hsa-miR-30b*	IVGN-novel-miR_3315
IVGN-novel-miR_3383	IVGN-novel-miR_3683	hsa-miR-646	hsa-miR-370	IVGN-novel-miR_3385
IVGN-novel-miR_3384		hsa-miR-768-3p	hsa-miR-373*	IVGN-novel-miR_3386 X
IVGN-novel-miR_3387 X		hsa-miR-98	hsa-miR-422a	IVGN-novel-miR_3429
IVGN-novel-miR_3390 X		IVGN-novel-miR_3306 X	hsa-miR-485-5p	IVGN-novel-miR_3433
IVGN-novel-miR_3394 X		IVGN-novel-miR_3310 X	hsa-miR-486-3p	IVGN-novel-miR_3435
IVGN-novel-miR_3397		IVGN-novel-miR_3316 X	hsa-miR-518c*	IVGN-novel-miR_3436
IVGN-novel-miR_3399 X		IVGN-novel-miR_3322 X	hsa-miR-548c-5p	IVGN-novel-miR_3437
IVGN-novel-miR_3401		IVGN-novel-miR_3332	hsa-miR-564	IVGN-novel-miR_3453
IVGN-novel-miR_3402		IVGN-novel-miR_3341	hsa-miR-608	IVGN-novel-miR_3463
IVGN-novel-miR_3403		IVGN-novel-miR_3354 X	hsa-miR-610	IVGN-novel-miR_3468
IVGN-novel-miR_3410 X		IVGN-novel-miR_3355	hsa-miR-616	IVGN-novel-miR_3474
IVGN-novel-miR_3411		IVGN-novel-miR_3391 X	hsa-miR-630	IVGN-novel-miR_3515
IVGN-novel-miR_3412 X		IVGN-novel-miR_3422	hsa-miR-650	IVGN-novel-miR_3537
IVGN-novel-miR_3415		IVGN-novel-miR_3428	hsa-miR-659	IVGN-novel-miR_3538
IVGN-novel-miR_3418		IVGN-novel-miR_3460	hsa-miR-671-5p	IVGN-novel-miR_3559
IVGN-novel-miR_3423		IVGN-novel-miR_3502	hsa-miR-674	IVGN-novel-miR_3579
IVGN-novel-miR_3424		IVGN-novel-miR_3504	hsa-miR-760	IVGN-novel-miR_3593
IVGN-novel-miR_3438 X		IVGN-novel-miR_3525	hsa-miR-933	IVGN-novel-miR_3694
IVGN-novel-miR_3458		IVGN-novel-miR_3541	IVGN-novel-miR_3328	IVGN-novel-miR_3695
IVGN-novel-miR_3461		IVGN-novel-miR_3560	IVGN-novel-miR_3329	
IVGN-novel-miR_3465		IVGN-novel-miR_3570	IVGN-novel-miR_3359	
IVGN-novel-miR_3485		IVGN-novel-miR_3573 X	IVGN-novel-miR_3361	
IVGN-novel-miR_3486		IVGN-novel-miR_3614	IVGN-novel-miR_3377	
IVGN-novel-miR_3495		IVGN-novel-miR_3624	IVGN-novel-miR_3378	
IVGN-novel-miR_3497		IVGN-novel-miR_3628	IVGN-novel-miR_3400	
IVGN-novel-miR_3503		IVGN-novel-miR_3650	IVGN-novel-miR_3425	
IVGN-novel-miR_3520		IVGN-novel-miR_3672 X	IVGN-novel-miR_3434	
IVGN-novel-miR_3535 X		IVGN-novel-miR_3673	IVGN-novel-miR_3452	
IVGN-novel-miR_3543			IVGN-novel-miR_3466	
IVGN-novel-miR_3548			IVGN-novel-miR_3467	
IVGN-novel-miR_3550 X			IVGN-novel-miR_3470	
IVGN-novel-miR_3552			IVGN-novel-miR_3471	
IVGN-novel-miR_3553 X			IVGN-novel-miR_3507	
IVGN-novel-miR_3556			IVGN-novel-miR_3516	
IVGN-novel-miR_3557			IVGN-novel-miR_3522	
IVGN-novel-miR_3563			IVGN-novel-miR_3526	
IVGN-novel-miR_3564			IVGN-novel-miR_3527	
IVGN-novel-miR_3566 X			IVGN-novel-miR_3536	
IVGN-novel-miR_3568 X			IVGN-novel-miR_3549	
IVGN-novel-miR_3582			IVGN-novel-miR_3586	
IVGN-novel-miR_3583			IVGN-novel-miR_3591	
IVGN-novel-miR_3595			IVGN-novel-miR_3604	
IVGN-novel-miR_3599			IVGN-novel-miR_3606	
IVGN-novel-miR_3607 X			IVGN-novel-miR_3649	
IVGN-novel-miR_3626			IVGN-novel-miR_3651	
IVGN-novel-miR_3657			IVGN-novel-miR_3668	
IVGN-novel-miR_3659			IVGN-novel-miR_3688	
IVGN-novel-miR_3679				
IVGN-novel-miR_3680				
IVGN-novel-miR_3681				
IVGN-novel-miR_3682 X				
IVGN-novel-miR_3697 X				
IVGN-novel-miR_3698 X				
IVGN-novel-miR_3699 X				

Class 6: F=A>Y	Class 7: F<Y<A	Class 9: Y>F>A	Class 10: F>Y>A	Class 12: Y<F<A
1526-mut1-has-mir-93	hsa-miR-22	1552-rev-mmu-mir-292	hsa-miR-505*	1518-mut1-rno-mir-16
hsa-miR-106a	IVGN-novel-miR_3353	hsa-miR-129-5p	hsa-miR-550	hsa-let-7a
hsa-miR-106b	IVGN-novel-miR_3357	hsa-miR-185*	hsa-miR-551b*	hsa-let-7b
hsa-miR-124	IVGN-novel-miR_3413	hsa-miR-193a-5p	hsa-miR-920	hsa-let-7c
hsa-miR-125b	IVGN-novel-miR_3454	hsa-miR-194*	IVGN-novel-miR_3335	hsa-let-7d
hsa-miR-181a	IVGN-novel-miR_3489	hsa-miR-202		hsa-let-7g
hsa-miR-181b	IVGN-novel-miR_3542	hsa-miR-215		hsa-let-7i
hsa-miR-206	IVGN-novel-miR_3551	hsa-miR-25*		hsa-miR-10b
hsa-miR-20a	IVGN-novel-miR_3580	hsa-miR-30c-2*		hsa-miR-16
hsa-miR-28-5p	IVGN-novel-miR_3666	hsa-miR-371-5p		hsa-miR-195
hsa-miR-297		hsa-miR-449b		hsa-miR-330-3p
hsa-miR-541*		hsa-miR-498		hsa-miR-574-5p X
hsa-miR-9		hsa-miR-557		hsa-miR-768-5p
hsa-miR-93		hsa-miR-602		IVGN-novel-miR_3302
IVGN-novel-miR_3303		hsa-miR-637		IVGN-novel-miR_3379
IVGN-novel-miR_3388		hsa-miR-638		IVGN-novel-miR_3395
IVGN-novel-miR_3409		hsa-miR-663		IVGN-novel-miR_3439
IVGN-novel-miR_3440		hsa-miR-675		IVGN-novel-miR_3490
IVGN-novel-miR_3491		hsa-miR-885-3p		IVGN-novel-miR_3501
IVGN-novel-miR_3505		hsa-miR-886-5p		IVGN-novel-miR_3615
IVGN-novel-miR_3506		hsa-miR-939		IVGN-novel-miR_3616
IVGN-novel-miR_3508		IVGN-novel-miR_3476		IVGN-novel-miR_3617
IVGN-novel-miR_3528		IVGN-novel-miR_3545		IVGN-novel-miR_3618
IVGN-novel-miR_3544		IVGN-novel-miR_3546		IVGN-novel-miR_3619
IVGN-novel-miR_3561		IVGN-novel-miR_3547		IVGN-novel-miR_3627
IVGN-novel-miR_3660		IVGN-novel-miR_3603		IVGN-novel-miR_3632
IVGN-novel-miR_3662		IVGN-novel-miR_3700		IVGN-novel-miR_3639 X
IVGN-novel-miR_3663				IVGN-novel-miR_3647

X-flagged as potentially being a larger ncRNA based on profiling of distinct RNA size fractions

Analysis was performed on the fetal samples alone to determine if the gestational age (in weeks) had a significant impact on expression. After adjusting for multiple testing it was found that there were no significantly misexpressed miRNAs present in the data. This may be due, in part, to the small sample sizes representing each developmental time point. Similarly, an analysis was run on the young samples alone to determine if age (in days) had a significant impact on miRNA expression. After adjusting for multiple testing, no significantly misexpressed miRNAs were present in the data set.

Figure 2.3: Hierarchical clustering of miRNAs with distinct expression signatures at fetal time points. Hierarchical clustering was performed on miRNAs with significantly different expression levels at fetal time points compared to young and adult. However, expression levels of these miRNAs do not vary between young and adult samples.

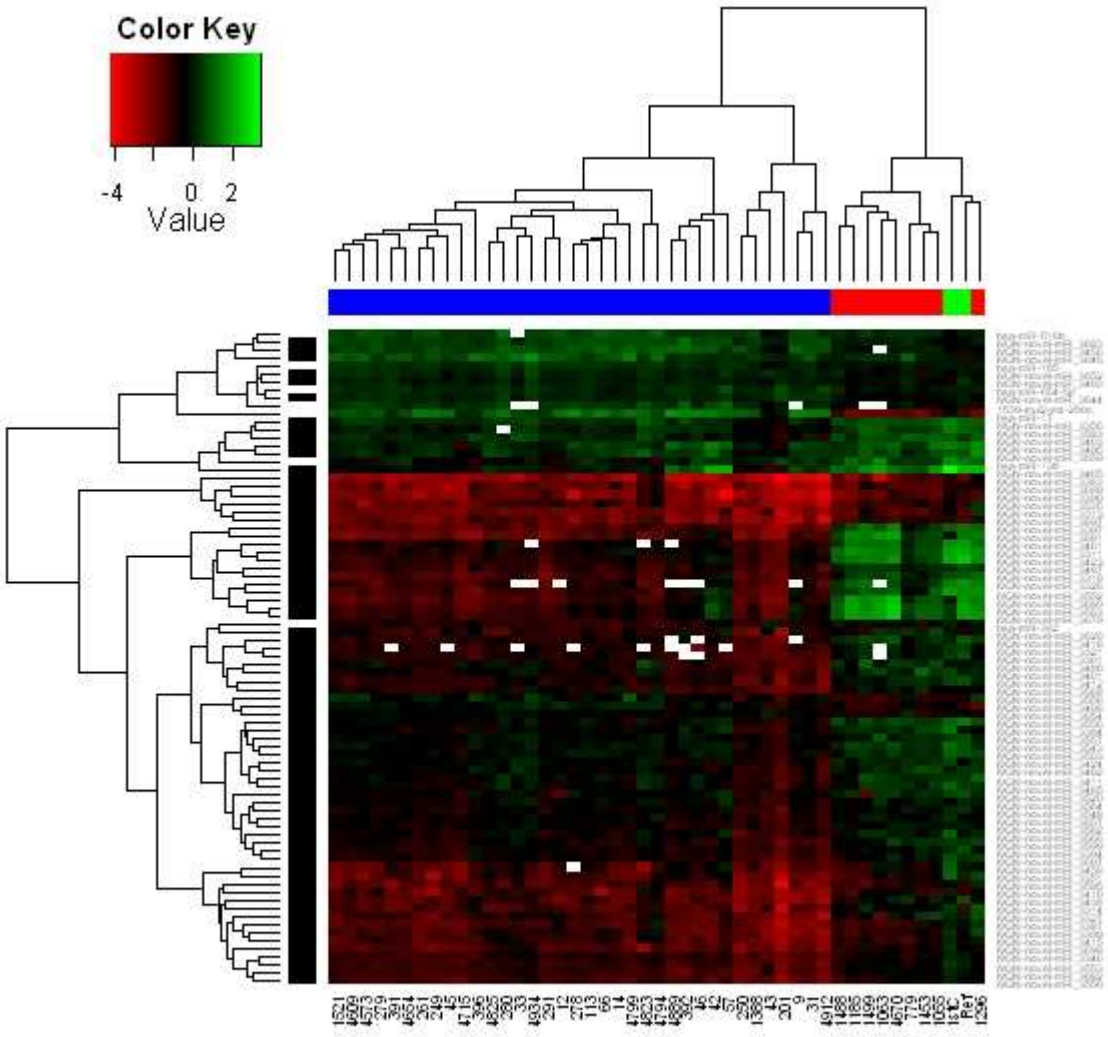

Samples comprising each distinct time point were mixed to form 10 sample pools, and miRNA expression analysis was performed using the TaqMan® MicroRNA Array v2.0. TaqMan methodology is widely hailed as the gold standard for sensitivity, and the use of looped reverse transcription primers ensures detection of only mature miRNAs. Many of the validated, Sanger miRNAs that were detected and quantifed on TaqMan arrays fell

below the threshold of detection on the NCode microarrays. Even though pooling of samples from each developmental age precluded formal statistical analysis, we summarized the expression fold changes between groups (**Table 2.3**), and all real-time qPCR data is presented in **appendix 1**.

Table 2.3: Temporal expression analysis using real-time quantitative PCR. Sample pools were constructed to represent each unique time point, and expression analysis was performed using Taqman miRNA arrays. The number of miRNAs that exceed the indicated fold difference are tabulated for each pair-wise sample type comparison.

Fold Increase	Fetal vs. Adult	Young vs. Adult	Fetal vs. Young	Fold Decrease	Fetal vs. Adult	Young vs. Adult	Fetal vs. Young
>2	145	188	90	**>2**	253	113	267
>5	92	85	47	**>5**	136	63	130
>10	68	48	27	**>10**	87	49	74
>100	23	23	2	**>100**	21	10	7

DISCUSSION

MicroRNAs have emerged as critical regulators of mammalian brain development. Early expression studies uncovered a subset of miRNAs that are uniquely expressed in brain or neuronal cell lines [52]. More recently, massive parallel sequencing of human and chimpanzee brain tissue has revealed hundreds of novel miRNAs, many with primate-specific expression signatures [110]. Though functional characterization is pending, it is reasonable to speculate that these evolutionarily young miRNAs help to establish the complex cellular architecture of the primate brain. Cells express characteristic miRNA signatures as they transition from an immature to a differentiated state, and contrary to the restrictive model of gene expression [111, 112], miRNA expression profiles become increasingly complex and diverse as cells mature [113]. The requirement for miRNAs in the developing nervous system has been assessed by disrupting miRNA biogenesis. Convergent lines of evidence from several Dicer

knockout models implicate miRNAs in cell survival and differentiation in the CNS [56, 57, 101], however, ES cells deficient for DGCR8, a requisite cofactor in the first enzymatic miRNA processing step, do not display cell proliferation or apoptotic defects [114]. With this ever evolving backdrop of global and specific miRNA functional studies, we sought to establish a detailed miRNA expression atlas of the developing human brain by comparing fetal, young, and adult miRNA signatures.

We reported 312 out of 464 detected features with temporally distinct expression patterns in the human brain. Differentially expressed species formed ten unique model classes with contrasting fetal, young, and adult expression profiles. Notably, many miRNAs fit a model that did not depict a consistent trend in expression along the fetal to adult timeline, but instead sharply increased or decreased at early postnatal stages. For example, the ubiquitously expressed let-7 family members are conserved from nematodes to primates, and are well-known markers of a terminally differentiated state [115-117]. In our study, expression levels of most let-7 family members dramatically peaked at the adult time point, as expected, but we also observed a surprising decline in expression at early postnatal stages relative to fetal. We would also like to draw attention to several miRNAs with well-characterized roles in CNS development. miR-124 and miR-9 are brain-specific miRNAs [118] that are highly up-regulated at the onset of embryonic neurogenesis. Over-expression of these miRNAs in cultured cells promotes adaptation of a neuronal fate, while down-regulation has the opposite effect [58]. Recently, developmental expression profiling of the murine CNS revealed 12 miRNAs (miR-9, miR-17-5p, miR-124a, miR-125a, miR-125b, miR-130a, miR-140, miR-181a, miR-199a, miR-205, miR-214, miR-301) with significantly higher expression at embryonic versus

postnatal time points. Expression profiling was not performed in the fully mature mouse. In the present study, 4 miRNAs (miR-9, miR-124, miR-125b, miR-181a) fit the model F=A>Y. The decrease in expression at early postnatal stages is consistent with observations in the mouse, however, expression levels appear to rebound in the adult human brain. It is intriguing to note that, with regard to several neuronal miRNAs as well as the let-7 family, the early postnatal brain appears to adopt a more immature, dedifferentiated state. However, we did not observe expression of the pluripotency markers miR-290, -295, -293, -294, or the -302 family [113] at any developmental time point. With the exception of certain neurogenic brain regions, such as the dentate gyrus of the hippocampus [119], neurogenesis is mostly complete by the 18th week of gestation. Our data support a role for miRNAs in later stages of neuronal development, such as the formation and pruning of synapses [120], which continues throughout infancy and early childhood. At these developmental stages, we observe transient down-regulation of several well-characterized neuronal miRNAs, with concomitant spikes in expression of 31 other Sanger miRNAs (model classes 5 and 9).

We investigated 373 novel, putative miRNAs that are exclusively present on the NCode Human miRNA microarray V3 (Invitrogen), and found that 194 of these exhibited significant temporal expression changes. These novel species were discovered through deep sequencing of a human heart total RNA reference sample. Sequences were mapped to genomic hairpins and validated by qPCR with probes for the “mature” region. Subsequent bioinformatic analysis was performed using the miRDeep algorithm, which evaluates enrichment of sequence reads derived from the stem versus loop region of genomic hairpins, suggestive of miRNA processing [29]. This analysis revealed that

most of the small RNA sequences were unlikely to be classic miRNAs. By comparing expression profiles of various RNA size fractions, we determined that a significant proportion of the novel sequences were likely derived from larger non-coding RNAs. In a comprehensive analysis of the mammalian transcriptome, the FANTOM consortium estimated that 63% of the mouse genome is transcribed [121], strongly refuting the idea that everything besides 1.5% coding sequence in the genome is merely "junk DNA." Several classes of ncRNA are dynamically regulated during development, and they may serve especially prominent roles in the developing brain (reviewed in [122]). For these reasons, all microarray features were retained for significance analysis, regardless of whether they represented miRNAs or other types of RNA. Model classes 1 (F<Y=A) and 7 (F<Y<A) are comprised of 67 and 10 genes, respectively. Of these 77 genes with lowest expression during fetal stages, 74 are novel ncRNAs. From our RNA size fractionation experiments, 29 of the 312 genes with significant developmental changes in expression level were flagged as potentially being larger ncRNAs, and 26 of these flagged species were novel ncRNAs from either model class 1 (F<Y<A) or 3 (F=Y<A). Taken together, these data implicate a class of longer ncRNAs that are progressively up-regulated during development and may serve important neurobiological functions in the adult brain.

In summary, we have established the first miRNA and non-coding RNA expression atlas of the developing human brain. Expression signatures varied significantly between fetal, early postnatal, and adult brain tissue samples, analogous to patterns of temporal regulation previously observed in animal model systems. Despite attempts to match samples with respect to demographic variables, factors pertaining to sample selection and

handling can skew the results of post-mortem expression studies. Experimental and statistical methods were adopted to optimize sensitivity and accuracy of measured miRNA expression levels, yet some caveats still remain. Most importantly, we could not ensure that brain tissue samples originated from anatomically homogeneous regions from all subjects. Expression levels were averaged across multiple samples from a given developmental age to minimize regional effects, but the relative contribution of specific cellular populations to detected expression levels could vary across time points. Ultimately, our expression results and the proposed classification scheme should guide future studies of miRNA expression and function during brain development.

Chapter 3:

Improvements to Bead Based Oligonucleotide Ligation SNP Genotyping Assays

ABSTRACT:

We describe a bead-based, multiplexed, oligonucleotide ligation assay (OLA) performed on the Luminex flow cytometer. Differences between this method and those previously reported include the use of far fewer beads and the use of a universal oligonucleotide for signal detection. These innovations serve to significantly reduce the cost of the assay, while maintaining robustness and accuracy. Comparisons are made between the Luminex OLA and both pyrosequencing and direct sequencing. Experiments to assess conversion rates, call rates, and concordance across technical replicates are also presented.

INTRODUCTION

Single nucleotide polymorphisms (SNPs) represent a major source of genetic variation in human beings; the NCBI database dbSNP contains nearly 12 million unique SNPs, which correlates to an average of 1 SNP every 250 base pairs. Due to their frequency, SNPs are an important type of marker used in association studies of human disease, and can themselves induce functional changes that contribute to disease and drug response variability [123, 124]. In a relatively short time, SNP genotyping technologies have evolved from rudimentary and simplexed gel-based assays to highly multiplexed arrays designed to simultaneously interrogate more than 1 million SNPs. Ultra-high throughput array-based genotyping technologies, such as those offered by Illumina [125] and Affymetrix [126], are utilized in genome-wide studies requiring genotyping of hundreds of thousands of SNPs in hundreds (or low thousands) of samples. However, fine-mapping, candidate gene, and other targeted genetic studies often require genotyping of dozens or hundreds of SNPs in thousands of samples, and ultra-high throughput methods are not ideal for these applications. Though too numerous to list in their entirety, popular medium-throughput commercial methods include technologies such as Biotage's pyrosequencing [127], Third Waves's Invader assay [128], ABI's TaqMan SNP assay [129], and ABI's SNPplex platform [130]. Drawbacks of commercial genotyping platforms include equipment costs and the need to purchase proprietary reagents. The genotyping method presented here utilizes the Luminex flow cytometer, which is within the budget of many academic labs, and is a relatively open source platform readily amenable to "home-brew" assays not requiring expensive and proprietary reagents.

Additionally, unlike many SNP genotyping platforms, the Luminex flow cytometer is one of the few instruments capable of quantifying both proteins and nucleic acids (DNA, mRNA, and miRNA) [131-134], providing it with uses beyond the SNP genotyping assay presented here.

Our method uses the robust chemistry of the oligonucleotide ligation assay (OLA) in conjunction with the Luminex flow cytometry platform (**Figure 3.1**) [135-140]. The assay is performed in 96-well plate format and has an upper multiplex capability of 50 SNPs per well, making it suitable for a moderate number of SNPs in a large number of samples. Two key modifications make this method less expensive and easier to perform than similar published methods. First, we use fewer beads than are traditionally used in quantitative Luminex assays [141-144]. The most significant expense of typical Luminex-based assays is the polystyrene beads used. Typical recommendations for SNP typing assays are to use 2500 input beads while counting 100 beads, but our experience indicates that these numbers can be substantially reduced, with a significant savings in cost per genotype.

Second, a universal biotinylated oligonucleotide is employed for signal quantification. For a biallelic SNP the OLA assay requires two allele specific oligonucleotides and a common oligonucleotide. Traditionally, the common oligonucleotide is labeled (during synthesis) with a detector molecule (i.e. biotin), which allows for quantification of the OLA product. In contrast, we synthesize the common oligonucleotide to have an attached sequence which is complementary to a universal oligonucleotide double-labeled with biotin, thus saving on the cost of synthesizing biotin-labeled common oligonucleotides for each SNP assay. In addition to being less expensive, the method

presented here does not employ typical wash or centrifugation steps, making it simpler to perform.

MATERIALS AND METHODS

Oligonucleotide primer and probe sets

The multiplex PCR primer selection program used in this study was an enhanced version of the program that was used to create 1000+ plex PCRs for parallel genotyping [145]. Amplicon size in multiplexed PCRs is generally below 400 base pairs, though we have successfully genotyped from amplicons as large as 1200 base pairs. PCR primers were ordered in 96-well plate format (IDT, Coralville, Iowa) and purified using standard desalting.

The OLA requires two allele-specific and one common probe for each SNP being assayed. Allele-specific probe pairs consist of a 5' tag sequence and a 3' locus specific portion which differs only at the terminal position of the probe. Each allele specific probe contains a unique 24-base FlexMAP™ tag (Luminex® Corporation, Austin, TX) at the 5' end to allow hybridization to a reverse complement anti-tag coupled to a unique FlexMAP™ microsphere. Common probes contain a locus specific portion at the 5' end, a universal capture sequence at the 3' end, and are 5' phosphorylated by the manufacturer (Integrated DNA Technologies, Coralville, IA). The universal capture sequence is the reverse complement of a doubly biotinylated "universal oligonucleotide" which is included in the bead hybridization step. For the universal capture sequence we employed the "tag" of FlexMAP™ bead 100 and the "universal oligonucleotide" sequence is the anti-tag of bead 100; for this reason, FlexMAP™ bead 100 is not utilized in our assays. All OLA probe sets are designed so that the locus-specific portion of both the common

and allele-specific probes have a melting temperature of approximately 64˚ C. Module 1 of the HyTher server was used to determine melting temperature (http://ozone3.chem.wayne.edu/). OLA probe sets were ordered in 96-well plate format and purified using standard desalting. All primer and probe sets are contained in **appendix 2**.

Genomic DNA Samples and Multiplex PCR Reaction

Samples previously genotyped in our laboratory were used in this study [146, 147]. Genomic DNA was isolated from whole blood or cell lines. All PCR reactions presented in this paper were fully multiplexed; for example, the 19 SNP assay presented involved a 19-plex PCR. We have performed as high as 40-plex PCR reactions (data not shown). Amplifications were performed in a solution (30 μl) containing 1.5 U AmpliTaq Gold DNA polymerase (Applied Biosystems); 1:10 dilution of 10X Buffer II (supplied with AmpliTaq Gold); 200 μM of each dNTP; 166 nM (5 pmol) of each primer; 2.5 mM MgCl; and 40 ng genomic DNA. Reactions were initially heated at 94 ˚C for 10 minutes, followed by 40 cycles of 94 ˚C for 40 seconds, 60 ˚C for 30 seconds, ramping from 60 ˚C to 65 ˚C using fifty 0.1 ˚C two second cycles, and 72 ˚C for 2 minutes. Reactions were completed at 72 ˚C for 10 minutes and 20 ˚C for 5 minutes. All reactions were performed in 96-well plates.

Oligonucleotide Ligation Reaction

All OLA reactions presented in this paper were fully multiplexed; for example, the 19 SNP assay presented involved a 19-plex OLA. We have performed as high as 40-plex OLA reactions (data not shown). OLA reactions were performed in a solution (15 μl) containing 20 mM Tris/HCl buffer pH 7.6; 25 mM KOAc; 10 mM MgOAc; 1 mM

NAD+; 10 mM DTT; 0.1% Triton X-100; 10 nM (150 fmol) of each OLA probe; 2 µl of multiplexed PCR product; and 3 U of Taq DNA ligase (New England Biolabs, Beverly, MA). Reactions were initially heated for 1 minute at 95 ˚C, followed by 32 thermal cycles of 95 ˚C for 15 seconds (denaturation) and 58 ˚C for 2 minutes (annealing/ligation). Reactions were then cooled to 4 ˚C, and were used immediately in the hybridization step or stored at -20 ˚C for up to 1 week before proceeding with the hybridization step. All reactions were performed in 96-well plates.

Hybridization of OLA Products to Microspheres and Universal Oligonucleotide

50 µl of TMAC hybridization solution (3 M tetramethylammonium chloride, 50 mM Tris-HCl, pH 8.0, 3 mM EDTA, pH 8.0, 0.10% SDS) containing 20nM (1000 fmol) of universal oligonucleotide and 200 beads (unless otherwise noted) from each FlexMAP™ microsphere set was added directly to a well containing a completed 15 µl OLA reaction. Note that TMAC hybridization solution should be warmed to 37 ˚C prior to use as the SDS falls out of solution at room temperature. Hybridization reactions were denatured at 95 ˚C for 90 seconds and hybridized at 37 ˚C for 20 minutes.

Fluorescent Labeling and Flow Cytometric Analysis

Following hybridization, 6 µl of TMAC hybridization solution containing 180 ng streptavidin-R-phycoerythrin (Molecular Probes – Invitrogen Corporation, Carlsbad, CA) was added directly to the well containing the hybridization reaction. Labeling reactions were incubated at 37 ˚C for 40 minutes. Care must be taken to avoid exposing SA-PE to excessive amounts of light. Unless otherwise noted, 20 of each FlexMAP™ bead included in the multiplexed assay were sorted and quantitated using a Luminex 100 or

Luminex 200 flow cytometer. The Luminex XY plate should be heated to 37 ˚C for the duration of bead sorting.

Figure 3.1: Overview of Luminex OLA assay. The assay consists of four steps: 1) multiplexed PCR, 2) multiplexed OLA, 3) hybridization with beads and SA-PE, and 4) detection using the Luminex flow cytometer. Steps 2–4 take place in the same 96-well plate.

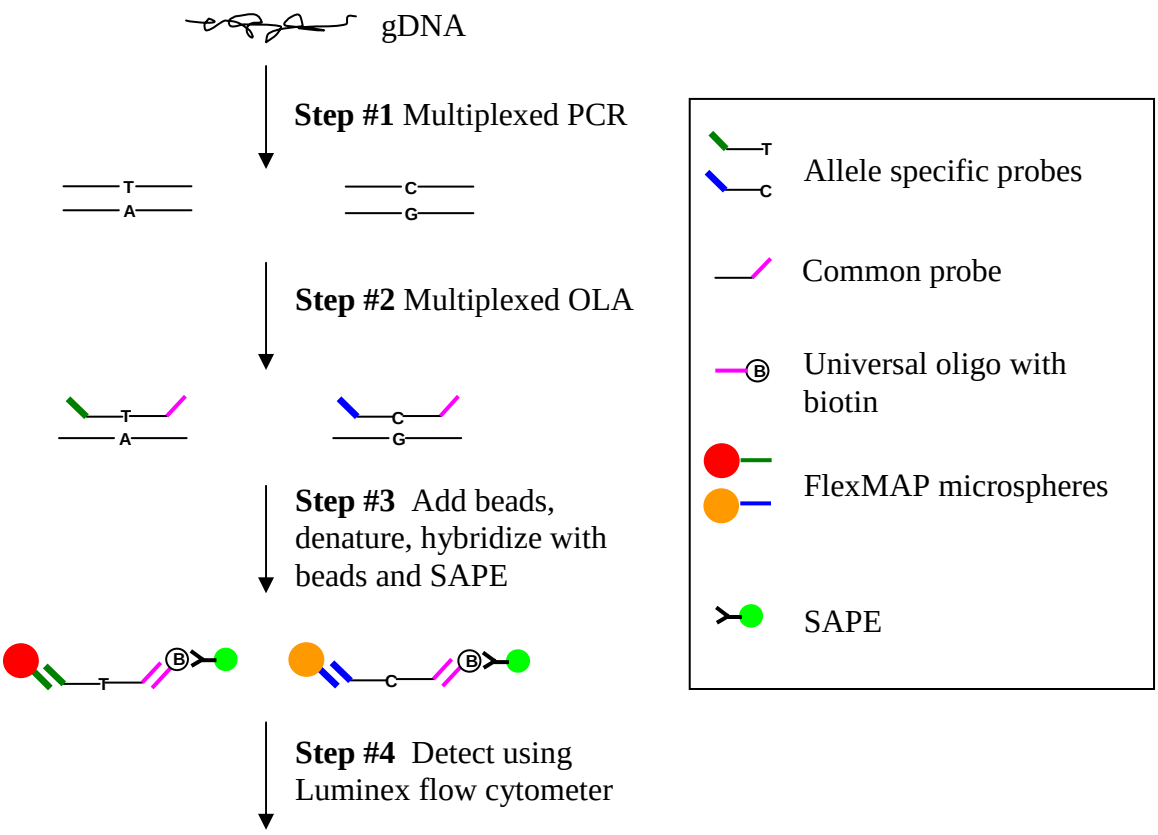

Direct sequencing and pyrosequencing

Semiautomated fluorescent direct sequencing was performed on the Beckman CEQ 8000 instrument. Pyrosequencing assays were performed as simplexed reactions on the automated PSQ HS96A platform [148, 149]. PCR primers were designed using Primer3 (Whitehead Institute) and the sequencing primer used for the Pyrosequencing assay was

designed using the Pyrosequencing SNP Primer Design Software v1.0. PCR reactions contained 40 ng of template DNA, 0.5 U Taq polymerase, 0.03 µM of each primer, 0.1 mM of dNTP, 3.0 mM of MgCl2, 50mM of KCl, 10mM of Tris—HCl (pH 9.0), and 0.1% Triton X-100 in a 20 µl volume. A touchdown amplification program was used. After 8 minutes at 95°C, 15 cycles were done at 94°C for 30 s, annealing for 20 seconds, and at 72°C for 20 seconds, with the annealing temperature starting at 60°C and decreasing by 0.5°C for each cycle. This was followed by 35 cycles at 94°C for 20 seconds, at 52°C for 20 seconds, at 72°C for 30 seconds, and then a final extension step at 72°C for 15 minutes.

Genotype calling for OLA/Luminex assay

A semi-automated method of assessing cluster quality and designating genotypes was applied to each SNP assay. Raw data is outputted as the median fluorescence intensity (MFI) for each allele. As an initial filter, data where neither allele has an MFI greater than 1000 (using the high PMT setting when calibrating the Luminex flow cytometer) were removed from analysis. This filter is based on our observation that the cluster quality (described below) decreases significantly for assays where the majority of MFI values for both alleles are below 1000. After this initial data cleaning step the raw data from both alleles was converted to a single number, the allelic ratio, as follows:

$$\frac{MFI\ (a_1)}{MFI\ (a_1 + a_2)}$$

Next, using the program Cluster 3.0 (http://bonsai.ims.u-tokyo.ac.jp/~mdehoon/software/cluster/software.htm) k-means clustering was applied to the allelic ratio to designate one of three genotypes [150]. The following settings were assigned in the Cluster 3.0 graphical user interface: (1) Organize genes (2) k = 3 (3) Iterations = 100 (4)

k-Means (5) Similarity metric = Euclidean distance. Resulting genotype assignments were then used to generate Silhouette scores for assessment of cluster quality [151]. SNP assays resulting in Silhouette scores less than 0.70 were considered failed assays when assessing conversion rate. As a final step, manual inspection of scatter plots was performed by expert technicians. Data points not clearly belonging to one of three clusters were considered failed genotypes when assessing call rates. For assessment of concordance with other SNP genotyping methods, all Luminex OLA calls were made blinded to the results obtained from those other methods.

RESULTS

As shown in **Figure 3.1**, the SNP genotyping assay can be divided into four steps: 1) multiplexed PCR, 2) multiplexed OLA, 3) hybridization/labeling 4) and detection using the Luminex flow cytometer. For an individual SNP the OLA involves a pair of allele specific primers and a 5' phosphorylated common primer, with tag and capture sequences utilized in downstream hybridization and labeling reactions. If an allele is present, Taq DNA ligase facilitates ligation between the allele specific and common oligonucleotides, using PCR product as a template. The OLA product is then simultaneously hybridized to FlexMAP™ beads and the universal oligonucleotide, followed by labeling with streptavidin-phycoerythrin (SA-PE). The Luminex flow cytometer is then used to sort the FlexMAP™ beads and quantitate the signal from each unique bead, thereby allowing determination of the absence or presence of each allele. Of note, different signal to noise ratios are achieved with different SA-PE conjugates. Five SA-PE conjugates were tested, one from Invitrogen/Molecular Probes and four from ProZyme (PJ31S, PJ70S, PJ35S,

PJ37S) with the best signal to noise ratio achieved with the Invitrogen/Molecular Probes SA-PE (data not shown).

Table 3.1: Inter-well CV and MFI range using low and high number of beads in control experiment.

200 input/20 count	**Positive control**	**Negative control**
Avg. inter-well CV	2%	26%
Avg. MFI*	21,968	192
MFI range	21,003-22,842	62-299
5000 input/300 count	**Positive control**	**Negative control**
Avg. inter-well CV	2%	20%
Avg. MFI*	22,619	162
MFI range	21,496-23,022	115-205

*Median fluorescence intensity (MFI) was assessed using the high PMT setting of the Luminex 100 flow cytometer. Inter-well CVs were calculated manually and are based on the median.

A control experiment was performed to demonstrate that counting as few as 20 beads allows one to distinguish a positive and negative population of beads. In order to mimic an OLA reaction, we used a synthesized OLA product as a positive control and unligated OLA probes as a negative control (see **appendix 2**). Sixteen replicate wells were assessed for each of four conditions: low beads/positive control, low beads/negative control, high beads/positive control, and high beads/negative control. Each of the four conditions was performed in a separate quadrant of the same 96-well plate, and positive and negative wells were alternated within each quadrant. **Table 3.1** shows that inter-well CVs and range of MFIs are very similar when counting 20 beads versus 300, and that positive and

negative MFIs differ by approximately an order of magnitude, providing a signal to noise ratio more than sufficient for accurate genotype calling. Importantly, inter-well CV and MFI were based on the median values obtained from each number of beads counted (20 or 300), and not the mean. Inter-well and intra-well CVs calculated using the mean were higher when counting low versus high number of beads (data not shown), likely due to a small percentage of bead carryover that occurs with the Luminex flow cytometer.

Table 3.2: Pyrosequencing concordance

SNP	concordant calls	% concordant
rs56387268	231/232	99.60%
rs1123005	287/289	99.30%
rs11806859	168/170	98.80%
rs12122048	58/58	100.00%
rs4657179	290/290	100.00%
rs4657187	167/168	99.40%
rs905720	263/264	99.62%
Total	**1464/1471**	**99.52%**

The Luminex-based OLA assay, using 200 input beads and counting 20, was compared to two other genotyping methods to assess validity (see **appendix 2**). First, eight SNPs were compared to direct sequencing in fourteen human DNA samples representing both homozygotes and heterozygotes, and concordance with direct sequencing was 100%. Second, a comparison was made between the multiplexed Luminex OLA and simplexed pyrosequencing. We compared 1471 genotypes from seven

SNPs (**Table 3.2**), and concordance between Luminex OLA and pyrosequencing was excellent, averaging 99.52%, with the lowest concordance for any SNP at 98.80 %.

Table 3.3: Call rates of technical replicates

Assay	call rate	% call rate
OLA 1 – PCR 1	670/672	99.7%
OLA 2 – PCR 1	672/672	100%
OLA 3 – PCR 2	671/672	99.9%
OLA 4 – PCR 2	672/672	100%
Total	**2685/2688**	**99.9%**

To assess robustness when counting 20 beads, replicate genotyping of an 8-plex assay was performed in 84 human genomic DNA samples (see **appendix 2**). Two separate PCR amplifications were performed, and an OLA was performed in duplicate on each PCR product, for a total of four OLA assays on the same 8 SNPs in the same 84 individuals. 2685 of 2688 genotypes were "callable", with a concordance of 100% between the 99.9% of genotypes that were callable (**Table 3.3**).

A 19-plex assay is presented in order to demonstrate typical results obtained from "first-pass" genotyping of 750 samples (see Supplementary Material – Primer and Probe Sets). Fifteen of nineteen assays were converted, with four failing due to the majority of MFI values falling below 1000. The approximately 80% conversion rate observed in this 19-plex assay is typical of the results observed across dozens of similar multiplexed panels, though more recent work indicates that this conversion rate can be increased by predicting nucleic acid interactions at the OLA step and carefully dividing multiplexed panels accordingly. **Figure 3.2** shows allelic ratios (Y-axis) plotted against samples (X-

axis) for the 15 working assays within the 19-plex assay. **Figure 3.3** shows representative raw data corresponding to the allelic ratios for four of the SNPs presented in Figure 3.2. **Table 3.4** gives the complete set of call rates and silhouette scores for the 15 working assays. 11,224 of 11,250 genotypes were callable (first-pass call rate 99.77 %), and the average silhouette score is >0.90.

Figure 3.2: Genotype clusters for 15-plex assay. Individual figures represent the allelic ratios (y-axis) produced from a first pass genotyping of 750 human genomic DNA samples (x-axis). Variability in allelic ratios is observed for different SNP assays, generally with skewing of heterozyote clusters, though homozygote clusters can also be skewed (i.e., rs9606240). Nonetheless, clusters are robust for each SNP genotype (see Table 3.4 for Silhouette scores).

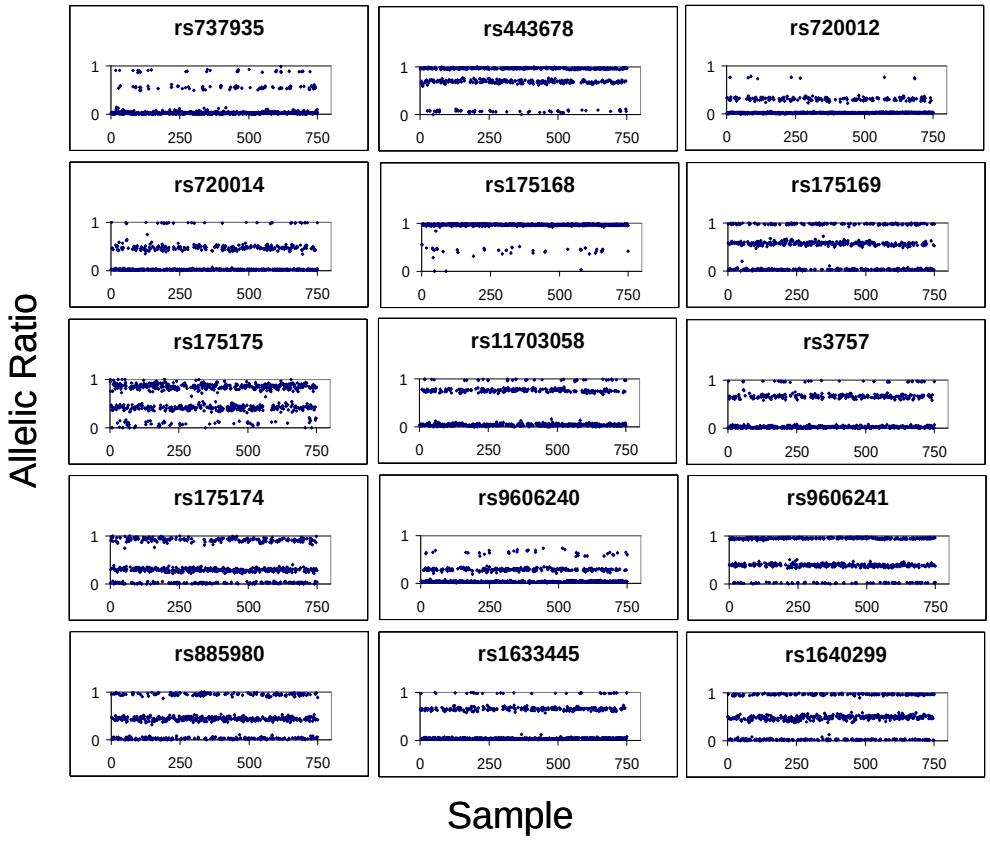

Figure 3.3: Raw data of 4 representative SNP assays. Each scatterplot represents the median fluorescence intensity (MFI) of allele 1 and allele 2 for four SNPs. The scatterplots represent the raw data from which allelic ratios (Figure 3.2) were calculated.

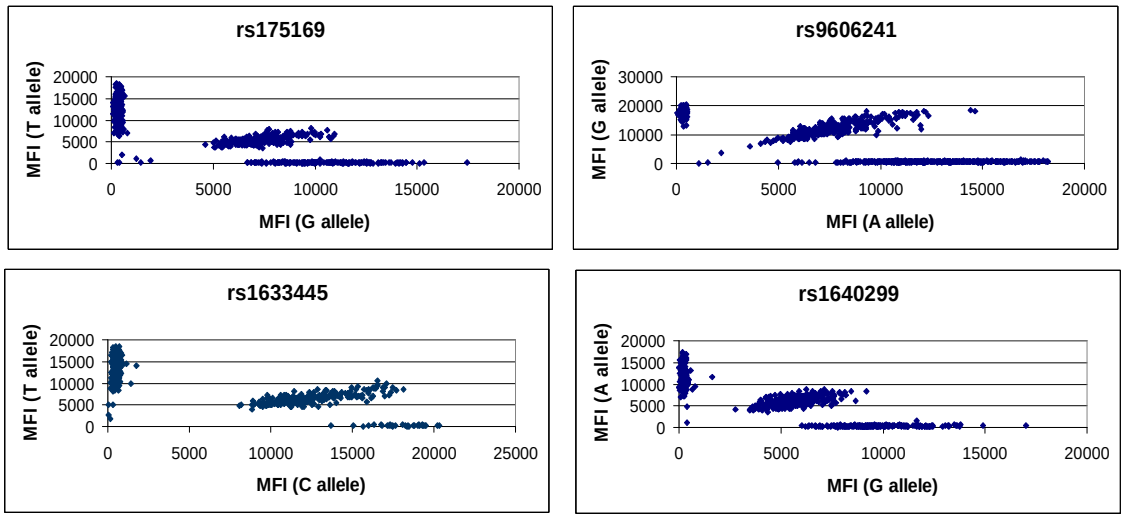

Table 3.4: Call rates and silhouette scores for 15-plex assay.

	Calls made	Percent callable	Silhouette score
rs737935	746/750	99.5%	0.938
rs443678	750/750	100.0%	0.932
rs720012	750/750	100.0%	0.876
rs720014	750/750	100%	0.916
rs175168	748/750	99.7%	0.914
rs175169	748/750	99.7%	0.942
rs175175	744/750	99.2%	0.777
rs11703058	748/750	99.7%	0.921
rs3757	749/750	99.9%	0.931
rs175174	745/750	99.3%	0.845
rs9606240	750/750	100.0%	0.821
rs9606241	750/750	100.0%	0.946
rs885980	746/750	99.5%	0.910
rs1633445	750/750	100.0%	0.952
rs1640299	750/750	100.0%	0.912
Total or average	**11224/11250**	**99.77%**	**0.902**

DISCUSSION

We have presented a method for multiplexed SNP genotyping on the Luminex platform that is accurate, robust, and significantly less inexpensive than previously published methods. Differences between this method and previously published Luminex-based methods include the use of significantly fewer beads, use of a universal biotinylated oligonucleotide for signal quantification, and no wash or centrifugation steps. We assessed concordance with both direct sequencing and pyrosequencing to establish validity, and observed 100% and >99% concordance respectively. Additional experiments with separate multiplexed assays demonstrated complete concordance across technical replicates and high call rates (>99%). Additionally, we presented a 19-plex assay in which 15 of 19 assays were converted. It should be noted that secondary SNPs within OLA probe binding sites can negatively impact conversion rates [139], and careful assay design requires knowledge of secondary SNPs. Cross-hybridization between nucleic acids present within single-tube, multiplexed OLA reaction can also reduce conversion rates (data not shown). Bioinformatics approaches which predict unwanted nucleic acid interactions could be used to rationally partition multiplexed OLA reactions and increase the conversion rate.

The cost is approximately $0.085 per genotype when performing both the PCR and OLA reactions in a 15-plex format (**Table 3.5**). The cost of other SNP genotyping methods is difficult to estimate, as innovations continue to drive down the cost of established methods and individual users find ways to achieve economies of scale. For example, while service-based TaqMan SNP genotyping costs are approximately $0.50 per genotype, advances in microfluidics are likely to significantly drive down this cost

(http://www.fluidigm.com/). In general, per genotype costs of $0.085 are on the low-end of informal estimates of other medium throughput genotyping technologies, and our method should be useful to academic labs on limited budgets as well to core facilities requiring flexibility in performing targeted genetic studies. While the PCR step of our assay is time consuming (5 hours) due to specialized cycling parameters required for the multiplexed PCR reaction, workflows can be established that result in approximately 40,000 genotypes per day. In practice, we perform multiple PCR and OLA reactions in parallel, and can then analyze one plate per hour on the Luminex flow cytometer, with each 96-well plate producing 4,800 genotypes when multiplexing at 50 SNP assays per well.

Table 3.5: Reagent costs per genotype. Calculations show the cost of each reagent per genotype generated. Cost of each reagent assumes that 15 SNPs are multiplexed at both the PCR and OLA steps; reagent costs decrease as multiplexing increases. Cost of PCR and OLA oligonucleotides assumes a sample size of 2000; oligonucleotide costs decrease as sample size increases, given that only a small portion of a typical OLA oligonucleotide order is utilized to genotype 2000 samples.

Reagent	Cost ($)
FlexMAP™ microspheres	0.0560
PCR + OLA oligos	0.0200
Taq DNA ligase	0.0030
SA-PE	0.0020
96-well plate	0.0030
Hybridization buffer	0.0002
Sheath fluid	0.0007
Total	**$0.0849**

For this study, a combination of k-means clustering, Silhouette scores, and manual inspection of raw data was used for genotype calling (outlined in Methods). While this provides a method for semi-automated genotype calling, k-means clustering requires manual inspection of the raw data to ensure that the algorithm arrives at a reasonable solution. In this study there were two SNPs for which k-means clustering resulted in genotype designations which clearly did not agree with visual inspection of scatterplots. It appeared in both cases that high density genotype clusters were incorrectly divided, a problem for k-means clustering that has been noted elsewhere [152]. In both cases, running the k-means algorithm multiple times eventually resulted in a visually "correct" solution. Alternatively, we found that we could resolve the problem by splitting data from 750 samples into two separate data sets containing allelic ratios from 375 samples each. Neither of these solutions are ideal and refinements to the clustering algorithm, such as careful seeding of k centers, may prove to be useful [153].

No reports directly assess the "bead count" issue when performing SNP genotyping assays on the Luminex platform. One previous report has assessed the variability in measurements when counting different numbers of beads using limiting amounts of SA-PE or analyte, and concluded that under the appropriate conditions counting as few as ten beads can distinguish two populations [154]. The appropriate conditions included a high amount of SA-PE (or analyte) relative to bead number. The conditions of our assay utilize massively saturating amounts of SA-PE (equivalent to 1.5 x 10^8 molecules per bead) and analyte, so it is not surprising that we can clearly and robustly distinguish two populations when counting as few as 20 beads (and perhaps less). Of note, run times on the Luminex flow cytometer are impacted by the number of input beads and the

proportion of those input bead one attempts to count. A typical 96-well plate assay using 5000 input beads (per well) and counting 100 beads has an approximately 30 minute run time, while using 200 input beads and counting 20 requires approximately 45 minutes; the degree of multiplexing does not dramatically affect run times. Issues of machine time-out begin to appear when trying to use less than 200 beads while still counting 20, or when trying to count more than 20 beads with only 200 input beads. Also, there may be a small percentage of well-to-well bead carryover using the Luminex flow cytometer. Using the median, rather than the mean, ensures that this carryover will not significantly affect the MFI and subsequent genotype calls when counting 20 beads. It is important to point out that we have only assessed using low bead counts for a qualitative, OLA SNP genotyping assay. In quantitative assays, where minimizing intra and inter-well variance is paramount, it may not be appropriate to use bead counts as low as 20. Using low bead counts may also not be appropriate for assays utilizing the direct hybridization format, where the non-target DNA strand will be available to compete with the probe-coupled microsphere for annealing to the target strand.

Chapter 4:

A Genetic Association Study of the MicroRNA Processing Gene DGCR8

ABSTRACT

Schizophrenia is a severe psychiatric disorder believed to be caused by a mixture of genetic, epigenetic, and environmental factors. A 3.1 Mb hemizygous deletion on chromosome 22q11.2 that causes DiGeorge syndrome is also one of the greatest known genetic risk factors for schizophrenia. Previous fine mapping studies identified a disease-associated haplotype block that encompasses the four closely positioned genes DGCR8, HTF9C, RANBP, and ZDHHC8. DGCR8 encodes a requisite cofactor in the biogenesis pathway of microRNAs, which are potent regulatory molecules that repress the expression of 20-30% of human genes. We hypothesized that genetic polymorphisms in DGCR8 are associated with schizophrenia spectrum disorders. We genotyped a panel of SNPs that span a 75 Kb region of chromosome 22q11.2, and performed family-based association testing in two independent collections of Caucasian pedigrees. Association analysis was performed using the Posterior Probability of Linkage Disequilibrium (PPLD). We did not observe evidence for association within the region. This suggests that common variants within DGCR8 are unlikely to contribute to schizophrenia etiology. Detailed mutation analysis and resequencing are needed to investigate possible rare mutations that alter DGCR8 expression or function in individuals with psychotic illness.

INTRODUCTION

Schizophrenia is a debilitating psychiatric disease affecting 0.5-1% of the world's population [155]. Heritability is high, estimated to be 80-85% [156], although this value reflects an average based on the as yet unknown mix of individual forms of schizophrenia. Despite evidence for a strong genetic component that contributes to disease etiology in schizophrenia, the results of genetic linkage and association studies have been inconsistent. However, meta-analyses have identified several linkage regions likely to contain susceptibility variants [157, 158], and promising candidate genes have emerged [159-162]. Chromosome 22q11 is one such region that has shown suggestive linkage in meta-analyses and independent studies [81, 157, 163-166].

Notably, 22q11.2 deletions associated with 22q11.2 deletion syndrome (22q11.2DS) are a major genetic risk factor for schizophrenia. 22q11.2DS, known also as velo-cardiofacial or DiGeorge syndrome, involves a common (1 in 4000 live births) hemizygous 22q11.2 deletion that results in a range of clinical phenotypes, including craniofacial anomalies and psychiatric disorders. 22q11.2DS increases the risk for schizophrenia about 25-fold, and the 22q11.2 deletion is present in approximately 1% of patients with schizophrenia, a 30-45-fold higher rate than in the general population [167, 168]. Although 22q11.2 deletions are observed in a small proportion of patients with schizophrenia, common variants of genes within this region may contribute to risk in non-deleted patients with schizophrenia.

The 22q11.2 deletion associated with 22q11.2DS is typically 3.1 Mb and encompasses ~40-50 genes, although deletions of smaller size are observed in a minority (~15%) of cases [169]. Genetic polymorphisms from a number of genes within the

deletion region - including COMT, TBX1, PICK4CA, PRODH, ZDHHC8, CLDN5, DGCR14, and DGCR2 - have been associated with schizophrenia in candidate gene studies (reviewed in [170, 171]). A fine mapping study of common variants in the proximal 1.5 Mb 22q11.2 deletion region identified two subregions that were positively associated with schizophrenia [172]. One of these subregions contained a disease-associated haplotype block that encompasses the four closely positioned genes examined in the current study (DGCR8, HTF9C, RANBP, and ZDHHC8).

DGCR8, a ~31.5 Kb gene encoding an RNA-binding protein necessary for proper maturation of microRNAs (miRNAs), is a particularly attractive schizophrenia candidate gene. miRNAs are small RNAs (~22 nucleotides) that regulate gene expression in a wide diversity of organisms by targeting mRNAs for translational repression or degradation [25]. Cell line knock-outs reveal that DGCR8 is necessary for processing the majority of, if not all, miRNAs [114]. Importantly, a recent study utilizing a mouse model demonstrated that haploinsufficiency of the DGCR8 gene leads to alterations in processing of specific subsets of microRNAs [173]. Additionally, this study identified neuronal and behavioral alterations consistent with changes observed in patients with schizophrenia [173]. Subtle alterations in miRNA expression levels can have profound effects on mammalian organ systems [174] and miRNAs are abundantly expressed in the developing and adult mammalian brain [7]. Of particular note, recent reports indicate misexpression of miRNAs in post-mortem brain samples from patients with schizophrenia [70, 71, 175].

In this study, we hypothesized that genetic polymorphisms in DGCR8 are associated with schizophrenia and/or schizophrenia spectrum disorders. Two distinct collections of

Caucasian pedigrees ascertained through a proband with a diagnosis of schizophrenia or schizoaffective disorder were used in this study. Given the prior (although inconsistent) evidence implicating ZDHHC8 in schizophrenia, we genotyped a panel of SNPs from a 75 Kb region of chromosome 22q11.2 that includes DGCR8, ZDHHC8, and the intervening genes HTF9C and RANBP1 (**Figure 4.1**). Additional genotyping and analysis was performed to account for updated intermarker LD data among common SNPs in the region.

Figure 4.1: TagSNPs in the chromosome 22 candidate gene region. This figure shows 17 tagSNPs spanning four genes in a 75 kb region on chr22q11.21. tagSNPs cover the entire region shown here, from 2 kb upstream of DGCR8 to 2 kb downstream of ZDHHC8. The SNP producing strong evidence of association to schizophrenia is numbered in red.

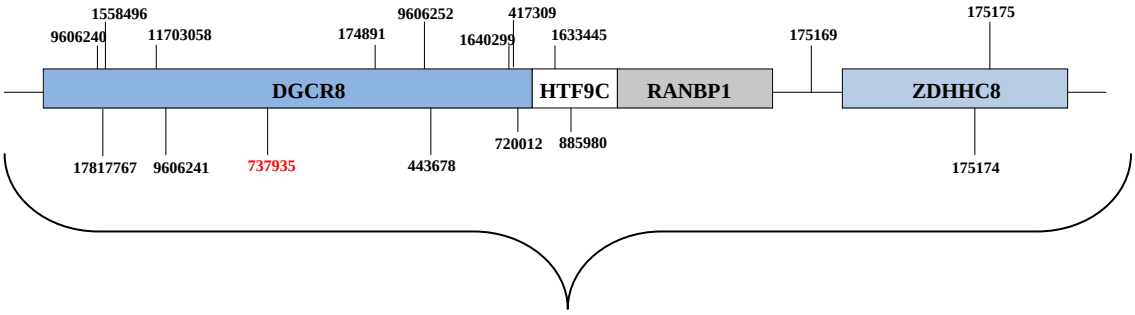

MATERIALS AND METHODS

Subjects

Two distinct samples of schizophrenia families were used for this study: (1) a sample selected from the NIMH Human Genetics Initiative (http://nimhgenetics.org/) schizophrenia collection and (2) a sample of Canadian subjects of northern European descent, selected for genetic study because multiple relatives were clinically diagnosed

with schizophrenia or schizoaffective disorder [82]. The two samples had important differences in ascertainment scheme, exclusionary criteria, and assessment battery.

NIMH Sample

The NIMH sample (277 families) was obtained from the National Institute of Mental Health (NIMH) Human Genetics Initiative. Families were selected from Schizophrenia Distribution 3.0. Caucasian pedigrees in this collection were ascertained from multiple independent sites as part of two large collaborative studies [176, 177], with probands and family members assessed using the Diagnostic Interview for Genetic Studies [176, 178, 179]. Families for both studies were recruited on the basis of at least two individuals meeting DSM-IIIR or IV criteria for schizophrenia or schizoaffective disorder. To reduce potential heterogeneity in the sample selected from this collection, families with multiple members exhibiting diagnoses that might result from other genetics risk factors were excluded from this study. Specifically, families with 1) two or more individuals with mental retardation, 2) two or more individuals with a psychotic mood disorder, or 3) three or more individuals with substance use disorders for substances other than alcohol, cannabis, or nicotine were excluded. Only families with at least one individual classified as affected under the defined phenotypes were selected for analysis.

Detailed data on the family structures and individual family members, including psychiatric diagnosis and other clinically relevant information, as well as lymphoblastoid cell lines and DNA, are stored, maintained and distributed by the NIMH Center for Genetic Studies. The specific families used for this study are listed in **appendix 3**.

.

Canadian Sample

The Canadian sample (24 families) consists of moderately large pedigrees of northern European ancestry previously used for a genome-wide linkage scan for schizophrenia susceptibility loci [180]. Families were recruited for study if schizophrenic illness appeared to be segregating in a unilineal (one side of the family only) autosomal dominant, manner. Direct interviews conducted with the Structured Clinical Interview for DSM-III-R (SCID-I) for major disorders and the SCID-II for personality disorders, collateral information, and medical records were used to make consensus diagnoses based on DSM-III-R criteria. Further details regarding ascertainment criteria and clinical diagnostic methods have been described previously [181, 182]. Although consisting of relatively few pedigrees, this sample has yielded statistically significant association results in other studies [146, 183]. Families with a history of bipolar disorder were excluded from this sample. This sample has been followed for up to 20 years, with the opportunity to longitudinally observe the stability of the diagnoses in the subjects.

Phenotype Definitions

Recent studies have demonstrated that diagnostic stability varies among psychotic illnesses, with high prospective stability for psychotic individuals initially diagnosed with schizophrenia (>90%) and bipolar disorder (>80%) [184, 185]. The diagnosis of schizoaffective disorder appears to be significantly less stable, with less than 20% of individuals retaining this diagnosis over the course of seven years, with the diagnosis equally likely to change to a diagnosis of bipolar disorder as to a diagnosis of schizophrenia [186]. While schizophrenia and schizoaffective disorder are often both included in a narrow definition of affection for genetic studies of schizophrenia

(including in our own prior work [146, 180, 183, 187]), many subjects in the NIMH sample were early in their illness and had not been followed longitudinally. Concerned about potential diagnostic instability in these subjects, we defined the following three categorical definitions of affection:

Narrow Schizophrenia: Subjects with a DSM-III-R or DSM-IV diagnosis of schizophrenia were classified as affected. Individuals were considered diagnosis unknown if they had schizoaffective disorder, major depressive disorder with psychotic features, bipolar disorder, brief psychotic disorder, delusional disorder, psychosis NOS, or paranoid, schizoid, or schizotypal personality disorder.

Broad Schizophrenia: Subjects with a diagnosis of schizophrenia or schizoaffective disorder were classified as affected. Individuals were considered diagnosis unknown if they had major depressive disorder with psychotic features, bipolar disorder, brief psychotic disorder, delusional disorder, psychosis NOS, or paranoid, schizoid, or schizotypal personality disorder.

Schizophrenia Spectrum: Subjects with a diagnosis of schizophrenia, schizoaffective disorder, brief psychotic disorder, delusional disorder, psychosis NOS, or paranoid, schizoid, or schizotypal personality disorder were classified as affected. Individuals were considered diagnosis unknown if they had major depressive disorder with psychotic features or bipolar disorder.

Individuals with dementia, mental retardation, autism spectrum disorders, organic mental disorders, or substance use disorders for substances other than alcohol, cannabis, or nicotine were always classified as phenotype unknown.

Table 4.1 presents descriptive statistics for each sample as well as the distribution of the categorical phenotypes within those families.

Table 4.1: Descriptive statistics of NIMH and Canadian samples by Phenotype.

	Narrow		Broad		Schizophrenia	
	NIMH	CAN	NIMH	CAN	NIMH	CAN
Informative Families[a]	259	24	274	24	277	24
Subjects with DNA	978	332	1042	332	1058	332
Total Subjects	1307	455	1687	455	1404	455
Number of Affected	452	69	521	85	568	134
Number Unaffected	361	192	392	192	398	192
Number Phenotype Unknown[b]	495	194	474	178	438	129
Unknown due to Substance Use	66	0	93	0	100	0

[a] Families with at least one individual affected under the diagnostic classification
[b] Includes individuals with no genetic or phenotypic data who are needed to link pedigree members with data

TagSNP selection

A set of tagSNPs was selected from the approximately 75 kb region from 2 kb upstream of the 5' end of DGCR8 to 2 kb downstream of the 3' end of ZDHHC8 (chr22:18,445,000-18,520,000; build 35) using the Tagger-pairwise tagging algorithm with an r^2 cutoff of 0.8 and a MAF cutoff of 0.02 and release 23a (Phase II, March 2008) of the HapMap CEU database. This identified a set of 18 tag SNPs. The sequence surrounding one SNP, rs9605069, was not amenable to conversion to a genotyping assay using the oligonucleotide ligation assay. While this SNP was in a singleton LD bin using an r^2 cutoff of 0.8, it is in strong LD with another SNP in the panel, rs11703058, at r^2 of 0.76. Therefore genotyping of rs9605069 was not pursued further and a final panel of 17 SNPs was used to tag this region (**Figure 4.1**). This set includes rs1633445 and rs175174, previously suggested to be associated with schizophrenia [188, 189].

Genotyping

The genotyping method was a bead-based, multiplexed oligonucleotide ligation assay (OLA) performed on a Luminex flow cytometer. Multiplexed PCR primer sets were designed to avoid spurious products [190]. The OLA requires two allele-specific and one common probe for each SNP being assayed. Allele-specific probe pairs consist of a 5' tag sequence and a 3' locus specific portion that differs only at the base-pair containing the SNP. Each allele specific probe contains a unique 24-base FlexMAP™ tag (Luminex® Corporation, Austin, TX) at the 5' end to allow hybridization to a reverse complement anti-tag coupled to a unique FlexMAP microsphere. Common probes contain a locus-specific portion at the 5' end, a universal capture sequence at the 3' end, and are 5' phosphorylated by the manufacturer (Integrated DNA Technologies, Coralville, IA). PCR and OLA reactions were conducted under the conditions described in Bruse et al. 2008 [191]. Multiplexed assays were sorted and quantified using a Luminex 100 or Luminex 200 flow cytometer. All primer and probe sequences are contained within **appendix 3**.

Statistical analysis and error checking

Genotypes were checked for Mendelian errors using the program PEDCHECK (version 1.1) [192], for unlikely genotypes based on recombination using the program SIMWALK2 (version 2.91) [193], and for departures from Hardy-Weinberg Equilibrium with PEDSTATS (version 0.6.12) [194] . Genotypes identified as potential errors were re-genotyped, and genotypes were removed for individuals involved in unresolved Mendelian errors for a given marker (0.2% of total genotypes). Marker allele frequencies

were estimated using MENDEL (version 7.0) [195]; Minor allele frequencies for each SNP in each sample are given in **Table 4.2**.

In this study, genetic association analysis was performed using the posterior probability of linkage disequilibrium (PPLD), an extension of the posterior probability of linkage (PPL) method of Vieland [196] as implemented in the program KELVIN (version 0.37.5) [197]. The PPL assesses the evidence for linkage and LD and estimates LD between the SNP marker and the disease phenotype [196]. The PPL was developed as a Bayesian alternative to traditional linkage analysis [198, 199]. The PPLD integrates over the trait parameters, rather than maximizing over them or fixing them at specific values. It also makes full use of all pedigree data. It intrinsically measures LD due only to close physical proximity (or perhaps epistasis), and it has been shown to be robust to departures from Hardy Weinberg equilibrium at the marker [200].

In computing the usual form of the PPL, the prior probability of linkage is set to 2% based on theoretical calculations [201]. For comparability of scale, therefore, we also set the prior probability of LD given linkage to 2% (so that the joint prior probability of linkage and linkage disequilibrium is just 0.04%). Values of the PPLD < 2% therefore represent evidence against LD in the presence of linkage, while values > 2% indicate evidence in favor of LD in the presence of linkage. As with any form of the PPL, the PPLD has a direct interpretation as a probability: a PPLD of 25% can be interpreted in the same way as a 25% probability of rain, or winning a bet, or of a successful medical intervention.

The PPLD applies to one SNP at a time (two-point analysis) and measures the evidence for or against LD to that SNP. As a measure of evidence, the PPLD does not

require "correction" for multiple testing, any more than measurements of length for various pieces of rope would require "correction" as a function of the number of pieces measured. On the other hand, the very small prior probability implicit in the calculation effectively adjusts for the biological fact that even at a linked locus, any given SNP may have only a very small chance of exhibiting LD.

RESULTS

An initial set of seventeen tag SNPs from a 75 kB region on chromosome 22q11.2 containing the genes DGCR8, HTF9C, RANBP1, and ZDHHC8 (**Figure 4.1**) were genotyped in both samples (NIMH and Canadian) and evaluated for evidence of linkage disequilibrium (**Table 4.2**). All of the SNPs tested produced either no evidence for or against association (PPLD = 2%) or evidence against association (PPLD < 2%) in the NIMH sample for all phenotypes, with the exception of rs175169 which produced small PPLD scores ranging from 2.2% to 4% (**Table 4.2**). In the Canadian sample all SNPs tested produced evidence against association under all three phenotypes.

Approximately 10-15% of subjects in the NIMH families selected for study were classified as phenotype unknown instead of as affected due to comorbid substance use disorders. To determine the potential effect of excluding the phenotypes of these subjects from our analysis, we modified the Narrow Schizophrenia phenotype definition to remove the substance use exclusion and recalculated the PPLD results. This change converted 51 subjects previously coded as phenotype unknown to affected, but no increased evidence of association was detected.

Table 4.2: Posterior Probability of Linkage Disequilibrium (PPLD) Results.

	Build 36.1	Minor Allele Freq		Narrow Schizophrenia		Broad Schizophrenia		Schizophrenia Spectrum	
SNP	bp position	NIMH	CAN	NIMH	CAN	NIMH	CAN	NIMH	CAN
rs9606240	18,451,423	0.22	0.25	0.016	0.016	0.018	0.016	0.018	0.016
rs17817767	18,451,630	0.04	0.04	0.017	0.018	0.018	0.018	0.018	0.019
rs1558496	18,451,737	0.28	0.25	0.016	0.014	0.020	0.013	0.019	0.013
rs11703058	18,455,048	0.21	0.23	0.016	0.016	0.018	0.016	0.018	0.016
rs9606241	18,455,858	0.32	0.29	0.014	0.016	0.018	0.016	0.017	0.016
rs737935	18,462,570	0.08	0.02	0.015	0.018	0.015	0.018	0.016	0.018
rs174891	18,469,751	0.06	0.10	0.015	0.017	0.016	0.017	0.016	0.015
rs9606252	18,472,996	0.22	0.24	0.016	0.014	0.018	0.014	0.018	0.013
rs443678	18,473,126	0.27	0.32	0.016	0.015	0.014	0.016	0.014	0.016
rs1640299	18,478,359	0.50	0.45	0.016	0.014	0.016	0.013	0.016	0.014
rs417309	18,478,544	0.09	0.11	0.015	0.017	0.016	0.017	0.015	0.016
rs720012	18,478,582	0.13	0.11	0.018	0.016	0.017	0.017	0.016	0.015
rs1633445	18,480,596	0.22	0.22	0.014	0.018	0.013	0.017	0.013	0.017
rs885980	18,482,090	0.45	0.39	0.020	0.016	0.018	0.016	0.017	0.016
rs737871	18,485,641	0.06	0.01	0.014	0.019	0.016	0.018	0.016	0.019
rs175169	18,497,345	0.41	0.38	0.040	0.017	0.022	0.017	0.022	0.018
rs175174	18,507,554	0.44	0.36	0.016	0.015	0.015	0.016	0.014	0.015
rs175175	18,508,651	0.28	0.37	0.015	0.015	0.014	0.015	0.014	0.015

DISCUSSION

In this study seventeen tag SNPs spanning four genes (75 kb total) located within a 22q11DS sub-region were genotyped and analyzed for LD with schizophrenia, schizoaffective disorder, and schizophrenia spectrum disorders. The full 3Mb 22q11DS region contains 40 to 50 protein coding genes, and has been implicated in markedly increased risk for schizophrenia and other psychiatric disorders [202]. Our findings fail to provide evidence for LD between the DGCR8 gene and schizophrenia, suggesting that common variants are unlikely to contribute to disease. We were also unable to confirm the two reported associations [172, 188] between ZDHHC8 and schizophrenia in either of

our samples. Our negative findings with respect to schizophrenia and schizoaffective disorder are consistent with those reported by a number of other groups [203-208].

Our analyses evaluated evidence for association using the posterior probability of linkage disequilibrium framework, a relatively new method. The PPL was originally developed as an alternative to traditional linkage analysis [209, 210], and has undergone continuous development over the past decade (see [211]), including extension to the testing of LD [212]. The PPLD has several key advantages over other approaches to testing for association. First, the PPLD directly measures the probability of LD, in stark contrast to p-values. As it is on the probability scale (0,..,1), it can be readily interpreted in the same way as any other probability. Second, unknown trait parameters are integrated out of the model, rather than maximized over or fixed at arbitrary values. This means that, although the PPLD is "model-based," it does not assume any particular trait model, and it retains the same scale even as new parameters are added to the model, unlike maximized statistics which must be adjusted for additional 'degrees of freedom.' Third, the PPLD measures evidence against, as well as in favor of, linkage disequilibrium. Thus the PPLD distinguishes between data that are merely failing to support LD and data that are actually providing support against LD, very different from p-value based methods. This feature is clearly illustrated by **Table 4.2** of our results, where the data produced evidence against involvement of most of the tested SNPs.

In this study, a thorough tagging strategy was employed using intermarker LD data from the HapMap database. Importantly, only validated SNPs with minor allele frequencies greater than 2% in the CEU sample were included. Thus, the study was restricted to common genetic variants present throughout the population. This negative

association finding, combined with the severe phenotypic consequences of a hemizygous deletion, seem to underscore the importance of genes within this critical region. Even though common genetic variants failed to show association, this does not preclude the possibility of rare, private mutations in individuals with psychotic illness.

In conclusion, this study represents negative evidence for association of the DGCR8 gene - a gene involved in miRNA biogenesis - with psychiatric disorders. A previous report has identified misexpressed miRNAs in post-mortem samples from patients with schizophrenia and schizoaffective disorder [71]. Through a comparison of the expression of intronic miRNAs and the mRNAs in which they are located, Perkins et. al. [71] hypothesized that altered biogenesis of miRNAs might be responsible for the miRNA misexpression that was observed in their study. A later study has provided compelling *in vivo* evidence linking DGCR8 haploinsuffiency to altered miRNA processing and behavioral and neuronal phenotypes relevant to schizophrenia [173]. However, the findings of our genetic study indicate that common polymorphisms within DGCR8 are unlikely to contribute to the etiology of schizophrenia and schizoaffective disorder. It is possible that rare, undiscovered mutations may alter the function or expression of DGCR8, leading to altered expression of miRNAs in the developing and/or adult brain of patients with schizophrenia. Comprehensive mutation analysis using a deep resequencing approach is required to evaluate this possibility.

Chapter 5: Altered microRNA expression profiles in post-mortem brain samples from individuals with schizophrenia and bipolar disorder

ABSTRACT

MicroRNAs (miRNAs) are potent regulators of gene expression with proposed roles in brain development and function. We hypothesized that miRNA expression profiles are altered in individuals with severe psychiatric disorders. Using quantitative real-time PCR, we compared the expression of 435 miRNAs and 18 snoRNAs in post-mortem brain tissue samples from individuals with schizophrenia, individuals with bipolar disorder, and psychiatrically healthy control subjects (n = 35 each group). Detailed demographic data, sample selection and storage conditions, and drug and substance exposure histories were available for all subjects. Bayesian model averaging was used to simultaneously assess the impact of these covariates as well as the psychiatric phenotype on miRNA expression profiles. Of the variables considered, sample storage time, brain pH, alcohol at time of death, and post-mortem interval were found to affect the greatest proportion of miRNAs. 19% of miRNAs analyzed exhibited positive evidence of altered expression due to a diagnosis of schizophrenia or bipolar disorder. Both conditions were associated with reduced miRNA expression levels, with a much more pronounced effect observed for bipolar disorder. This study suggests that modest under-expression of several miRNAs may be involved in the complex pathogenesis of major psychosis.

INTRODUCTION

Schizophrenia and bipolar disorder are severe psychiatric conditions for which disease pathophysiology is still poorly understood. The association of psychotic features with severe mood disorders, combined with recent genetic insights, suggests that schizophrenia and bipolar disorder are etiologically related [213]. Though highly heritable, the complex pathogenesis of major psychosis may involve dozens of genes, as well as epigenetic and environmental factors (reviewed in [76]). Positional cloning strategies have traditionally focused on protein coding genes within established linkage regions for fine mapping of disease susceptibility loci. Difficulties in identifying susceptibility genes in some regions suggest that candidate gene studies should be expanded to include other elements beneath linkage peaks, such as non-coding RNA genes.

In the last decade, the discovery of small non-coding RNAs (sncRNAs) has unveiled a new layer of gene expression regulation. MicroRNAs (miRNAs) comprise a growing class of endogenous molecules that regulate gene expression post-transcriptionally. By binding to partially complementary regions at the 3' end of messenger RNAs, these ~22 nucleotide single-stranded molecules direct target site recognition by the macromolecular RNA-induced silencing complex (RISC). The RISC complex induces cleavage or translational repression of targeted transcripts. Based on a widely accepted and highly empirical framework of miRNA-target interactions, several independent studies predict that 20-30% of human genes are regulated by miRNAs [214, 215], but a sensitive pattern-based target prediction algorithm boosts this estimate considerably to 74-92% of genes [2].

The majority of miRNA genes occur in tandem, operon-like clusters that form polycistronic transcripts. Most miRNAs fall within intergenic regions or within the introns of protein-coding genes [216]. Mammalian miRNA biosynthesis begins with RNA polymerase II-dependent transcription, which yields long primary miRNA (pri-miRNA) transcripts [7]. While intronic miRNAs may be coincidentally transcribed with their host gene, the nature of intergenic pri-miRNA transcription has only recently been investigated [217]. Thorough sequence analysis and annotation of transcription start sites, transcription factor binding sites, and other regulatory elements suggest that most intergenic primary miRNA transcripts are 3-4 kb in length [32].

Enrichment of predicted miRNA target sites within brain-expressed mRNAs [39], as well as emerging functional evidence, suggests that miRNAs serve important neurobiological roles. Approximately 70% of known miRNAs are expressed in the nervous system, often with a high degree of spatial and temporal specificity [51]. A survey of miRNA expression patterns in various organ and tissue types identified several brain-specific and brain-enriched miRNAs, many of which were up-regulated in embryonal carcinoma cells induced to adopt a neural cell fate [52]. Additionally, miRNA profiling of the developing and adult mouse brain revealed a “chronological wave” of expression [54]. Thus, the appearance of sequentially expressed groups of miRNAs may correlate with the onset of neurodevelopmental processes, such as neuronal proliferation and migration, neurite growth, and synaptogenesis. The global developmental impact of miRNAs has been evaluated in model systems by knocking out essential factors in the miRNA biosynthetic pathway. Genetic ablation of Dicer1, a gene involved in the second enzymatic processing step of miRNA biogenesis, results in early embryonic lethality in

mice, seemingly caused by defects in cell proliferation and maintenance of stem cell populations [55]. In other mouse models, generation of conditional alleles that bypass this early requirement for Dicer reveal that miRNAs are essential for limb morphogenesis but dispensable for axis formation and patterning [56]. In zebrafish Dicer knockouts, elimination of mature miRNAs produced gross morphological abnormalities in the nervous system [57]. While miRNA ablation results in profound defects in morphogenesis, abolishing hundreds of regulatory molecules and derepressing thousands of targets has remarkably subtle phenotypic effects on cell differentiation and patterning. With a few notable exceptions, miRNAs may act primarily to fine-tune transcriptional programs in a cell- or tissue-specific manner, rather than serving a wide-spread obligatory function [95].

Altered expression of miRNAs in post-mortem brain samples from individuals with schizophrenia has recently been reported [71]. Additionally, miRNA genes within established schizophrenia susceptibility loci have been investigated using genetic association coupled with expression analysis [218]. In the present study, we have performed miRNA expression analysis of 435 miRNAs and 18 small nucleolar RNAs (Sanger miRBase v9.2) using TaqMan® real-time PCR methodology. Expression signatures were obtained from post-mortem brain samples originating from individuals with schizophrenia, individuals with bipolar disorder, and psychiatrically healthy controls. Sample covariates pertaining to demographic variables, sample handling, and substance exposure history were assessed in a statistically rigorous manner.

MATERIALS AND METHODS

Post-mortem brain tissue samples

A set of samples from individuals with schizophrenia, bipolar disorder, and psychiatrically normal controls were obtained from the Stanley Medical Research Institute. This collection contains many more individual subjects than is typical for post-mortem studies of human brain (n=35 each group), and the samples were collected and stored in a standardized fashion with an emphasis on obtaining high-quality RNA for expression studies. Employing DSM-IV criteria, diagnoses were made by two senior psychiatrists using medical records and, when necessary, telephone interviews with family members. Diagnoses of unaffected controls were based on structured interviews by a senior psychiatrist with family member(s) to rule out Axis I diagnoses. Specimens were collected, with informed consent from next-of-kin, by participating medical examiners between January 1995 and June 2002. Exclusion criteria for all specimens included: 1) significant structural brain pathology on post-mortem examination by a qualified neuropathologist, or by pre-mortem imaging; 2) a history of significant focal neurological signs pre-mortem; 3) a history of central nervous system disease that could be expected to alter gene expression in a persistent way; 4) a documented IQ < 70; or 5) Poor RNA quality. Additional exclusion criteria for unaffected controls included an age less than 30 (thus, still in the period of maximum risk) and substance abuse within one year of death or evidence of significant alcohol-related changes in the liver. Expression analyses were conducted with the samples coded to keep investigators blind to diagnostic status. After the blind was broken, diagnostic status and a range of clinical variables were provided for analysis. These included gender, race, age at time of death, age of

onset, post-mortem interval (PMI), brain pH, total brain weight, hemisphere used for RNA extraction, smoking status at time of death (coded as non-smoking for individuals who smoked previously but had quit), antipsychotic status at time of death, and lifetime antipsychotic exposure in fluphenazine milligram equivalents. In addition, lifetime alcohol and substance use were each rated on a scale of 0 to 5 using the categories "little or none", "social", "moderate past", "moderate present", "heavy past", and "heavy present". Total sample storage time was calculated from date of death to date of experiment, and so represents the sum of storage time of the brain tissue prior to RNA extraction and storage time of the extracted RNA. Overall, the sample set was 66% male, with a mean age at death of 44 years (S.D. 8.9, range of 19 to 64), and was predominantly Caucasian (97%). The mean PMI was 33 hours (S.D. 16, range of 9 to 84), and the mean storage time was 8.0 years (S.D. 1.9, range of 5.1 to 12.7). Smoking status at time of death was available for 67 subjects, with 72% of the sample smokers. Lifetime alcohol use estimates were available on all but one subject, with 57% of the sample reporting no, little, or social use, 17% reporting past or present moderate use, and 26% reporting past or present heavy use. Lifetime substance use estimates were available on all but two subjects, with 65% of the sample reporting no, little, or social use, 16% reporting past or present moderate use, and 19% reporting past or present heavy use. The mean age of onset for the schizophrenia group was 21.3 years (S.D. 6.1, range of 9 to 34) and for the bipolar group was 25.1 years (S.D. 9.1, range of 14 to 48). Further information about the Stanley Array Collection is available from the Stanley Medical Research Institute (http://www.stanleyresearch.org).

Purification of RNA from tissue samples

Frozen tissue samples originating from Brodmann area 9 (BA9) of the prefrontal cortex were obtained from the Stanley Medical Research Institute, and total RNA extractions were performed using the *mir*VANA miRNA Isolation Kit (Ambion, Austin, TX). 300-500 mg sections of frozen tissue were added to 3 mL of chilled RNALaterICE (Ambion) and stored at -20°C for a minimum of 16 hours. To prepare samples for RNA purification, RNALaterICE was decanted, and the tissue sample lightly blotted to wick away excess RNALaterICE. Next, 3mL of chilled *mir*Vana lysis buffer was added to the tissue and the tissue homogenized with a Fisher PowerGen 35 handheld homogenizer. The *mir*Vana miRNA isolation kit was used to purify total RNA from a 750 µL aliquot of lysate. Yield and purity were determined using a NanoDrop ND-1000 spectrophotometer.

Real-time quantitative PCR

Real-time qPCR was performed using the TaqMan® (Applied Biosystems) single tube human miRNA assay panel (Sanger miRBase v9.2). Multiplexed RT reactions were performed using the TaqMan® MicroRNA Reverse Transcription Kit (Applied Biosystems). Compatible 8-plexed RT primer pools were selected as subsets of the manufacturer recommended 48-plexed RT pools (Applied Biosystems, Human Multiplex RT Pools 1-8 v1.0). For a 1X reaction, cDNA synthesis was performed in a solution (20 µL) containing 2.0 mM dNTPs (0.50 mM each), 200 U MultiScribe Reverse Transcriptase, 2 µL 10x RT Buffer, 5 U RNase Inhibitor, 0.35 µL nuclease-free water, 12 nM each stem-loop RT primer and 50 ng input RNA. Reactions were incubated in a PTC-200 Thermal Cycler (MJ Research) in 96-well format for 30 min at 16˚C, 30 min at 42˚C, 5 min at 85˚C, and then held at 4˚C. Real-time PCR reactions were performed using

TaqMan® single tube microRNA assays (Applied Biosystems). Reactions were performed in solution (5 μL) containing 1.5 μL nuclease-free water, 2.5 μL TaqMan® Universal PCR Master Mix (No AmpErase UNG), 0.25 μL assay-specific 20x probe/primer mix, and 0.75 μL RT product (1:20 dilution). Reactions were incubated in 384-well format at 95˚C for 10 min, followed by 40 cycles of 95˚C for 15 s and 60˚C for 1 min. All reactions were carried out in quadruplicate using a 7900HT Real-Time PCR System (Applied Biosystems). Pipetting operations were performed using a JANUS® Automated Workstation (Perkin Elmer) to ensure accuracy and reproducibility of relative expression data.

Control RNAs for normalization of miRNA expression

Evaluation of putative internal control genes requires prior knowledge of a stably expressed housekeeper, thus creating a circular problem. One way to solve this problem is to utilize non-normalized expression data, by relying on the principle that the expression ratio of two ideal control genes should be identical from sample to sample. The expression of a set of putative housekeepers can be measured across a number of samples, and the average expression stability, *M*, can be determined. *M* is defined as the average pair-wise variation of a particular gene with all other control genes. Thus a lower *M* score denotes a more stable control gene. This procedure (implemented in the GeNorm analysis software) is a common method used to assess the suitability of putative housekeeping genes as normalization controls [219].

To identify stably expressed control genes in BA9 of the prefrontal cortex, 16 samples representing all three diagnostic categories (schizophrenia, bipolar, control) were randomly selected from the total sample set. GeNorm analysis was used in conjunction

with TaqMan® expression assays to evaluate a panel of small nucleolar RNAs. 150ng of total RNA from each of the 16 samples was subjected to two-step RT-PCR as previously described. The 16 samples were divided into two groups of 8 so that the RT and PCR reactions were performed separately for each group, resulting in a replication of the GeNorm analysis. Based on results of the GeNorm analysis, RNU24, RNU48 and RNU44 were used to normalize expression data from the Stanley samples. Relative expression analysis was performed using the $2^{-\Delta\Delta CT}$ method [109].

Statistical analysis of miRNA expression

Three samples were removed from the statistical analysis due to poor RNA quality or yield following the RNA extraction, and one additional sample was excluded due to organic brain pathology. Statistical analysis was performed using 35, 33, and 33 samples from the schizophrenia, control, and bipolar groups, respectively. Because of concerns that sample covariates may have affected detected expression levels, Bayesian model averaging (BMA) was used to simultaneously assess the impact of these covariates as well as psychiatric diagnosis on miRNA expression profiles. BMA averages over many regression models, using weights equal to the estimated probability of those models, and achieves better predictive performance than use of a single statistical model [220]. Because some covariates were missing for some samples, ten distinct imputations of covariates were created [221]; missing miRNA expression values (35 total) were not imputed, and were left as missing. The analysis was performed with miRNA expression levels transformed to the $\log_2$ scale.

Bayesian simultaneous variable selection and outlier identification was used to determine outliers in miRNA expression levels via Markov Chain Monte Carlo model

composition [222]. The regression analyses were also run with no automatic outlier detection. miRNAs for which either of the analyses gave greater than 90% posterior probability of non-zero diagnosis coefficients were checked manually for outliers; that determination was used for the final analysis. There were a total of 269 automatically detected outliers, an average of just over one per miRNA, and there were 49 individuals with no outliers at all. Outlier detection was based on a regression model including the following set of covariates in addition to diagnosis: age, sex, brain pH, brain hemisphere, lifetime alcohol use, lifetime drug use, time of death (TOD) alcohol use, TOD drug use, smoking at TOD, mood stabilizer at death, antidepressants at death, anticholinergics at death, reaction plate, storage, refrigerator interval, post-mortem interval (PMI), and brain weight. With outliers removed, the same set of covariates was used in a reiterated BMA procedure and results averaged over the 10 covariate imputations.

RESULTS

The superior sensitivity of TaqMan® assays allows detection of miRNAs that are expressed at less than one copy per cell. Only 9 out of 435 assayed species produced a detection signal that was indistinguishable from background. However, when approaching the limit of detection, the standard deviation in measured expression values across technical replicates dramatically increases due to random sampling error. Therefore, quantitative analysis was restricted to 234 miRNAs and 18 snoRNAs that produced mean Ct values ≤ 34. 10 miRNAs accounted for greater than 66% of total miRNA expression (**Figure 5.1**). Those species found to be highly expressed included several ubiquitously expressed let-7 family members (let-7b, let-7c, and let-7g) as well as miRNAs previously classified as brain-enriched (miR-125b).

Figure 5.1: Highly expressed miRNAs in the adult human brain. Expression levels are presented as a proportion of total miRNA expression.

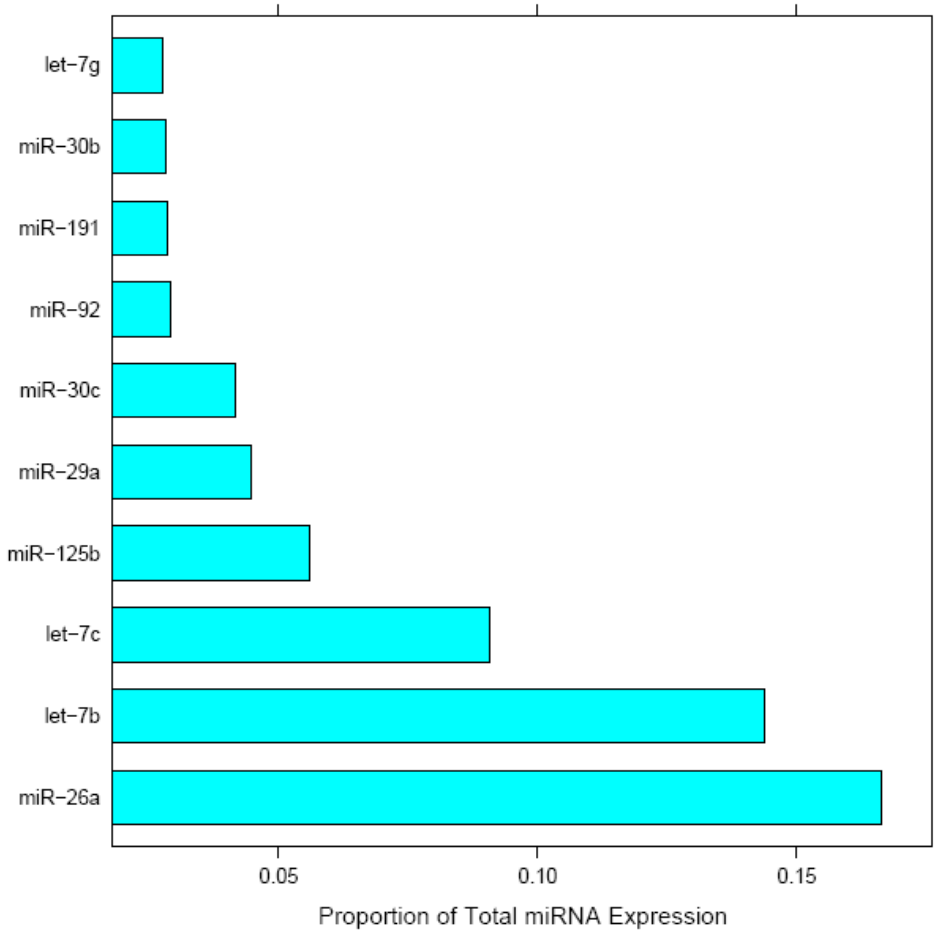

Bayesian model averaging (BMA) was used to assess the degree to which psychiatric diagnosis as well as sample covariates influence miRNA expression profiles. The regressions implemented through BMA revealed that for most miRNAs, sample covariates accounted for only a small proportion of the variation. The increase in the coefficient of determination R^2 (which measures the proportion of variability in the data accounted for by the models) over a model incorporating only plate effect ranged from 0 to 0.3. BMA yields posterior probabilities that a given variable has a nonzero regression

coefficient, as well as distributions for each regression coefficient. A common interpretation of the posterior probabilities in this context is that a posterior probability less than 50% gives no evidence that the variable affects expression, 50% to 75% is weak evidence, 75% to 95% represents positive evidence, 95% to 99% represents strong evidence, and a posterior probability greater than 99% represents very strong evidence [223]. Of all sample covariates considered, storage, brain pH, alcohol at TOD, and post-mortem interval influenced the expression of the greatest proportion of miRNAs (25%, 18%, 9%, and 8%, respectively, showing positive evidence) (**Table 5.1**).

Table 5.3: Posterior probabilities of covariate inclusion. Values in cells indicate the percentage of analyzed miRNAs for which the posterior probability of a non-zero covariate effect falls into the bin in the column heading.

Covariates	[0,75]	(75,95]	(95,99]	(99,100]
Diagnosis	81	7	2	10
Age	95	2	0	2
Sex	99	1	0	0
Brain PH	82	9	4	5
Brain Hemisphere	99	0	1	0
Lifetime Alcohol Use	100	0	0	0
Lifetime Drug Use	99	1	0	0
TOD Alcohol Use	91	5	1	3
TOD Drug Use	100	0	0	0
Smoking at TOD	100	0	0	0
Mood Stabilizer at death	99	0	1	0
Antidepressants at death	97	2	1	0
Anticholinergic at death	100	0	0	0
Storage	75	10	2	13
Refrigerator Interval	100	0	0	0
PMI	92	5	1	2
Brain Weight	100	0	0	0

According to the above significance thresholds, 19% of miRNAs analyzed exhibited positive evidence of altered expression based on diagnostic classification, with 12% showing strong or very strong evidence. miRNAs with posterior probabilities of a nonzero diagnostic effect greater than 95% are listed in **Table 5.2**. None of the identified miRNAs are among the most highly expressed miRNAs in the adult prefrontal cortex, but are instead expressed at intermediate or modest levels. None of the listed miRNAs arise from genomically proximal hairpins, suggesting that transcriptional co-regulation is unlikely. Only two of the misexpressed miRNAs, miR-193a and miR-193b, are closely related family members with nearly identical sequences.

Table 5.4: Misexpressed miRNAs. miRNAs having greater than 95% posterior probability of non-zero effect of psychiatric diagnosis are listed, along with chromosomal positions and host genes.

miRNA	Posterior probability diagnosis	Chromosomal Position	Host Gene	Under-expressed in 22q11 Del mouse PFC*
miR.330	100	19q13.32	EML2	
miR.33	100	22q13.2	SREBF2	Below detection threshold
miR.193b	100	16p13.12	intergenic	No probe for sequence
miR.545	100	Xq13.2	intergenic	No probe for sequence
miR.138	100	3p21.33 / 16q13	Intergenic	
miR.151	100	8q24.3	PTK2	Yes**
miR.210	100	11p15.5	intergenic	
miR.324.3p	100	17p13.1	ACADVL	Yes
miR.22	100	17p13.3	C17orf91	Yes
miR.425	100	3p21.31	DALRD3	Yes
miR.181a	100	1q31.3 / 9q33.3	Intergenic / NR6A1	
miR.106b	100	7q22.1	MCM7	Yes
miR.193a	99.95	17q11.2	intergenic	
miR.192	99.92	11q13.1	intergenic	Yes
miR.301	99.91	17q22	FAM33A	
miR.27b	99.82	9q22.32	C9orf3	
miR.148b	99.8	12q13.13	COPZ1	
miR.338	99.58	17q25.3	AATK	Yes
miR.639	99.57	19p12.13	GPSN2	No probe for sequence
miR.15a	99.5	13q14.3	DLEU2	
miR.186	98.8	1p31.1	ZRANB2	Yes
miR.99a	98.52	21q21.1	C21orf34	
miR.190	97.25	15q22.2	TLN2	Below detection threshold
miR.339	96.09	7p22.3	C7orf50	

* From Stark et. al., 2008
** The mouse homolog mmu-miR-151 differs at a single base pair position from the corresponding human sequence

A diagnostic classification of either schizophrenia or bipolar disorder, but especially bipolar disorder, seemingly corresponds to reduced miRNA expression levels. All miRNAs that are under-expressed in the schizophrenia group relative to controls are also under-expressed in the bipolar group, and to a greater degree (**Figure 5.2**). Notably, eight of the identified miRNAs were also found to be under-expressed in the prefrontal cortex of a 22q11 hemizygous knockout mouse with haploinsufficiency of the DGCR8 miRNA processing gene [224] (**Table 5.2**). The observed overlap in differentially expressed miRNAs between these expression studies is unlikely to occur by chance ($p=0.0373$ using Fisher's exact test), and suggests that aberrant miRNA processing may underlie observed expression changes. The overall trend toward under-expression of miRNAs in bipolar disorder is especially evident when examining standardized effect sizes of all analyzed miRNAs (**Figure 5.3**). Regression coefficients depicted in this figure are standardized so that expression levels have a standard deviation equal to 1. For example, a standardized coefficient of 0.5 corresponds to a change in miRNA expression of 0.5 standard deviations. Taken together, the data suggest that the presence of major psychosis is associated with globally reduced miRNA expression levels in the prefrontal cortex of affected adults.

Figure 5.2: Magnitude of expression changes. Fold changes with 95% confidence intervals for miRNAs with posterior probability of non-zero effect of diagnosis exceeding 95% (black bars represent the bipolar group, gray bars represent the schizophrenia group).

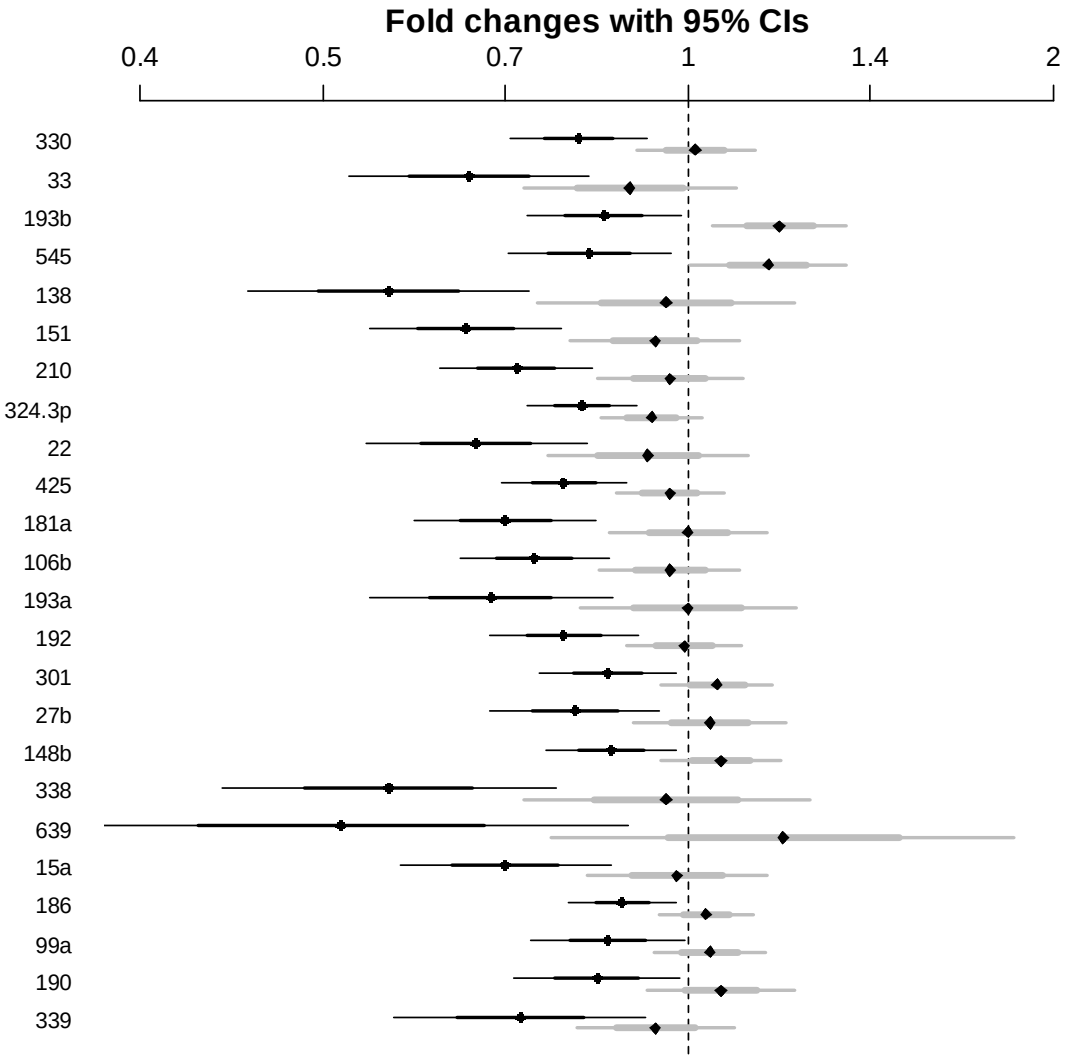

Figure 5.3: Separately sorted effect sizes for diagnostic classes. Expression levels were standardized such that transitioning from normal to the indicated affected category shifts miRNA expression by units of standard deviation on the Y-axis. Bolder negative effects for the bipolar group are evident.

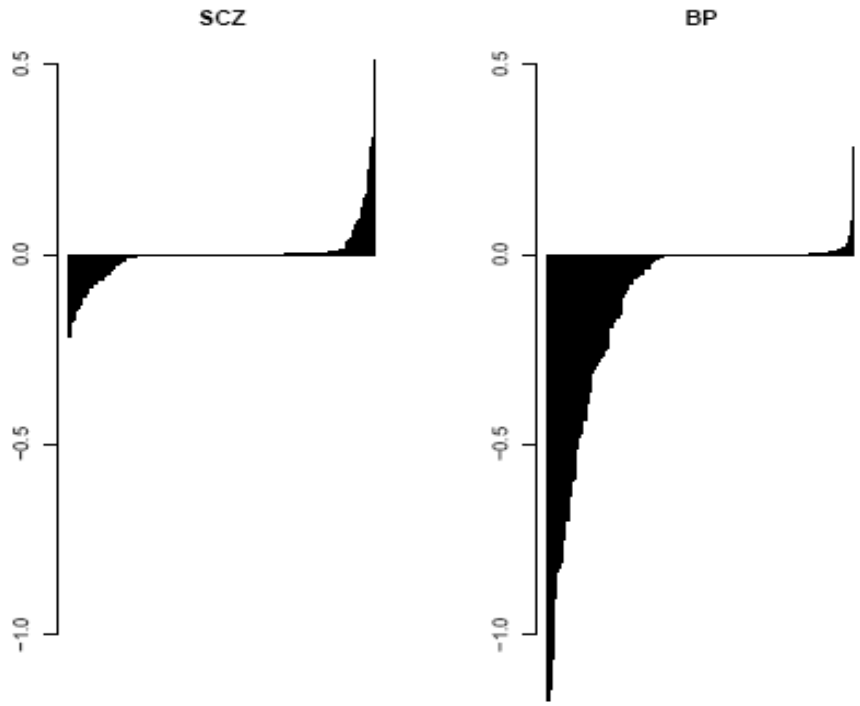

DISCUSSION

MicroRNA expression profiling of Brodmann Area 9 of the adult prefrontal cortex has revealed altered expression of several miRNAs in individuals affected with schizophrenia or bipolar disorder as compared to psychiatrically normal controls. Sensitivity and accuracy are essential when evaluating subtle differences in expression between closely related sample groups, and the TaqMan® assay has demonstrated superior sensitivity and linear dynamic range compared to Northern blotting and microarrays [225]. Furthermore, expression values were normalized to multiple internal control genes with empirically validated expression stability in this tissue.

Post-mortem expression studies are frequently confounded by variables pertaining to tissue source and quality. This study used a collection of anatomically homogeneous samples, collected and stored with an emphasis on obtaining high quality RNA for expression studies. The sample group was composed of specimens originating from 105 subjects divided equally among three diagnostic groups, many more than is typical for expression studies of post-mortem human brain. Besides basic demographic variables (age, race, and sex), lifetime exposure histories to alcohol, nicotine, psychoactive medications, and illicit drugs were also available. The effect of all sample covariates was assessed in a statistically rigorous manner, such that the influence of underlying neuropathology on miRNA expression levels could be evaluated.

Bayesian model averaging takes into account the inherent uncertainty in modeling the effect size of sample covariates in case-control studies [220]. The output of BMA is the posterior probability that a given covariate influences the dependent variable, in this case miRNA expression. BMA revealed that basic demographic variables such as age and sex were unlikely to influence miRNA expression levels. Pre-mortem acidosis and post-mortem interval have been shown to affect mRNA expression levels in past studies [226]. Variables related to sample selection and handling, particularly storage time, pH, and post-mortem interval, appeared to influence expression levels of many miRNAs, with storage time having a particularly strong influence. Thus, it is critical to control for these variables either experimentally [227], or statistically.

Besides sample selection and handling variables, we also assessed the potentially confounding effects of exposure to psychoactive drugs and medications. Given the severity of schizophrenia and bipolar disorder, it is tremendously difficult to find large

collections of brain tissue from untreated subjects for gene expression studies. Importantly, treatment with antipsychotics was excluded from BMA because all subjects with schizophrenia and more than two-thirds of those with bipolar disorder received such treatment. In this sample set, antipsychotic treatment history acts as a proxy for the presence of psychosis, the phenotype of interest. Thus, inclusion of this variable would obscure the detection of disease-related alterations in miRNA expression. The psychoactive substances considered affected only a small proportion of miRNAs, with the exception of alcohol at time of death. To clarify, this variable describes an individual's pattern of alcohol use prior to death, not their actual state upon autopsy. Alcohol at TOD influenced the expression of 9% of miRNAs analyzed, even though lifetime alcohol use had no measurable effect, implying a short term effect of alcohol on miRNA expression levels in the brain.

BMA revealed that psychiatric diagnosis strongly influenced brain expression levels of 24 miRNAs. Notably, most of the differentially expressed miRNAs were under-expressed in both the schizophrenia and bipolar sample groups relative to controls. This observation of *under*-expression of the majority of misexpressed miRNAs is in agreement with the work of others [71]. Although expression differences are subtle, consistent trends toward under-expression of several miRNAs in both of the affected groups not only legitimizes these characteristic expression signatures, but also further supports the idea of genetic overlap in the etiologies of schizophrenia and bipolar disorder.

Contrary to dramatic expression differences of individual miRNAs observed in human cancers [228], subtle perturbations in expression levels suggest that combinatorial effects

of several misexpressed miRNAs may contribute to the pathogenesis of major psychosis. This finding holds critical implications for future studies of miRNAs in psychiatric illness. First, miRNAs appear to be very tightly regulated in the human adult brain, with little inter-individual variability. Consequently, it is important to implement the most sensitive and precise technical methodologies in order to detect subtle expression differences between sample groups. Second, rather than selecting particular miRNA genes as candidate susceptibility loci, genetic studies should focus on factors that regulate transcription or processing of several miRNAs. We did not observe altered expression of genomically co-localized miRNAs. For example, even though miR-25, miR-106b, and miR-93 comprise a well-characterized co-transcribed miRNA cluster on chromosome 7, only miR-106b was found to be significantly misexpressed in this study. This observation seems to imply a selective alteration in miRNA processing or degradation, as opposed to aberrant transcriptional regulation. Haploinsufficiency of the DGCR8 gene, an RNA binding protein involved in the Drosha processing step, has recently been demonstrated to decrease the levels of at least 25 mature miRNAs in the prefrontal cortex and hippocampus of mice [224]. This same study demonstrated compelling schizophrenia-like behaviors associated with DGCR8 haploinsufficiency. It may be that alterations in the mammalian biosynthesis pathway lead to subtle alterations of subsets of miRNAs that contribute to psychiatric disorders.

In conclusion, the findings of this study support a role for miRNAs in schizophrenia and bipolar disorder. We employed technical and statistical methods to control for factors that often confound post-mortem expression studies, yet some important caveats remain. All tissue samples originated from a single anatomically defined region of the

adult prefrontal cortex, thus providing only a single spatiotemporal snapshot of miRNA expression profiles. Detailed functional characterization as well as expression profiling over a developmental time course may help to assign specific neurobiological roles to brain-expressed miRNAs, including those that are mis-expessed in individuals with psychiatric illness.

Chapter 6: Genetic Association of a microRNA Target Site Polymorphism in H3F3B with Schizophrenia

ABSTRACT

MicroRNAs (miRNAs) are endogenous ~21 nucleotide molecules that play important roles in gene repression. Single nucleotide polymorphisms (SNPs) that disrupt miRNA binding sites, known as miRSNPs, make up a new class of functional genetic polymorphisms. We describe a pattern-based miRNA target prediction algorithm called miRSNiPer, which is capable of detecting target site enhancement or disruption by SNPs. We used the algorithm to construct a panel of 48 putative functional SNPs, which were genotyped and tested for association to schizophrenia spectrum disorders. A SNP (rs1060120) within the 3'UTR of H3F3B, was found to be associated with schizophrenia (PPLD = 17%). An analysis method allowing for epistasis showed increased evidence of association (PPLD = 32%), suggesting a genetic interaction with a previously identified risk variant in the gene NOS1AP.

Polymorphic microRNA (miRNA) target sites are a newly recognized source of genetic variation that can have pronounced biological effects. miRNAs are ~21 nucleotide single-stranded molecules that negatively regulate the expression of 20-30% of human genes [214, 215]. They bind to recognition sites in the 3'UTRs of messenger RNAs to direct their posttranscriptional repression by the RNA-induced silencing complex (RISC). Altered expression of miRNAs has been implicated as a factor in several human disease states, including cancer, heart disease, and neurological conditions [71, 229, 230]. Recently, researchers have also begun to investigate the impact of genetic variation in miRNA target sites. A class of functional single nucleotide polymorphisms known as "miRSNPs" act to strengthen or weaken miRNA binding sites, thereby altering the stability or translatability of targeted transcripts. A prominent role for miRSNPs has been observed in several complex genetic traits, including Tourette's syndrome [231], methotrexate drug resistance [232], and even musculature of sheep [233].

Many key principles of miRNA target recognition have emerged in recent years, which have helped to guide genome-wide computational prediction strategies. Early reports showed that the 5' region is the most conserved portion of metazoan miRNAs [27], and miRNA regulation was most sensitive to nucleotide substitutions in positions 2-7 of the mature sequence [35, 234]. The requirement for perfect Watson-Crick pairing of this so-called "seed" region markedly reduced the occurrence of false-positive target predictions [34, 214]. However, early experimental validation approaches used *in vitro* reporter assays that were confounded by the artificiality of miRNA over-expression and a lack of endogenous cofactors. The use of sensor constructs in an endogenous context has shown that seed pairing is not sufficient to reliably predict miRNA-target interactions

[36]. Newly recognized targeting motifs, such as 3' compensatory sites, can bypass the seed-pairing rule and demonstrate similar binding efficacy [35]. Furthermore, 3' compensatory motifs may promote spatially restricted regulation by specific miRNA family members with closely related seed sequences. This phenomenon may be especially relevant in humans, given the dramatic expansion and divergence of the miRNA-ome in comparison to lower animals.

Accurate prediction of miRNA target sites is complicated due to the small size of miRNAs and their ability to bind to target sites with partial complementarity. "Signature-based" prediction algorithms strive for a balance of sensitivity and noise reduction by integrating novel classes of miRNA binding motifs, 3'UTR context determinants, binding energy measures, and especially evolutionary conservation. For example, the target-finding algorithm PicTar detects sites with perfect seed matches as well as imperfect nuclei bearing a 3' compensatory motif, and then applies a free energy filter to assess binding thermodynamics [39]. PicTar also exploits cross-species comparisons among divergent *Drosophila* lineages to further distinguish accurate site predictions from noise. Unfortunately, one cannot use evolutionary conservation to aid in target predictions for a growing number of human-specific miRNAs.

Rna22, in stark contrast with signature-based alignment methods, detects enriched, noncontiguous sequence motifs in a set of mature miRNA sequences [2]. The algorithm relies on the fundamental principle that recurring sequence patterns across distinct miRNAs are innately important, and perhaps contribute to target site recognition. A comprehensive miRNA sequence database is used to train a motif discovery algorithm called Teiresias [235], which identifies elementary sequence patterns. These basic

patterns are convolved and filtered for statistical significance, and their reverse complements are then mapped onto a gene or region of interest. Pattern instances that cluster around a specific 3'UTR location define a putative miRNA binding site, known as a "target island." One or more specific miRNAs are associated with a target island using such parameters as the overall number of base-pair matches and the maximum allowed number of unpaired bases in the miRNA seed region.

We have developed a target prediction algorithm called miRSNiPer, which expands upon the rna22 method to detect target site enhancement or disruption by SNPs. In the present study, we describe the application of the miRSNiPer algorithm to mine for functional variants involved in schizophrenia. Schizophrenia is a severe psychiatric disorder that affects 0.5-1% of the general population worldwide. Family and twin studies suggest a strong genetic component in disease etiology [75]. More than 20 genome-wide linkage scans have been performed to date, and meta-analyses have revealed consistency among identified susceptibility loci [81-93]. However, efforts to fine map causal mutations within specific genes have been considerably more difficult, and non-replication is typical among genetic association studies. This may be due, in part, to the prioritization of coding regions and upstream regulatory elements for in depth mutation analysis. We used miRSNiPer to identify miRSNPs within positional candidate regions, and we constructed a panel of SNPs for genotyping and family-based association analysis.

Genomic regions of interest were selected based on previous linkage findings in a well-characterized set of Canadian pedigrees. In 2000, a genome-wide linkage scan provided highly significant evidence of linkage (HLOD = 6.50) to the chromosomal

region 1q21-22 [82]. This data was reanalyzed in 2006 using a Bayesian linkage analysis technique called the posterior probability of linkage (PPL) [236]. The PPL has several key advantages over traditional likelihood-based linkage statistics. Results are presented on the probability scale, and can easily be interpreted in the same way as any other probability. While PPL analysis is model-based, unknown trait parameters are integrated out of the model, rather than maximized over arbitrary values [209, 237]. The genome-scan reanalysis also illustrates superior signal-to-noise discrimination of the PPL (**Figure 6.1a**), and confirms strong linkage evidence in the 1q21 region (PPL = 99.7%).

The PPL has undergone continuous development over the past decade, including extension to testing of linkage disequilibrium [196]. Fine mapping of the 1q21-22 region led to the discovery of several disease-associated SNPs within the NOS1AP gene, and functional allelic testing supported a causal role for rs12742393 [238]. The PPL has also been extended to support two locus analysis through the use of liability classes to specify a genotype at a fixed locus. A two-locus scan with the rs12742393 risk SNP as the fixed locus may implicate genes that interact with NOS1AP epistatically and contribute to schizophrenia pathogenesis. Therefore, linkage peaks from such a two-locus scan (**Figure 6.1b**) were used to establish boundaries for the genomic regions investigated in the present study.

Figure 6.1: Genome scan reanalysis using the Posterior Probability of Linkage. A. Single locus scan. **B.** Two-locus scan, with the NOS1AP risk SNP set as the fixed locus.

A

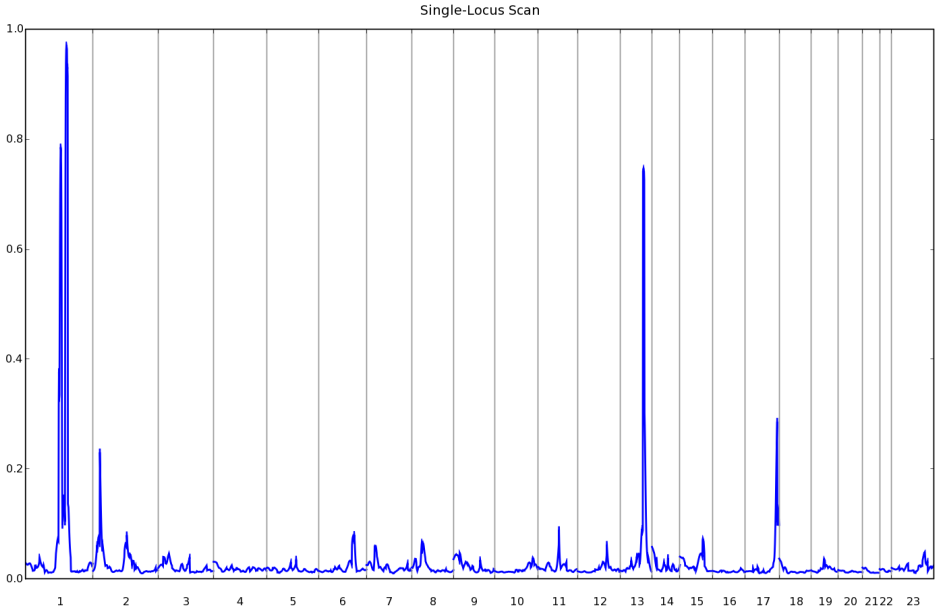
Single-Locus Scan
1.0
0.8
0.6
0.4
0.2
0.0
1 2 3 4 5 6 7 8 9 10 11 12 13 14 15 16 17 18 19 20 2122 23

B

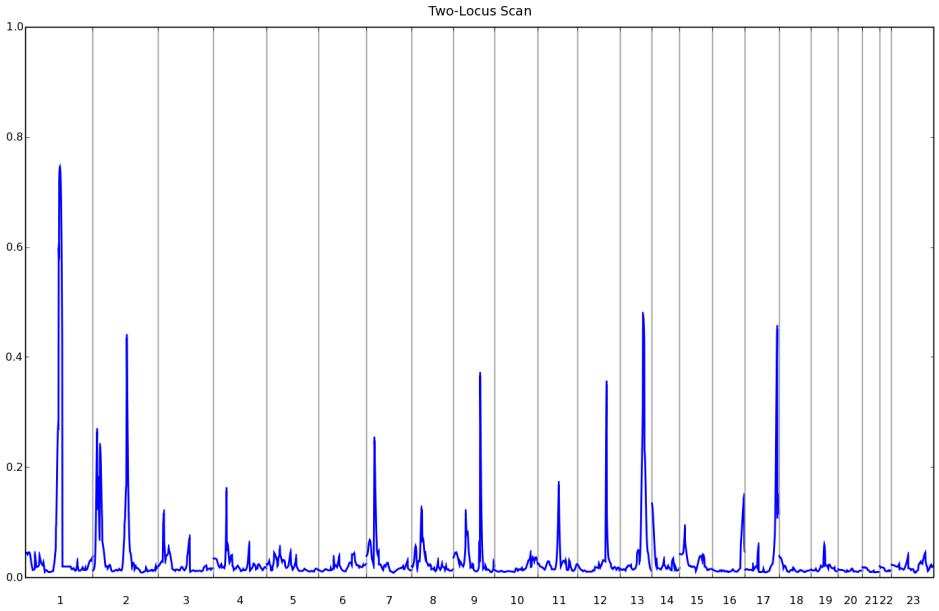
Two-Locus Scan
1.0
0.8
0.6
0.4
0.2
0.0
1 2 3 4 5 6 7 8 9 10 11 12 13 14 15 16 17 18 19 20 2122 23

Detection of polymorphic miRNA target sites requires three sources of input data for the miRSNiPer algorithm. The AceView database [239] provides a comprehensive representation of the human transcriptome, including all variably spliced and polyadenylated mRNA isoforms. 3'UTRs of all AceView transcripts beneath the aforementioned linkage peaks were extracted and concatenated, acting as a sequence of interest for mapping of miRNA binding sites. Following the removal of closely related entries, all mature miRNA sequences from the RNA families database of alignments and covariance models (Rfam 9.0) were used to train the Teiresias pattern discovery program. A detailed description of Teiresias parameters and statistical assessment of enriched sequence motifs is presented in **appendix 6**. Significant patterns were mapped to the joined 3'UTR sequences, along with all validated SNPs from the dbSNP (NCBI) database. Contiguous sequence blocks with 30 or more aligned patterns comprised probable miRNA binding sites, or "target islands." SNPs that resulted in a 2-fold or greater difference in the number of aligned patterns were identified as putative miRSNPs, acting to create, strengthen, weaken, or destroy miRNA target sites.

A total of 6467 transcripts originating from identified schizophrenia susceptibility regions served as target sequence for the miRSNiPer algorithm, and several criteria were used to select a panel of miRSNPs for genotyping and family-based association analysis. A simple ranking metric was devised consisting of three components: 1) miRNA target score, based on the number of aligned pattern matches, 2) transcript score, based on the number of identified clones reported in AceView, and 3) gene score, based on the presence or absence of known neurobiological function of the host gene. Ultimately a total of 48 putative miRSNPs were selected for association testing.

The subjects for this study included the individuals that were used in the genome-wide linkage scan, with the addition of two new families as well as additional members of previously studied families. Currently, the sample set consists of 455 subjects (332 with DNA available) from 24 extended pedigrees of Canadian Celtic ancestry. Families were recruited for study if schizophrenic illness appeared to be segregating in a unilineal (one side of the family only) autosomal dominant, manner. Ascertainment criteria and clinical diagnostic methods were described previously (see chapter 4). Families with a history of bipolar disorder were excluded from this sample. This sample has been followed for up to 20 years, with the opportunity to longitudinally observe the stability of the diagnoses in the subjects. Two categorical definitions of affection, "narrow" and "broad" were used. Individuals were considered affected under the narrow diagnostic classification if they were diagnosed with schizophrenia or chronic schizoaffective disorder. Individuals were considered affected under the broad diagnostic classification if they had been diagnosed with one of those disorders or with a nonaffective psychotic disorder, schizotypal personality disorder, or paranoid personality disorder.

Genotyping was performed using a bead-based oligonucleotide ligation SNP typing assay on the Luminex 100 platform (see chapter 3). Genotypes were checked for Mendelian errors and for departures from Hardy-Weinberg Equilibrium using the program PEDSTATS (version 0.6.12) [194]. Genotypes were removed for individuals exhibiting unresolved Mendelian errors for a given marker (0.17% of total genotypes). Marker allele frequencies were estimated using MENDEL (version 7.0) [195]. Genetic association analysis was performed using the posterior probability of linkage disequilibrium (PPLD), an extension of the posterior probability of linkage (PPL) method

of Vieland [196] as implemented in the program KELVIN (version 0.37.5) [197]. The PPL assesses the evidence for linkage and LD and estimates LD between the SNP marker and the disease phenotype [196].

In computing the usual form of the PPL, the prior probability of linkage is set to 2% based on theoretical calculations [201]. For comparability of scale, therefore, we also set the prior probability of LD given linkage to 2% (so that the joint prior probability of linkage and linkage disequilibrium is just 0.04%). Values of the PPLD < 2% therefore represent evidence against LD in the presence of linkage, while values > 2% indicate evidence in favor of LD in the presence of linkage. As with any form of the PPL, the PPLD has a direct interpretation as a probability. The PPLD applies to one SNP at a time (two-point analysis) and measures the evidence for or against LD to that SNP. As a direct measure of evidence, the PPLD does not require "correction" for multiple testing.

Three markers failed to convert to working genotyping assays, and two additional markers were monomorphic in our sample set. PPLD results for 43 analyzed markers are displayed in **table 6.1**. Most of the SNPs tested produced either no evidence for or against association (PPLD = 2%) or evidence against association (PPLD < 2%) under both phenotype definitions. Four markers, rs17575427, rs3736147, rs1060120, and rs10923444 displayed modest evidence of linkage disequilibrium under the narrow phenotype, with PPLD scores ranging from 3% to 6%. We observed evidence of association for the marker rs1060120 (PPLD = 17%) under the broad phenotype.

Table 6.1: Posterior Probability of Linkage Disequilibrium analysis results.

Marker	Host gene	Band	Broad Phenotype			Narrow Phenotype		
			Uncond	Dom LC	Rec LC	Uncond	Dom LC	Rec LC
rs575797	RBM14, RBM4	11q13.1	0.018	0.019	0.018	0.018	0.019	0.019
rs10898932	RAB6A	11q13.4	0.011	0.012	0.012	0.015	0.016	0.015
rs3825003	RAB6A	11q13.4	0.018	0.017	0.019	0.020	0.021	0.023
rs17132305	RAB6A	11q13.4	0.015	0.016	0.016	0.018	0.018	0.017
rs10898931	RAB6A	11q13.4	0.010	0.011	0.011	0.013	0.015	0.015
rs11768	LOC100128191	12q23.1	0.017	0.016	0.018	0.015	0.015	0.016
rs2282136	HS6ST3	13q32.1	0.015	0.018	0.017	0.025	0.030	0.040
rs1953550	TTC5	14q11.2	0.018	0.020	0.019	0.016	0.016	0.016
rs12920360	C16orf44	16q24.1	0.023	0.030	0.030	0.023	0.030	0.030
rs1060120	**H3F3B**	**17q25.1**	**0.170**	**0.190**	**0.340**	**0.050**	**0.050**	0.120
rs4969391	BAIAP2	17q25.3	0.018	0.017	0.018	0.017	0.017	0.017
rs7211218	LOC283999	17q25.3	0.017	0.017	0.018	0.018	0.019	0.019
rs1663196	TBC1D16	17q25.3	0.017	0.017	0.017	0.017	0.017	0.017
rs1128687	CHMP6	17q25.3	0.004	0.007	0.006	0.012	0.012	0.011
rs835575	NOTCH2	1p12	0.017	0.015	0.018	0.014	0.012	0.015
rs10923444	GDAP2	1p12	0.020	0.019	0.030	**0.060**	0.030	0.050
rs2050892	HSD3B2	1p12	0.016	0.016	0.017	0.017	0.016	0.017
rs17034228	VANGL1	1p13.1	0.021	0.030	0.024	0.022	0.022	0.020
rs2798566	ADORA3	1p13.2	0.020	0.020	0.021	0.015	0.014	0.015
rs1415793	ADORA3	1p13.2	0.020	0.020	0.021	0.015	0.014	0.015
rs17575427	AMIGO1	1p13.3	0.019	0.018	0.018	**0.030**	0.030	0.030
rs1043293	RPRD2	1q21.2	0.014	0.014	0.015	0.013	0.016	0.015
rs7539	YY1AP1	1q22	0.019	0.021	0.020	0.018	0.019	0.019
rs1271	APOA1BP	1q23.1	0.018	0.018	0.018	0.019	0.019	0.019
rs12402294	ARHGEF11	1q23.1	0.016	0.014	0.014	0.015	0.014	0.014
rs16837530	GPATCH4	1q23.1	0.019	0.019	0.019	0.018	0.019	0.018
rs7418910	VSIG8	1q23.2	0.014	0.014	0.014	0.010	0.010	0.011
rs924834	NOS1AP	1q23.3	0.015	0.011	0.013	0.015	0.011	0.012
rs480104	CD244	1q23.3	0.012	0.011	0.012	0.015	0.009	0.014
rs164149	NOS1AP	1q23.3	0.013	0.040	0.023	0.013	0.060	0.030
rs12311	DDR2	1q23.3	0.015	0.017	0.016	0.016	0.016	0.015
rs2272916	SCYL3	1q24.2	0.020	0.024	0.023	0.020	0.022	0.020
rs11688303	GPR17	2q14.3	0.017	0.016	0.016	0.018	0.016	0.016
rs9857007	RNPC3	3p14.1	0.016	0.016	0.015	0.016	0.015	0.015
rs13084430	RNPC3	3p14.1	0.015	0.015	0.016	0.016	0.015	0.018
rs2279974	LMCD1	3p26.1	0.017	0.018	0.017	0.019	0.018	0.018
rs4624663	TLR6, TLR1	4p14	0.018	0.018	0.018	0.019	0.019	0.019
rs11895	FBXO16, ZNF395	8p21.1	0.018	0.019	0.019	0.017	0.017	0.017
rs3736147	BIN3	8p21.3	0.022	0.023	0.030	**0.040**	0.030	0.050
rs17411988	ATP6V1B2	8p21.3	0.013	0.015	0.015	0.015	0.016	0.016
rs10117507	MTAP	9p21.3	0.015	0.014	0.015	0.016	0.016	0.016
rs4977494	FAM29A, SCARNA8	9p22.1	0.018	0.018	0.017	0.018	0.017	0.017
rs4289885	PALM2-AKAP2	9q31.3	0.013	0.012	0.013	0.015	0.014	0.014

We are operating under the hypothesis that these SNPs are functional variants that disrupt miRNA binding. Results from simulated datasets with an extended pedigree structure suggest that PPLD scores above 10% are quite rare, and likely represent a positive association finding. The PPLD for rs1060120 increased to 32% under the two-locus model, with rs12742393, the NOS1AP risk SNP.

rs1060120 falls within the 3'UTR of the gene H3F3B, which encodes a core histone protein. Patterns of LD with nearby SNPs were examined in order to better localize the association signal. rs1060120 falls within a haplotype block that spans 32 kb (**Figure 6.2**). The flanking markers rs7432 and rs10338 are 250 base pairs apart and exhibit perfect intermarker LD (r^2=1), but rs1060120 is not in strong LD (r^2<0.4) with these or any other markers in a 40 kb radius (**Table 6.2**). Recently, genome-wide SNP data was obtained on this sample set using the Affymetrix 6.0 SNP array. PPLD analysis was performed on 1800 SNPs beneath a known linkage peak on chromosome 17 (cM positions 113.2914-137.7255). Remarkably, under the liability class model, only four markers exceeded a PPLD score of 10%, with the highest score being 12%. This sharply contrasts with the PPLD score of 32% for rs1060120 (**Figure 6.3**), which was not present on the Affymetrix 6.0 array. Of note is that no SNPs in strong or even moderate LD with rs1060120 are present on the Affymetrix 6.0 array, so the lack of a strong LD signal from the Affymetrix SNPs is not unexpected. From this finding, the association signal appears to be localized to the 3'UTR of H3F3B. Furthermore, this finding supports the use of a two-stage fine mapping strategy that first uses linkage evidence for course localization of disease susceptibility loci. In this case, an unbiased genome-wide association approach

that simultaneously profiles over 900,000 SNP genotypes would not have been sufficient to detect allelic association to H3F3B.

Figure 6.2: Linkage disequilibrium plot of a 40 kb region encompassing H3F3B. Red arrow indicates the position of rs1060120, flanked by the markers rs7342 and rs10338.

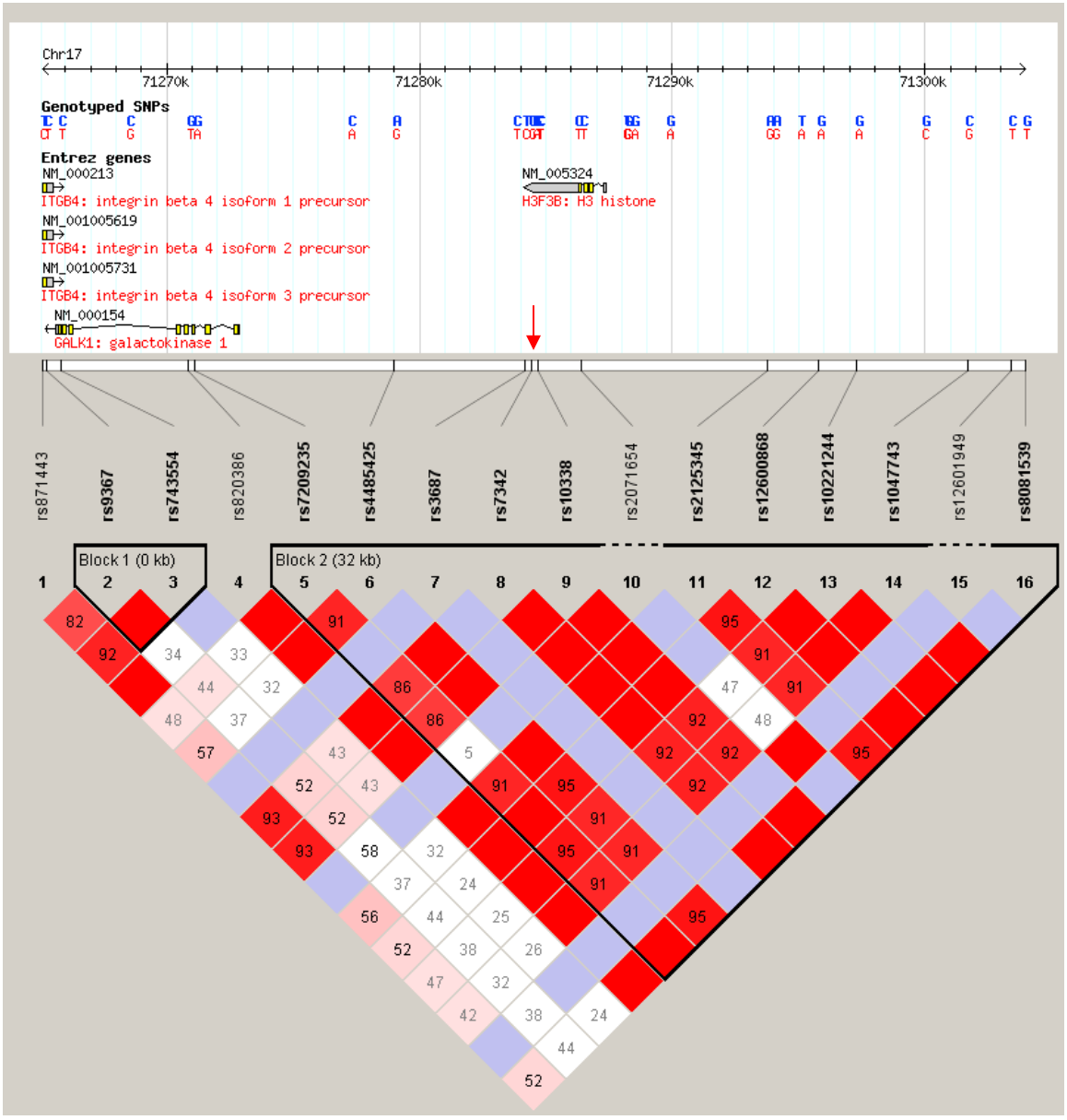

Table 6.2: Inter-marker LD measures for validated SNPs in a 40 kb interval encompassing H3F3B.

pos1	pos2	marker1	marker2	D'	r^2
71265098	71284595	rs871443	rs1060120	0.905	**0.249**
71265256	71284595	rs9367	rs1060120	0.799	**0.155**
71265843	71284595	rs743554	rs1060120	0.848	**0.119**
71270899	71284595	rs820386	rs1060120	1	**0.059**
71271147	71284595	rs7209235	rs1060120	1	**0.391**
71279032	71284595	rs4485425	rs1060120	1	**0.39**
71284185	71284595	rs3687	rs1060120	1	**0.069**
71284451	71284595	rs7342	rs1060120	1	**0.215**
71284595	71284701	rs1060120	rs10338	1	**0.215**
71284595	71286436	rs1060120	rs2071654	1	**0.029**
71284595	71293786	rs1060120	rs2125345	0.929	**0.353**
71284595	71295809	rs1060120	rs12600868	0.547	**0.173**
71284595	71297313	rs1060120	rs10221244	0.532	**0.157**
71284595	71301688	rs1060120	rs1047743	0.526	**0.147**
71284595	71303410	rs1060120	rs12601949	1	**0.019**
71284595	71303967	rs1060120	rs8081539	0.547	**0.173**
71284595	71304196	rs1060120	rs8069105	0.552	**0.181**

Figure 6.3: Two-Locus PPLD results for 1800 SNPs spanning a 25 cM region on chromosome 17. Two-locus analysis was performed under the broad phenotype definition with rs12742393 from NOS1AP. The PPLD score for rs1060120 from the present study is superimposed in pink.

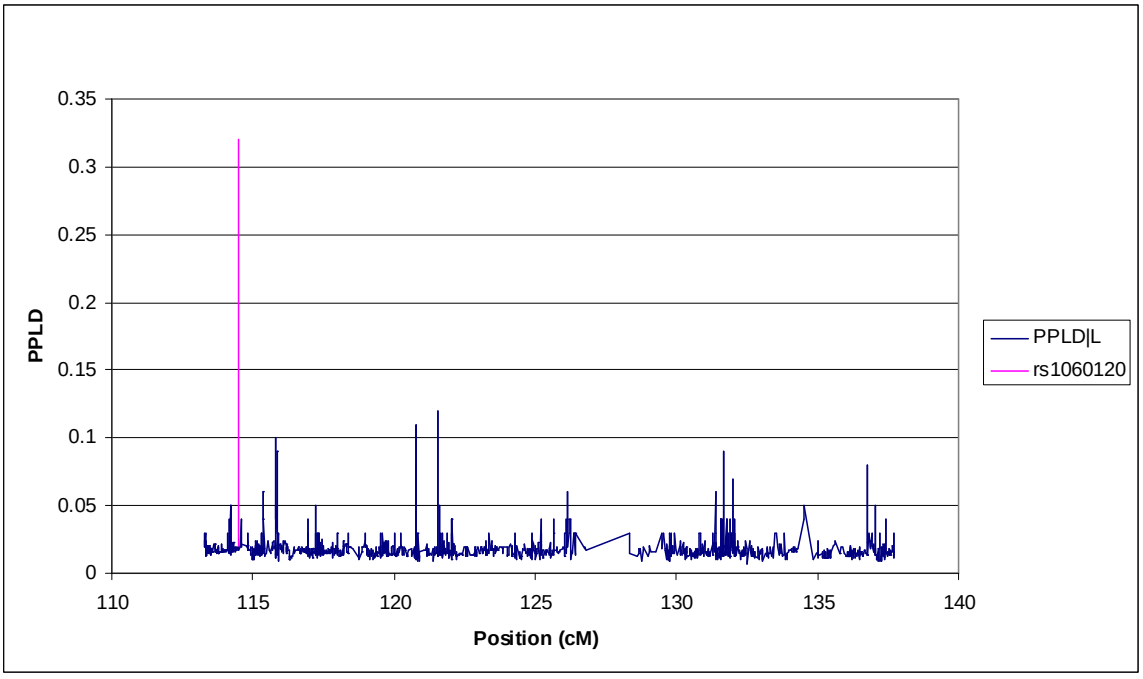

Direct sequencing was performed in a single extended pedigree in order to validate genotype calls for rs1060120, and also to identify any unknown nearby mutations. Semi-automated fluorescent direct sequencing was performed on the Beckman CEQ 8000 instrument. PCR primers and internal sequencing primers were designed using Primer3 (Whitehead Institute). We observed 100% concordance between genotype calls derived from sequencing those generated using bead-based OLA. We confirmed the two flanking SNPs, rs7432 and rs10338, but we did not identify any additional mutations. Phased haplotypes were generated for rs1060120 and the adjacent markers using SIMWALK2 [193], and a graphical pedigree display was drawn using Haplopainter [240] (**Figure 6.4**). In this particular example, the A allele of rs1060120 appears to be over-transmitted to affected individuals.

As mentioned, the miRNA target site in H3F3B was predicted using a pattern-based algorithm that did not require a pre-specified miRNA as input for sequence alignment. Thermodynamically favorable miRNA-mRNA duplex formations were predicted using RNAFold from the Vienna Software Package [241], revealing probable interactions with two miRNAs (**Figure 6.5**). miR-616 bears a perfect 7 nucleotide seed match, as well as a 3' supplementary interaction. Contiguous pairing of 4 consecutive nucleotides in the 3' region, especially at positions 13-16, has been characterized as a productive interaction that leads a greater degree of target gene repression [38]. The A allele of rs1060120 converts a G-U wobble base pair to a Watson-Crick A-U pairing at position 15, potentially enhancing the degree of miRNA binding. From previous expression studies, we observed only trace expression levels of miR-616 in post-mortem fetal, early postnatal, or adult brain tissue (see **appendix 1**). However, this does not preclude

expression of miR-616 in specific neural cell populations. miR-886-3p, on the other hand, is highly expressed in the brain at levels comparable to the let-7 family of miRNAs. The G allele of rs1060120 shifts the position of a G-C pairing to the 3' end of the miRNA-mRNA duplex. This alignment is predicted to be more energetically favorable, perhaps because the competing 5' G-C pairing requires a bulge in the miRNA secondary structure.

DNA of eukaryotic cells is compacted into chromatin, and packaged into basic structural units called nucleosomes. In the nucleosome, DNA is wrapped around a histone octamer, which is comprised of a central H3-H4 core tetramer flanked by two H2A-H2B dimers. Histone genes fall into two major classes, replicative histones that are expressed only during DNA replication, and replacement histones that are continually expressed throughout the cell cycle [242]. Replacement histones, such as the H3.3 family, were once thought to serve a redundant role as substitutes for replicative classes. However, H3.3 distribution patterns and characterization of posttranslational modifications suggest that they are markers of actively transcribed chromatin [243]. Recent models suggest that H3.3 histones set up a "transition" signature to modify chromatin architecture independent of DNA replication. This mode of epigenetic reprogramming may activate key transcriptional switches during development [244]. We believe that a G to A transition in the 3'UTR of H3F3B alters the binding affinity of two miRNAs, miR-616 and miR-886-3p, which, in turn affects gene expression. The SNP rs1060120 is associated with schizophrenia and schizophrenia spectrum disorders, and the association signal doubles in strength upon allowing for epistasis with a known risk

variant in NOS1AP. Taken together, the data suggest that two functional variants in NOS1AP and H3F3B contribute to schizophrenia etiology in a cooperative manner.

Figure 6.4: Phased haplotypes in a large, extended pedigree. Haplotypes were computed based on sequencing results for rs1060120, and two flanking markers. Genotypes for rs12742393, a known functional SNP in the NOS1AP gene, are also shown.

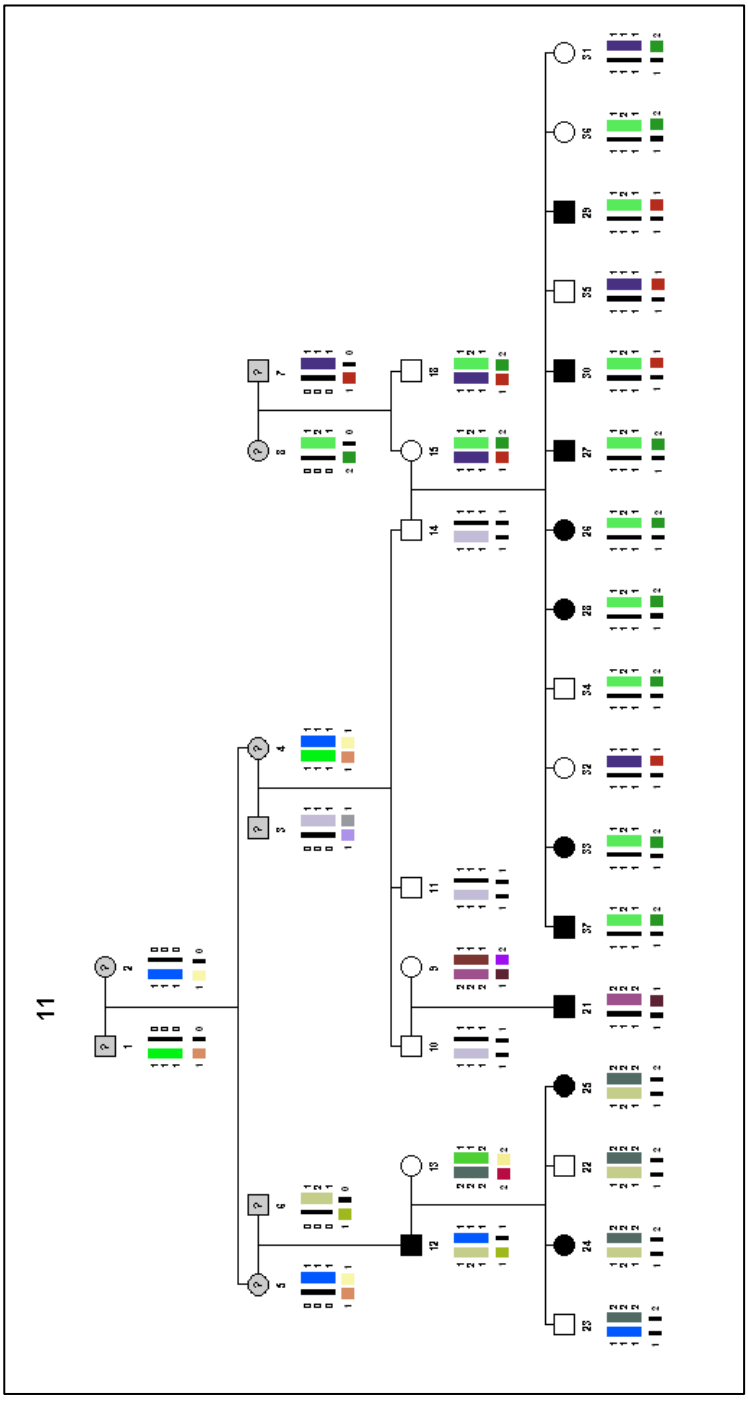

Figure Legend: Marker and allele identifiers are shown below; those in Red show evidence of association to schizophrenia. Genotypes of the three linked markers were determined by direct sequencing. The single marker, separated by a line, is a proposed functional variant described in [183].

Marker name	**Allele 1/2**
rs7432	**C/G**
rs1060120	**G/A**
rs10338	**T/C**
rs12742393	**A/C**

Figure 6.5: Sequence alignments of two miRNAs to a polymorphic target site in H3F3B.

Chapter 7: Conclusions

REVIEW OF MAJOR FINDINGS

The work presented here describes the integration of genetic, molecular profiling, and computational techniques to better understand how altered miRNA regulatory networks contribute to schizophrenia spectrum disorders. First, we performed microarray-based expression analysis of over 1000 miRNAs and other non-coding RNAs in fetal, early postnatal and adult post-mortem brain tissue samples. This study revealed dramatic changes in miRNA expression signatures over a developmental time course, which formed the basis for a miRNA classification system. A novel bead-based multiplexed SNP genotyping assay was developed and used in a family-based association study of DGCR8, a miRNA processing gene. An intronic SNP in DGCR8 showed strong evidence of association to schizophrenia, possibly implicating altered miRNA processing in disease pathogenesis. Furthermore, comprehensive miRNA expression profiling revealed several moderately under-expressed miRNAs in the prefrontal cortex of individuals with major psychosis relative to psychiatrically healthy subjects. A pattern-based miRNA target prediction algorithm called miRSNiPer was used to construct a panel of SNPs predicted to alter miRNA binding sites. One of these miRSNPs, located in the 3'UTR of the H3F3B replacement histone gene, showed evidence of genetic association to schizophrenia and schizoaffective disorder. Finally, the miRSNiPer algorithm was used to identify the targets of misexpressed miRNAs in order to uncover disrupted networks and pathways.

Several expression studies conducted in animal models have depicted a chronological wave of miRNA expression in the brain throughout the course of development, but

researchers had yet to investigate miRNA expression profiles in the developing human brain. We selected a commercially available microarray with enhanced feature content comprised of nearly all validated Sanger 10.0 miRNAs as well as 373 novel, proprietary miRNAs. Microarray analysis was performed on 48 post-mortem brain tissue samples representing gestational ages 14-24 weeks, as well as early postnatal and adult time points. A total of 464 expressed species passed quality control filters, and 312 of them showed significantly different expression levels between fetal, young, and adult sample types. Reverse F-test model selection was used to assign these developmentally regulated species to 12 distinct model classes. We not only characterized hundreds of miRNAs and ncRNAs in a developmental context for the first time, but we found that in the human brain many canonical miRNAs depart from previously observed expression trends from model systems. Previous studies have depicted the let-7 family of miRNAs as markers of differentiation with gradually increasing expression levels throughout development. Conversely, expression levels of brain-enriched neuronal markers such as miR-124 and miR-9 were shown to peak at fetal time points and gradually decline. Surprisingly, we found that the human brain adopts an immature, dedifferentiated miRNA expression signature in early childhood, marked by dramatically reduced expression of brain specific miRNAs and let-7 family members relative to other time points. These observations support a model stating that miRNA regulatory networks are "recalibrated" after critical developmental milestones are achieved. Ultimately, our proposed miRNA classification scheme may help to guide future studies of miRNA expression and function in the brain.

At the outset of this research project, no cost-effective medium-throughput multiplexed SNP genotyping assay was commercially available. Therefore, an efficient and flexible assay, built on existing methods, was developed and optimized in-house. Robust oligonucleotide ligation assay chemistry was used in conjunction with colored polystyrene beads, and allelic discrimination was achieved using two-color flow cytometry on the Luminex platform. Three innovations helped reduce the cost and improve efficiency of the assay, relative to previously published work. First, we established through extensive experimental trial that far fewer beads than previously reported could be used to obtain accurate and reproducible genotypes. Second, a biotinylated universal oligonucleotide was used to reduce the cost of assay-specific reagents. Third, reagent concentrations were optimized such that bead washing and filtration steps could be omitted, in contrast to all previously published Luminex-based genotyping protocols. While new methods are continually being developed and old methods are becoming less expensive, our method remains a very inexpensive and reliable one that is widely useful for performing targeted genetic studies.

Our custom bead-based multiplexed SNP typing assay was utilized in a candidate gene study of the miRNA processing gene, DGCR8. A tagSNP strategy was employed to investigate several adjacent genes within a 75 kb region on chromosome 22q11.2. This region is likely to harbor schizophrenia susceptibility genes, with evidence from two sources. First, this sub-region is part of a common 3.1 Mb hemizygous deletion that causes velocardiofacial syndrome, and is also one of the greatest known genetic risk factors for schizophrenia. Second, several other genes in this region, including ZDHHC8 and COMT, have been implicated in previous association studies. We either observed no

evidence of association, or evidence against association for all genotyped markers in two unique sample sets. Globally reduced miRNA expression levels have been observed in a 22q11 hemizygous knockout mouse, suggesting that a polymorphism affecting DGCR8 expression or function can have broad biological implications. Our findings suggest that common genetic variants within DGCR8 are unlikely to play a role in the etiology of schizophrenia. However, this does not preclude the existence of rare, private mutations in individuals with psychotic illness. Findings of miRNA under-expression in the 22q11 hemizygous knockout mouse combined with findings of several misexpressed miRNAs in postmortem brain samples from individuals with schizophrenia seem to implicate a miRNA processing defect. Therefore, detailed mutation analysis of DGCR8 using a deep sequencing approach is warranted.

We performed miRNA expression profiling in post-mortem prefrontal cortex tissue samples from patients with schizophrenia, patients with bipolar disorder, and psychiatrically healthy control subjects. In contrast with other post-mortem studies, tissue samples originated from anatomically homogeneous brain regions, and samples were prepared and stored in a standardized fashion. With 35 samples per diagnostic group, we were able to assess demographic and substance exposure covariates in a statistically rigorous manner. This approach, combined with the use of gold-standard TaqMan methodology, allowed us to reliably detect subtle but consistent expression changes that correlate with psychotic illness. 24 miRNAs exceeded a statistical threshold indicating a strong effect of psychiatric diagnosis, and a global trend toward under-expression was especially evident in the bipolar group. Several of these miRNAs were also found to be under-expressed in the prefrontal cortex of the 22q11 hemizygous

knockout mouse. Therefore, molecular profiling and genetic association data both suggest that global down-regulation of miRNAs likely factors into the pathogenesis of schizophrenia spectrum disorders.

FUTURE WORK: DECIPHERING THE SCHIZOPHRENIA PHENOCODE

Gennadi Glinsky coined the term "phenocode" to describe the phenotype-defining functions of interacting non-coding RNA pathways. Through sequence homology profiling, he deduced that several classes of ncRNAs could be transacting repressors of miRNAs. Furthermore, he proposed that many disease-associated, functionally ambiguous intergenic SNPs identified in whole genome association studies could reside within these ncRNAs and disrupt their miRNA binding capacity. Due to inconsistent results across candidate gene studies of schizophrenia, Glinsky's SNP-guided strategy was supplanted by a miRNA-guided approach in the present research project. A re-envisioned two-hit hypothesis states that miRNAs act to offset the effects of mutations in *cis*-regulatory elements, and disease manifestation occurs upon dysregulation of this miRNA buffering system. Two experimental observations support this theory. First, expression profiling of brain tissue samples from individuals with psychotic illness revealed several significantly *under*-expressed miRNAs, as well as a global trend toward miRNA under-expression. Second, the significantly misexpressed miRNAs tended to have low to moderate expression levels in the adult brain. While highly expressed miRNAs may act to sharpen developmental transitions by suppressing the products of leaky transcription, it is these moderately expressed miRNAs that are thought to buffer stochastic effects of suboptimal promoters to maintain appropriate gene expression levels.

If misexpressed miRNAs truly can reveal something fundamental about disrupted genetic pathways in disease, then one should focus on the targets of these misexpressed miRNAs to mine for causal regulatory mutations. Over the course of this project, we have identified a set of moderately under-expressed miRNAs in individuals with psychotic illness, we have classified hundreds of miRNAs according to their patterns of expression over a developmental time course, and we have developed a sensitive miRNA target prediction algorithm. With these three components in place, we next attempted to identify disrupted networks of genes using the Ingenuity Pathway Analysis (IPA) software.

Figure 7.1: Classification of misexpressed miRNAs based on developmental time course data. Expression levels are indicated as ΔCt values, using the mammalian U6 small nuclear RNA as an internal control. Higher ΔCt values indicate that more PCR cycles are required to reach the fluorescence threshold during the real-time PCR reaction, therefore bar height is inversely proportional to expression level.

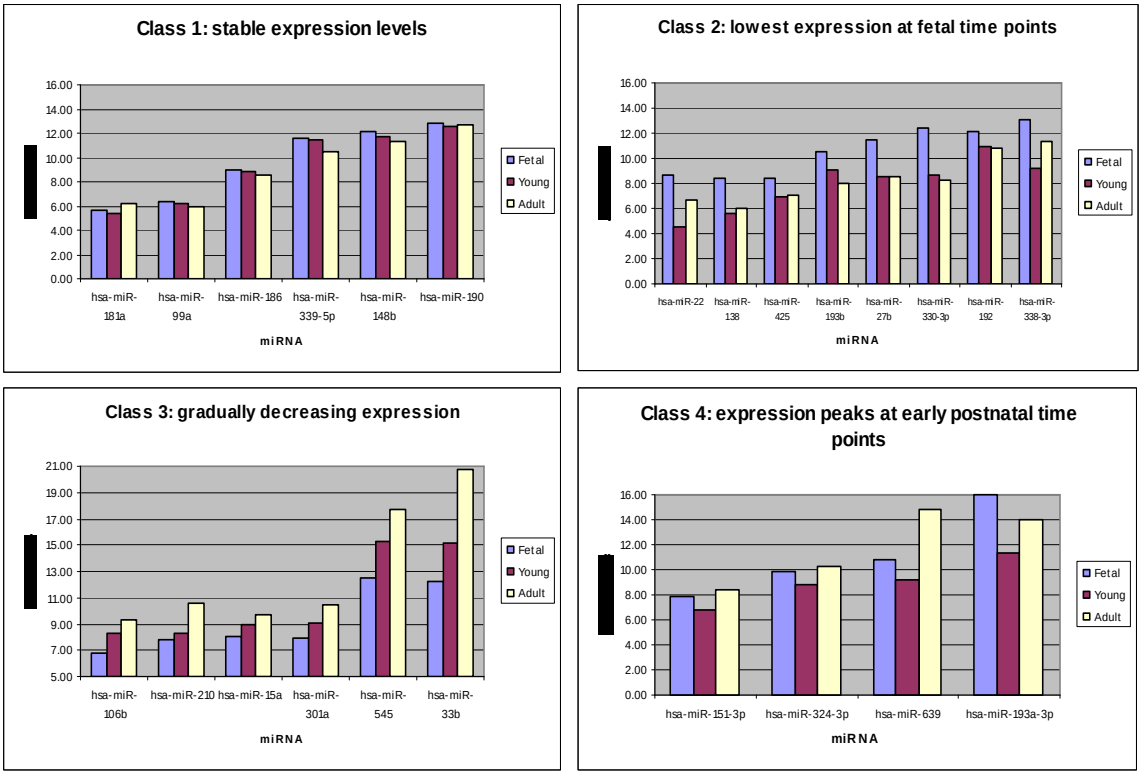

The miRNAs found to be misexpressed in individuals with psychotic illness were divided into four classes based on their temporal expression signatures. Having low to moderate expression levels, many of these miRNAs were undetectable on glass slide arrays, and therefore TaqMan expression data from pooled samples was used for classification (**Figure 7.1**). A genome-wide scan for miRNA target sites was performed using miRSNiPer, and lists of aligned pattern matches were extracted for each of the four miRNA classes. These lists served as the input for IPA. IPA is a tremendously useful software application that extracts information from the full text of scientific literature so as to assign genes to functional categories, disease processes, and interacting networks. A basic or "core" analysis was performed by submitting each of the four lists of gene identifiers. Upon initial inspection, "neurological disease" was among the highest ranked biological categories for all four sets of genes (**Figure 7.2**). Since each list had several thousand members, this ranking could have simply reflected the distribution of ontology labels for all known human genes. To address this possibility, three lists of random gene identifiers were constructed and submitted for core pathway analysis. Even though these random lists were similar in size to the four sets of miRNA targets, "neurological disease" received an intermediate ranking among the assigned biological categories, ranking 30^{th} for one list and 33^{rd} for the other two Therefore, there appears to be a meaningful enrichment in miRNA-targeted genes that are associated with neurological disorders.

Figure 7.2: Biological functions of genes targeted by misexpressed miRNAs. IPA functional assignments of target gene classes 1-4 are displayed in the four bar charts. Red ovals indicate the position of the "neurological disease" functional category.

Analysis: unique1 - 2009-07-28 04:19 PM

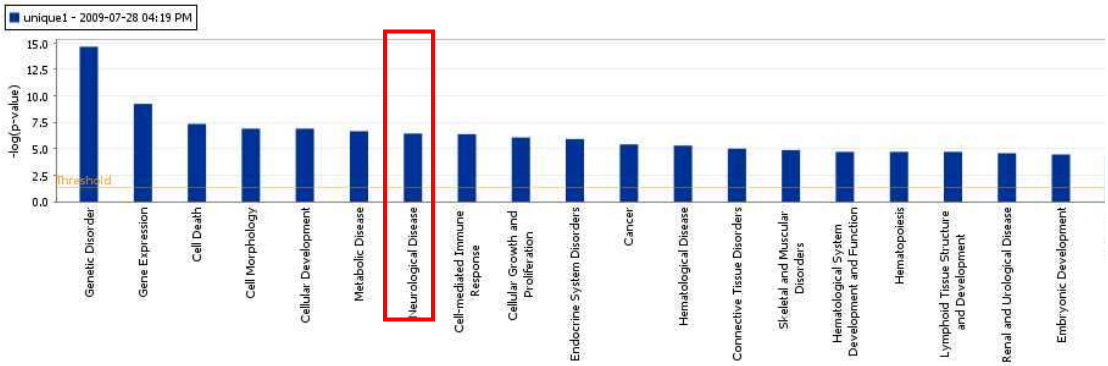

Analysis: unique2 - 2009-07-28 04:20 PM

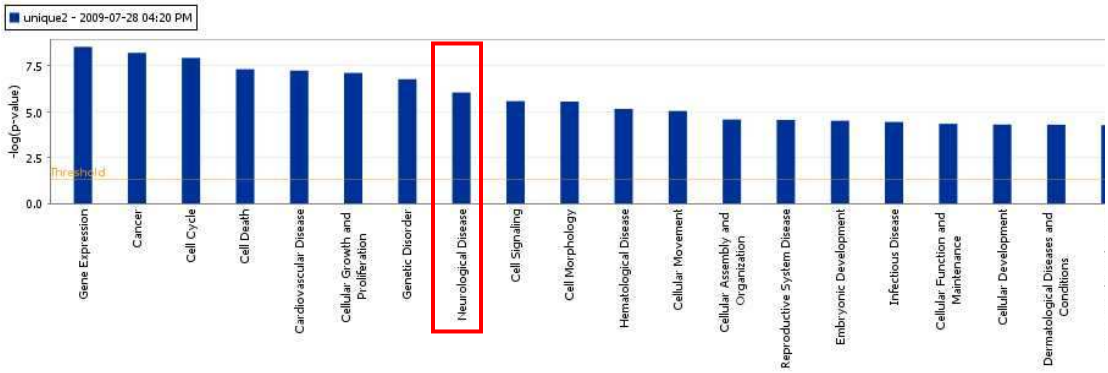

Analysis: unique3 - 2009-07-28 04:21 PM

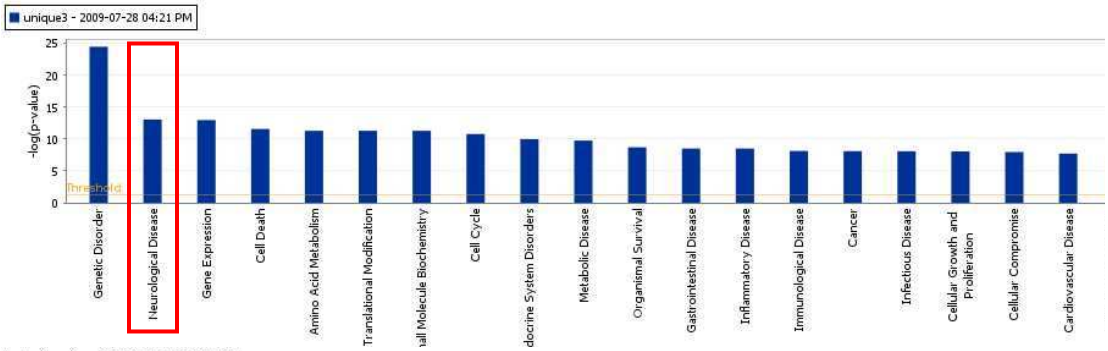

Analysis: unique4 - 2009-07-28 04:22 PM

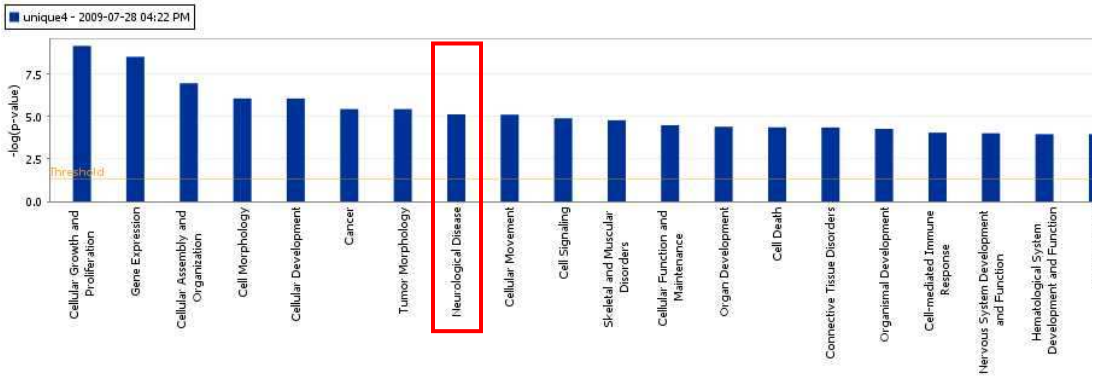

For each of the four miRNA target classes, lists of genes related to “neurological disease” were extracted and the core analysis was reiterated. Not surprisingly, “psychological disorders” appeared as the highest ranked biological process for all classes, but more importantly, “bipolar affective disorder” and “schizophrenia” were consistently the most strongly implicated disease states under this header. IPA organizes lists of genes into networks based on experimentally supported interactions, and lists these networks according to their score. The score is based on a p-value calculation, which calculates the likelihood that the network eligible molecules that are part of a network are found therein by random chance alone.

Table 7.1: Schizophrenia candidate genes. The Schizophrenia Research Forum indentifies these genes as the most promising schizophrenia candidate genes based on meta-analysis of published association findings.

Gene ID
DISC1
SLC18A1
GABRB2
DRD2
GWA 10q26.13
AKT1
GRIN2B
DGCR2
PLXNA2
RPGRIP1L

To interpret these networks in a meaningful context, one should be cognizant of well-supported etiological models of schizophrenia. The Schizophrenia Research Forum (http://www.schizophreniaforum.org/) is a comprehensive database of positive and negative genetic association findings. This database includes a frequently updated list of

the most promising schizophrenia candidate genes, based on meta-analysis results (**Table 7.1**). Among the listed genes, DISC1 and PLXNA2 are involved in neurite outgrowth and guidance, while AKT1 acts in growth-factor induced neuronal survival. DRD2, GRIN2B, and GABRB2 are receptor subunits involved in dopamine, glutamate, and GABA signaling, respectively, and SLC18A is a monoamine transporter. Therefore, the most promising schizophrenia candidate genes converge on both axonal guidance and signal transduction pathways.

The highest scoring networks from all four miRNA target classes were examined, and marked overlap was observed between class 1 and class 3 targets, as well as between class 2 and class 4 targets. Therefore, two networks emerged as the most consistent targets of misexpressed miRNAs. The first of these networks was highly enriched ($p = 10^{-42}$) for targets of miRNAs with stable or gradually declining expression levels over time (**Figure 7.3 A, B**). The members of this network include a group of metabotrobic glutamate receptors, the DRD2 dopamine receptor gene, and perhaps most strikingly, DISC1 and 10 of its direct binding partners. The second major gene network is highly enriched ($p = 10^{-28}$) for targets of miRNAs with lower expression levels in the fetal brain, as well as those that spike at early postnatal time points (**Figure 7.3 C, D**). This vast network includes several NMDA receptor subunits as well as the NOS1 and AKT genes that function downstream in the nitric oxide signaling cascade. Remarkably, the influential glutamate model of schizophrenia has once again risen to the forefront using our novel miRNA-guided approach.

Figure 7.3: Gene networks targeted by misexpressed miRNAs. A. Genes targeted by miRNAs from class 3 are shaded in blue, and those targeted by miRNAs from classes 1 and 3 are shaded in pink. **B.** Genes with published evidence of genetic association to schizophrenia and bipolar disorder are indicated among the class 1 and 3 miRNA targets. **C.** Genes targeted by miRNAs from class 2 are shaded in grey, and those targeted by miRNAs from classes 2 and 4 are shaded in pink. **D.** Genes with published evidence of genetic association to schizophrenia and bipolar disorder are indicated among the class 2 and 4 miRNA targets.

A

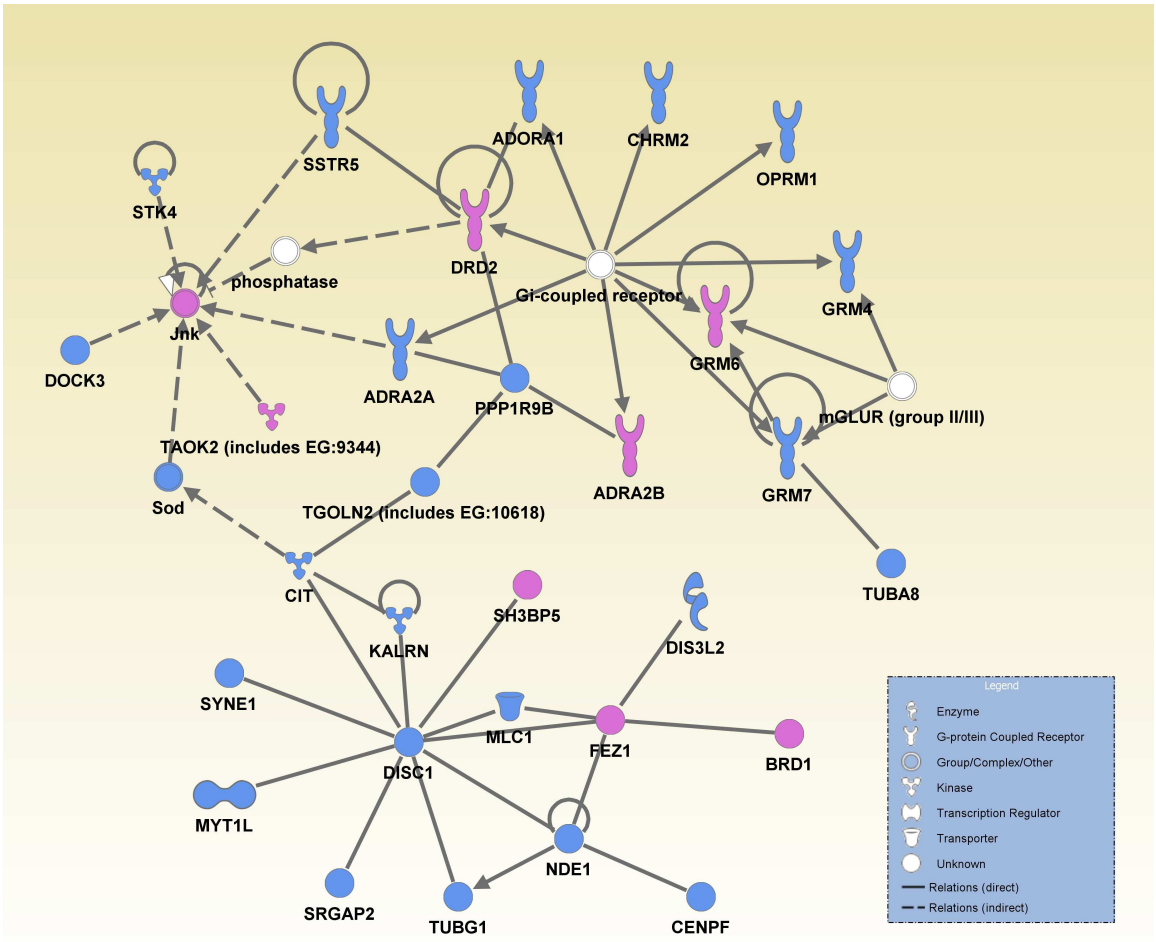

B

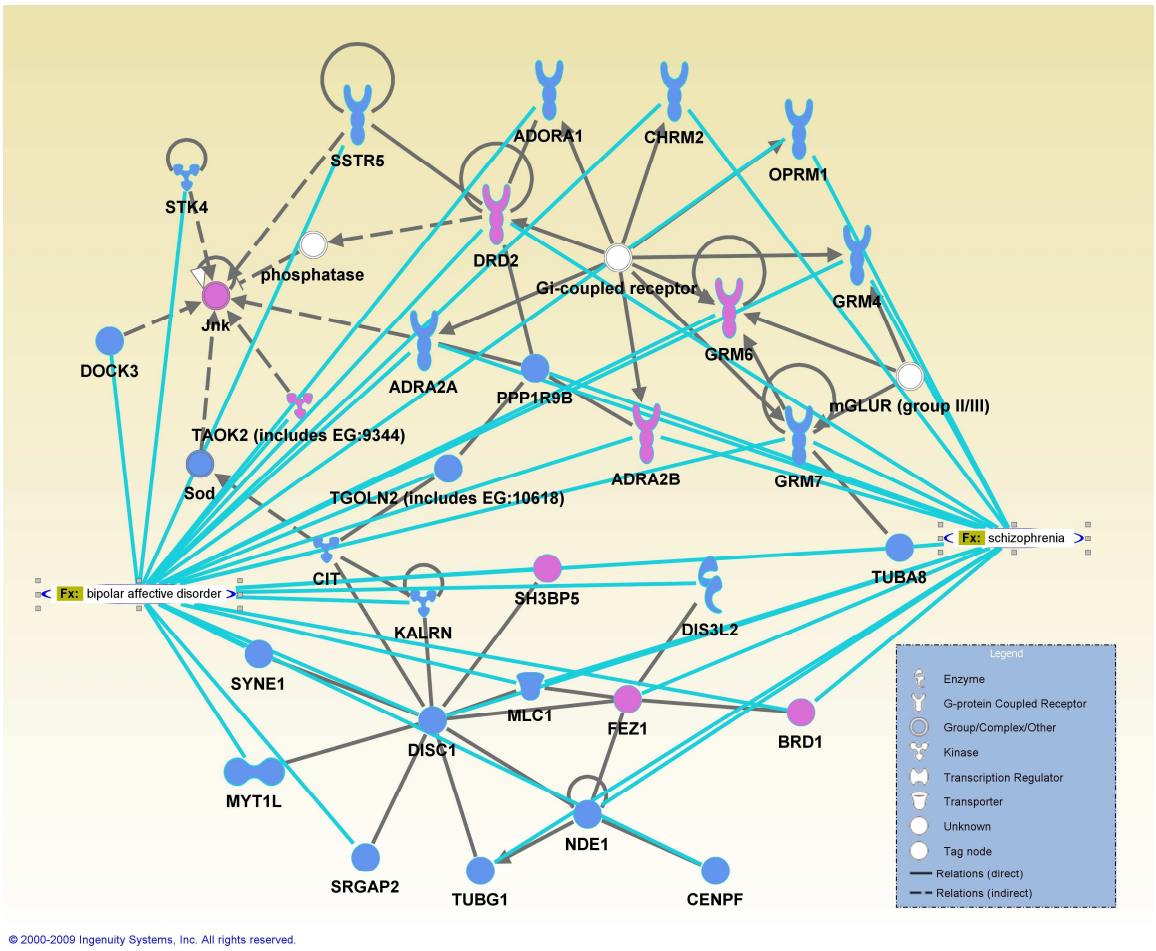

C

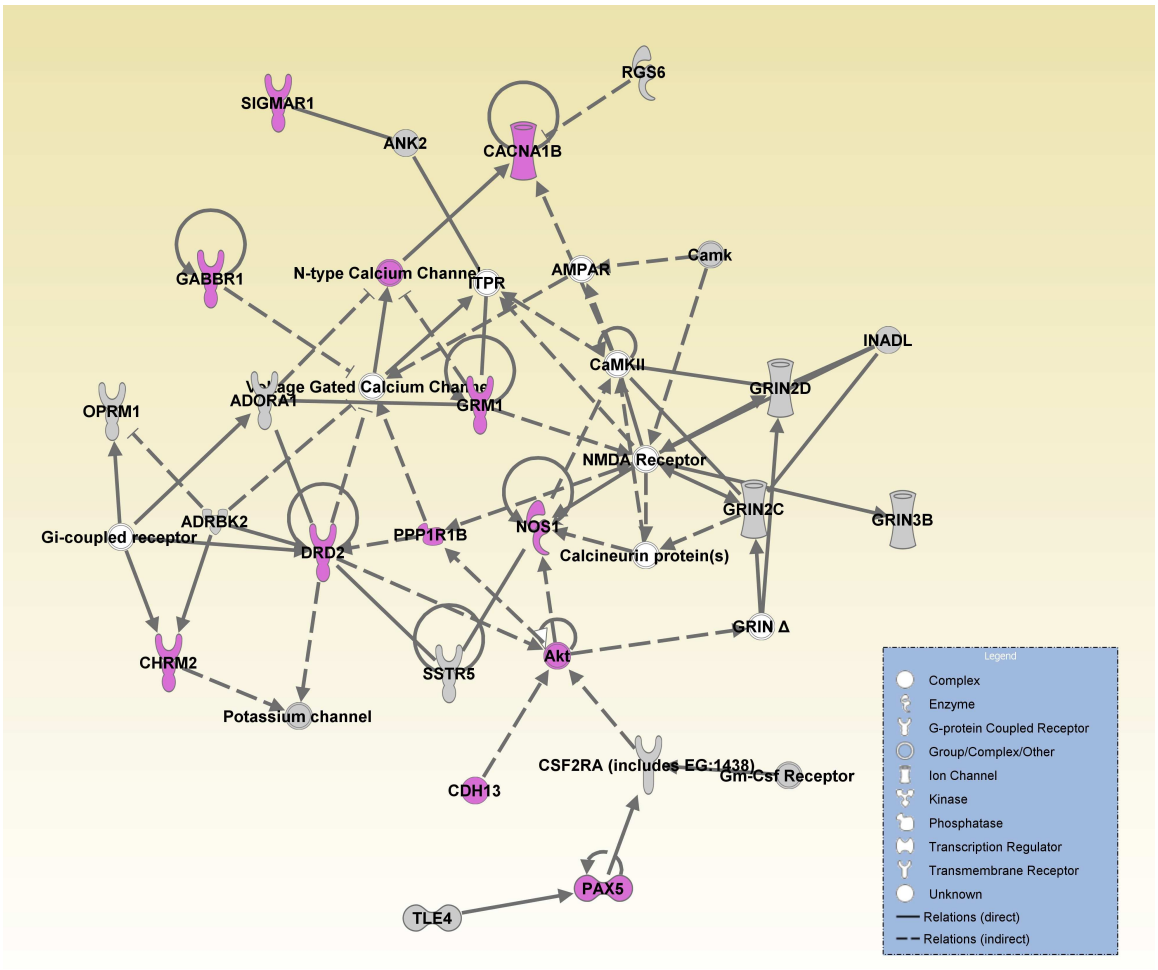

D

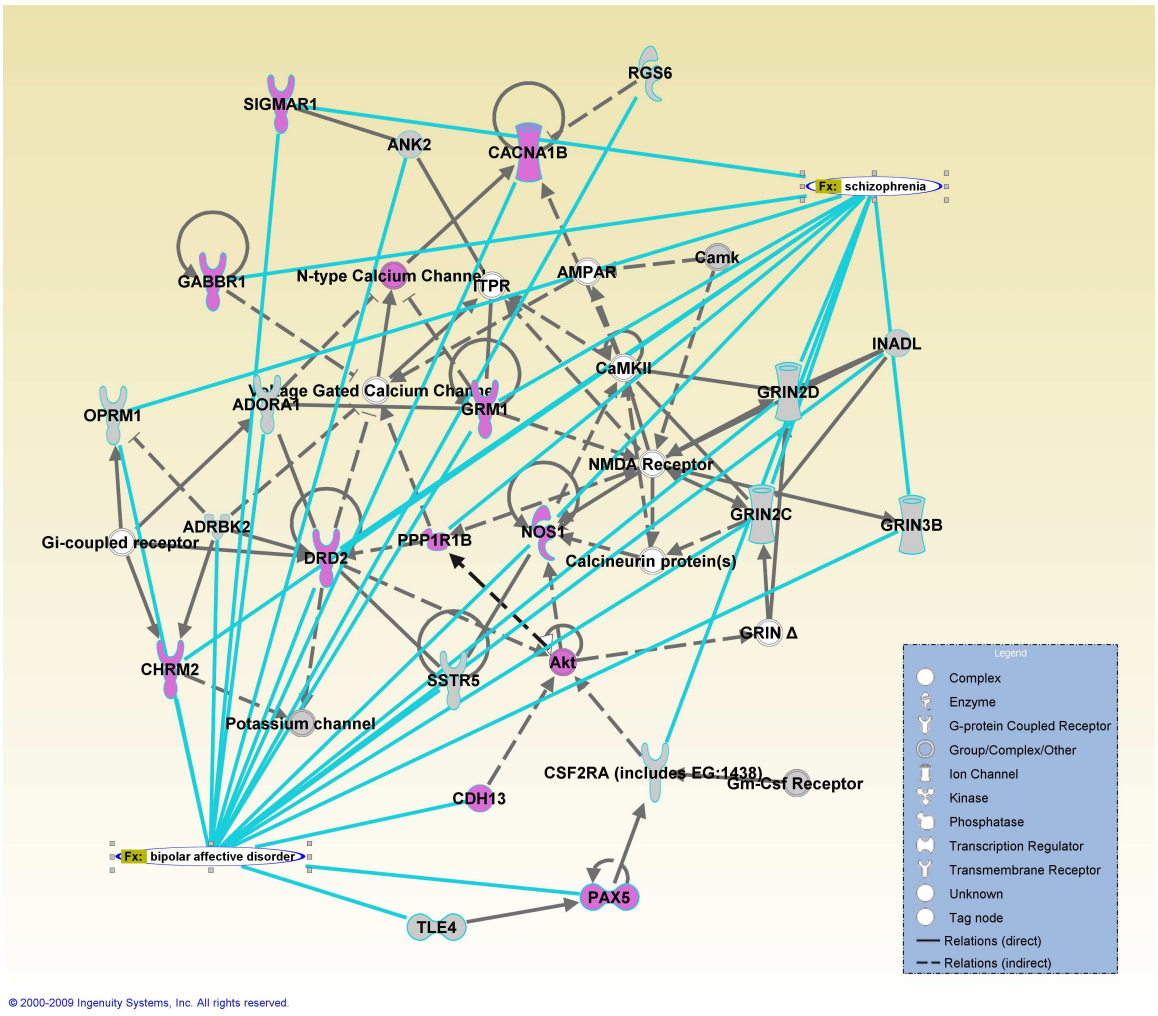

Global miRNA expression profiling was performed following a rapid release of commercially available assays in 2006-2007. Since that time hundreds of additional miRNAs have been discovered and experimentally validated. In general, ubiquitous, highly expressed miRNAs were characterized years ago, and many of these newly

discovered species have tightly restricted spatiotemporal expression signatures. However, the structural and functional complexity of the human brain necessitates updated, comprehensive miRNA expression profiling. Therefore phase II of the expression study is currently underway. Preliminary pathway analysis was performed on the predicted targets of misexpressed miRNAs, and the degree of overlap with established etiological models of schizophrenia was very compelling. However, further benchmarking of the miRSNiPer algorithm and experimental validation of high-priority miRNA target sites are required. Additionally, misexpressed miRNAs must be functionally tested to understand their potential role in the schizophrenic brain, and this functional data can help to refine classification methods. Though we have made several contributions to this young and rapidly evolving research field, there is still much work to be done before miRNAs can be considered reliable biomarkers or therapeutic targets in psychiatric disease.

APPENDIX 1

TaqMan data from developmental miRNA expression study (Chapter 2)

Sample Key:

Pool 1 = gestational age 14 weeks
Pool 2 = gestational age 16 weeks
Pool 3 = gestational age 17 weeks
Pool 4 = gestational age 18 weeks
Pool 5 = gestational age 19 weeks
Pool 6 = gestational age 20 weeks
Pool 7 = age 5 - 98 days
Pool 8 = age 443 - 502 days
Pool 9 = age 1630 - 1733 days
Pool 10 = adult - FirstChoice Human Brain Reference RNA (Ambion)

Expression data, averaged over four technical replicates:

detector	ave Ct 1	ave Ct 2	ave Ct 3	ave Ct 4	ave Ct 5	ave Ct 6	ave Ct 7	ave Ct 8	ave Ct 9	ave Ct 10
MammU6-4395470	18.49	19.52	18.78	18.53	18.33	18.85	20.86	20.85	20.20	18.84
MammU6-4395470	19.30	19.51	18.88	18.62	18.27	18.96	20.62	20.80	20.06	19.19
hsa-miR-9-4373285	18.70	19.10	18.68	18.91	18.70	18.77	20.06	20.97	20.63	20.95
hsa-miR-19b-4373098	20.34	20.38	20.18	20.26	19.97	20.39	22.78	23.91	23.77	23.20
hsa-miR-923-4395264	22.91	20.26	21.23	21.43	21.59	22.29	22.31	21.21	21.24	22.83
hsa-miR-801-4395183	20.33	20.39	20.72	20.87	20.87	21.22	22.37	23.25	23.27	27.95
hsa-miR-17-4395419	21.15	21.62	21.33	21.43	21.14	21.64	24.93	25.66	25.95	25.22
hsa-miR-125b-4373148	23.21	22.58	22.57	22.53	21.98	22.11	24.24	24.60	24.21	22.59
hsa-miR-9*-4395342	22.64	22.80	22.54	22.95	22.83	22.90	23.40	23.63	23.37	25.97
hsa-miR-106a-4395280	21.51	22.00	21.80	21.85	21.61	21.96	25.31	25.92	26.14	25.58
hsa-miR-16-4373121	22.70	22.78	22.50	22.30	22.13	22.96	25.26	25.35	25.27	23.65
RNU48-4373383	24.01	23.96	23.55	23.36	23.03	22.86	24.02	24.68	24.54	22.51
RNU48-4373383	23.92	23.79	23.52	23.31	23.33	23.12	24.44	24.70	24.64	22.44
hsa-miR-26a-4395166	23.76	24.24	23.90	23.99	23.36	23.89	24.71	24.37	24.29	22.56
hsa-miR-19a-4373099	21.73	21.96	21.90	22.25	22.12	22.74	25.70	27.27	27.52	26.20
hsa-miR-126-4395339	24.87	24.96	24.86	24.28	24.29	24.40	23.45	23.46	22.95	22.37
hsa-miR-20a-4373286	22.06	22.42	22.33	22.66	22.05	22.65	25.99	26.96	27.19	26.33
hsa-miR-342-3p-4395371	24.39	24.16	23.97	24.05	22.99	23.55	24.85	24.45	24.83	23.42
hsa-miR-149-4395366	23.73	23.95	23.97	23.87	23.38	23.54	25.27	24.95	24.82	23.73
hsa-miR-484-4381032	23.37	23.95	23.48	23.70	22.92	23.53	25.46	25.46	25.60	23.88
hsa-miR-29a-4395223	24.40	25.30	25.39	25.14	24.93	25.53	24.19	22.88	22.36	22.07
hsa-miR-24-4373072	24.45	24.97	24.92	24.83	24.53	24.94	23.98	23.78	23.12	23.56
hsa-miR-124-4373295	24.96	24.24	24.31	24.13	23.80	23.54	24.73	24.85	24.69	24.92
hsa-let-7b-4395446	24.80	24.40	24.45	24.58	23.93	24.01	25.12	25.97	25.80	23.57
hsa-let-7e-4395517	24.96	24.96	24.98	24.88	24.12	24.63	25.20	25.83	25.68	23.63
hsa-miR-191-4395410	24.97	25.40	24.96	24.95	24.62	24.82	25.60	25.10	24.68	23.87
hsa-miR-331-3p-4373046	24.49	24.92	24.76	24.61	24.19	24.48	25.98	26.07	25.38	24.40
hsa-miR-222-4395387	24.23	25.27	25.19	25.34	25.06	25.69	25.64	24.94	24.64	24.28
hsa-miR-181a-4373117	25.66	24.96	24.62	24.58	23.69	23.95	25.64	25.96	25.96	25.42
hsa-miR-139-5p-4395400	25.87	26.26	25.97	25.48	25.59	25.70	24.57	24.20	23.95	23.86
hsa-miR-132-4373143	26.81	26.45	26.22	25.94	25.97	26.11	23.35	23.25	22.69	24.92
hsa-miR-30c-4373060	25.61	25.74	25.40	25.17	24.96	25.31	25.96	25.38	24.77	23.75
hsa-miR-320-4395388	24.33	24.59	24.67	24.48	24.36	24.49	26.79	26.93	26.96	24.54
hsa-miR-100-4373160	25.84	25.14	24.95	24.96	24.49	24.55	26.46	26.54	26.06	24.60
RNU43-4373375	24.35	24.52	24.66	24.61	24.51	24.66	26.84	26.63	26.11	27.05
hsa-miR-768-3p-4395188	26.56	25.47	25.42	25.14	24.85	24.82	26.08	26.32	25.86	24.40
hsa-miR-939-4395293	25.61	25.30	25.85	25.64	25.95	25.74	25.43	25.73	25.30	25.02
hsa-miR-596-4380959	26.00	25.24	25.72	25.93	25.71	25.64	25.67	25.91	25.75	24.44
hsa-miR-30b-4373290	25.97	26.07	25.76	25.66	25.47	25.78	26.15	26.14	25.33	24.32
hsa-miR-99a-4373008	26.23	25.30	25.34	25.15	24.62	24.63	26.72	26.96	26.51	25.18
hsa-miR-93-4373302	23.69	24.65	24.42	24.59	24.12	24.64	27.76	28.17	27.97	27.28
RNU44-4373384	25.77	25.93	25.56	25.35	25.03	25.27	27.18	27.18	26.80	23.65
hsa-miR-454-4395434	24.13	24.96	24.96	24.98	24.72	25.38	27.71	27.81	27.74	26.66
hsa-miR-218-4373081	26.95	27.03	27.08	26.53	26.41	26.32	25.36	24.96	24.41	24.58

hsa-miR-135b-4395372	23.96	24.24	24.24	23.99	23.82	24.13	27.74	30.46	31.80	26.00
hsa-miR-374b-4381045	25.83	25.79	25.32	25.48	25.38	25.66	26.97	27.52	27.64	26.87
RNU44-4373384	27.01	26.81	26.18	25.96	25.76	25.81	27.45	27.38	27.29	24.21
hsa-miR-149*-4395275	26.77	26.19	26.24	26.49	26.74	26.45	26.63	26.87	26.96	24.86
hsa-miR-204-4373094	28.30	26.98	26.46	26.64	25.61	26.02	27.16	26.83	26.46	23.84
hsa-miR-708-4395452	25.95	26.03	25.89	25.93	25.61	25.62	27.30	27.62	26.98	28.06
hsa-miR-137-4373301	27.70	26.40	25.96	25.76	25.32	25.25	26.25	26.62	27.17	28.61
hsa-miR-140-5p-4373374	26.70	26.91	26.55	26.49	25.85	26.15	27.37	26.95	26.60	25.86
hsa-miR-26b-4395167	25.96	26.57	26.56	26.65	26.33	26.92	27.38	27.13	26.99	25.54
hsa-miR-30a*-4373062	26.93	26.65	26.85	26.93	26.55	27.16	26.67	26.67	26.05	25.91
hsa-let-7g-4395393	26.91	26.78	26.65	26.44	26.02	26.47	27.45	27.56	26.95	25.15
hsa-miR-128-4395327	28.36	26.91	26.95	26.62	26.23	26.14	26.38	26.72	25.95	26.17
hsa-miR-30e*-4373057	26.74	26.93	26.67	26.52	26.57	26.90	26.94	26.73	26.38	26.19
hsa-miR-195-4373105	26.99	27.02	26.99	26.66	26.79	27.21	26.38	27.04	26.22	25.34
hsa-miR-22-4373079	27.67	27.75	27.58	27.07	27.64	27.94	25.28	25.26	24.74	25.86
hsa-miR-138-4395395	29.26	27.70	27.43	26.55	26.60	26.66	26.17	25.96	25.96	25.26
hsa-miR-30e-4395334	27.37	26.95	26.84	26.83	26.53	26.92	27.63	26.94	26.75	25.27
hsa-miR-99b-4373007	25.92	26.93	26.72	26.88	26.41	26.77	27.97	27.87	27.32	25.39
hsa-miR-151-3p-4395365	25.72	26.91	26.70	26.74	26.67	26.92	27.92	27.10	27.14	27.21
hsa-miR-30d-4373059	26.76	26.97	28.27	26.82	26.46	26.88	27.66	27.15	26.74	25.42
hsa-miR-106b-4373155	25.36	25.88	25.80	25.90	25.44	25.82	28.62	28.96	28.85	28.54
hsa-miR-125a-5p-4395309	26.95	27.00	26.64	26.88	26.47	26.53	27.66	27.83	27.58	25.97
hsa-miR-30a-4373061	27.04	27.19	26.94	26.98	26.65	27.04	27.90	27.25	26.89	25.82
hsa-miR-885-5p-4395407	27.97	28.46	27.82	27.83	27.70	27.96	26.77	26.44	25.42	25.37
RNU6B-4373381	25.89	26.75	26.86	26.85	26.70	27.07	28.76	28.61	28.05	26.49
hsa-miR-103-4373158	26.68	27.62	27.49	27.25	27.02	27.04	27.66	27.70	27.00	26.96
hsa-miR-340-4395369	26.84	26.89	26.63	26.79	26.31	26.38	28.03	28.24	28.46	27.96
hsa-miR-425-4380926	26.97	27.60	27.30	27.71	27.34	27.26	27.98	27.18	27.09	26.28
hsa-miR-766-4395177	28.13	27.35	27.22	26.87	26.54	26.94	27.40	27.65	27.22	27.60
RNU24-4373379	26.70	26.74	26.74	26.71	26.57	26.64	28.77	29.06	28.89	27.12
hsa-miR-221-4373077	25.95	27.40	27.40	27.37	27.18	27.48	28.34	27.79	27.34	27.69
hsa-let-7c-4373167	27.74	26.97	27.24	26.82	26.38	26.67	28.06	28.74	28.65	26.77
hsa-miR-376c-4395233	27.92	27.99	27.59	27.05	27.29	27.65	27.56	27.79	27.84	26.22
hsa-miR-378-4395354	27.79	28.03	28.19	27.92	28.30	28.24	27.22	26.74	26.94	26.79
hsa-miR-210-4373089	26.56	26.85	26.70	26.76	26.50	26.69	28.36	29.19	28.93	29.73
hsa-let-7a-4373169	27.93	27.99	27.86	27.59	26.96	27.34	27.98	28.51	28.33	26.12
hsa-miR-21-4373090	27.96	27.94	27.84	27.56	27.40	27.85	28.34	26.60	28.13	27.17
hsa-miR-598-4395179	27.96	28.26	28.18	27.93	28.00	28.25	27.96	27.67	27.22	25.95
hsa-let-7f-4373164	28.04	28.05	27.87	27.67	26.77	27.93	28.30	28.46	27.76	26.79
hsa-miR-886-3p-4395305	26.88	27.18	27.33	26.82	26.81	27.33	29.44	28.96	28.19	28.69
hsa-miR-197-4373102	26.96	27.61	27.38	27.66	27.07	27.82	28.98	28.99	28.19	27.13
hsa-miR-139-3p-4395424	28.73	29.02	28.61	27.96	28.13	28.01	26.91	26.49	25.75	28.19
hsa-miR-650-4381006	27.09	27.18	27.62	27.78	27.30	27.53	28.49	27.96	28.35	28.52
hsa-miR-874-4395379	28.95	28.90	28.39	28.88	28.07	27.93	27.54	26.92	26.71	26.18
hsa-miR-15a-4373123	26.99	26.93	27.16	26.81	26.47	27.50	29.42	29.76	29.00	28.92
hsa-miR-135a-4373140	27.35	26.98	27.01	26.42	26.89	27.96	28.30	29.96	29.69	28.45
hsa-miR-145-4395389	28.97	28.92	28.89	28.17	28.59	28.30	27.83	27.50	27.01	24.85
hsa-miR-124*-4395308	26.91	26.99	26.96	26.91	26.73	26.66	29.11	29.44	28.45	31.04
hsa-miR-301a-4373064	26.35	27.24	26.98	26.96	26.70	27.19	29.31	29.77	29.57	29.65
hsa-miR-15b-4373122	25.98	26.91	26.73	26.96	26.40	27.46	30.06	30.64	30.54	28.28
hsa-miR-15b*-4395284	24.73	25.89	26.18	26.04	25.58	26.84	31.26	32.10	30.65	30.88
hsa-miR-223-4395406	29.95	29.52	29.67	28.67	28.60	28.75	27.24	25.95	26.65	25.54
hsa-miR-7-1*-4381118	27.84	28.16	27.98	27.97	27.30	27.69	29.68	28.67	28.55	26.92
hsa-miR-661-4381009	28.09	27.19	27.29	28.10	28.13	27.71	28.00	27.56	28.78	30.00
hsa-miR-92a-4395169	26.19	26.81	26.60	26.97	26.45	27.12	30.42	30.87	30.66	28.89
hsa-miR-744-4395435	27.57	28.33	28.21	28.24	28.03	28.06	28.95	28.17	27.83	27.95
hsa-miR-135a*-4395343	28.58	27.96	28.09	28.38	28.23	28.16	28.51	27.95	28.28	27.19
hsa-miR-93*-4395250	26.11	27.20	26.96	27.05	26.71	27.10	30.95	30.27	30.08	29.12
hsa-miR-95-4373011	29.40	28.65	28.19	27.90	27.84	28.51	27.65	28.08	27.96	27.63
hsa-miR-769-5p-4395186	28.84	28.64	28.58	28.84	28.68	28.73	27.70	27.09	27.31	27.47
hsa-miR-565-4380942	29.07	28.35	28.01	27.33	27.53	26.95	31.02	29.08	28.20	26.61
hsa-let-7d-4395394	27.95	28.22	28.42	28.32	28.19	28.54	28.99	28.80	28.25	26.68
hsa-miR-126*-4373269	29.35	29.26	28.97	28.48	28.45	28.70	28.38	27.58	27.52	26.46
hsa-miR-374a-4373028	27.58	27.96	27.61	27.80	27.57	27.88	29.68	29.16	29.27	28.63
hsa-miR-130b-4373144	25.68	26.91	26.93	26.70	26.66	26.99	30.92	30.95	30.44	30.98
hsa-miR-186-4395396	27.84	28.58	27.97	27.96	27.24	27.89	29.63	29.24	29.26	27.69
hsa-miR-574-3p-4395460	27.54	28.50	28.10	28.11	27.87	28.23	29.98	28.94	29.41	26.64
hsa-miR-324-5p-4373052	27.69	28.20	28.19	28.13	28.00	27.84	29.22	28.94	28.62	28.53
hsa-miR-127-3p-4373147	28.88	29.10	29.25	28.29	28.87	28.94	28.62	27.99	27.75	25.95
hsa-miR-370-4395386	29.19	28.99	28.79	28.36	29.61	28.69	28.22	27.74	27.53	27.02
hsa-miR-31-4395390	29.91	30.21	30.99	29.44	30.61	30.60	27.63	25.63	25.27	23.89
hsa-miR-424*-4395420	27.68	27.06	28.18	28.11	27.93	28.69	28.95	27.92	28.89	30.87
hsa-miR-328-4373049	29.17	29.17	29.13	28.97	28.44	28.76	28.78	28.41	27.79	25.91
hsa-miR-92b*-4395454	25.46	27.35	27.19	27.03	27.06	28.61	29.25	30.19	29.24	33.16

hsa-miR-660-4380925	27.48	28.45	28.43	28.42	28.41	28.78	28.88	28.92	28.89	27.96
hsa-miR-675-4395192	28.22	27.95	28.20	28.57	29.02	28.72	28.40	28.58	28.49	28.50
hsa-miR-423-5p-4395451	27.25	28.79	28.72	27.75	27.36	28.26	28.97	29.72	29.97	27.94
hsa-miR-382-4373019	28.86	29.77	29.45	29.00	28.41	28.24	27.84	27.82	28.19	27.36
hsa-miR-20b-4373263	26.73	27.95	27.87	27.90	27.91	28.38	29.90	29.60	29.44	29.81
hsa-miR-628-5p-4395544	29.08	28.94	28.95	28.58	28.27	28.85	28.35	28.21	28.13	28.53
hsa-miR-146a-4373132	30.42	29.52	29.18	28.71	28.97	29.32	27.39	27.54	27.49	27.42
hsa-miR-181a*-4373086	28.10	27.98	27.86	27.51	27.45	27.55	29.76	29.97	29.35	30.54
hsa-miR-323-3p-4395338	29.46	29.72	29.50	28.67	28.99	29.23	28.34	27.81	27.95	26.42
hsa-miR-146b-5p-4373178	30.40	29.95	30.03	29.72	29.26	29.17	27.96	26.52	26.12	27.06
hsa-miR-566-4380943	28.49	27.25	27.41	28.18	28.43	27.95	28.99	28.94	30.33	30.22
hsa-miR-625*-4395543	28.35	28.01	28.13	28.54	28.39	28.24	29.78	29.50	29.97	27.57
hsa-miR-345-4395297	27.26	28.29	27.96	27.83	27.55	27.76	30.83	30.80	31.40	27.65
hsa-miR-760-4395439	28.61	28.79	28.89	28.64	28.51	28.79	28.95	28.94	28.87	28.45
hsa-miR-494-4395476	28.44	29.11	29.91	28.98	29.51	28.26	28.22	28.69	28.16	28.47
hsa-miR-181c*-4395444	28.70	27.96	27.77	27.91	27.41	27.91	29.56	30.32	29.38	31.02
hsa-miR-361-3p-4395227	28.81	28.75	29.12	28.63	28.97	29.39	29.63	28.97	28.05	27.78
hsa-miR-411-4381013	29.83	29.58	29.90	28.59	28.72	29.31	28.47	28.36	27.97	27.43
hsa-miR-129-3p-4373297	29.22	29.98	29.75	28.94	29.58	29.65	28.97	28.19	27.81	26.17
hsa-miR-886-5p-4395304	27.41	27.99	28.00	27.64	27.31	27.97	31.28	30.24	29.95	30.95
hsa-miR-130b*-4395225	26.45	27.30	27.26	27.37	26.73	27.26	31.42	32.67	31.81	30.95
hsa-miR-379-4373349	29.95	29.79	29.91	28.98	29.70	29.50	28.18	27.98	27.42	27.97
hsa-miR-125b-2*-4395269	30.09	27.77	28.08	27.67	26.95	28.12	31.54	31.66	29.86	27.74
hsa-miR-181c-4373115	28.56	27.80	27.71	28.00	27.53	28.29	29.78	30.40	30.96	30.52
hsa-miR-222*-4395208	26.14	28.29	28.57	27.68	27.81	28.17	31.55	29.95	29.50	32.07
hsa-miR-324-3p-4395272	28.69	28.89	28.97	28.87	28.78	28.49	29.57	29.22	29.04	29.52
hsa-miR-92a-1*-4395248	28.13	27.42	28.84	28.58	28.62	27.81	30.36	30.06	29.72	30.58
hsa-miR-590-5p-4395176	28.34	28.47	28.03	28.09	28.02	28.75	30.48	30.94	30.63	28.40
hsa-miR-567-4380944	28.31	28.08	28.48	29.94	30.92	29.11	28.91	29.75	29.35	27.79
hsa-miR-143-4395360	29.94	30.53	30.98	29.18	29.46	29.09	28.77	28.64	28.26	26.12
hsa-miR-486-5p-4378096	29.46	29.96	29.33	29.68	29.43	29.15	29.31	28.90	29.77	26.02
hsa-miR-571-4381016	29.61	28.78	29.20	29.17	29.15	28.81	28.68	29.01	29.10	29.51
hsa-miR-431-4395173	29.18	30.37	30.14	28.38	29.19	31.02	29.44	27.46	27.99	28.28
hsa-miR-657-4380922	28.84	28.95	28.14	29.30	29.37	29.64	29.36	29.59	29.49	28.83
hsa-miR-130a-4373145	27.44	28.49	27.97	27.97	27.67	27.83	30.77	31.85	31.37	30.31
hsa-miR-532-5p-4380928	27.68	28.99	28.98	28.82	28.65	29.90	30.66	30.01	30.42	27.86
hsa-miR-491-5p-4381053	30.58	29.80	29.97	29.37	29.62	29.63	29.76	28.66	27.87	26.78
hsa-miR-935-4395289	30.01	29.69	29.35	29.49	29.52	29.46	30.00	29.64	28.98	26.11
hsa-miR-23a-4373074	28.39	30.06	29.91	29.51	29.02	29.65	27.90	29.31	29.51	29.11
hsa-miR-214-4395417	28.82	29.82	29.99	29.45	28.37	28.42	28.89	29.06	29.49	30.34
hsa-miR-193b-4395478	29.22	29.90	29.96	29.10	29.62	29.21	29.80	29.27	29.47	27.22
hsa-miR-134-4373299	29.95	29.44	29.43	29.14	29.66	30.03	29.01	29.24	29.13	28.16
hsa-miR-340*-4395370	29.03	29.10	28.98	28.76	28.44	28.97	30.67	30.76	30.01	28.62
hsa-miR-584-4381026	30.10	29.26	30.02	29.48	30.09	30.42	28.80	28.36	28.34	28.49
hsa-miR-433-4373205	30.65	30.11	30.16	29.36	30.91	31.01	28.63	27.71	27.97	26.90
hsa-miR-150-4373127	30.81	30.95	30.32	29.53	29.77	30.14	28.53	28.39	28.07	27.21
hsa-miR-125b-1*-4395489	27.68	27.69	27.86	27.75	27.52	27.92	30.76	31.37	31.47	33.97
hsa-miR-497-4373222	31.94	29.75	30.84	29.99	29.47	29.82	28.47	29.04	28.16	26.74
hsa-miR-877-4395402	29.25	28.63	29.21	29.97	29.82	29.41	29.61	29.15	29.65	29.79
hsa-miR-27a-4373287	28.97	30.19	29.79	29.81	29.19	30.21	28.42	29.64	28.95	29.36
hsa-miR-34a-4395168	30.98	30.95	31.38	30.93	30.46	31.85	28.86	26.98	26.37	25.92
hsa-miR-383-4373018	33.02	30.94	30.25	30.03	29.88	30.48	27.66	27.71	27.48	27.31
hsa-miR-339-3p-4395295	29.66	29.31	29.32	29.13	28.66	28.98	30.75	29.96	29.95	29.19
hsa-miR-592-4380956	30.50	30.21	29.96	29.38	29.80	30.08	28.77	28.73	28.12	29.46
hsa-miR-539-4378103	30.94	30.51	30.48	30.08	29.99	31.21	29.60	28.38	27.63	26.57
hsa-miR-335-4373045	29.97	29.47	29.34	29.04	29.33	29.78	29.45	29.77	29.24	30.60
hsa-miR-181a-2*-4395428	28.05	28.52	28.64	28.84	28.31	29.42	31.25	31.98	31.69	29.69
hsa-miR-941-4395294	28.53	29.03	28.94	29.60	28.41	29.09	30.93	31.74	30.37	29.83
hsa-miR-27b-4373068	30.96	30.25	30.39	29.66	29.95	30.96	29.68	29.01	28.40	27.67
hsa-miR-487b-4378102	30.32	30.96	30.61	30.23	30.16	30.52	29.47	28.92	28.82	27.75
hsa-miR-23b-4373073	30.56	30.48	30.06	30.38	29.94	32.06	29.57	29.02	28.46	27.26
hsa-miR-644-4380999	29.88	29.34	29.44	29.70	30.27	29.57	29.97	29.95	30.22	29.72
hsa-miR-99a*-4395252	29.63	28.73	28.86	28.62	28.40	28.57	31.71	31.37	31.36	30.97
hsa-miR-140-3p-4395345	29.87	30.32	29.69	29.99	29.12	29.83	30.63	29.97	30.35	28.75
hsa-miR-409-3p-4395443	29.45	30.61	31.13	29.96	30.85	30.30	30.50	29.61	29.35	27.07
hsa-miR-7-4378130	32.18	30.60	29.31	29.66	31.30	31.73	28.59	27.34	27.92	30.37
hsa-miR-652-4395463	29.74	30.38	29.99	29.81	30.23	29.84	30.64	29.93	29.93	28.68
hsa-miR-28-3p-4395557	29.59	29.90	29.98	29.97	29.74	29.62	30.87	30.54	30.53	29.19
hsa-miR-604-4380973	29.45	29.36	29.79	30.64	29.94	29.97	30.34	29.85	30.06	30.54
hsa-miR-29c-4395171	30.36	31.23	31.17	30.81	30.98	31.39	30.03	28.36	27.98	27.64
hsa-miR-135b*-4395270	26.41	27.77	27.30	27.29	27.59	27.25	32.81	36.43	32.45	34.85
hsa-miR-639-4380987	29.31	28.99	29.01	29.52	30.18	29.99	30.27	29.93	29.40	33.62
hsa-miR-432-4373280	30.08	30.78	31.28	29.89	31.61	30.72	29.77	29.11	29.35	27.66
hsa-miR-185-4395382	29.98	30.53	30.70	30.55	29.96	30.24	30.29	28.98	29.44	29.61

hsa-miR-564-4380941	30.03	29.14	29.61	30.99	30.22	29.88	29.65	29.67	30.26	31.11
hsa-miR-18a-4395533	27.64	28.58	28.62	28.91	28.53	28.89	31.95	32.35	32.42	32.90
hsa-miR-486-3p-4395204	30.23	30.99	30.17	30.29	28.92	30.42	29.98	30.53	30.73	28.67
hsa-miR-25-4373071	27.62	28.96	28.94	29.02	28.68	29.66	32.74	32.45	32.77	30.13
hsa-miR-106b*-4395491	26.42	27.81	27.38	27.81	27.25	28.30	35.35	33.67	35.92	31.13
hsa-miR-770-5p-4395189	31.97	30.49	31.04	30.23	30.82	30.70	30.07	28.92	28.91	28.31
hsa-miR-187-4373307	32.26	31.00	32.00	30.18	29.91	33.19	28.33	27.95	28.74	28.32
hsa-miR-449b-4381011	31.96	29.75	28.05	28.12	28.63	31.33	31.29	31.89	30.97	29.98
hsa-miR-199a-3p-4395415	29.58	31.36	31.36	29.98	30.00	29.32	30.28	30.68	30.21	29.45
hsa-miR-490-3p-4373215	32.01	29.87	30.45	29.96	30.61	30.65	28.52	29.30	28.91	32.15
hsa-miR-449a-4373207	33.16	28.75	26.75	27.15	28.23	35.84	31.13	30.45	31.46	29.52
hsa-miR-488-4395468	30.95	30.76	29.96	30.39	29.42	29.50	30.27	30.41	30.17	30.62
hsa-miR-495-4381078	30.45	31.30	31.42	30.83	30.86	30.94	30.11	29.13	29.06	28.43
hsa-miR-335*-4395296	29.96	30.11	29.89	29.82	29.96	30.00	30.80	30.36	30.98	30.78
hsa-miR-330-3p-4373047	31.07	31.98	31.75	31.69	30.90	30.55	29.75	28.94	28.61	27.52
hsa-miR-668-4395181	30.32	31.02	31.37	30.00	31.78	33.27	29.73	28.51	28.27	28.51
hsa-miR-331-5p-4395344	29.32	29.27	30.08	29.05	29.14	30.01	30.96	31.44	30.62	32.96
hsa-miR-505*-4395198	29.06	29.47	29.67	29.40	29.41	29.68	31.59	32.98	31.35	30.60
hsa-miR-107-4373154	29.64	30.35	30.19	29.59	31.01	30.30	30.82	31.30	30.23	30.04
hsa-miR-767-5p-4395182	28.53	29.29	29.12	28.86	29.38	29.47	31.77	32.78	31.79	32.85
hsa-miR-654-5p-4381014	29.34	30.04	29.51	29.28	29.95	32.82	29.84	28.83	29.44	34.86
hsa-miR-605-4386742	30.44	29.49	29.99	30.75	29.25	31.09	32.53	30.72	30.34	29.40
hsa-miR-18b-4395328	28.27	29.06	29.62	29.98	28.68	28.86	31.85	31.96	32.93	32.87
hsa-miR-628-3p-4395545	31.45	30.94	31.05	30.82	30.70	30.75	30.06	29.46	29.35	29.87
hsa-miR-646-4381002	29.68	29.32	29.65	29.04	30.71	30.45	31.99	30.84	31.30	31.50
hsa-miR-188-5p-4395431	30.39	29.62	30.13	30.58	30.34	30.52	30.48	31.01	31.43	29.98
hsa-miR-1-4395333	30.95	30.47	32.08	31.31	31.29	31.97	29.12	28.95	29.08	29.46
hsa-miR-376a-4373026	30.64	30.54	30.28	29.85	30.53	30.97	30.46	30.60	30.80	30.02
hsa-miR-610-4380980	30.71	30.95	30.17	30.30	31.37	29.76	29.78	30.66	30.95	30.12
hsa-miR-361-5p-4373035	30.51	31.02	30.14	30.29	29.75	30.13	30.83	30.84	30.58	30.82
hsa-miR-136*-4395211	31.43	31.44	31.26	30.46	30.97	31.28	30.31	29.77	29.29	28.70
hsa-miR-101-4395364	30.37	30.38	30.12	29.94	29.64	30.30	31.40	31.02	30.87	30.96
hsa-miR-659-4380924	29.96	29.25	30.19	30.52	30.86	30.16	30.98	31.50	32.32	29.46
hsa-miR-505-4395200	28.23	29.82	29.68	29.02	28.74	28.46	29.95	30.22	40.00	31.09
hsa-miR-33a*-4395247	28.90	29.83	30.00	29.11	29.52	29.40	32.90	32.83	32.02	31.08
hsa-miR-501-5p-4373226	28.09	31.62	29.48	30.21	31.08	30.99	33.00	31.66	30.04	29.47
hsa-miR-138-2*-4395255	30.46	31.49	31.39	30.22	30.06	31.50	32.05	31.15	30.18	27.73
hsa-miR-638-4380986	31.88	29.79	30.34	30.77	30.83	30.37	30.98	30.21	30.80	30.44
hsa-miR-583-4381025	30.77	29.77	30.46	30.38	30.47	30.60	30.87	30.89	31.28	30.97
hsa-miR-152-4395170	30.90	31.98	31.95	30.43	30.84	31.00	30.24	29.81	29.70	29.99
hsa-miR-630-4380970	29.77	29.70	30.52	30.48	29.66	30.52	31.45	31.39	31.52	32.00
hsa-miR-532-3p-4395466	28.94	30.95	30.53	30.37	30.75	31.07	31.94	31.83	32.01	28.79
hsa-miR-301b-4395503	27.85	29.35	28.97	29.48	28.80	29.28	32.84	33.43	33.32	33.94
hsa-miR-487a-4378097	30.75	32.97	30.58	30.21	31.08	30.81	31.08	30.66	31.17	28.56
hsa-miR-575-4381020	30.65	29.76	29.44	29.98	30.73	30.03	31.13	31.19	32.09	32.95
hsa-miR-20a*-4395548	29.34	29.55	29.36	29.24	29.14	29.65	32.63	33.64	33.70	31.95
hsa-miR-17*-4395532	27.65	27.97	27.68	27.50	27.78	28.55	36.16	33.24	31.70	40.00
hsa-miR-342-5p-4395258	31.94	31.56	31.79	30.54	30.08	29.60	31.10	31.63	30.65	29.45
hsa-miR-455-5p-4378098	29.79	30.85	30.57	30.88	31.03	31.48	31.99	31.57	31.96	28.36
hsa-miR-208b-4395401	30.63	30.95	29.56	29.02	29.97	28.95	30.55	29.90	28.96	40.00
hsa-miR-887-4395485	28.41	30.45	29.33	29.89	29.56	31.20	40.00	29.64	30.53	29.53
hsa-miR-550*-4380954	30.33	30.90	29.99	29.95	29.86	29.89	31.95	31.89	32.97	30.97
hsa-miR-339-5p-4395368	29.57	31.01	29.99	31.26	30.63	30.65	32.36	32.19	31.45	29.68
hsa-miR-485-5p-4373212	29.01	28.92	31.89	28.45	40.00	40.00	28.13	28.19	28.03	26.21
hsa-miR-29c*-4381131	31.71	32.11	33.03	32.14	32.41	32.00	30.73	28.83	28.21	27.77
hsa-miR-643-4380997	30.75	29.35	30.12	31.05	32.01	30.68	30.79	30.95	31.32	31.93
hsa-miR-409-5p-4395442	29.63	31.10	35.18	30.49	30.51	31.93	30.71	30.45	29.41	29.69
hsa-miR-22*-4395412	32.46	31.60	31.51	31.80	30.97	32.01	30.63	29.44	29.24	29.59
hsa-miR-212-4373087	32.58	31.96	31.93	31.42	31.98	32.64	29.31	29.32	29.02	29.10
hsa-miR-365-4373194	31.65	32.41	32.37	31.95	31.85	31.36	30.47	30.06	29.28	27.87
hsa-miR-591-4380955	30.06	29.96	31.14	30.60	30.48	31.28	31.36	31.33	30.10	32.95
hsa-miR-632-4380977	29.36	30.64	30.39	30.68	30.50	30.46	30.99	32.48	31.04	32.98
hsa-miR-34a*-4395427	32.29	31.59	34.34	30.61	29.74	34.44	30.61	29.93	28.78	27.30
hsa-miR-28-5p-4373067	30.81	31.68	31.12	30.89	30.59	30.82	31.32	30.97	31.01	30.58
hsa-miR-193b*-4395477	29.37	30.17	30.97	29.53	40.00	30.02	30.98	29.78	29.62	29.58
hsa-miR-483-5p-4395449	30.00	30.63	31.85	30.21	30.88	29.81	30.35	31.97	31.07	33.26
hsa-miR-509-3p-4395347	32.08	31.05	31.50	30.77	31.97	31.59	29.65	29.80	30.94	30.95
hsa-miR-10a-4373153	31.83	31.15	31.47	30.51	30.94	30.13	30.99	32.66	31.80	29.40
hsa-miR-192-4373108	31.44	31.62	30.97	30.62	30.96	31.12	31.22	31.56	31.41	30.00
hsa-miR-19b-1*-4395536	29.30	29.42	29.46	29.50	29.04	29.63	33.99	33.00	34.58	33.62
hsa-miR-338-3p-4395363	32.45	32.32	31.95	32.00	30.96	32.38	30.57	29.55	29.14	30.49
hsa-miR-142-3p-4373136	31.97	32.27	31.83	31.69	32.36	32.15	30.20	29.53	30.58	29.34
hsa-miR-30d*-4395416	30.55	30.99	31.08	31.01	30.44	30.67	32.33	31.80	31.36	31.98
hsa-miR-223*-4395209	30.91	33.22	31.15	32.35	31.93	30.76	31.43	28.93	30.54	31.14

hsa-miR-455-3p-4395355	29.30	31.59	30.39	30.52	31.21	31.45	31.85	36.05	32.94	27.33
hsa-miR-648-4381004	31.02	30.61	31.00	31.03	31.30	31.32	31.94	31.94	31.59	31.18
hsa-miR-215-4373084	31.61	31.78	30.79	31.66	30.04	31.53	30.99	31.01	32.46	31.06
hsa-miR-98-4373009	30.95	31.73	32.02	31.84	30.98	31.08	31.38	31.65	31.34	30.01
hsa-miR-148b-4373129	30.31	30.95	31.23	31.11	30.92	31.53	32.46	32.29	31.76	30.45
hsa-miR-200c-4395411	31.68	30.98	31.13	30.99	30.53	30.84	35.02	30.69	31.40	29.79
hsa-miR-380*-4373021	31.83	30.75	31.18	30.50	31.47	31.14	31.94	31.02	30.72	32.49
hsa-miR-219-5p-4373080	31.53	31.87	34.00	33.88	33.99	33.04	29.83	28.37	27.76	28.97
hsa-miR-517a-4395513	32.18	31.42	34.75	33.40	31.24	32.17	30.07	29.28	29.13	29.60
hsa-miR-432*-4378076	31.44	31.59	31.89	30.84	32.02	32.04	30.94	32.08	30.66	29.78
hsa-miR-302a*-4395492	31.58	31.71	31.37	31.71	31.01	31.09	30.72	31.67	31.18	31.25
hsa-miR-600-4380963	31.61	30.15	30.81	29.98	30.51	29.85	30.45	30.88	29.58	40.00
hsa-miR-129-5p-4373171	31.89	32.53	31.56	32.97	31.23	33.29	29.77	30.11	30.26	30.27
hsa-miR-200a-4378069	31.86	31.59	31.03	31.44	31.10	30.72	31.90	31.64	31.63	30.99
hsa-miR-589*-4380953	30.52	30.44	30.08	31.11	32.85	32.65	33.11	33.96	30.18	29.12
hsa-let-7g*-4395229	31.02	31.13	31.68	30.84	30.50	31.92	32.96	31.60	31.48	31.06
hsa-miR-576-3p-4395462	30.00	29.81	29.95	30.77	30.56	30.59	32.06	31.98	33.04	35.98
hsa-miR-744*-4395436	31.46	32.05	31.44	31.35	31.03	31.34	32.97	31.50	31.21	30.48
hsa-miR-518d-3p-4373248	32.03	40.00	29.66	31.43	31.06	29.79	29.58	29.45	30.23	31.65
hsa-miR-27b*-4395285	31.29	31.54	30.98	32.25	33.97	30.81	30.59	32.61	31.11	29.91
hsa-miR-194-4373106	31.57	31.30	31.80	31.27	31.34	31.42	32.20	31.97	31.93	30.52
hsa-miR-452-4395440	29.79	30.87	30.90	31.29	32.00	31.34	33.00	32.73	31.45	32.18
hsa-miR-587-4380950	31.71	30.68	31.60	32.03	31.99	31.53	31.54	31.33	31.55	31.72
hsa-miR-504-4395195	32.95	32.33	31.40	30.93	30.18	31.37	31.49	33.56	31.39	30.08
hsa-miR-99b*-4395307	30.09	32.53	31.79	30.40	30.87	32.99	32.39	32.05	32.30	30.45
hsa-miR-451-4373360	32.75	32.51	32.95	32.50	32.58	32.66	29.96	30.29	30.95	28.75
hsa-miR-148a-4373130	31.64	32.41	32.08	31.97	30.95	30.48	30.59	31.72	32.83	31.34
hsa-miR-127-5p-4395340	34.04	31.49	31.53	34.20	31.40	31.34	30.81	32.04	29.67	29.52
hsa-miR-219-2-3p-4395501	40.00	33.11	34.90	30.38	40.00	32.33	27.25	26.49	26.57	25.06
hsa-miR-362-5p-4378092	30.72	31.54	31.60	31.45	31.18	32.45	31.96	31.75	32.98	30.62
hsa-miR-30c-1*-4395219	29.95	28.94	29.37	31.42	29.63	30.73	31.54	40.00	31.80	32.92
hsa-miR-758-4395180	31.71	32.89	32.34	31.82	32.96	31.65	31.37	30.61	30.58	30.50
hsa-miR-640-4386743	32.28	30.01	31.55	31.63	31.95	32.24	31.47	31.63	31.53	32.33
hsa-miR-655-4381015	32.53	32.65	31.95	31.58	31.81	32.15	31.94	31.81	30.82	29.41
hsa-miR-509-5p-4395346	32.70	32.49	30.89	31.26	33.97	31.72	30.46	30.30	32.27	30.80
hsa-miR-216b-4395437	27.13	30.82	31.42	29.66	29.31	28.98	40.00	32.44	35.88	31.47
hsa-miR-105-4395278	31.00	32.27	31.23	30.19	31.24	30.29	31.66	32.35	33.93	33.04
hsa-miR-377*-4395239	31.75	33.91	31.16	30.70	33.90	30.68	32.05	32.16	30.70	30.31
hsa-miR-296-5p-4373066	29.95	30.75	30.71	30.25	29.80	30.98	33.63	36.06	33.61	31.61
hsa-miR-330-5p-4395341	40.00	33.26	34.09	29.33	30.02	31.22	30.75	29.67	29.22	29.87
hsa-miR-410-4378093	32.96	32.98	32.80	31.94	32.50	32.02	31.11	30.76	30.35	30.02
hsa-miR-153-4373305	33.80	31.76	31.45	30.91	30.75	31.42	31.02	31.96	31.61	32.95
hsa-miR-522-4395524	33.95	31.51	32.02	31.93	30.01	30.89	31.30	32.00	33.06	31.08
hsa-miR-485-3p-4378095	32.43	33.27	32.26	31.99	31.54	32.11	32.92	31.48	31.37	28.53
hsa-miR-133a-4395357	35.86	32.96	33.05	31.87	32.81	33.91	30.95	29.56	28.78	28.39
hsa-miR-190-4373110	30.82	31.96	31.79	31.73	31.83	32.07	32.05	32.18	32.09	31.83
hsa-miR-582-3p-4395510	31.50	33.89	30.91	30.27	30.59	29.43	31.93	31.72	36.98	31.24
hsa-miR-508-3p-4373233	31.98	31.18	30.80	31.25	30.81	31.50	28.94	30.87	31.46	40.00
hsa-miR-425*-4395413	31.60	32.39	32.96	32.30	32.13	32.56	31.58	32.03	32.02	29.25
hsa-miR-572-4381017	32.06	31.74	31.03	31.78	31.89	31.48	31.81	32.57	32.48	32.04
hsa-miR-888-4395323	31.63	33.33	30.92	31.81	30.05	30.02	30.92	32.80	35.95	31.63
hsa-miR-15a*-4395530	30.74	31.27	30.54	30.62	30.78	31.71	32.97	33.10	34.96	32.82
hsa-miR-595-4395178	30.55	30.92	31.53	31.36	30.25	30.21	40.00	32.84	31.10	30.82
hsa-miR-885-3p-4395483	29.68	40.00	29.92	40.00	28.62	40.00	28.74	28.26	25.68	28.80
hsa-miR-892b-4395325	33.05	31.40	30.59	31.65	31.97	31.31	32.98	33.71	31.34	31.75
hsa-miR-617-4380994	33.10	30.55	32.18	31.04	30.96	30.99	31.29	33.66	32.24	33.87
hsa-miR-656-4380920	33.62	32.70	33.63	33.07	32.32	32.69	31.73	31.32	29.94	29.00
hsa-miR-203-4373095	32.23	33.39	31.66	32.96	31.91	32.48	33.08	30.88	30.99	30.46
hsa-miR-202-4395474	32.09	31.71	31.59	32.42	31.59	30.91	31.59	31.71	33.93	32.58
hsa-miR-138-1*-4395273	32.41	32.00	31.70	32.10	32.70	32.10	32.61	31.76	31.79	31.09
hsa-miR-582-5p-4395175	32.97	30.93	31.80	30.97	30.84	30.52	33.21	33.59	33.57	32.21
hsa-miR-200b-4395362	31.26	31.71	32.48	32.00	31.02	32.21	33.74	33.72	31.55	30.96
hsa-miR-513-3p-4395202	31.62	31.30	32.16	32.06	31.63	32.18	31.98	33.16	33.95	30.76
hsa-miR-625-4395542	31.96	31.96	31.77	31.56	31.26	31.68	34.09	33.26	33.25	30.10
hsa-miR-543-4395487	32.97	32.80	33.43	31.75	32.70	33.35	32.02	31.71	31.23	29.02
hsa-miR-649-4381005	32.31	30.80	31.48	31.49	32.23	31.58	33.13	31.97	32.13	33.97
hsa-miR-500-4395539	31.13	32.89	31.98	31.91	31.64	32.15	33.65	33.08	32.02	30.98
hsa-miR-21*-4395549	30.45	32.14	31.00	32.05	31.75	32.52	36.00	31.19	32.58	32.71
hsa-miR-337-5p-4395267	31.20	33.34	33.99	31.75	32.46	32.09	32.11	32.43	32.03	31.04
hsa-miR-623-4386740	32.53	31.91	31.89	33.10	32.82	32.14	32.36	32.05	33.16	30.55
hsa-miR-573-4381018	31.63	32.17	32.20	31.42	32.56	32.19	32.47	33.01	33.18	31.84
hsa-miR-489-4395469	35.64	32.96	29.74	29.88	33.53	36.93	32.62	30.68	30.49	30.37
hsa-miR-373*-4373279	28.07	28.31	28.99	29.89	29.16	28.88	40.00	40.00	40.00	29.62
hsa-miR-629-4395547	33.29	31.11	31.00	30.94	31.80	30.92	32.35	32.88	35.93	32.95

hsa-miR-29b-4373288	32.21	33.12	33.99	35.56	34.71	33.99	32.15	29.08	29.23	29.16
hsa-miR-873-4395467	34.98	33.19	31.77	31.18	32.62	32.84	31.23	31.92	31.50	32.09
hsa-miR-876-5p-4395316	32.92	32.41	31.11	31.16	31.73	32.24	30.18	31.19	30.64	40.00
hsa-miR-100*-4395253	31.24	30.77	30.79	30.73	30.64	30.48	35.01	34.08	35.64	34.97
hsa-miR-145*-4395260	37.00	31.84	31.57	33.53	31.84	32.50	32.62	32.44	31.09	30.06
hsa-miR-629*-4380969	31.60	31.24	30.58	30.80	31.12	31.33	34.33	34.54	33.96	35.39
hsa-miR-190b-4395374	32.12	33.99	31.30	32.50	32.09	32.30	33.39	32.07	32.71	32.69
hsa-miR-524-3p-4378087	32.70	32.26	32.61	33.28	31.92	32.81	32.63	31.07	31.38	34.51
hsa-miR-101*-4395254	31.70	30.37	31.11	30.49	31.16	30.98	33.14	34.71	31.66	40.00
hsa-miR-302d-4373063	31.15	30.43	30.58	32.03	32.45	31.11	40.00	34.17	31.88	31.57
hsa-miR-519a-4395526	31.98	33.15	32.69	32.14	32.02	33.04	36.03	31.44	31.45	31.75
hsa-miR-875-5p-4395314	33.56	32.04	32.33	32.64	33.39	32.98	32.70	32.63	32.79	30.63
hsa-miR-548b-5p-4395519	30.64	32.89	34.94	31.19	31.11	31.07	33.10	31.95	33.39	35.66
hsa-miR-769-3p-4395190	40.00	31.30	40.00	31.60	29.98	31.73	30.99	32.08	29.24	29.08
hsa-miR-422a-4395408	31.77	32.98	32.30	32.60	32.33	33.61	32.78	32.83	33.75	31.14
hsa-miR-326-4373050	32.12	33.99	32.80	32.47	30.84	31.03	33.82	34.18	33.85	31.29
hsa-miR-29a*-4395558	31.55	32.26	32.65	32.96	32.40	33.86	35.01	31.66	31.49	32.76
hsa-miR-346-4373038	32.07	40.00	30.62	40.00	32.43	30.46	30.98	31.12	31.64	27.37
hsa-miR-876-3p-4395336	32.63	34.01	36.03	30.91	32.36	31.83	32.29	32.67	31.08	32.89
hsa-miR-889-4395313	33.69	33.95	35.38	32.32	32.96	34.16	32.24	31.56	30.94	30.18
hsa-miR-551b*-4395457	32.00	33.00	32.52	32.61	31.52	31.84	33.86	32.87	33.05	34.98
hsa-miR-193a-5p-4395392	35.03	33.83	35.95	32.62	33.16	32.73	32.54	31.89	31.78	28.87
hsa-miR-922-4395263	33.47	31.75	31.32	33.02	31.62	32.04	33.50	34.04	31.75	35.98
hsa-miR-16-1*-4395531	29.93	30.03	30.33	31.55	30.27	30.80	40.00	40.00	31.70	33.90
hsa-miR-7-2*-4395425	33.74	32.77	33.99	31.93	32.53	33.47	34.90	32.85	31.07	31.44
hsa-miR-891a-4395302	34.23	32.28	30.38	31.64	31.94	30.64	35.73	36.87	34.08	31.32
hsa-miR-144*-4395259	33.80	32.82	32.29	33.96	33.97	33.67	31.93	32.55	33.21	30.96
hsa-miR-636-4395199	33.95	32.98	33.16	32.88	32.94	32.24	32.53	34.04	33.63	31.07
hsa-miR-221*-4395207	30.43	36.34	32.34	30.94	31.85	30.35	36.72	30.02	30.46	40.00
hsa-miR-29b-2*-4395277	35.90	40.00	40.00	31.41	33.23	32.23	29.49	29.75	28.91	29.19
hsa-miR-198-4395384	31.01	31.80	31.56	32.01	31.90	35.77	30.70	33.04	32.73	40.00
hsa-miR-519d-4395514	34.05	31.26	32.01	33.64	40.00	30.94	31.45	31.56	31.99	33.79
hsa-miR-550-4395521	32.39	32.68	33.49	32.41	32.67	32.35	33.30	33.97	34.11	33.35
hsa-miR-518e-4395506	33.10	32.13	32.04	33.83	32.87	34.06	32.23	31.40	35.35	33.76
hsa-miR-224-4395210	29.52	31.12	31.76	30.83	31.37	31.46	35.97	33.25	40.00	35.84
hsa-miR-672-4395438	30.36	31.83	30.55	32.26	31.76	32.62	32.99	40.00	34.58	34.33
hsa-miR-671-3p-4395433	31.96	33.42	31.90	31.99	31.11	31.96	40.00	33.98	32.50	32.55
hsa-miR-548c-5p-4395540	32.49	31.74	32.46	34.16	31.98	32.05	32.24	34.88	32.49	36.96
hsa-miR-184-4373113	37.08	39.42	33.48	32.34	36.74	32.69	30.56	30.73	30.58	28.00
hsa-miR-516a-3p-4373183	34.01	33.98	32.07	33.91	32.61	33.25	33.36	32.95	34.22	31.42
hsa-let-7i*-4395283	33.37	32.48	32.73	32.88	32.99	32.46	34.83	34.98	33.47	31.61
hsa-miR-302a-4378070	37.78	36.36	31.63	33.98	33.84	36.60	36.28	10.42	40.00	35.08
hsa-miR-206-4373092	35.13	31.92	34.93	32.01	31.13	30.73	36.54	35.88	33.90	29.90
hsa-miR-369-5p-4373195	32.27	32.47	32.49	31.97	36.99	31.29	33.35	33.28	34.96	33.14
hsa-miR-545-4395378	31.13	32.33	31.08	31.77	30.42	31.82	32.03	40.00	35.47	36.93
hsa-miR-363-4378090	32.39	33.60	33.37	33.96	32.54	33.19	33.72	33.85	33.65	32.72
hsa-let-7f-2*-4395529	33.67	34.83	34.14	32.64	30.32	32.69	35.97	35.19	31.31	32.36
hsa-miR-545*-4395377	31.69	32.10	33.38	34.26	32.42	31.80	34.90	34.71	35.32	32.54
hsa-miR-555-4380933	32.54	30.10	31.36	34.45	30.95	30.59	40.00	40.00	31.43	32.00
hsa-miR-526b*-4395494	32.82	32.88	32.33	32.95	33.31	35.00	32.74	34.32	33.50	33.61
hsa-let-7e*-4395518	30.87	32.63	31.09	30.91	36.03	34.99	40.00	31.49	34.48	31.28
hsa-miR-33b-4395196	28.76	40.00	30.01	28.34	29.86	29.93	40.00	27.00	40.00	40.00
hsa-miR-618-4380996	33.73	32.76	33.53	35.00	32.73	32.42	32.96	33.46	34.00	33.35
hsa-miR-214*-4395404	34.01	40.00	35.97	32.31	31.91	30.67	32.04	31.71	33.16	32.36
hsa-miR-208-4373091	30.69	33.64	32.34	34.77	33.93	33.85	33.92	34.88	33.24	33.01
hsa-miR-499-5p-4381047	33.41	40.00	40.00	32.82	29.56	40.00	29.18	31.13	29.57	28.80
hsa-miR-502-3p-4395194	30.81	32.76	32.67	36.31	31.99	33.98	40.00	31.90	33.76	30.30
hsa-miR-622-4380961	35.21	32.22	31.22	33.15	32.93	31.96	33.98	32.68	31.38	40.00
hsa-miR-502-5p-4373227	33.56	40.00	32.33	31.15	31.99	36.03	33.63	32.06	32.57	31.54
hsa-miR-518b-4373246	32.30	32.41	32.20	32.69	32.69	32.81	32.32	33.50	33.96	40.00
hsa-miR-580-4381024	34.31	33.11	34.17	33.57	32.99	32.56	33.67	34.13	33.85	32.59
hsa-miR-133b-4395358	40.00	33.78	40.00	32.95	32.15	32.76	31.77	31.01	30.40	30.17
hsa-miR-376a*-4395238	33.31	32.63	32.99	33.40	35.95	33.85	36.13	32.51	33.04	31.36
hsa-miR-381-4373020	35.41	34.95	31.57	31.42	34.60	36.46	31.84	32.26	35.66	31.02
hsa-miR-597-4380960	32.62	33.82	32.04	32.96	32.72	32.54	33.91	35.30	34.36	34.98
hsa-miR-302c*-4373277	40.00	32.13	32.29	32.54	34.53	32.96	32.74	32.39	31.60	34.08
hsa-miR-552-4380930	32.35	30.91	40.00	34.80	32.48	31.71	40.00	31.55	31.10	30.51
hsa-miR-26a-1*-4395554	34.02	33.86	33.23	33.30	32.62	33.60	33.59	33.47	33.97	33.99
hsa-miR-10b*-4395426	31.19	34.30	33.13	36.01	33.14	31.62	34.96	35.16	33.84	32.37
hsa-miR-662-4381010	30.26	30.13	40.00	30.73	32.73	30.90	30.03	40.00	40.00	30.96
hsa-miR-559-4380937	34.22	32.02	33.46	33.74	34.11	33.12	34.65	33.75	34.43	32.40
hsa-miR-429-4373203	36.00	33.78	31.86	31.49	32.90	32.14	40.00	33.25	33.54	31.47
hsa-miR-493-4395475	31.47	30.35	33.34	31.83	35.93	36.00	32.01	33.11	36.96	35.50
hsa-miR-299-5p-4373188	33.84	34.99	33.83	33.28	33.14	35.00	34.74	32.98	33.91	31.17

hsa-miR-548d-5p-4395348	32.88	33.07	32.35	33.63	32.54	31.79	33.28	35.74	34.66	36.97
hsa-miR-517c-4373264	36.02	33.46	35.64	36.23	33.96	33.00	34.33	33.20	30.53	30.54
hsa-miR-32-4395220	32.49	33.94	32.99	33.13	32.51	33.57	33.43	33.70	35.35	35.99
hsa-miR-503-4373228	31.00	31.21	40.00	31.55	31.12	33.02	30.77	32.67	35.92	40.00
hsa-miR-511-4373236	33.05	33.99	35.52	34.42	35.96	33.65	33.22	31.98	32.08	33.67
hsa-miR-606-4380974	34.63	32.62	34.44	34.03	32.30	33.66	35.51	33.25	36.01	31.71
hsa-miR-193a-3p-4395361	33.45	33.47	40.00	32.85	36.09	33.82	32.07	31.36	31.98	33.21
hsa-let-7a*-4395418	33.13	31.98	32.06	33.04	32.25	33.02	32.89	40.00	36.00	34.11
hsa-miR-519b-3p-4395495	33.56	33.39	33.03	34.30	33.80	34.95	34.45	33.20	33.65	34.19
hsa-miR-488*-4373213	33.31	33.20	34.56	31.64	31.38	32.70	34.67	40.00	35.96	31.25
hsa-miR-586-4380949	35.20	32.62	33.76	33.93	34.13	32.36	34.74	36.10	33.86	32.29
hsa-miR-520h-4373258	34.09	30.57	32.11	31.80	32.80	33.78	40.00	33.14	30.81	40.00
hsa-miR-641-4380988	32.49	31.31	31.47	31.19	32.85	32.97	34.11	40.00	40.00	32.92
hsa-miR-18a*-4395534	29.81	31.70	31.35	31.94	32.16	33.97	40.00	35.08	40.00	33.44
hsa-miR-921-4395262	31.33	31.05	40.00	33.04	34.01	32.35	32.70	31.82	40.00	33.18
hsa-miR-26b*-4395555	35.42	33.98	33.47	33.69	32.60	33.35	33.96	35.90	35.32	31.83
hsa-miR-362-3p-4395228	32.51	33.92	34.04	33.39	33.71	35.95	34.42	33.85	35.51	32.34
hsa-miR-136-4373173	32.41	33.74	33.05	33.33	33.16	35.11	33.85	37.42	34.27	33.35
hsa-miR-454*-4395185	31.54	32.72	33.52	32.67	33.14	32.96	40.00	34.03	35.97	33.44
hsa-miR-125a-3p-4395310	32.77	33.99	33.40	33.71	33.32	33.03	33.92	34.34	35.67	35.92
hsa-miR-34c-5p-4373036	34.24	34.62	32.53	32.18	32.28	32.98	33.92	35.97	40.00	31.59
hsa-miR-182-4395445	38.27	30.78	32.60	32.13	29.63	35.16	33.47	37.16	40.00	31.34
hsa-miR-378*-4373024	33.35	34.95	33.51	33.44	34.69	34.95	34.32	33.43	34.69	33.27
hsa-miR-579-4395509	33.16	34.60	33.24	33.95	32.37	32.80	35.41	34.47	35.05	35.86
hsa-miR-27a*-4395556	32.89	40.00	33.64	33.63	33.16	33.26	32.80	32.64	32.96	35.94
hsa-miR-34b*-4373037	40.00	31.06	30.69	30.52	30.41	31.69	34.96	40.00	40.00	31.68
hsa-miR-627-4380967	32.13	33.78	32.43	32.49	31.76	31.80	34.99	37.04	34.84	39.86
hsa-miR-412-4373199	40.00	31.87	31.29	33.30	32.10	34.44	32.78	33.48	31.95	40.00
hsa-miR-612-4380983	40.00	40.00	40.00	40.00	40.00	5.53	15.82	40.00	40.00	40.00
hsa-miR-642-4380995	37.01	33.56	40.00	30.94	31.62	32.14	40.00	32.08	35.73	28.61
hsa-miR-296-3p-4395212	30.65	30.77	30.51	32.19	30.92	31.06	36.01	40.00	40.00	40.00
hsa-miR-542-5p-4395351	31.05	40.00	32.97	30.89	31.63	40.00	29.63	32.43	33.94	40.00
hsa-miR-424-4373201	40.00	39.40	32.33	34.11	37.02	32.65	31.54	31.67	32.18	31.70
hsa-miR-148b*-4395271	32.72	34.86	33.02	35.01	33.98	33.46	36.63	33.60	33.74	35.96
hsa-miR-621-4381001	30.41	31.80	40.00	31.45	32.39	31.03	32.11	34.05	40.00	40.00
hsa-miR-938-4395292	31.23	31.40	32.65	32.53	32.78	31.64	35.70	40.00	40.00	35.73
hsa-miR-520c-3p-4395511	34.96	33.28	33.34	34.83	35.57	34.80	33.84	34.99	34.86	33.29
hsa-miR-654-3p-4395350	30.33	33.96	32.00	37.19	31.72	35.03	35.86	32.43	40.00	35.74
hsa-miR-551b-4380945	32.58	34.85	35.56	33.96	33.77	32.51	35.26	34.89	34.27	36.91
hsa-miR-363*-4380917	29.68	40.00	28.13	40.00	31.51	33.25	40.00	40.00	31.64	31.00
hsa-miR-411*-4395349	40.00	40.00	32.90	32.22	36.00	32.39	33.56	35.20	31.21	31.97
hsa-miR-708*-4395453	34.03	30.95	31.42	33.00	32.72	40.00	31.91	40.00	31.68	40.00
hsa-miR-374a*-4395236	34.96	34.39	33.33	33.01	32.63	32.20	40.00	36.96	32.81	35.43
hsa-miR-942-4395298	32.18	33.55	32.97	33.02	33.46	34.57	36.00	35.38	40.00	34.83
hsa-miR-523-4395497	32.67	32.79	35.49	33.43	34.87	32.93	35.02	34.90	37.05	36.82
hsa-miR-26a-2*-4395226	31.65	32.91	32.29	32.16	31.60	33.54	36.96	40.00	40.00	35.38
hsa-miR-581-4386744	34.93	32.12	33.61	33.59	34.38	40.00	34.59	36.28	34.09	32.93
hsa-miR-186*-4395216	29.87	31.32	32.04	30.89	30.43	32.05	40.00	40.00	40.00	40.00
hsa-miR-601-4380965	34.85	34.52	34.46	34.96	34.85	34.04	34.16	34.54	35.94	34.55
hsa-miR-10a*-4395399	32.76	33.11	31.83	35.86	40.00	34.90	35.15	32.56	40.00	31.26
hsa-miR-635-4380982	32.18	34.93	32.49	32.52	35.40	33.29	31.85	40.00	36.90	38.10
hsa-miR-616*-4380992	40.00	35.09	34.69	40.00	13.50	40.00	40.00	35.52	38.85	30.98
hsa-miR-542-3p-4378101	31.47	34.90	33.76	40.00	31.26	40.00	30.82	40.00	32.69	33.80
hsa-miR-614-4380990	40.00	33.47	34.06	33.11	33.18	33.35	34.19	32.55	34.87	40.00
hsa-miR-569-4380946	33.91	31.53	32.97	31.62	40.00	32.33	34.51	35.21	36.75	40.00
hsa-miR-517b-4373244	40.00	40.00	32.97	31.80	32.88	36.81	32.07	40.00	31.67	30.85
hsa-miR-633-4380979	40.00	26.74	40.00	32.01	25.90	40.00	40.00	40.00	40.00	25.65
hsa-miR-154-4373270	33.75	33.72	33.49	31.64	40.00	40.00	36.02	33.61	33.26	34.91
hsa-miR-148a*-4395245	28.97	40.00	40.00	31.14	40.00	30.87	40.00	40.00	29.65	29.90
hsa-miR-943-4395299	40.00	35.20	33.22	34.07	34.30	31.58	36.61	40.00	31.01	35.10
hsa-miR-154*-4378065	40.00	33.45	35.99	40.00	32.28	34.21	40.00	33.83	30.91	31.44
hsa-miR-122-4395356	31.91	28.62	40.00	32.60	30.74	36.39	31.97	40.00	40.00	40.00
hsa-miR-216a-4395331	30.45	34.33	34.25	32.69	34.00	32.23	40.00	40.00	34.51	40.00
hsa-miR-183*-4395381	32.76	32.88	34.97	31.68	40.00	36.36	35.30	40.00	34.72	34.77
hsa-miR-578-4381022	30.72	33.65	32.66	31.70	36.16	40.00	31.89	40.00	40.00	36.69
hsa-miR-450a-4395414	40.00	40.00	40.00	32.96	32.08	40.00	34.26	30.49	33.90	29.94
hsa-miR-512-3p-4381034	30.85	31.81	40.00	40.00	33.04	34.07	31.69	40.00	40.00	32.82
hsa-miR-25*-4395553	30.92	29.84	34.74	32.10	34.51	32.17	40.00	40.00	40.00	40.00
hsa-miR-299-3p-4373189	33.83	40.00	35.25	35.08	34.23	31.32	40.00	33.60	31.09	40.00
hsa-miR-374b*-4395502	32.99	35.71	35.98	32.22	32.60	32.41	40.00	40.00	40.00	32.72
hsa-miR-518f-4395499	35.01	35.56	34.31	36.54	35.93	36.83	35.52	38.70	32.76	33.56
hsa-miR-23a*-4395550	31.54	32.25	36.32	32.28	36.24	36.30	34.50	40.00	40.00	35.35
hsa-miR-142-5p-4395359	33.68	40.00	40.00	33.93	40.00	35.60	32.84	33.12	32.96	32.69
hsa-miR-219-1-3p-4395206	28.85	33.72	32.71	33.12	31.39	35.93	40.00	40.00	40.00	40.00

hsa-miR-141-4373137	33.88	32.46	34.03	35.53	33.95	36.94	40.00	34.01	35.12	40.00
hsa-miR-218-2*-4395405	33.74	34.96	34.54	33.98	34.34	34.90	40.00	40.00	34.81	34.69
hsa-miR-519e-4395481	33.08	35.50	40.00	33.69	32.82	40.00	33.10	40.00	33.35	34.81
hsa-miR-329-4373191	37.21	33.33	40.00	31.97	40.00	31.19	36.76	40.00	36.42	30.16
hsa-miR-561-4380938	32.61	32.54	40.00	36.27	35.96	35.79	35.47	34.82	40.00	33.99
hsa-miR-130a*-4395242	35.05	40.00	40.00	32.61	30.54	32.79	40.00	34.83	35.71	36.03
hsa-miR-132*-4395243	40.00	34.03	40.00	40.00	40.00	40.00	31.06	30.91	30.00	31.55
hsa-miR-541-4395312	34.05	32.55	40.00	40.00	31.49	40.00	35.83	31.96	31.94	40.00
hsa-miR-202*-4395473	40.00	28.14	28.43	40.00	40.00	32.12	40.00	40.00	40.00	29.17
hsa-miR-19a*-4395535	32.12	35.07	31.65	33.02	33.74	33.98	40.00	40.00	40.00	40.00
hsa-miR-674-4395193	40.00	40.00	8.24	40.00	40.00	40.00	40.00	31.42	40.00	40.00
hsa-miR-626-4380966	30.82	40.00	40.00	40.00	40.00	31.48	40.00	31.38	34.79	31.19
hsa-let-7b*-4395515	33.12	32.93	36.04	32.29	40.00	40.00	40.00	36.83	36.68	31.97
hsa-miR-450b-3p-4395319	40.00	40.00	36.56	40.00	35.88	32.88	32.62	34.72	35.20	32.47
hsa-miR-589-4395520	37.00	33.71	40.00	33.56	37.45	34.25	36.86	40.00	35.87	32.42
hsa-miR-20b*-4395422	30.90	40.00	32.62	34.74	34.11	35.84	33.03	40.00	40.00	40.00
hsa-miR-603-4380972	40.00	31.97	40.00	40.00	40.00	9.43	40.00	40.00	40.00	40.00
hsa-miR-613-4380989	33.83	33.07	36.08	40.00	32.89	34.00	40.00	40.00	40.00	32.05
hsa-miR-217-4395448	31.68	33.75	35.66	33.97	33.70	33.77	40.00	40.00	40.00	40.00
hsa-miR-375-4373027	40.00	33.50	35.89	33.25	40.00	40.00	36.95	40.00	34.03	29.87
hsa-miR-609-4380978	40.00	33.12	33.80	33.17	33.30	40.00	40.00	40.00	40.00	30.37
hsa-miR-937-4395291	31.30	32.03	40.00	40.00	31.43	33.98	40.00	40.00	40.00	35.10
hsa-miR-496-4386771	40.00	40.00	40.00	32.01	35.87	32.82	32.04	40.00	36.03	35.11
hsa-miR-369-3p-4373032	40.00	33.76	40.00	35.96	35.68	33.09	40.00	33.71	36.15	35.59
hsa-miR-631-4380971	40.00	26.49	29.84	40.00	40.00	40.00	40.00	28.84	40.00	40.00
hsa-miR-302c-4378072	40.00	37.21	35.69	40.00	36.92	40.00	35.12	30.52	40.00	30.69
hsa-miR-196b-4395326	32.97	35.79	36.69	32.03	40.00	40.00	31.97	36.99	40.00	40.00
hsa-miR-448-4373206	40.00	40.00	32.51	32.06	33.99	40.00	35.99	32.98	40.00	40.00
hsa-miR-450b-5p-4395318	33.91	31.96	40.00	40.00	40.00	40.00	35.10	32.14	34.54	40.00
hsa-miR-570-4395458	40.00	34.17	34.95	40.00	40.00	33.72	34.93	40.00	34.34	35.94
hsa-miR-192*-4395383	37.00	40.00	32.82	40.00	40.00	31.69	40.00	35.19	40.00	31.45
hsa-miR-585-4381027	40.00	40.00	40.00	30.28	29.17	40.00	40.00	40.00	40.00	28.73
hsa-miR-373-4378073	36.98	36.05	34.02	36.09	35.30	36.06	40.00	40.00	40.00	33.73
hsa-miR-637-4380985	40.00	31.69	40.00	33.68	22.96	40.00	40.00	40.00	40.00	40.00
hsa-miR-380-4373022	35.96	40.00	40.00	34.98	37.79	34.37	40.00	38.93	33.67	33.16
hsa-miR-563-4380940	40.00	31.70	34.51	37.17	34.01	40.00	40.00	40.00	40.00	31.98
hsa-miR-767-3p-4395184	36.17	31.62	40.00	34.48	40.00	40.00	40.00	40.00	32.77	34.63
hsa-miR-607-4380975	40.00	32.40	40.00	40.00	40.00	30.47	40.00	40.00	40.00	27.89
hsa-miR-518a-3p-4395508	31.66	40.00	40.00	40.00	40.00	32.16	40.00	40.00	40.00	27.06
hsa-miR-645-4381000	40.00	40.00	37.43	33.85	40.00	35.50	36.83	35.96	33.75	37.68
hsa-miR-302b-4378071	40.00	33.92	40.00	40.00	40.00	37.12	35.25	40.00	33.35	31.75
hsa-miR-551a-4380929	32.21	32.05	34.28	40.00	40.00	40.00	40.00	40.00	33.21	40.00
hsa-miR-220c-4395322	29.99	40.00	40.00	40.00	31.24	40.00	40.00	40.00	30.82	40.00
has-miR-155-4395459	36.99	36.19	40.00	35.45	35.35	40.00	40.00	34.51	34.25	40.00
hsa-miR-220b-4395317	33.04	35.33	33.12	40.00	40.00	40.00	40.00	40.00	40.00	31.88
hsa-miR-199a-5p-4373272	31.94	40.00	40.00	32.34	40.00	37.06	40.00	40.00	40.00	32.23
hsa-let-7d*-4378108	40.00	32.63	40.00	40.00	40.00	40.00	40.00	33.24	40.00	28.49
hsa-miR-520f-4373256	33.24	40.00	34.79	40.00	36.03	38.38	40.00	34.27	40.00	37.66
hsa-miR-933-4395287	40.00	31.05	40.00	31.72	40.00	40.00	40.00	40.00	40.00	32.21
hsa-miR-520a-3p-4373268	40.00	35.38	40.00	40.00	33.87	40.00	33.07	32.77	40.00	40.00
hsa-miR-367*-4395232	40.00	40.00	32.21	40.00	40.00	40.00	31.55	40.00	40.00	31.35
hsa-miR-517*-4378078	40.00	33.76	40.00	34.92	40.00	32.40	40.00	34.11	40.00	40.00
hsa-let-7f-1*-4395528	33.47	33.80	35.98	40.00	40.00	40.00	40.00	40.00	40.00	32.09
hsa-miR-337-3p-4395268	31.68	40.00	40.00	31.96	40.00	40.00	40.00	40.00	40.00	31.87
hsa-miR-624*-4380964	36.69	36.44	40.00	36.74	40.00	32.63	37.14	40.00	40.00	35.96
hsa-miR-562-4380939	35.49	40.00	34.11	40.00	40.00	34.96	40.00	40.00	34.93	36.20
hsa-miR-501-3p-4395546	40.00	32.10	31.36	40.00	40.00	32.39	40.00	40.00	40.00	40.00
hsa-miR-372-4373029	35.62	40.00	40.00	33.95	36.94	40.00	40.00	40.00	34.15	35.66
hsa-miR-500*-4373225	29.00	40.00	40.00	36.00	40.00	40.00	40.00	40.00	40.00	31.86
hsa-miR-199b-5p-4373100	40.00	40.00	36.92	33.22	40.00	40.00	32.09	40.00	35.67	40.00
hsa-miR-541*-4395311	40.00	40.00	40.00	34.57	40.00	40.00	40.00	36.77	35.97	31.20
hsa-miR-548d-3p-4381008	35.65	33.19	40.00	40.00	40.00	34.42	35.98	40.00	40.00	40.00
hsa-miR-520g-4373257	39.30	40.00	40.00	40.00	40.00	40.00	34.72	36.10	33.72	35.53
hsa-miR-379*-4395244	40.00	40.00	40.00	34.27	35.03	34.55	40.00	35.76	40.00	40.00
hsa-miR-549-4380921	32.46	40.00	40.00	40.00	34.04	40.00	40.00	40.00	40.00	33.88
hsa-miR-554-4380932	40.00	33.67	33.99	40.00	40.00	32.91	40.00	40.00	40.00	40.00
hsa-miR-521-4373259	40.00	40.00	40.00	40.00	34.19	33.46	40.00	33.23	40.00	40.00
hsa-miR-30b*-4395240	33.10	40.00	40.00	34.89	40.00	40.00	40.00	40.00	40.00	33.04
hsa-miR-634-4380981	40.00	40.00	40.00	40.00	40.00	40.00	30.77	40.00	30.75	40.00
hsa-miR-183-4395380	34.65	40.00	32.32	35.02	40.00	40.00	40.00	40.00	40.00	40.00
hsa-miR-593*-4380957	40.00	40.00	40.00	40.00	31.25	40.00	30.79	40.00	40.00	40.00
hsa-miR-599-4380962	40.00	40.00	33.76	40.00	40.00	40.00	40.00	36.47	40.00	32.82
hsa-miR-515-3p-4395480	40.00	40.00	35.61	35.48	40.00	40.00	40.00	37.13	35.05	40.00
hsa-miR-658-4380923	40.00	31.19	40.00	40.00	40.00	40.00	40.00	40.00	32.73	40.00

hsa-miR-32*-4395222	40.00	40.00	40.00	40.00	40.00	29.31	40.00	40.00	35.02	40.00
hsa-miR-200a*-4373273	36.00	33.95	40.00	40.00	40.00	40.00	40.00	34.66	40.00	40.00
hsa-miR-143*-4395257	40.00	40.00	40.00	40.00	40.00	40.00	40.00	40.00	40.00	25.25
hsa-miR-616-4395525	34.09	40.00	35.73	40.00	40.00	35.66	40.00	40.00	40.00	40.00
hsa-miR-518d-5p-4395500	33.23	40.00	40.00	40.00	32.61	40.00	40.00	40.00	40.00	40.00
hsa-miR-920-4395261	40.00	31.12	40.00	40.00	40.00	40.00	40.00	40.00	40.00	34.72
hsa-miR-302d*-4395231	40.00	40.00	40.00	40.00	40.00	32.96	40.00	40.00	32.94	40.00
hsa-miR-576-5p-4395461	37.22	40.00	40.00	33.95	35.05	40.00	40.00	40.00	40.00	40.00
hsa-miR-875-3p-4395315	34.35	32.00	40.00	40.00	40.00	40.00	40.00	40.00	40.00	40.00
hsa-miR-146b-3p-4395472	40.00	40.00	40.00	40.00	34.02	40.00	40.00	40.00	32.63	40.00
hsa-miR-491-3p-4395471	40.00	40.00	40.00	40.00	40.00	40.00	40.00	40.00	33.94	33.91
hsa-miR-452*-4395441	40.00	33.93	40.00	40.00	40.00	33.97	40.00	40.00	40.00	40.00
hsa-miR-520d-5p-4395504	40.00	40.00	40.00	40.00	40.00	33.84	40.00	40.00	40.00	34.14
hsa-miR-544-4395376	40.00	40.00	40.00	35.50	40.00	36.98	35.60	40.00	40.00	40.00
hsa-miR-615-3p-4386777	40.00	40.00	28.46	40.00	40.00	40.00	40.00	40.00	40.00	40.00
hsa-miR-519c-3p-4373251	35.76	40.00	32.79	40.00	40.00	40.00	40.00	40.00	40.00	40.00
hsa-miR-872-4395375	36.62	40.00	40.00	40.00	34.70	40.00	40.00	40.00	37.38	40.00
hsa-miR-205-4373093	40.00	40.00	40.00	40.00	40.00	40.00	40.00	29.11	40.00	40.00
hsa-miR-106a*-4395281	34.01	40.00	40.00	40.00	40.00	40.00	40.00	40.00	35.12	40.00
hsa-miR-553-4380931	40.00	40.00	40.00	40.00	40.00	40.00	40.00	29.18	40.00	40.00
hsa-miR-10b-4395329	40.00	40.00	40.00	40.00	40.00	40.00	40.00	40.00	35.92	33.42
hsa-miR-377-4373025	40.00	40.00	33.89	40.00	40.00	40.00	40.00	40.00	36.00	40.00
hsa-miR-558-4380936	40.00	30.05	40.00	40.00	40.00	40.00	40.00	40.00	40.00	40.00
hsa-miR-651-4381007	40.00	34.83	40.00	40.00	40.00	40.00	40.00	40.00	35.88	40.00
hsa-miR-431*-4395423	40.00	40.00	40.00	40.00	40.00	40.00	40.00	35.13	40.00	35.86
hsa-miR-188-3p-4395217	40.00	40.00	40.00	40.00	40.00	40.00	40.00	40.00	31.05	40.00
hsa-miR-23b*-4395237	40.00	40.00	40.00	40.00	31.17	40.00	40.00	40.00	40.00	40.00
hsa-miR-498-4373223	40.00	31.38	40.00	40.00	40.00	40.00	40.00	40.00	40.00	40.00
hsa-miR-367-4373034	40.00	40.00	40.00	40.00	34.77	40.00	40.00	40.00	40.00	36.94
hsa-miR-924-4395265	40.00	40.00	40.00	40.00	40.00	40.00	40.00	35.72	40.00	36.02
hsa-miR-593-4395522	40.00	40.00	40.00	40.00	40.00	40.00	40.00	40.00	40.00	31.93
hsa-miR-96-4373372	35.97	40.00	40.00	40.00	35.98	40.00	40.00	40.00	40.00	40.00
hsa-miR-608-4380976	40.00	40.00	40.00	32.50	40.00	40.00	40.00	40.00	40.00	40.00
hsa-miR-944-4395300	40.00	40.00	35.63	40.00	40.00	40.00	40.00	40.00	40.00	36.93
hsa-miR-525-5p-4378088	40.00	40.00	40.00	40.00	32.87	40.00	40.00	40.00	40.00	40.00
hsa-miR-506-4373231	33.05	40.00	40.00	40.00	40.00	40.00	40.00	40.00	40.00	40.00
hsa-miR-18b*-4395421	40.00	40.00	33.19	40.00	40.00	40.00	40.00	40.00	40.00	40.00
hsa-miR-16-2*-4395282	40.00	40.00	40.00	40.00	40.00	33.24	40.00	40.00	40.00	40.00
hsa-miR-520b-4373252	40.00	40.00	35.85	37.44	40.00	40.00	40.00	40.00	40.00	40.00
hsa-miR-24-1*-4395551	40.00	40.00	40.00	40.00	40.00	40.00	40.00	40.00	40.00	33.90
hsa-miR-619-4380998	40.00	40.00	40.00	40.00	33.92	40.00	40.00	40.00	40.00	40.00
hsa-miR-509-3-5p-4395266	40.00	40.00	40.00	40.00	33.94	40.00	40.00	40.00	40.00	40.00
hsa-miR-516a-5p-4395527	40.00	40.00	40.00	40.00	34.00	40.00	40.00	40.00	40.00	40.00
hsa-miR-141*-4395256	40.00	40.00	40.00	40.00	40.00	37.62	40.00	40.00	40.00	36.41
hsa-miR-510-4395352	40.00	40.00	40.00	40.00	40.00	40.00	34.05	40.00	40.00	40.00
hsa-miR-371-3p-4395235	40.00	40.00	40.00	40.00	40.00	40.00	40.00	40.00	34.82	40.00
hsa-miR-934-4395288	40.00	40.00	40.00	40.00	40.00	34.97	40.00	40.00	40.00	40.00
hsa-miR-105*-4395279	40.00	40.00	40.00	40.00	35.05	40.00	40.00	40.00	40.00	40.00
hsa-miR-302b*-4395230	40.00	40.00	40.00	40.00	40.00	40.00	35.31	40.00	40.00	40.00
hsa-miR-548a-3p-4380948	40.00	40.00	40.00	40.00	35.83	40.00	40.00	40.00	40.00	40.00
hsa-miR-936-4395290	40.00	35.86	40.00	40.00	40.00	40.00	40.00	40.00	40.00	40.00
hsa-miR-515-5p-4373242	40.00	40.00	40.00	40.00	40.00	40.00	40.00	40.00	40.00	35.93
hsa-miR-525-3p-4395496	40.00	40.00	40.00	40.00	40.00	40.00	40.00	40.00	35.96	40.00
hsa-miR-29b-1*-4395276	40.00	40.00	40.00	40.00	40.00	40.00	40.00	35.99	40.00	40.00
hsa-miR-497*-4395479	40.00	40.00	40.00	35.99	40.00	40.00	40.00	40.00	40.00	40.00
hsa-miR-325-4373051	40.00	40.00	40.00	36.00	40.00	40.00	40.00	40.00	40.00	40.00
hsa-miR-146a*-4395274	40.00	40.00	36.00	40.00	40.00	40.00	40.00	40.00	40.00	40.00
hsa-miR-453-4395429	40.00	40.00	40.00	36.00	40.00	40.00	40.00	40.00	40.00	40.00
hsa-miR-147-4373131	36.01	40.00	40.00	40.00	40.00	40.00	40.00	40.00	40.00	40.00
hsa-miR-518c-4395512	40.00	40.00	36.04	40.00	40.00	40.00	40.00	40.00	40.00	40.00
hsa-miR-871-4395465	40.00	36.09	40.00	40.00	40.00	40.00	40.00	40.00	40.00	40.00
hsa-miR-516b-4395172	40.00	40.00	40.00	40.00	40.00	40.00	40.00	36.18	40.00	40.00
hsa-miR-624-4395541	40.00	40.00	40.00	40.00	36.62	40.00	40.00	40.00	40.00	40.00
hsa-miR-512-5p-4373238	40.00	40.00	40.00	40.00	40.00	40.00	36.69	40.00	40.00	40.00
hsa-miR-220-4373078	40.00	40.00	36.69	40.00	40.00	40.00	40.00	40.00	40.00	40.00
hsa-miR-155*-4395398	40.00	40.00	40.00	40.00	40.00	40.00	36.97	40.00	40.00	40.00
hsa-miR-96*-4395251	40.00	38.00	40.00	40.00	40.00	40.00	40.00	40.00	40.00	40.00
ath-miR159a-4373390	40.00	40.00	40.00	40.00	40.00	40.00	40.00	40.00	40.00	40.00
hsa-miR-147b-4395373	40.00	40.00	40.00	40.00	40.00	40.00	40.00	40.00	40.00	40.00
hsa-miR-211-4373088	40.00	40.00	40.00	40.00	40.00	40.00	40.00	40.00	40.00	40.00
hsa-miR-298-4395301	40.00	40.00	40.00	40.00	40.00	40.00	40.00	40.00	40.00	40.00
hsa-miR-376b-4373196	40.00	40.00	40.00	40.00	40.00	40.00	40.00	40.00	40.00	40.00
hsa-miR-384-4373017	40.00	40.00	40.00	40.00	40.00	40.00	40.00	40.00	40.00	40.00
hsa-miR-492-4373217	40.00	40.00	40.00	40.00	40.00	40.00	40.00	40.00	40.00	40.00

hsa-miR-499-3p-4395538	40.00	40.00	40.00	40.00	40.00	40.00	40.00	40.00	40.00	40.00
hsa-miR-507-4373232	40.00	40.00	40.00	40.00	40.00	40.00	40.00	40.00	40.00	40.00
hsa-miR-508-5p-4395203	40.00	40.00	40.00	40.00	40.00	40.00	40.00	40.00	40.00	40.00
hsa-miR-513-5p-4395201	40.00	40.00	40.00	40.00	40.00	40.00	40.00	40.00	40.00	40.00
hsa-miR-518a-5p-4395507	40.00	40.00	40.00	40.00	40.00	40.00	40.00	40.00	40.00	40.00
hsa-miR-520a-5p-4378085	40.00	40.00	40.00	40.00	40.00	40.00	40.00	40.00	40.00	40.00
hsa-miR-520e-4373255	40.00	40.00	40.00	40.00	40.00	40.00	40.00	40.00	40.00	40.00
hsa-miR-524-5p-4395174	40.00	40.00	40.00	40.00	40.00	40.00	40.00	40.00	40.00	40.00
hsa-miR-526b-4395493	40.00	40.00	40.00	40.00	40.00	40.00	40.00	40.00	40.00	40.00
hsa-miR-548a-5p-4395523	40.00	40.00	40.00	40.00	40.00	40.00	40.00	40.00	40.00	40.00
hsa-miR-548b-3p-4380951	40.00	40.00	40.00	40.00	40.00	40.00	40.00	40.00	40.00	40.00
hsa-miR-548c-3p-4380993	40.00	40.00	40.00	40.00	40.00	40.00	40.00	40.00	40.00	40.00
hsa-miR-556-3p-4395456	40.00	40.00	40.00	40.00	40.00	40.00	40.00	40.00	40.00	40.00
hsa-miR-556-5p-4395455	40.00	40.00	40.00	40.00	40.00	40.00	40.00	40.00	40.00	40.00
hsa-miR-615-5p-4395464	40.00	40.00	40.00	40.00	40.00	40.00	40.00	40.00	40.00	40.00
hsa-miR-653-4395403	40.00	40.00	40.00	40.00	40.00	40.00	40.00	40.00	40.00	40.00
hsa-miR-890-4395320	40.00	40.00	40.00	40.00	40.00	40.00	40.00	40.00	40.00	40.00
hsa-miR-891b-4395321	40.00	40.00	40.00	40.00	40.00	40.00	40.00	40.00	40.00	40.00
hsa-miR-892a-4395306	40.00	40.00	40.00	40.00	40.00	40.00	40.00	40.00	40.00	40.00
ath-miR159a-4373390	40.00	40.00	40.00	40.00	40.00	40.00	40.00	40.00	40.00	40.00
hsa-miR-122*-4395241	40.00	40.00	40.00	40.00	40.00	40.00	40.00	40.00	40.00	40.00
hsa-miR-182*-4378066	40.00	40.00	40.00	40.00	40.00	40.00	40.00	40.00	40.00	40.00
hsa-miR-185*-4395215	40.00	40.00	40.00	40.00	40.00	40.00	40.00	40.00	40.00	40.00
hsa-miR-194*-4395490	40.00	40.00	40.00	40.00	40.00	40.00	40.00	40.00	40.00	40.00
hsa-miR-195*-4395218	40.00	40.00	40.00	40.00	40.00	40.00	40.00	40.00	40.00	40.00
hsa-miR-19b-2*-4395537	40.00	40.00	40.00	40.00	40.00	40.00	40.00	40.00	40.00	40.00
hsa-miR-200b*-4395385	40.00	40.00	40.00	40.00	40.00	40.00	40.00	40.00	40.00	40.00
hsa-miR-200c*-4395397	40.00	40.00	40.00	40.00	40.00	40.00	40.00	40.00	40.00	40.00
hsa-miR-30c-2*-4395221	40.00	40.00	40.00	40.00	40.00	40.00	40.00	40.00	40.00	40.00
hsa-miR-493*-4373218	40.00	40.00	40.00	40.00	40.00	40.00	40.00	40.00	40.00	40.00
hsa-miR-518c*-4378082	40.00	40.00	40.00	40.00	40.00	40.00	40.00	40.00	40.00	40.00
hsa-miR-518e*-4395482	40.00	40.00	40.00	40.00	40.00	40.00	40.00	40.00	40.00	40.00
hsa-miR-518f*-4395498	40.00	40.00	40.00	40.00	40.00	40.00	40.00	40.00	40.00	40.00
hsa-miR-519e*-4378084	40.00	40.00	40.00	40.00	40.00	40.00	40.00	40.00	40.00	40.00
hsa-miR-557-4380935	40.00	40.00	40.00	40.00	40.00	40.00	40.00	40.00	40.00	40.00
hsa-miR-588-4380952	40.00	40.00	40.00	40.00	40.00	40.00	40.00	40.00	40.00	40.00
hsa-miR-647-4381003	40.00	40.00	40.00	40.00	40.00	40.00	40.00	40.00	40.00	40.00
hsa-miR-888*-4395324	40.00	40.00	40.00	40.00	40.00	40.00	40.00	40.00	40.00	40.00
hsa-miR-92a-2*-4395249	40.00	40.00	40.00	40.00	40.00	40.00	40.00	40.00	40.00	40.00

APPENDIX 2

Oligonucleotide sequences for development of bead-based genotyping assay (Chapter 3)

Universal oligo, double biotinylated
5'-/5Biosg/GTT AGA TTT GTA GT/iBiodT/ TAA AGA TAG -3'

OLA controls for data shown in Table 3.1	
Positive control	
rs5993882-g ligation product	AATCTACACTAACAATTTCATAACCAAAAAGTTACGCTTAATAATGAATGT TGCAGCACTTTCTTCTCTTCAGGCTATCTTTAAACTACAAATCTAAC
Negative control	
rs5993882-g allele specific	AATCTACACTAACAATTTCATAACCAAAAAGTTACGCTTAATAATGAATGTTG
rs5993882-g common	TTGCAGCACTTTCTTCTCTTCAGGCTATCTTTAAACTACAAATCTAAC

Sequencing primers for Sanger sequencing		
SNP	Forward	Reverse
rs945713	GGGAATCTAGGATTCACTTCTAAGC	CTGTCTATGAAACACAACAGTCTGG
rs1572495	TTGTATGCTAAATGCATCAGTTTTT	TCTAAAGGGACTGTACGATTTGCTA
rs1415263	CTTGTTTCATGTATAGCCCGTAAGT	AATACAGAAAGAGCGTGGTATCAAC
rs1538018	AGCCCTGAAATCCATATTTTACCTC	AATGAGGAGGGACCAATATAATAAC
rs348624	CATTCATGTCCCTCTCTTCTCTC	TATACTAATGGGGAAACAAAGCTG
rs6680461	CTGGGTGTTTCTGGGACTCT	ACACGGAGACAGGAGGAAACT
rs12125293	TTTAGAGACGGACAGACTGTGG	AAAGCAGCAAAGCAGGGTGACC
rs4657187	TCACAGGACTTGAAAATACCTGAA	TTATTCATCTTCCATTTTCTTTGGA

Primers and probes for OLA comparison to Sanger sequencing	
PCR primer	Sequence
rs945713-F	CCCTGTTTAACCAAATGTCAGTCCA
rs945713-R	CACTGCGGCAGCTGTCTATGA
rs1572495-F	TAGCCCACAGCATCTACTCCCTATT
rs1572495-R	CTGCTGTGGACCCAACACCA
rs1415263-F	GGAAATCTGTCAACTGCTTCTGGGT
rs1415263-R	CTGGAGCAGACTGCACATTCCT
rs1538018-F	TTTGTCCAGGAGTCACTTTATCCCT
rs1538018-R	AGGGACGAAATTGCCAGCACTAA
rs348624-F	TAGTGATGCATCATGGCCCTCC
rs348624-R	GGAGATGTGCTGGAGCATGTCC
rs6680461-F	CTCTTCAGCCTTTAACTTCCACCTG
rs6680461-R	GGACAGGACCTCAGCCATATAACAA
rs12125293-F	GGGTCTCAGAAAGCCGTAAGTGT
rs12125293-R	AGGTGGCAGGCCATTTCTAGC
rs4657187-F	TGCCTAGGGAGTACCCAACAGA
rs4657187-R	TAACTGGCACTTATTGAGGGCTCTC

Probe	Sequence (tags in red)	Bead
rs945713-A	TACAAATCATCAATCACTTTAATCCCATTTGGATATCCCAAAGA	11
rs945713-G	TCAACTAACTAATCATCTATCAATCCATTTGGATATCCCAAAGG	84
rs945713-com	CACCTTAAATTCAATATGTCAAAAAACCTATCTTTAAACTACAAATCTAAC	
rs1572495-A	TCATCAATCTTTCAATTTACTTACGCTTCTATAGATCTATTTGTCCTAATA	49
rs1572495-G	TTACCTTTATACCTTTCTTTTTACGCTTCTATAGATCTATTTGTCCTAATG	30
rs1572495-com	GGCTCAGCTCAAATCTGCTATCTTTAAACTACAAATCTAAC	
rs1415263-C	CTTTAATCTACACTTTCTAACAATGAAGGCAACATACTTGATGAC	81
rs1415263-T	TACACTTTAAACTTACTACACTAAGAAGGCAACATACTTGATGAT	95
rs1415263-com	GATAAAGGAATTGGGAATGCCTATCTTTAAACTACAAATCTAAC	
rs1538018-C	CTTTTCATCAATAATCTTACCTTTCAGCACCATTTACTCCTTTC	65
rs1538018-G	AATCCTTTTACATTCATTACTTACCAGCACCATTTACTCCTTTG	8
rs1538018-com	TCATTGTTCTCCTTTTCATCCCTATCTTTAAACTACAAATCTAAC	
rs348624-C	AATCTAACAAACTCATCTAAATACGCCCAGGCTCGC	76
rs348624-T	CTTTTCATCTTTTCATCTTTCAATGCCCAGGCTCGT	37
rs348624-com	GTGCATCAGCTTTTGCTGCTATCTTTAAACTACAAATCTAAC	
rs6680461-G	TCAATCAATTACTTACTCAAATACGAGCCATGTCCTCAAGG	19
rs6680461-T	TCAACAATCTTTTACAATCAAATCGAGCCATGTCCTCAAGT	6
rs6680461-com	GCATGCCAATCAAACCAACCTATCTTTAAACTACAAATCTAAC	
rs12125293-A	AATCTACAAATCCAATAATCTCATCTCAGCAACCACAACCA	60
rs12125293-G	TCAAAATCTCAAATACTCAAATCACTCAGCAACCACAACCG	18
rs12125293-com	CCATCCCTCACGAGCCTATCTTTAAACTACAAATCTAAC	
rs4657187-C	TCAATCATAATCTCATAATCCAATGCTCACACCTGTAGTCC	62
rs4657187-T	TCATTTACCAATCTTTCTTTATACGCTCACACCTGTAGTCT	44
rs4657187-com	CAGCACTTTGGGAGGCCTATCTTTAAACTACAAATCTAAC	

Pyrosequencing oligos (Table 3.2)			
rs #	PCR forward	PCR reverse	Pyrosequencing primer
rs11806859	GGTGGGGTGGGTTGAAAGT	TCCAGCCGAGGAAATGTTTCT	GGTGTCTTGCTGTCCTT
rs56387268	AATGAACACCAGATGGAAGAGATG	CGGGCAGCTGAACATTTAGA	GCATAGGGCAGGGTC
rs1123005	TGGACCAGGCCAAAAGCTACT	TCTACTCCTTGGGCTCTGGTTCT	TTCTTGGTTTGGCAC
rs12122048	CATTAGTGCTGGCTCAGGCAGTAG	TGCCATGAGAAAATGCTCCTTGTA	TTTTCAAGTCCTGTGAAT
rs4657179	GAGGCCGGATGTTCAAAA	CCTAAAATGCCACACCCATATC	GCCACACCCATATCAA
rs4657187	GCCTAGGGAGTACCCAACAGAC	CGCCACCACACCTAGCTAATTT	CTCGGCCTCCCAAAG
rs905720	ACAAGAACACCCTTTTCCCCATAA	AGTTCTCCAGGGAGCATTTCA	TTTTCCCCATAAGCTAC

Primers and probes for OLA data presented in Table 3.2	
PCR primers	Sequence
rs11806859-F	ACTTACTGCCTGGGTTCTGATTTGA
rs11806859-R	GCCCAGGTGATGGCTCTGTC
345549-F	ACCCTCTCCTTGGACTCAACTGA
345549-R	TTTAGAGGTTCCTGGAGGGTGGT
rs1123005-F	TGACAAGCTTCACCAGCGGT
rs1123005-R	CCTGCCCAGGTGATGGCTC
rs12122048-F	TTTGGGTTCTCCTGCAGCACA
rs12122048-R	TGCAGGTACCCAAGTTCAATGGT
rs4657179-F	CGCTTGAGGCCGGATGTTC
rs4657179-R	GACCTTGGGCACTTCACATGC
rs4657187-F	TGCCTAGGGAGTACCCAACAGA
rs4657187-R	TAACTGGCACTTATTGAGGGCTCTC
rs905720-F	AGCCACGGTATCCACAAGTGTAA
rs905720-R	TGAGTTAGAAGGCCAATACCAGTGT

OLA probes	Sequence (tags in red)	Bead
rs11806859-A	AATCCTTTTACATTCATTACTTACGTGTCTTGCTGTCCTTAAGA	8
rs11806859-G	TCATTTACCAATCTTTCTTTATACGTGTCTTGCTGTCCTTAAGG	44
rs11806859-com	CATGTGTGTTTATTGTCATTAACCCTATCTTTAAACTACAAATCTAAC	
rs56387268-G	TCATCAATCAATCTTTTTCACTTTGGCAGGGTCTGTGG	59
rs56387268-T	TCATCAATCTTTCAATTTACTTACGGCAGGGTCTGTGT	49
rs56387268-com	GAAGGGTGGCAGAGCCTATCTTTAAACTACAAATCTAAC	
rs1123005-A	ATCATACATACATACAAATCTACACTGAAATTGCTAAGGCCTA	10
rs1123005-G	ATACTACATCATAATCAAACATCACTGAAATTGCTAAGGCCTG	85
rs1123005-com	TGTGCCAAACCAAGAACCTATCTTTAAACTACAAATCTAAC	
rs12122048-A	CAATATACCAATATCATCATTTACGCAGTAGCAGCAGTGA	50
rs12122048-G	CTTTAATCTCAATCAATACAAATCGCAGTAGCAGCAGTGG	1
rs12122048-com	GTGCTCACATATTCACAGGACTATCTTTAAACTACAAATCTAAC	
rs4657179-G	AAACTAACATCAATACTTACATCACTCTAATATATATATATATAAATCAAAAGACCTTTG	87
rs4657179-T	TAATTATACATCTCATCTTCTACACTCTAATATATATATATATAAATCAAAAGACCTTTT	53
rs4657179-com	TTGATATGGGTGTGGCATTTTCTATCTTTAAACTACAAATCTAAC	
rs4657187-C	TCAATCATAATCTCATAATCCAATGCTCACACCTGTAGTCC	62
rs4657187-T	TCATTTACCAATCTTTCTTTATACGCTCACACCTGTAGTCT	44
rs4657187-com	CAGCACTTTGGGAGGCCTATCTTTAAACTACAAATCTAAC	
rs905720-C	CAATTCAAATCACAATAATCAATCCCTTTTCCCCATAAGCTACAC	5
rs905720-T	TCAATTACTTCACTTTAATCCTTTCCTTTTCCCCATAAGCTACAT	33
rs905720-com	TGGTCCAGGCCATAAAAATTCTATCTTTAAACTACAAATCTAAC	

Primers and probes for data presented in Table 3.3	
PCR primer	Sequence
rs363039-F	GCCCAGACTCGTGATTCCCAAA
rs363039-R	CCTTGGGGCAACGCTTCTGT
rs362602-F	ATGTGCATAGGTTGTACTCACTGGA
rs362602-R	TAGAACTGTGGAGCGTAAAAGTCGT
rs362548-F	CCGATGCTGGTCTGGGGAAC
rs362548-R	ACTCCCTAAGTCCCCTCATTGAAAG
rs175169-F	GAATGGGGTCCTGCCGGT
rs175169-R	GGCCTTGGGATCCCTTTTCCT
rs443678-F	GCACAGTGGGCAATGTCTCTG
rs443678-R	AGGCCCACCTTATTTGGATCTGATT
rs885980-F	ACTGCCGTGTGTACCTCTAGGT
rs885980-R	GAGTGACCTGCCTCTACTTCGT
rs175174-F	CATCGGGCGTCGAAACTATCG
rs175174-R	CTGCTCGTTGGTGGTGCG
rs175175-F	GACAACGGGCTGAAGGCTG
rs175175-R	AGGGAGCGGGGTCAGTGG

Probe	Sequence	Bead
rs363039-C	CTTTATCAATACATACTACAATCAGTCAGGGGGCTTCTACC	2
rs363039-T	TCATTTACCAATCTTTCTTTATACGTCAGGGGGCTTCTACT	44
rs363039-com	CTGTCTTGTCCTCCTCTGCCTATCTTTAAACTACAAATCTAAC	
rs362602-A	TCAACAATCTTTTACAATCAAATCCAAGTATCTCCATGTTCCCAA	6
rs362602-G	TCATTTCAATCAATCATCAACAATCAAGTATCTCCATGTTCCCAG	51
rs362602-com	TTGTAGCAGTGGGGGTACCTATCTTTAAACTACAAATCTAAC	
rs362548-A	CAATAAACTATACTTCTTCACTAAACCTGGGGCAAATTCTGA	13
rs362548-G	CTATCTATCTAACTATCTATATCAACCTGGGGCAAATTCTGG	78
rs362548-com	TGATTCAGAAAATGGAAGGAATCACTATCTTTAAACTACAAATCTAAC	
rs175169-T	CTTTTCATCAATAATCTTACCTTTGCAGCCATGTTGGGT	65
rs175169-G	TATATACACTTCTCAATAACTAACGCAGCCATGTTGGGG	55
rs175169-com	GGAATGGCTGGGAGACACTATCTTTAAACTACAAATCTAAC	
rs443678-T	CTTTAATCCTTTATCACTTTATCACCTGTCTGCCTCTCTTGT	17
rs443678-C	TTACTTCACTTTCTATTTACAATCCCTGTCTGCCTCTCTTGC	88
rs443678-com	TAAATTCCCTGAGCCAGTAAGTCTATCTTTAAACTACAAATCTAAC	
rs885980-T	AATCTACACTAACAATTTCATAACCCCACCAGGGACTCAT	99
rs885980-C	AATCTAACAAACTCATCTAAATACCCCACCAGGGACTCAC	76
rs885980-com	GTGTCCTCGTTCCCGTCTATCTTTAAACTACAAATCTAAC	
rs175174-A	CTTTCAATTACAATACTCATTACATCCCTAGGTTGGGAGGA	43
rs175174-G	CAATTTACTCATATACATCACTTTTCCCTAGGTTGGGAGGG	56
rs175174-com	TTACCAGACAGTGAGTGGCCTATCTTTAAACTACAAATCTAAC	
rs175175-T	CTATAAACATATTACATTCACATCCAGAGCCGTAGACAGATTCTT	69
rs175175-G	CTATTACACTTTAAACATCAATACCAGAGCCGTAGACAGATTCTG	92
rs175175-com	GGTTTGTCCACAGGCACCTATCTTTAAACTACAAATCTAAC	

Primers and probes for data presented in Table 3.4	
Primer	Sequence
rs2292570-F	ACATGAACAGATGCCTTAACTTCCT
rs2292570-R	GGCTTTCTCGTCCCCAAATGG
rs175175-F	GACAACGGGCTGAAGGCTG
rs175175-R	AGGGAGCGGGGTCAGTGG
rs175168-F	GTACAGGTGTCAGTTGGAGGCTT
rs175168-R	CCCACATGGGCGTCCTTGTATAG
rs175169-F	GAATGGGGTCCTGCCGGT
rs175169-R	GGCCTTGGGATCCCTTTTCCT
rs1640299-F	CCACCTCCTGGAGTTACCCTG
rs1640299-R	GGTGGACATATGGACTCGACTGC
rs737935-F	GTGTCCGTGGGCTGTGCT
rs737935-R	GGTCAAGATCAAACTCTGTCACTGC
rs7288396-F	GGGCCCTTTAGCTGAGTGGTC
rs7288396-R	GAGGCTGGGGCACTAGTTGG
rs720014-F	CTGGTGGCCCCTATGGGTG
rs720014-R	TTCACAGGCGCATCTGGCT
rs443678-F	GCACAGTGGGCAATGTCTCTG
rs443678-R	AGGCCCACCTTATTTGGATCTGATT
rs9606241-F	TGCTGCCTATGTCGTGTTGGTAG
rs9606241-R	CACTGCGTGGGCTCTCTCC
rs9606240-F	GTCTCTATGGGACTGCCAGGTTC
rs9606240-R	TCACACCGTATGTTCCCAAAGATGT
rs175162-F	GAAGTGTGTCGTGTGGGCTG
rs175162-R	GCAGCTTGGACGATCTGGACTG
rs175172-F	AAGGGGTTCTGTTGGGTCGG
rs175172-R	GGAGGGGTCCCTGGTTCTCA
rs175174-F	CATCGGGCGTCGAAACTATCG
rs175174-R	CTGCTCGTTGGTGGTGCG
rs11703058-F	AGTGGAGGGGTGGTTGCTTC
rs11703058-R	ACCCACCTTGCCCTTGGTC
rs1633445-F	CGCCTGAGGTTCTTAGCTCTCC
rs1633445-R	TGGCTTGCGTGAGTGGCTT
rs885980-F	ACTGCCGTGTGTACCTCTAGGT
rs885980-R	GAGTGACCTGCCTCTACTTCGT
rs720012-F	CCACCTCCTGGAGTTACCCTG
rs720012-R	GCAGAACGCTGGACTCTTGC
rs3757-F	GCCAAGCATGGGTATGAATCGTG
rs3757-R	TTCCCTTCTGGACAGTTTGCTTTAT

Probe	Sequence (tags in red)	Bead
rs9606240-C	TCATTTACCTTTAATCCAATAATCTGAGCGTCTTCAGCACTTC	72
rs9606240-T	TCATCAATCAATCTTTTTCACTTTTGAGCGTCTTCAGCACTTT	59
rs11703058-G	ATACTAACTCAACTAACTTTAAACATGCGGATCCTGGTGTG	96
rs11703058-A	CTTTTCAAATCAATACTCAACTTTATGCGGATCCTGGTGTA	27
rs9606241-G	TACACTTTCTTTCTTTCTTTCTTTGGTTTGGTGCTGCATTTTCAG	12
rs9606241-A	CTTTCTATCTTTCTACTCAATAATGGTTTGGTGCTGCATTTTCAA	94
rs737935-A	CAATATACCAATATCATCATTTACGCATTGAGTGTGCACCA	50
rs737935-G	TAATCTTCTATATCAACATCTTACGCATTGAGTGTGCACCG	9
rs7288396-T	CTACTATACATCTTACTATACTTTGCTTGGACAGGGATTTTCT	14
rs7288396-G	CTACATATTCAAATTACTACTTACGCTTGGACAGGGATTTTCG	64
rs443678-T	CTTTAATCCTTTATCACTTTATCACCTGTCTGCCTCTCTTGT	17
rs443678-C	TTACTTCACTTTCTATTTACAATCCCTGTCTGCCTCTCTTGC	88
rs1640299-T	TCATAATCTCAACAATCTTTCTTTCCCCTTTTTCTGATGAAGTCTTAATT	68
rs1640299-G	AATCTTACTACAAATCCTTTCTTTCCCCTTTTTCTGATGAAGTCTTAATG	29
rs720012-A	CTACAAACAAACAAACATTATCAATTGTTGAAACAGGAAGCAAGA	28
rs720012-G	TCAAAATCTCAAATACTCAAATCATTGTTGAAACAGGAAGCAAGG	18
rs720014-T	CAATAAACTATACTTCTTCACTAACCTACAGGCGGTACTGAT	13
rs720014-C	CTAACTAACAATAATCTAACTAACCCTACAGGCGGTACTGAC	80
rs3757-A	AATCCTTTTACATTCATTACTTACGCTGATGCCATCCAGA	8
rs3757-G	TCATTTACCAATCTTTCTTTATACGCTGATGCCATCCAGG	44
rs1633445-T	CTTTTACAATACTTCAATACAATCGGTGAGCCACCCCAT	20
rs1633445-C	CTTTATCAATACATACTACAATCAGGTGAGCCACCCCAC	2
rs885980-T	AATCTACACTAACAATTTCATAACCCCACCAGGGACTCAT	99
rs885980-C	AATCTAACAAACTCATCTAAATACCCCACCAGGGACTCAC	76
rs175162-T	CAATTTCATCATTCATTCATTTCAGCTCCGGTTCCCATTAGT	35
rs175162-G	TCATCAATCTTTCAATTTACTTACGCTCCGGTTCCCATTAGG	49
rs175168-T	CAATTAACTACATACAATACATACCAGTGAGAAGGCCCCTT	77
rs175168-C	ATCATACATACATACAAATCTACACAGTGAGAAGGCCCCTC	10
rs175169-T	CTTTTCATCAATAATCTTACCTTTGCAGCCATGTTGGGT	65
rs175169-G	TATATACACTTCTCAATAACTAACGCAGCCATGTTGGGG	55
rs175172-T	TTACCTTTATACCTTTCTTTTTACTGTTTGCTCCTCGGACT	30
rs175172-G	TCAATTACTTCACTTTAATCCTTTTGTTTGCTCCTCGGACG	33
rs175174-A	CTTTCAATTACAATACTCATTACATCCCTAGGTTGGGAGGA	43
rs175174-G	CAATTTACTCATATACATCACTTTTCCCTAGGTTGGGAGGG	56
rs175175-T	CTATAAACATATTACATTCACATCCAGAGCCGTAGACAGATTCTT	69
rs175175-G	CTATTACACTTTAAACATCAATACCAGAGCCGTAGACAGATTCTG	92
rs2292570-T	CTTTTCATCTTTTCATCTTTCAATCTGTGTCCTCCAGCAGT	37
rs2292570-C	CTTTAATCTCAATCAATACAAATCCTGTGTCCTCCAGCAGC	1
rs2292570-com	GGTACGGCCTGCGGCTATCTTTAAACTACAAATCTAAC	
rs11703058-com	ATAGTCAGTTGTTAGCTCTGTGCCTATCTTTAAACTACAAATCTAAC	
rs9606241-com	TGCTATGGAAACCACAGAGCTATCTTTAAACTACAAATCTAAC	
rs737935-com	CAGGCTCATTCAGAAGGTAAACCTATCTTTAAACTACAAATCTAAC	
rs7288396-com	TAAATGTCGGGTACACATAGGTCTATCTTTAAACTACAAATCTAAC	
rs443678-com	TAAATTCCCTGAGCCAGTAAGTCTATCTTTAAACTACAAATCTAAC	
rs1640299-com	CCTTCCTGTGTGTTCTTGGCTATCTTTAAACTACAAATCTAAC	
rs720012-com	CCCTAAAAGCGCCTCTTTGCTATCTTTAAACTACAAATCTAAC	
rs720014-com	GCCTTCAGTGTAGCCCACTATCTTTAAACTACAAATCTAAC	
rs3757-com	GGCGCNTTTTTTTTTTTTTTCTGTCTATCTTTAAACTACAAATCTAAC	
rs1633445-com	GCACTGGGCTGTGCCTATCTTTAAACTACAAATCTAAC	
rs885980-com	GTGTCCTCGTTCCCGTCTATCTTTAAACTACAAATCTAAC	
rs175162-com	GGCTACCTGGAAGAAGGCCTATCTTTAAACTACAAATCTAAC	
rs175168-com	TGTTGCGGAGCCTGACTATCTTTAAACTACAAATCTAAC	
rs175169-com	GGAATGGCTGGGAGACACTATCTTTAAACTACAAATCTAAC	
rs175172-com	GGGGAGGCCGGTGCTATCTTTAAACTACAAATCTAAC	
rs175174-com	TTACCAGACAGTGAGTGGCCTATCTTTAAACTACAAATCTAAC	
rs175175-com	GGTTTGTCCACAGGCACCTATCTTTAAACTACAAATCTAAC	
rs2292570-com	GGGAGGGGGCTAGGTCTATCTTTAAACTACAAATCTAAC	

APPENDIX 3

Oligonucleotide sequences for DGCR8 association study (Chapter 4)

Primers and probes for data presented in Table 4.2	
Primer	Sequence
rs175175-F	GACAACGGGCTGAAGGCTG
rs175175-R	AGGGAGCGGGGTCAGTGG
rs175169-F	GAATGGGGTCCTGCCGGT
rs175169-R	GGCCTTGGGATCCCTTTTCCT
rs1640299-F	CCACCTCCTGGAGTTACCCTG
rs1640299-R	GGTGGACATATGGACTCGACTGC
rs737935-F	GTGTCCGTGGGCTGTGCT
rs737935-R	GGTCAAGATCAAACTCTGTCACTGC
rs443678-F	GCACAGTGGGCAATGTCTCTG
rs443678-R	AGGCCCACCTTATTTGGATCTGATT
rs9606241-F	TGCTGCCTATGTCGTGTTGGTAG
rs9606241-R	CACTGCGTGGGCTCTCTCC
rs9606240-F	GTCTCTATGGGACTGCCAGGTTC
rs9606240-R	TCACACCGTATGTTCCCAAAGATGT
rs175174-F	CATCGGGCGTCGAAACTATCG
rs175174-R	CTGCTCGTTGGTGGTGCG
rs11703058-F	AGTGGAGGGGTGGTTGCTTC
rs11703058-R	ACCCACCTTGCCCTTGGTC
rs1633445-F	CGCCTGAGGTTCTTAGCTCTCC
rs1633445-R	TGGCTTGCGTGAGTGGCTT
rs885980-F	ACTGCCGTGTGTACCTCTAGGT
rs885980-R	GAGTGACCTGCCTCTACTTCGT
rs720012-F	CCACCTCCTGGAGTTACCCTG
rs720012-R	GCAGAACGCTGGACTCTTGC
rs17817767_rs1558496-F	GAATCCAGGAAATGGGGTGA
rs17817767_rs1558496-R	CCCGGAAAGAACAGGAGAT
rs174891-F	ACCAACACTGCAATCAAGATG
rs174891-R	AGGACATTCAGGATCTGGC
rs9606252-F	GTTGTCCATGCTCCAGAGT
rs9606252-R	GACAGGGAAACAAGAGGTGA
rs417309-F	TCCATATGTCCACCCATTGATT
rs417309-R	CTGCCTTTGACATCCAGAGA
rs737871-F	TTCGGTTCTTACGTCTGGAA
rs737871-R	TCGCTGCTCTTCACTGTT

Probe	Sequence (tags in red)	Bead
rs9606240-C	TCATTTACCTTTAATCCAATAATCTGAGCGTCTTCAGCACTTC	72
rs9606240-T	TCATCAATCAATCTTTTTCACTTTTGAGCGTCTTCAGCACTTT	59
rs11703058-G	ATACTAACTCAACTAACTTTAAACATGCGGATCCTGGTGTG	96
rs11703058-A	CTTTTCAAATCAATACTCAACTTTATGCGGATCCTGGTGTA	27
rs9606241-G	TACACTTTCTTTCTTTCTTTCTTTGGTTTGGTGCTGCATTTTCAG	12
rs9606241-A	CTTTCTATCTTTCTACTCAATAATGGTTTGGTGCTGCATTTTCAA	94
rs737935-A	CAATATACCAATATCATCATTTACGCATTGAGTGTGCACCA	50
rs737935-G	TAATCTTCTATATCAACATCTTACGCATTGAGTGTGCACCG	9
rs443678-T	CTTTAATCCTTTATCACTTTATCACCTGTCTGCCTCTCTTGT	17
rs443678-C	TTACTTCACTTTCTATTTACAATCCCTGTCTGCCTCTCTTGC	88
rs1640299-T	TCATAATCTCAACAATCTTTCTTTCCCTTTTTCTGATGAAGTCTTAATT	68
rs1640299-G	AATCTTACTACAAATCCTTTCTTTCCCTTTTTCTGATGAAGTCTTAATG	29
rs720012-A	CTACAAACAAACAAACATTATCAATTGTTGAAACAGGAAGCAAGA	28
rs720012-G	TCAAAATCTCAAATACTCAAATCATTGTTGAAACAGGAAGCAAGG	18
rs1633445-T	CTTTTACAATACTTCAATACAATCGGTGAGCCACCCCAT	20
rs1633445-C	CTTTATCAATACATACTACAATCAGGTGAGCCACCCCAC	2
rs885980-T	AATCTACACTAACAATTTCATAACCCCACCAGGGACTCAT	99
rs885980-C	AATCTAACAAACTCATCTAAATACCCCACCAGGGACTCAC	76
rs175169-T	CTTTTCATCAATAATCTTACCTTTGCAGCCATGTTGGGT	65
rs175169-G	TATATACACTTCTCAATAACTAACGCAGCCATGTTGGGG	55
rs175174-A	CTTTCAATTACAATACTCATTACATCCCTAGGTTGGGAGGA	43
rs175174-G	CAATTTACTCATATACATCACTTTTCCCTAGGTTGGGAGGG	56
rs175175-T	CTATAAACATATTACATTCACATCCAGAGCCGTAGACAGATTCTT	69
rs175175-G	CTATTACACTTTAAACATCAATACCAGAGCCGTAGACAGATTCTG	92
rs17817767-A	TCATTTACTCAACAATTACAAATCTGTCTCTTGTCCATATAGTGCA	67
rs17817767-G	AAACTAACATCAATACTTACATCATGTCTCTTGTCCATATAGTGCG	87
rs1558496-C	TCAATTACTTCACTTTAATCCTTTAAGTACATCCACCATGCCC	33
rs1558496-T	TCATTCATATACATACCAATTCATAAGTACATCCACCATGCCT	34
rs174891-A	TCATCAATCAATCTTTTTCACTTTTGGGAGAGTTTGACCAACA	59
rs174891-G	AATCCTTTTACATTCATTACTTACTGGGAGAGTTTGACCAACG	8
rs9606252-C	TAACATTACAACTATACTATCTACCAGGAGGCACTCTCAGC	66
rs9606252-T	AATCTAACAAACTCATCTAAATACCAGGAGGCACTCTCAGT	76
rs417309-C	TCAACTAACTAATCATCTATCAATACAAGTCCACTTGCTAAAATGC	84
rs417309-T	CAATTCATTTCATTCACAATCAATACAAGTCCACTTGCTAAAATGT	36
rs737871-A	AATCCTTTTTACTCAATTCAATCAAGAAGCTCGCGTTCCA	22
rs737871-T	CTACAAACAAACAAACATTATCAAAGAAGCTCGCGTTCCT	28
rs11703058-com	ATAGTCAGTTGTTAGCTCTGTGCCTATCTTTAAACTACAAATCTAAC	
rs9606241-com	TGCTATGGAAACCACAGAGCTATCTTTAAACTACAAATCTAAC	
rs737935-com	CAGGCTCATTCAGAAGGTAAACCTATCTTTAAACTACAAATCTAAC	
rs443678-com	TAAATTCCCTGAGCCAGTAAGTCTATCTTTAAACTACAAATCTAAC	
rs1640299-com	CCTTCCTGTGTGTTCTTGGCTATCTTTAAACTACAAATCTAAC	
rs720012-com	CCCTAAAAGCGCCTCTTTGCTATCTTTAAACTACAAATCTAAC	
rs1633445-com	GCACTGGGCTGTGCCTATCTTTAAACTACAAATCTAAC	
rs885980-com	GTGTCCTCGTTCCCGTCTATCTTTAAACTACAAATCTAAC	
rs175169-com	GGAATGGCTGGGAGACACTATCTTTAAACTACAAATCTAAC	
rs175174-com	TTACCAGACAGTGAGTGGCCTATCTTTAAACTACAAATCTAAC	
rs175175-com	GGTTTGTCCACAGGCACCTATCTTTAAACTACAAATCTAAC	
rs17817767-com	TTCCTCGGAGTAGATGGCCTATCTTTAAACTACAAATCTAAC	
rs1558496-com	TGTCCCTTGTTAAATGTGTGATGCTATCTTTAAACTACAAATCTAAC	
rs174891-com	AAGAAGAATGTTGGAATGTACAGAAACTATCTTTAAACTACAAATCTAAC	
rs9606252-com	TTCAGCCAAAGTCCTAGTCTGCTATCTTTAAACTACAAATCTAAC	
rs417309-com	ATGATTCCAAATCTACCTTCTACTCTCCTATCTTTAAACTACAAATCTAAC	
rs737871-com	GCGTGGGGCACAGGTCTATCTTTAAACTACAAATCTAAC	

List of pedigrees from the National Institute of Mental Health Human Genetics Initiative included in DGCR8 association study.

Affection statuses under three categorical phenotypes are listed.
1 – unaffected
2 – affected
0 – phenotype unknown
* pedigree uninformative

Pedigree	Person	Narrow	Broad	Spectrum
30-30144	1	0	0	0
30-30144	2	1	1	1
30-30144	3	2	2	2
30-30144	4	1	1	1
30-30144	5	2	2	2
32-32107	1	0	0	0
32-32107	2	0	0	0
32-32107	3	2	2	2
32-32107	4	2	2	2
41-0007	1	1	1	1
41-0007	2	1	1	1
41-0007	3	2	2	2
41-0007	4	2	2	2
41-0033	1	1	1	1
41-0033	2	1	1	1
41-0033	3	2	2	2
41-0033	4	2	2	2
41-0033	5	1	1	1
41-0033	6	1	1	1
41-0033	7	0	0	2
41-0042	1	1	1	1
41-0042	2	1	1	1
41-0042	3	2	2	2
41-0042	4	0	0	0
41-0080	1	1	1	1
41-0080	2	1	1	1
41-0080	3	0	0	0
41-0080	4	2	2	2
41-0083	1	1	1	1
41-0083	2	1	1	1
41-0083	3	2	2	2
41-0083	4	2	2	2
43-1002	1	0	0	0
43-1002	2	0	0	0
43-1002	3	0	0	0
43-1002	4	2	2	2
43-1002	5	2	2	2
43-1008	1	0	0	0
43-1008	2	0	0	0
43-1008	3	0	0	0
43-1008	4	2	2	2
43-1008	5	2	2	2
43-1024	1	0	0	0
43-1024	2	0	0	0
43-1024	3	0	0	0
43-1024	4	0	0	0
43-1024	5	0	0	0
43-1024	6	2	2	2
43-1031	1	0	0	0
43-1031	2	0	0	0
43-1031	3	2	2	2
43-1031	4	2	2	2

43-1050	1	0	0	0
43-1050	2	0	0	0
43-1050	3	0	0	0
43-1050	4	2	2	2
43-1050	5	2	2	2
43-1054	1	0	0	0
43-1054	2	1	1	1
43-1054	3	2	2	2
43-1054	4	2	2	2
43-1054	5	0	0	0
43-1074	1	0	0	0
43-1074	2	2	2	2
43-1074	3	0	0	0
43-1074	4	2	2	2
44-1001	1	1	1	1
44-1001	2	1	1	1
44-1001	3	2	2	2
44-1001	4	2	2	2
44-1001	5	1	1	1
44-1001	6	1	1	1
45-1002	1	0	0	0
45-1002	2	0	0	0
45-1002	3	0	0	0
45-1002	4	2	2	2
45-1009	1	0	0	0
45-1009	2	1	1	1
45-1009	3	1	1	1
45-1009	4	1	1	1
45-1009	5	2	2	2
45-1009	6	2	2	2
45-1010	1	0	0	0
45-1010	2	1	1	1
45-1010	3	2	2	2
45-1010	4	2	2	2
45-1037	1	0	0	0
45-1037	2	0	0	0
45-1037	3	2	2	2
45-1037	4	2	2	2
45-1040	1	0	0	0
45-1040	2	0	0	0
45-1040	3	0	0	0
45-1040	4	0	0	0
45-1040	5	0	0	0
45-1040	6	2	2	2
45-1040	7	2	2	2
45-1040	8	2	2	2
45-1040	9	2	2	2
45-1040	10	2	2	2
45-1040	11	0	0	0
45-1040	12	0	0	0
45-1040	13	0	0	0
45-1041	1	0	0	0
45-1041	2	0	0	0
45-1041	3	2	2	2
45-1041	4	2	2	2
45-1044	1	0	0	0
45-1044	2	0	0	0
45-1044	3	0	0	0
45-1044	4	2	2	2
45-1044	5	2	2	2
45-1046	1	0	0	0
45-1046	2	0	0	0
45-1046	3	2	2	2
45-1046	4	2	2	2
46-1013	1	0	0	0
46-1013	2	0	0	0

46-1013	3	2	2	2
46-1013	4	2	2	2
46-1028	1	0	0	0
46-1028	2	1	1	1
46-1028	3	2	2	2
46-1028	4	0	0	0
46-1030	1	0	0	0
46-1030	2	0	0	0
46-1030	3	2	2	2
46-1030	4	2	2	2
46-1036	1	0	0	0
46-1036	2	0	0	0
46-1036	3	2	2	2
46-1036	4	2	2	2
46-1038	1	1	1	1
46-1038	2	0	0	0
46-1038	3	2	2	2
46-1038	4	0	0	0
46-1038	5	2	2	2
46-1040	1	1	1	1
46-1040	2	1	1	1
46-1040	3	0	0	0
46-1040	4	2	2	2
46-1040	5	2	2	2
46-1042	1	0	0	0
46-1042	2	0	0	0
46-1042	3	2	2	2
46-1042	4	2	2	2
46-1043	1	1	1	1
46-1043	2	0	0	0
46-1043	3	2	2	2
46-1043	4	0	0	0
47-1010	1	0	0	0
47-1010	2	0	0	0
47-1010	3	2	2	2
47-1010	4	1	1	1
47-1010	5	1	1	1
47-1010	6	2	2	2
47-1064	1	0	0	0
47-1064	2	0	0	0
47-1064	3	0	0	0
47-1064	4	2	2	2
47-1067	1	0	0	0
47-1067	2	0	0	0
47-1067	3	2	2	2
47-1067	4	2	2	2
47-1067	5	0	0	0
47-1093	1	0	0	0
47-1093	2	1	1	1
47-1093	3	2	2	2
47-1093	4	2	2	2
48-1004	1	1	1	1
48-1004	2	1	1	1
48-1004	3	2	2	2
48-1004	4	2	2	2
49-1016	1	1	1	1
49-1016	2	0	0	2
49-1016	3	0	0	0
49-1016	4	2	2	2
49-1023	1	1	1	1
49-1023	2	0	0	2
49-1023	3	1	1	1
49-1023	4	0	0	0
49-1023	5	2	2	2
49-1029	1	1	1	1
49-1029	2	0	0	0

49-1029	3	2	2	2
49-1029	4	0	0	0
49-1034	1	1	1	1
49-1034	2	0	0	0
49-1034	3	2	2	2
49-1034	4	0	0	0
32-32101	1	0	0	0
32-32101	2	0	0	0
32-32101	3	2	2	2
32-32101	4	2	2	2
32-32101	5	1	1	1
32-32101	6	0	0	0
32-32102	1	0	0	0
32-32102	2	0	0	0
32-32102	3	0	0	0
32-32102	4	2	2	2
32-32102	5	1	1	1
32-32108	1	0	0	0
32-32108	2	1	1	1
32-32108	3	2	2	2
32-32108	4	0	0	0
32-32108	5	1	1	1
32-32108	6	1	1	1
32-32202	1	0	0	0
32-32202	2	1	1	1
32-32202	3	2	2	2
32-32202	4	2	2	2
32-32202	5	1	1	1
32-32308	1	0	0	0
32-32308	2	2	2	2
32-32308	3	1	1	1
32-32308	4	0	0	0
32-32308	5	1	1	1
32-32308	6	1	1	1
32-32308	7	1	1	1
32-32308	8	1	1	1
32-32308	9	1	1	1
32-32311	1	1	1	1
32-32311	2	0	0	2
32-32311	3	0	0	0
32-32311	4	0	0	0
32-32311	5	2	2	2
32-32313	1	0	0	0
32-32313	2	1	1	1
32-32313	3	0	0	0
32-32313	4	1	1	1
32-32313	5	2	2	2
32-32321	1	0	0	0
32-32321	2	1	1	1
32-32321	3	0	0	0
32-32321	4	0	0	0
32-32321	5	2	2	2
32-32321	6	1	1	1
32-32407	1	0	0	0
32-32407	2	0	0	0
32-32407	3	0	0	0
32-32407	4	2	2	2
32-32407	5	1	1	1
32-32407	6	0	0	2
32-32407	7	0	0	0
32-32407	8	2	2	2
41-0001	1	1	1	1
41-0001	2	1	1	1
41-0001	3	1	1	1
41-0001	4	2	2	2
41-0001	5	2	2	2

41-0005	1	1	1	1
41-0005	2	1	1	1
41-0005	3	2	2	2
41-0005	4	2	2	2
41-0008	1	1	1	1
41-0008	2	1	1	1
41-0008	3	2	2	2
41-0008	4	2	2	2
41-0017	1	1	1	1
41-0017	2	1	1	1
41-0017	3	2	2	2
41-0017	4	2	2	2
41-0017	5	1	1	1
41-0034	1	1	1	1
41-0034	2	1	1	1
41-0034	3	2	2	2
41-0034	4	2	2	2
41-0048	1	1	1	1
41-0048	2	1	1	1
41-0048	3	2	2	2
41-0048	4	2	2	2
41-0048	5	2	2	2
41-0053	1	1	1	1
41-0053	2	1	1	1
41-0053	3	2	2	2
41-0053	4	2	2	2
41-0060	1	2	2	2
41-0060	2	1	1	1
41-0060	3	2	2	2
41-0060	4	2	2	2
41-0061	1	1	1	1
41-0061	2	2	2	2
41-0061	3	2	2	2
41-0061	4	2	2	2
41-0079	1	1	1	1
41-0079	2	1	1	1
41-0079	3	2	2	2
41-0079	4	2	2	2
42-1007	1	0	0	0
42-1007	2	0	0	0
42-1007	3	2	2	2
42-1007	4	2	2	2
42-1010	1	0	0	0
42-1010	2	0	0	0
42-1010	3	2	2	2
42-1010	4	2	2	2
42-1016	1	2	2	2
42-1016	2	0	0	0
42-1016	3	2	2	2
42-1016	4	0	0	0
42-1034	1	0	0	0
42-1034	2	0	0	0
42-1034	3	2	2	2
42-1034	4	2	2	2
42-1034	5	2	2	2
43-1004	1	0	0	0
43-1004	2	0	0	0
43-1004	3	2	2	2
43-1004	4	2	2	2
43-1023	1	0	0	0
43-1023	2	0	0	0
43-1023	3	0	0	0
43-1023	4	2	2	2
43-1023	5	0	0	0
43-1025	1	0	0	0
43-1025	2	0	0	0

43-1025	3	0	0	0
43-1025	4	2	2	2
43-1025	5	0	0	0
43-1040	1	0	0	0
43-1040	2	0	0	0
43-1040	3	1	1	1
43-1040	4	1	1	1
43-1040	5	2	2	2
43-1040	6	2	2	2
43-1046	1	1	1	1
43-1046	2	1	1	1
43-1046	3	2	2	2
43-1046	4	0	0	0
43-1052	1	1	1	1
43-1052	2	0	0	0
43-1052	3	2	2	2
43-1052	4	2	2	2
44-1025	1	0	0	0
44-1025	2	1	1	1
44-1025	3	1	1	1
44-1025	4	2	2	2
44-1025	5	0	0	0
45-1033	1	1	1	1
45-1033	2	1	1	1
45-1033	3	2	2	2
45-1033	4	2	2	2
46-1035	1	0	0	0
46-1035	2	0	0	0
46-1035	3	2	2	2
46-1035	4	2	2	2
47-1023	1	0	0	0
47-1023	2	0	0	0
47-1023	3	2	2	2
47-1023	4	1	1	1
47-1023	5	0	0	0
47-1056	1	1	1	1
47-1056	2	1	1	1
47-1056	3	2	2	2
47-1056	4	0	0	2
47-1056	5	2	2	2
47-1066	1	0	0	0
47-1066	2	0	0	0
47-1066	3	2	2	2
47-1066	4	2	2	2
47-1090	1	0	0	2
47-1090	2	0	0	0
47-1090	3	2	2	2
47-1090	4	2	2	2
47-1090	5	2	2	2
48-1021	1	0	0	0
48-1021	2	1	1	1
48-1021	3	2	2	2
48-1021	4	0	0	0
48-1034	1	0	0	2
48-1034	2	1	1	1
48-1034	3	2	2	2
48-1034	4	2	2	2
48-1034	5	1	1	1
48-1034	6	1	1	1
49-1003	1	1	1	1
49-1003	2	1	1	1
49-1003	3	0	0	0
49-1003	4	2	2	2
49-1031	1	1	1	1
49-1031	2	1	1	1
49-1031	3	0	0	0

49-1031	4	2	2	2
30-30106	1	2	2	2
30-30106	2	1	1	1
30-30106	3	0	0	0
30-30106	4	0	0	2
30-30106	5	0	0	0
30-30106	6	2	2	2
30-30106	7	2	2	2
30-30108	1	1	1	1
30-30108	2	1	1	1
30-30108	3	0	0	0
30-30108	4	0	0	0
30-30108	5	2	2	2
30-30108	6	2	2	2
30-30108	7	1	1	1
30-30108	8	1	1	1
30-30147	1	0	0	0
30-30147	2	1	1	1
30-30147	3	0	0	0
30-30147	4	0	0	2
30-30147	5	0	0	2
30-30147	6	0	0	0
30-30147	7	0	0	0
30-30147	8	1	1	1
30-30147	9	1	1	1
30-30147	10	2	2	2
30-30147	11	2	2	2
31-31152	1	1	1	1
31-31152	2	1	1	1
31-31152	3	2	2	2
31-31152	4	2	2	2
31-31158	1	0	0	0
31-31158	2	0	0	0
31-31158	3	2	2	2
31-31158	4	2	2	2
31-31158	5	1	1	1
31-31167	1	0	0	0
31-31167	2	1	1	1
31-31167	3	2	2	2
31-31167	4	2	2	2
31-31167	5	1	1	1
32-32103	1	0	0	0
32-32103	2	0	0	0
32-32103	3	2	2	2
32-32103	4	2	2	2
32-32103	5	1	1	1
32-32103	6	0	0	0
32-32106	1	0	0	0
32-32106	2	1	1	1
32-32106	3	0	0	0
32-32106	4	2	2	2
32-32106	5	2	2	2
32-32106	6	1	1	1
32-32106	7	0	0	2
32-32109	1	1	1	1
32-32109	2	0	0	0
32-32109	3	1	1	1
32-32109	4	0	0	0
32-32109	5	1	1	1
32-32109	6	1	1	1
32-32109	7	0	0	0
32-32109	8	1	1	1
32-32109	9	0	0	0
32-32109	10	2	2	2
32-32211	1	1	1	1
32-32211	2	1	1	1

32-32211	3	0	0	0
32-32211	4	2	2	2
32-32211	5	1	1	1
32-32211	6	1	1	1
32-32213	1	0	0	0
32-32213	2	0	0	0
32-32213	3	2	2	2
32-32213	4	2	2	2
32-32213	5	0	0	0
32-32213	6	1	1	1
32-32219	1	0	0	0
32-32219	2	0	0	0
32-32219	3	0	0	0
32-32219	4	0	0	0
32-32219	5	0	0	0
32-32219	6	0	0	2
32-32219	7	1	1	1
32-32219	8	1	1	1
32-32219	9	2	2	2
32-32219	10	2	2	2
32-32315	1	0	0	0
32-32315	2	1	1	1
32-32315	3	2	2	2
32-32315	4	0	0	0
32-32315	5	1	1	1
32-32317	1	0	0	0
32-32317	2	0	0	0
32-32317	3	0	0	0
32-32317	4	1	1	1
32-32317	5	1	1	1
32-32317	6	2	2	2
32-32317	7	2	2	2
32-32317	8	0	0	2
32-32319	1	0	0	0
32-32319	2	1	1	1
32-32319	3	0	0	2
32-32319	4	0	0	0
32-32319	5	2	2	2
32-32319	6	1	1	1
32-32402	1	0	0	2
32-32402	2	1	1	1
32-32402	3	2	2	2
32-32402	4	0	0	0
32-32402	5	1	1	1
41-0003	1	1	1	1
41-0003	2	1	1	1
41-0003	3	2	2	2
41-0003	4	1	1	1
41-0003	5	2	2	2
41-0012	1	1	1	1
41-0012	2	2	2	2
41-0012	3	2	2	2
41-0012	4	2	2	2
41-0014	1	1	1	1
41-0014	2	1	1	1
41-0014	3	2	2	2
41-0014	4	0	0	0
41-0014	5	1	1	1
41-0014	6	1	1	1
41-0016	1	0	0	2
41-0016	2	1	1	1
41-0016	3	2	2	2
41-0016	4	0	0	0
41-0018	1	1	1	1
41-0018	2	1	1	1
41-0018	3	2	2	2

41-0018	4	2	2	2
41-0020	1	1	1	1
41-0020	2	1	1	1
41-0020	3	2	2	2
41-0020	4	2	2	2
41-0028	1	1	1	1
41-0028	2	1	1	1
41-0028	3	2	2	2
41-0028	4	2	2	2
41-0029	1	1	1	1
41-0029	2	1	1	1
41-0029	3	2	2	2
41-0029	4	2	2	2
41-0029	5	1	1	1
41-0029	6	1	1	1
41-0030	1	1	1	1
41-0030	2	1	1	1
41-0030	3	1	1	1
41-0030	4	2	2	2
41-0030	5	2	2	2
41-0035	1	*	*	2
41-0035	2	*	*	1
41-0035	3	*	*	0
41-0035	4	*	*	0
41-0037	1	1	1	1
41-0037	2	1	1	1
41-0037	3	2	2	2
41-0037	4	2	2	2
41-0038	1	1	1	1
41-0038	2	1	1	1
41-0038	3	2	2	2
41-0038	4	2	2	2
41-0039	1	1	1	1
41-0039	2	1	1	1
41-0039	3	2	2	2
41-0039	4	2	2	2
41-0049	1	1	1	1
41-0049	2	1	1	1
41-0049	3	2	2	2
41-0049	4	2	2	2
41-0054	1	1	1	1
41-0054	2	1	1	1
41-0054	3	2	2	2
41-0054	4	2	2	2
41-0057	1	1	1	1
41-0057	2	1	1	1
41-0057	3	1	1	1
41-0057	4	2	2	2
41-0057	5	2	2	2
41-0057	6	1	1	1
41-0057	7	1	1	1
41-0057	8	1	1	1
41-0062	1	1	1	1
41-0062	2	0	0	2
41-0062	3	2	2	2
41-0062	4	0	0	0
41-0063	1	1	1	1
41-0063	2	1	1	1
41-0063	3	2	2	2
41-0063	4	0	0	0
41-0065	1	1	1	1
41-0065	2	1	1	1
41-0065	3	2	2	2
41-0065	4	0	0	0
41-0071	1	1	1	1
41-0071	2	1	1	1

41-0071	3	2	2	2
41-0071	4	2	2	2
41-0072	1	1	1	1
41-0072	2	1	1	1
41-0072	3	2	2	2
41-0072	4	2	2	2
41-0078	1	1	1	1
41-0078	2	1	1	1
41-0078	3	2	2	2
41-0078	4	2	2	2
41-0082	1	1	1	1
41-0082	2	1	1	1
41-0082	3	2	2	2
41-0082	4	2	2	2
41-0086	1	1	1	1
41-0086	2	1	1	1
41-0086	3	0	0	0
41-0086	4	2	2	2
41-0094	1	*	*	1
41-0094	2	*	*	1
41-0094	3	*	*	2
41-0094	4	*	*	0
41-0094	5	*	*	0
41-0096	1	1	1	1
41-0096	2	1	1	1
41-0096	3	2	2	2
41-0096	4	2	2	2
42-1006	1	1	1	1
42-1006	2	1	1	1
42-1006	3	2	2	2
42-1006	4	2	2	2
42-1024	1	1	1	1
42-1024	2	0	0	0
42-1024	3	1	1	1
42-1024	4	0	0	0
42-1024	5	2	2	2
42-1024	6	2	2	2
42-1025	1	0	0	2
42-1025	2	0	0	0
42-1025	3	2	2	2
42-1025	4	2	2	2
42-1030	1	0	0	0
42-1030	2	1	1	1
42-1030	3	2	2	2
42-1030	4	2	2	2
42-1032	1	1	1	1
42-1032	2	0	0	2
42-1032	3	2	2	2
42-1032	4	0	0	0
42-1032	5	2	2	2
42-1036	1	0	0	0
42-1036	2	1	1	1
42-1036	3	2	2	2
42-1036	4	2	2	2
42-1037	1	0	0	0
42-1037	2	0	0	0
42-1037	3	0	0	0
42-1037	4	2	2	2
42-1039	1	0	0	0
42-1039	2	0	0	0
42-1039	3	2	2	2
42-1039	4	2	2	2
42-1041	1	0	0	0
42-1041	2	0	0	2
42-1041	3	2	2	2
42-1041	4	2	2	2

42-1043	1	0	0	0
42-1043	2	2	2	2
42-1043	3	2	2	2
42-1043	4	2	2	2
43-1003	1	1	1	1
43-1003	2	0	0	0
43-1003	3	2	2	2
43-1003	4	2	2	2
43-1005	1	0	0	0
43-1005	2	0	0	0
43-1005	3	0	0	0
43-1005	4	0	0	0
43-1005	5	2	2	2
43-1005	6	2	2	2
43-1005	7	2	2	2
43-1005	8	2	2	2
43-1005	9	2	2	2
43-1005	10	0	0	0
43-1026	1	0	0	0
43-1026	2	0	0	0
43-1026	3	2	2	2
43-1026	4	0	0	0
43-1026	5	2	2	2
43-1029	1	0	0	0
43-1029	2	0	0	0
43-1029	3	2	2	2
43-1029	4	2	2	2
43-1034	1	1	1	1
43-1034	2	0	0	0
43-1034	3	2	2	2
43-1034	4	0	0	0
43-1044	1	0	0	0
43-1044	2	1	1	1
43-1044	3	2	2	2
43-1044	4	1	1	1
43-1044	5	2	2	2
43-1044	6	2	2	2
43-1051	1	1	1	1
43-1051	2	1	1	1
43-1051	3	2	2	2
43-1051	4	0	0	0
43-1066	1	0	0	0
43-1066	2	0	0	0
43-1066	3	2	2	2
43-1066	4	0	0	0
43-1066	5	2	2	2
43-1070	1	0	0	2
43-1070	2	0	0	0
43-1070	3	2	2	2
43-1070	4	2	2	2
44-1026	1	1	1	1
44-1026	2	0	0	0
44-1026	3	0	0	0
44-1026	4	2	2	2
44-1044	1	0	0	0
44-1044	2	2	2	2
44-1044	3	2	2	2
44-1044	4	2	2	2
44-1044	5	1	1	1
44-1048	1	2	2	2
44-1048	2	1	1	1
44-1048	3	2	2	2
44-1048	4	2	2	2
44-1069	1	1	1	1
44-1069	2	1	1	1
44-1069	3	2	2	2

44-1069	4	2	2	2
44-1075	1	1	1	1
44-1075	2	1	1	1
44-1075	3	2	2	2
44-1075	4	2	2	2
45-1001	1	0	0	0
45-1001	2	0	0	0
45-1001	3	0	0	0
45-1001	4	2	2	2
45-1004	1	0	0	0
45-1004	2	1	1	1
45-1004	3	2	2	2
45-1004	4	2	2	2
45-1007	1	0	0	0
45-1007	2	0	0	0
45-1007	3	2	2	2
45-1007	4	2	2	2
45-1011	1	0	0	0
45-1011	2	0	0	0
45-1011	3	2	2	2
45-1011	4	2	2	2
45-1030	1	1	1	1
45-1030	2	0	0	0
45-1030	3	2	2	2
45-1030	4	2	2	2
45-1030	5	2	2	2
46-1002	1	0	0	0
46-1002	2	0	0	0
46-1002	3	0	0	0
46-1002	4	0	0	0
46-1002	5	0	0	0
46-1002	6	2	2	2
46-1003	1	0	0	0
46-1003	2	0	0	0
46-1003	3	0	0	2
46-1003	4	2	2	2
46-1003	5	2	2	2
46-1003	6	2	2	2
46-1003	7	2	2	2
46-1007	1	0	0	0
46-1007	2	0	0	0
46-1007	3	2	2	2
46-1007	4	2	2	2
46-1009	1	0	0	0
46-1009	2	1	1	1
46-1009	3	0	0	0
46-1009	4	0	0	0
46-1009	5	2	2	2
46-1009	6	2	2	2
46-1010	1	0	0	0
46-1010	2	0	0	0
46-1010	3	0	0	0
46-1010	4	2	2	2
46-1015	1	0	0	0
46-1015	2	0	0	0
46-1015	3	2	2	2
46-1015	4	2	2	2
46-1017	1	0	0	0
46-1017	2	0	0	0
46-1017	3	2	2	2
46-1017	4	2	2	2
46-1022	1	0	0	0
46-1022	2	1	1	1
46-1022	3	2	2	2
46-1022	4	2	2	2
46-1025	1	0	0	0

46-1025	2	1	1	1
46-1025	3	0	0	0
46-1025	4	2	2	2
46-1025	5	2	2	2
46-1025	6	0	0	0
46-1045	1	0	0	0
46-1045	2	0	0	0
46-1045	3	2	2	2
46-1045	4	2	2	2
46-1052	1	0	0	0
46-1052	2	0	0	0
46-1052	3	0	0	0
46-1052	4	2	2	2
46-1052	5	2	2	2
47-1003	1	0	0	0
47-1003	2	0	0	0
47-1003	3	2	2	2
47-1003	4	0	0	0
47-1008	1	0	0	0
47-1008	2	0	0	0
47-1008	3	2	2	2
47-1008	4	2	2	2
47-1009	1	0	0	0
47-1009	2	0	0	0
47-1009	3	2	2	2
47-1009	4	2	2	2
47-1025	1	0	0	0
47-1025	2	0	0	0
47-1025	3	2	2	2
47-1025	4	2	2	2
47-1025	5	0	0	0
47-1025	6	2	2	2
47-1040	1	0	0	0
47-1040	2	0	0	0
47-1040	3	2	2	2
47-1040	4	2	2	2
47-1044	1	0	0	0
47-1044	2	0	0	0
47-1044	3	2	2	2
47-1044	4	0	0	0
47-1053	1	0	0	0
47-1053	2	0	0	2
47-1053	3	0	0	0
47-1053	4	2	2	2
47-1053	5	0	0	2
47-1059	1	0	0	0
47-1059	2	0	0	0
47-1059	3	2	2	2
47-1059	4	2	2	2
47-1062	1	0	0	0
47-1062	2	2	2	2
47-1062	3	2	2	2
47-1062	4	2	2	2
47-1062	5	2	2	2
47-1070	1	0	0	0
47-1070	2	0	0	0
47-1070	3	1	1	1
47-1070	4	2	2	2
47-1070	5	2	2	2
47-1085	1	0	0	0
47-1085	2	0	0	0
47-1085	3	2	2	2
47-1085	4	2	2	2
47-1091	1	0	0	0
47-1091	2	0	0	0
47-1091	3	2	2	2

47-1091	4	2	2	2
47-1092	1	0	0	0
47-1092	2	0	0	0
47-1092	3	2	2	2
47-1092	4	2	2	2
48-1001	1	0	0	0
48-1001	2	1	1	1
48-1001	3	2	2	2
48-1001	4	0	0	2
48-1001	5	2	2	2
48-1003	1	1	1	1
48-1003	2	2	2	2
48-1003	3	0	0	0
48-1003	4	2	2	2
48-1007	1	0	0	0
48-1007	2	1	1	1
48-1007	3	2	2	2
48-1007	4	1	1	1
48-1007	5	2	2	2
48-1010	1	0	0	0
48-1010	2	1	1	1
48-1010	3	2	2	2
48-1010	4	2	2	2
48-1016	1	1	1	1
48-1016	2	1	1	1
48-1016	3	2	2	2
48-1016	4	2	2	2
48-1017	1	1	1	1
48-1017	2	1	1	1
48-1017	3	0	0	0
48-1017	4	2	2	2
48-1026	1	1	1	1
48-1026	2	1	1	1
48-1026	3	0	0	0
48-1026	4	2	2	2
48-1026	5	2	2	2
48-1027	1	1	1	1
48-1027	2	1	1	1
48-1027	3	1	1	1
48-1027	4	1	1	1
48-1027	5	0	0	0
48-1027	6	2	2	2
48-1035	1	1	1	1
48-1035	2	1	1	1
48-1035	3	2	2	2
48-1035	4	2	2	2
48-1041	1	0	0	0
48-1041	2	0	0	0
48-1041	3	0	0	0
48-1041	4	2	2	2
48-1041	5	0	0	0
49-1006	1	1	1	1
49-1006	2	1	1	1
49-1006	3	2	2	2
49-1006	4	1	1	1
49-1006	5	2	2	2
49-1008	1	0	0	2
49-1008	2	1	1	1
49-1008	3	0	0	0
49-1008	4	2	2	2
49-1019	1	0	0	0
49-1019	2	1	1	1
49-1019	3	0	0	0
49-1019	4	1	1	1
49-1019	5	1	1	1
49-1019	6	2	2	2

49-1030	1	1	1	1
49-1030	2	2	2	2
49-1030	3	2	2	2
49-1030	4	2	2	2
49-1037	1	1	1	1
49-1037	2	1	1	1
49-1037	3	0	0	0
49-1037	4	2	2	2
49-1037	5	2	2	2
49-1038	1	1	1	1
49-1038	2	2	2	2
49-1038	3	2	2	2
49-1038	4	2	2	2
30-30134	1	0	0	0
30-30134	2	0	0	0
30-30134	3	0	0	0
30-30134	4	0	0	0
30-30134	5	0	0	0
30-30134	6	0	0	0
30-30134	7	1	1	1
30-30134	8	1	1	1
30-30134	9	0	2	2
30-30134	10	1	1	1
30-30134	11	1	1	1
30-30134	12	2	2	2
30-30134	13	2	2	2
30-30134	14	2	2	2
43-1016	1	1	1	1
43-1016	2	0	0	0
43-1016	3	0	0	0
43-1016	4	0	2	2
43-1016	5	0	0	0
43-1016	6	2	2	2
43-1016	7	2	2	2
43-1016	8	0	0	0
43-1016	9	1	1	1
43-1016	10	2	2	2
43-1016	11	2	2	2
43-1016	12	2	2	2
43-1016	13	2	2	2
32-32200	1	1	1	1
32-32200	2	0	0	0
32-32200	3	1	1	1
32-32200	4	1	1	1
32-32200	5	2	2	2
32-32200	6	1	1	1
46-1050	1	2	2	2
46-1050	2	0	0	0
46-1050	3	0	2	2
46-1050	4	0	0	2
46-1050	5	1	1	1
46-1050	6	2	2	2
44-1018	1	1	1	1
44-1018	2	1	1	1
44-1018	3	1	1	1
44-1018	4	0	0	0
44-1018	5	2	2	2
44-1031	1	1	1	1
44-1031	2	2	2	2
44-1031	3	0	0	0
44-1031	4	0	0	0
44-1045	1	0	0	2
44-1045	2	0	2	2
44-1045	3	0	0	0
44-1045	4	0	0	0
44-1045	5	2	2	2

44-1045	6	0	0	2
46-1044	1	0	0	2
46-1044	2	1	1	1
46-1044	3	0	2	2
46-1044	4	2	2	2
30-30111	1	1	1	1
30-30111	2	1	1	1
30-30111	3	2	2	2
30-30111	4	2	2	2
30-30111	5	0	0	0
30-30128	1	0	0	2
30-30128	2	0	0	0
30-30128	3	1	1	1
30-30128	4	1	1	1
30-30128	5	2	2	2
30-30128	6	2	2	2
30-30153	1	0	0	0
30-30153	2	1	1	1
30-30153	3	1	1	1
30-30153	4	0	0	2
30-30153	5	2	2	2
30-30153	6	1	1	1
30-30153	7	1	1	1
30-30153	8	2	2	2
30-30153	9	0	0	0
30-30153	10	0	2	2
31-31113	1	0	0	0
31-31113	2	0	0	0
31-31113	3	1	1	1
31-31113	4	1	1	1
31-31113	5	2	2	2
31-31113	6	0	2	2
31-31113	7	0	0	0
31-31113	8	0	0	0
31-31113	9	1	1	1
32-32208	1	0	0	0
32-32208	2	0	0	2
32-32208	3	2	2	2
32-32208	4	0	2	2
32-32312	1	1	1	1
32-32312	2	2	2	2
32-32312	3	1	1	1
32-32312	4	0	0	0
32-32312	5	0	0	0
32-32312	6	2	2	2
32-32400	1	1	1	1
32-32400	2	0	0	0
32-32400	3	1	1	1
32-32400	4	0	0	0
32-32400	5	1	1	1
32-32400	6	2	2	2
32-32403	1	0	0	0
32-32403	2	1	1	1
32-32403	3	1	1	1
32-32403	4	0	0	2
32-32403	5	2	2	2
32-32403	6	1	1	1
32-32403	7	1	1	1
32-32403	8	1	1	1
32-32403	9	0	0	0
32-32403	10	1	1	1
43-1061	1	0	0	0
43-1061	2	0	0	0
43-1061	3	2	2	2
43-1061	4	0	0	0
31-31130	1	0	0	0

31-31130	2	1	1	1
31-31130	3	1	1	1
31-31130	4	1	1	1
31-31130	5	1	1	1
31-31130	6	2	2	2
31-31130	7	1	1	1
31-31130	8	0	0	0
31-31130	9	0	2	2
31-31130	10	2	2	2
31-31130	11	1	1	1
31-31130	12	0	0	2
31-31130	13	0	0	0
41-0019	1	1	1	1
41-0019	2	0	0	0
41-0019	3	1	1	1
41-0019	4	0	2	2
41-0019	5	2	2	2
41-0041	1	1	1	1
41-0041	2	1	1	1
41-0041	3	0	2	2
41-0041	4	2	2	2
41-0056	1	1	1	1
41-0056	2	1	1	1
41-0056	3	2	2	2
41-0056	4	0	2	2
41-0066	1	1	1	1
41-0066	2	1	1	1
41-0066	3	0	2	2
41-0066	4	2	2	2
43-1027	1	0	0	0
43-1027	2	0	0	0
43-1027	3	0	2	2
43-1027	4	2	2	2
43-1065	1	0	0	0
43-1065	2	0	0	0
43-1065	3	0	0	0
43-1065	4	0	2	2
43-1065	5	2	2	2
44-1027	1	0	0	0
44-1027	2	0	0	2
44-1027	3	0	2	2
44-1027	4	1	1	1
44-1027	5	2	2	2
45-1012	1	0	0	0
45-1012	2	0	0	0
45-1012	3	0	2	2
45-1012	4	2	2	2
46-1011	1	0	0	0
46-1011	2	0	0	0
46-1011	3	2	2	2
46-1011	4	0	2	2
46-1021	1	*	1	1
46-1021	2	*	1	1
46-1021	3	*	2	2
46-1021	4	*	0	0
49-1027	1	1	1	1
49-1027	2	1	1	1
49-1027	3	2	2	2
49-1027	4	0	2	2
49-1035	1	*	1	1
49-1035	2	*	1	1
49-1035	3	*	0	0
49-1035	4	*	2	2
49-1036	1	0	0	0
49-1036	2	1	1	1
49-1036	3	2	2	2

49-1036	4	0	2	2
43-1007	1	*	1	1
43-1007	2	*	0	0
43-1007	3	*	0	0
43-1007	4	*	0	0
43-1007	5	*	1	1
43-1007	6	*	2	2
49-1021	1	*	1	1
49-1021	2	*	1	1
49-1021	3	*	0	0
49-1021	4	*	2	2
30-30142	1	0	0	0
30-30142	2	0	0	0
30-30142	3	1	1	1
30-30142	4	0	0	0
30-30142	5	0	0	0
30-30142	6	1	1	1
30-30142	7	2	2	2
30-30142	8	1	1	1
30-30142	9	1	1	1
30-30142	10	1	1	1
30-30142	11	0	2	2
30-30142	12	1	1	1
30-30142	13	0	2	2
30-30142	14	2	2	2
31-31118	1	*	0	0
31-31118	2	*	1	1
31-31118	3	*	0	0
31-31118	4	*	1	1
31-31118	5	*	0	0
31-31118	6	*	0	2
31-31118	7	*	2	2
41-0011	1	2	2	2
41-0011	2	1	1	1
41-0011	3	0	2	2
41-0011	4	2	2	2
41-0085	1	1	1	1
41-0085	2	1	1	1
41-0085	3	1	1	1
41-0085	4	0	2	2
41-0085	5	2	2	2
42-1011	1	2	2	2
42-1011	2	0	0	0
42-1011	3	0	2	2
42-1011	4	2	2	2
42-1026	1	0	0	0
42-1026	2	0	0	0
42-1026	3	0	2	2
42-1026	4	2	2	2
43-1036	1	0	0	0
43-1036	2	0	0	0
43-1036	3	0	0	0
43-1036	4	0	0	0
43-1036	5	0	0	0
43-1036	6	2	2	2
43-1036	7	2	2	2
43-1036	8	2	2	2
45-1039	1	0	0	0
45-1039	2	0	0	0
45-1039	3	0	2	2
45-1039	4	2	2	2
46-1051	1	0	0	0
46-1051	2	0	0	0
46-1051	3	2	2	2
46-1051	4	0	2	2
47-1024	1	0	0	0

47-1024	2	0	0	0
47-1024	3	0	2	2
47-1024	4	2	2	2
31-31141	1	*	0	0
31-31141	2	*	0	0
31-31141	3	*	0	0
31-31141	4	*	2	2
41-0013	1	*	1	1
41-0013	2	*	1	1
41-0013	3	*	0	0
41-0013	4	*	2	2
41-0015	1	1	1	1
41-0015	2	1	1	1
41-0015	3	2	2	2
41-0015	4	0	2	2
41-0076	1	1	1	1
41-0076	2	1	1	1
41-0076	3	0	2	2
41-0076	4	2	2	2
42-1001	1	0	0	2
42-1001	2	0	0	0
42-1001	3	2	2	2
42-1001	4	0	2	2
42-1001	5	1	1	1
42-1001	6	1	1	1
42-1035	1	1	1	1
42-1035	2	1	1	1
42-1035	3	0	2	2
42-1035	4	2	2	2
42-1035	5	2	2	2
44-1052	1	1	1	1
44-1052	2	0	0	2
44-1052	3	2	2	2
44-1052	4	0	0	0
44-1052	5	0	0	0
46-1004	1	1	1	1
46-1004	2	0	0	0
46-1004	3	0	2	2
46-1004	4	2	2	2
46-1004	5	0	0	0
47-1033	1	2	2	2
47-1033	2	2	2	2
47-1033	3	2	2	2
47-1033	4	0	2	2
48-1008	1	1	1	1
48-1008	2	0	0	0
48-1008	3	0	2	2
48-1008	4	2	2	2
48-1008	5	1	1	1
48-1031	1	1	1	1
48-1031	2	2	2	2
48-1031	3	0	2	2
48-1031	4	1	1	1
48-1031	5	1	1	1
48-1031	6	2	2	2
49-1012	1	1	1	1
49-1012	2	1	1	1
49-1012	3	1	1	1
49-1012	4	1	1	1
49-1012	5	0	2	2
49-1012	6	0	2	2
49-1012	7	2	2	2
41-0058	1	1	1	1
41-0058	2	1	1	1
41-0058	3	2	2	2
41-0058	4	0	2	2

41-0058	5	2	2	2
32-32401	1	0	0	0
32-32401	2	1	1	1
32-32401	3	2	2	2
32-32401	4	0	2	2
41-0075	1	1	1	1
41-0075	2	1	1	1
41-0075	3	2	2	2
41-0075	4	0	2	2
43-1001	1	0	0	0
43-1001	2	0	0	0
43-1001	3	2	2	2
43-1001	4	0	0	0
43-1001	5	2	2	2
43-1001	6	2	2	2
43-1058	1	*	1	1
43-1058	2	*	1	1
43-1058	3	*	2	2
43-1058	4	*	0	0
32-32322	1	0	0	0
32-32322	2	0	0	0
32-32322	3	2	2	2
32-32322	4	0	0	0
41-0036	1	1	1	1
41-0036	2	1	1	1
41-0036	3	0	0	0
41-0036	4	2	2	2
41-0044	1	*	1	1
41-0044	2	*	1	1
41-0044	3	*	2	2
41-0044	4	*	0	0
41-0046	1	*	1	1
41-0046	2	*	1	1
41-0046	3	*	0	0
41-0046	4	*	2	2
41-0047	1	1	1	1
41-0047	2	1	1	1
41-0047	3	2	2	2
41-0047	4	0	0	0
41-0067	1	1	1	1
41-0067	2	1	1	1
41-0067	3	2	2	2
41-0067	4	0	2	2
41-0090	1	1	1	1
41-0090	2	1	1	1
41-0090	3	2	2	2
41-0090	4	0	0	0
41-0092	1	1	1	1
41-0092	2	1	1	1
41-0092	3	2	2	2
41-0092	4	0	2	2
42-1027	1	0	0	0
42-1027	2	0	0	2
42-1027	3	2	2	2
42-1027	4	0	2	2
42-1040	1	0	0	0
42-1040	2	0	0	0
42-1040	3	2	2	2
42-1040	4	2	2	2
42-1044	1	0	0	0
42-1044	2	1	1	1
42-1044	3	2	2	2
42-1044	4	0	2	2
42-1053	1	0	0	0
42-1053	2	0	0	0
42-1053	3	0	2	2

42-1053	4	2	2	2
43-1068	1	*	0	0
43-1068	2	*	1	1
43-1068	3	*	0	0
43-1068	4	*	2	2
48-1014	1	0	0	0
48-1014	2	0	0	0
48-1014	3	2	2	2
48-1014	4	0	0	0
48-1014	5	2	2	2
48-1014	6	0	0	0
48-1039	1	0	0	2
48-1039	2	1	1	1
48-1039	3	2	2	2
48-1039	4	0	0	0
32-32212	1	0	0	2
32-32212	2	2	2	2
32-32212	3	2	2	2
32-32212	4	0	0	0
32-32212	5	0	0	0
41-0084	1	1	1	1
41-0084	2	1	1	1
41-0084	3	2	2	2
41-0084	4	0	2	2
30-30119	1	1	1	1
30-30119	2	1	1	1
30-30119	3	0	0	0
30-30119	4	1	1	1
30-30119	5	0	0	0
30-30119	6	0	0	0
30-30119	7	1	1	1
30-30119	8	2	2	2
30-30119	9	1	1	1
32-32205	1	*	*	0
32-32205	2	*	*	2
32-32205	3	*	*	1
32-32205	4	*	*	1
32-32205	5	*	*	0
32-32205	6	*	*	0
32-32205	7	*	*	0
32-32205	8	*	*	1
32-32201	1	*	0	0
32-32201	2	*	0	0
32-32201	3	*	0	0
32-32201	4	*	1	1
32-32201	5	*	1	1
32-32201	6	*	2	2
32-32201	7	*	0	0
32-32201	8	*	0	0
32-32201	9	*	1	1
32-32201	10	*	1	1
32-32201	11	*	1	1
32-32201	12	*	1	1
32-32201	13	*	0	0
32-32201	14	*	0	0
32-32201	15	*	0	0
31-31139	1	1	1	1
31-31139	2	0	0	0
31-31139	3	0	0	0
31-31139	4	1	1	1
31-31139	5	0	0	0
31-31139	6	1	1	1
31-31139	7	0	0	0
31-31139	8	2	2	2
41-0040	1	*	1	1
41-0040	2	*	1	1

41-0040	3	*	2	2
41-0040	4	*	2	2
42-1048	1	0	0	2
42-1048	2	1	1	1
42-1048	3	0	0	0
42-1048	4	2	2	2
42-1048	5	0	2	2
42-1048	6	0	2	2
42-1048	7	0	2	2
42-1074	1	*	0	0
42-1074	2	*	1	1
42-1074	3	*	0	0
42-1074	4	*	2	2
42-1074	5	*	0	0
42-1074	6	*	0	0
48-1037	1	*	1	1
48-1037	2	*	1	1
48-1037	3	*	1	1
48-1037	4	*	2	2
48-1037	5	*	2	2
48-1037	6	*	0	0
49-1009	1	1	1	1
49-1009	2	1	1	1
49-1009	3	0	0	0
49-1009	4	1	1	1
49-1009	5	1	1	1
49-1009	6	1	1	1
49-1009	7	1	1	1
49-1009	8	0	2	2
49-1009	9	2	2	2
49-1009	10	2	2	2
49-1009	11	2	2	2

APPENDIX 4

MicroRNA sequences (miRBase 9.2) detected by TaqMan probes (Chapter 5)

Assay Name	Target Sequence
U18	CAGUAGUGAUGAAAAUUCCACUUCAUUGGUCCGUGUUUCUGAACCACAUGAUUUUCUCGGAUGUUCUGAUG
hsa-let-7a	UGAGGUAGUAGGUUGUAUAGUU
hsa-let-7b	UGAGGUAGUAGGUUGUGUGGUU
hsa-let-7c	UGAGGUAGUAGGUUGUAUGGUU
hsa-let-7d	AGAGGUAGUAGGUUGCAUAGU
hsa-let-7e	UGAGGUAGGAGGUUGUAUAGU
hsa-let-7f	UGAGGUAGUAGAUUGUAUAGUU
hsa-let-7g	UGAGGUAGUAGUUUGUACAGU
hsa-let-7i	UGAGGUAGUAGUUUGUGCUGU
hsa-miR-1	UGGAAUGUAAAGAAGUAUGUA
hsa-miR-7	UGGAAGACUAGUGAUUUUGUUG
hsa-miR-10a	UACCCUGUAGAUCCGAAUUUGUG
hsa-miR-10b	UACCCUGUAGAACCGAAUUUGU
hsa-miR-15a	UAGCAGCACAUAAUGGUUUGUG
hsa-miR-15b	UAGCAGCACAUCAUGGUUUACA
hsa-miR-16	UAGCAGCACGUAAAUAUUGGCG
hsa-miR-17-3p	ACUGCAGUGAAGGCACUUGU
hsa-miR-17-5p	CAAAGUGCUUACAGUGCAGGUAGU
hsa-miR-18a	UAAGGUGCAUCUAGUGCAGAUA
hsa-miR-19a	UGUGCAAAUCUAUGCAAAACUGA
hsa-miR-19b	UGUGCAAAUCCAUGCAAAACUGA
hsa-miR-21	UAGCUUAUCAGACUGAUGUUGA
hsa-miR-22	AAGCUGCCAGUUGAAGAACUGU
hsa-miR-23a	AUCACAUUGCCAGGGAUUUCC
hsa-miR-23b	AUCACAUUGCCAGGGAUUACC
hsa-miR-24	UGGCUCAGUUCAGCAGGAACAG
hsa-miR-25	CAUUGCACUUGUCUCGGUCUGA
hsa-miR-26a	UUCAAGUAAUCCAGGAUAGGC
hsa-miR-26b	UUCAAGUAAUUCAGGAUAGGUU
hsa-miR-27a	UUCACAGUGGCUAAGUUCCGC
hsa-miR-27b	UUCACAGUGGCUAAGUUCUGC
hsa-miR-28	AAGGAGCUCACAGUCUAUUGAG
hsa-miR-29a	UAGCACCAUCUGAAAUCGGUU
hsa-miR-29b	UAGCACCAUUUGAAAUCAGUGUU
hsa-miR-29c	UAGCACCAUUUGAAAUCGGU
hsa-miR-30a-3p	CUUUCAGUCGGAUGUUUGCAGC
hsa-miR-30a-5p	UGUAAACAUCCUCGACUGGAAG
hsa-miR-30c	UGUAAACAUCCUACACUCUCAGC
hsa-miR-30d	UGUAAACAUCCCCGACUGGAAG
hsa-miR-30e-5p	UGUAAACAUCCUUGACUGGA
hsa-miR-30e-3p	CUUUCAGUCGGAUGUUUACAGC
hsa-miR-32	UAUUGCACAUUACUAAGUUGC
hsa-miR-33	GUGCAUUGUAGUUGCAUUG

hsa-miR-34a	UGGCAGUGUCUUAGCUGGUUGUU
hsa-miR-34b	UAGGCAGUGUCAUUAGCUGAUUG
hsa-miR-34c	AGGCAGUGUAGUUAGCUGAUUGC
hsa-miR-92	UAUUGCACUUGUCCCGGCCUG
hsa-miR-93	AAAGUGCUGUUCGUGCAGGUAG
hsa-miR-95	UUCAACGGGUAUUUAUUGAGCA
hsa-miR-96	UUUGGCACUAGCACAUUUUUGC
hsa-miR-99a	AACCCGUAGAUCCGAUCUUGUG
hsa-miR-99b	CACCCGUAGAACCGACCUUGCG
hsa-miR-100	AACCCGUAGAUCCGAACUUGUG
hsa-miR-101	UACAGUACUGUGAUAACUGAAG
hsa-miR-103	AGCAGCAUUGUACAGGGCUAUGA
hsa-miR-105	UCAAAUGCUCAGACUCCUGU
hsa-miR-106b	UAAAGUGCUGACAGUGCAGAU
hsa-miR-107	AGCAGCAUUGUACAGGGCUAUCA
hsa-miR-122a	UGGAGUGUGACAAUGGUGUUUGU
hsa-miR-124a	UUAAGGCACGCGGUGAAUGCCA
hsa-miR-125a	UCCCUGAGACCCUUUAACCUGUG
hsa-miR-125b	UCCCUGAGACCCUAACUUGUGA
hsa-miR-126	UCGUACCGUGAGUAAUAAUGC
hsa-miR-126#	CAUUAUUACUUUUGGUACGCG
hsa-miR-127	UCGGAUCCGUCUGAGCUUGGCU
hsa-miR-128a	UCACAGUGAACCGGUCUCUUUU
hsa-miR-130a	CAGUGCAAUGUUAAAAGGGCAU
hsa-miR-130b	CAGUGCAAUGAUGAAAGGGCAU
hsa-miR-132	UAACAGUCUACAGCCAUGGUCG
hsa-miR-133a	UUGGUCCCCUUCAACCAGCUGU
hsa-miR-134	UGUGACUGGUUGACCAGAGGG
hsa-miR-135a	UAUGGCUUUUUAUUCCUAUGUGA
hsa-miR-135b	UAUGGCUUUUCAUUCCUAUGUG
hsa-miR-140	AGUGGUUUUACCCUAUGGUAG
hsa-miR-141	UAACACUGUCUGGUAAAGAUGG
hsa-miR-142-3p	UGUAGUGUUUCCUACUUUAUGGA
hsa-miR-142-5p	CAUAAAGUAGAAAGCACUAC
hsa-miR-143	UGAGAUGAAGCACUGUAGCUCA
hsa-miR-145	GUCCAGUUUUCCCAGGAAUCCCUU
hsa-miR-146a	UGAGAACUGAAUUCCAUGGGUU
hsa-miR-147	GUGUGUGGAAAUGCUUCUGC
hsa-miR-148a	UCAGUGCACUACAGAACUUUGU
hsa-miR-148b	UCAGUGCAUCACAGAACUUUGU
hsa-miR-149	UCUGGCUCCGUGUCUUCACUCC
hsa-miR-150	UCUCCCAACCCUUGUACCAGUG
hsa-miR-152	UCAGUGCAUGACAGAACUUGGG
hsa-miR-153	UUGCAUAGUCACAAAAGUGA
hsa-miR-154	UAGGUUAUCCGUGUUGCCUUCG
hsa-miR-154#	AAUCAUACACGGUUGACCUAUU
hsa-miR-155	UUAAUGCUAAUCGUGAUAGGGG
hsa-miR-181a	AACAUUCAACGCUGUCGGUGAGU

hsa-miR-181c	AACAUUCAACCUGUCGGUGAGU
hsa-miR-182#	UGGUUCUAGACUUGCCAACUA
hsa-miR-183	UAUGGCACUGGUAGAAUUCACUG
hsa-miR-184	UGGACGGAGAACUGAUAAGGGU
hsa-miR-186	CAAAGAAUUCUCCUUUUGGGCUU
hsa-miR-187	UCGUGUCUUGUGUUGCAGCCG
hsa-miR-189	GUGCCUACUGAGCUGAUAUCAGU
hsa-miR-190	UGAUAUGUUUGAUAUAUUAGGU
hsa-miR-191	CAACGGAAUCCCAAAAGCAGCU
hsa-miR-192	CUGACCUAUGAAUUGACAGCC
hsa-miR-193a	AACUGGCCUACAAAGUCCCAG
hsa-miR-194	UGUAACAGCAACUCCAUGUGGA
hsa-miR-195	UAGCAGCACAGAAAUAUUGGC
hsa-miR-196a	UAGGUAGUUUCAUGUUGUUGG
hsa-miR-196b	UAGGUAGUUUCCUGUUGUUGG
hsa-miR-197	UUCACCACCUUCUCCACCCAGC
hsa-miR-199a	CCCAGUGUUCAGACUACCUGUUC
hsa-miR-199a#	UACAGUAGUCUGCACAUUGGUU
hsa-miR-199b	CCCAGUGUUUAGACUAUCUGUUC
hsa-miR-200a	UAACACUGUCUGGUAACGAUGU
hsa-miR-200c	UAAUACUGCCGGGUAAUGAUGG
hsa-miR-203	GUGAAAUGUUUAGGACCACUAG
hsa-miR-204	UUCCCUUUGUCAUCCUAUGCCU
hsa-miR-205	UCCUUCAUUCCACCGGAGUCUG
hsa-miR-206	UGGAAUGUAAGGAAGUGUGUGG
hsa-miR-208	AUAAGACGAGCAAAAAGCUUGU
hsa-miR-210	CUGUGCGUGUGACAGCGGCUGA
hsa-miR-211	UUCCCUUUGUCAUCCUUCGCCU
hsa-miR-212	UAACAGUCUCCAGUCACGGCC
hsa-miR-213	ACCAUCGACCGUUGAUUGUACC
hsa-miR-214	ACAGCAGGCACAGACAGGCAG
hsa-miR-215	AUGACCUAUGAAUUGACAGAC
hsa-miR-216	UAAUCUCAGCUGGCAACUGUG
hsa-miR-217	UACUGCAUCAGGAACUGAUUGGAU
hsa-miR-218	UUGUGCUUGAUCUAACCAUGU
hsa-miR-219	UGAUUGUCCAAACGCAAUUCU
hsa-miR-220	CCACACCGUAUCUGACACUUU
hsa-miR-221	AGCUACAUUGUCUGCUGGGUUUC
hsa-miR-222	AGCUACAUCUGGCUACUGGGUCUC
hsa-miR-223	UGUCAGUUUGUCAAAUACCCC
hsa-miR-296	AGGGCCCCCCCUCAAUCCUGU
hsa-miR-301	CAGUGCAAUAGUAUUGUCAAAGC
hsa-miR-302a	UAAGUGCUUCCAUGUUUUGGUGA
hsa-miR-302a#	UAAACGUGGAUGUACUUGCUUU
hsa-miR-302b	UAAGUGCUUCCAUGUUUUAGUAG
hsa-miR-302b#	ACUUUAACAUGGAAGUGCUUUCU
hsa-miR-302c	UAAGUGCUUCCAUGUUUCAGUGG
hsa-miR-302c#	UUUAACAUGGGGGUACCUGCUG

hsa-miR-302d	UAAGUGCUUCCAUGUUUGAGUGU
hsa-miR-320	AAAAGCUGGGUUGAGAGGGCGAA
hsa-miR-323	GCACAUUACACGGUCGACCUCU
hsa-miR-324-5p	CGCAUCCCCUAGGGCAUUGGUGU
hsa-miR-325	CCUAGUAGGUGUCCAGUAAGUGU
hsa-miR-326	CCUCUGGGCCCUUCCUCCAG
hsa-miR-328	CUGGCCCUCUCUGCCCUUCCGU
hsa-miR-330	GCAAAGCACACGGCCUGCAGAGA
hsa-miR-331	GCCCCUGGGCCUAUCCUAGAA
hsa-miR-335	UCAAGAGCAAUAACGAAAAAUGU
hsa-miR-337	UCCAGCUCCUAUAUGAUGCCUUU
hsa-miR-338	UCCAGCAUCAGUGAUUUUGUUGA
hsa-miR-339	UCCCUGUCCUCCAGGAGCUCA
hsa-miR-340	UCCGUCUCAGUUACUUUAUAGCC
hsa-miR-342	UCUCACACAGAAAUCGCACCCGUC
hsa-miR-345	UGCUGACUCCUAGUCCAGGGC
hsa-miR-346	UGUCUGCCCGCAUGCCUGCCUCU
hsa-miR-361	UUAUCAGAAUCUCCAGGGGUAC
hsa-miR-367	AAUUGCACUUUAGCAAUGGUGA
hsa-miR-368	ACAUAGAGGAAAUUCCACGUUU
hsa-miR-369-3p	AAUAAUACAUGGUUGAUCUUU
hsa-miR-370	GCCUGCUGGGGUGGAACCUGG
hsa-miR-371	GUGCCGCCAUCUUUUGAGUGU
hsa-miR-372	AAAGUGCUGCGACAUUUGAGCGU
hsa-miR-373	GAAGUGCUUCGAUUUUGGGGUGU
hsa-miR-373#	ACUCAAAAUGGGGGCGCUUUCC
hsa-miR-374	UUAUAAUACAACCUGAUAAGUG
hsa-miR-375	UUUGUUCGUUCGGCUCGCGUGA
hsa-miR-376a	AUCAUAGAGGAAAAUCCACGU
hsa-miR-377	AUCACACAAAGGCAACUUUUGU
hsa-miR-378	CUCCUGACUCCAGGUCCUGUGU
hsa-miR-379	UGGUAGACUAUGGAACGUA
hsa-miR-380-3p	UAUGUAAUAUGGUCCACAUCUU
hsa-miR-380-5p	UGGUUGACCAUAGAACAUGCGC
hsa-miR-381	UAUACAAGGGCAAGCUCUCUGU
hsa-miR-382	GAAGUUGUUCGUGGUGGAUUCG
hsa-miR-383	AGAUCAGAAGGUGAUUGUGGCU
hsa-miR-384	AUUCCUAGAAAUUGUUCAUA
hsa-miR-422b	CUGGACUUGGAGUCAGAAGGCC
hsa-miR-423	AGCUCGGUCUGAGGCCCCUCAG
hsa-miR-98	UGAGGUAGUAAGUUGUAUUGUU
hsa-miR-106a	AAAAGUGCUUACAGUGCAGGUAGC
hsa-miR-324-3p	CCACUGCCCCAGGUGCUGCUGG
hsa-miR-20a	UAAAGUGCUUAUAGUGCAGGUAG
hsa-miR-198	GGUCCAGAGGGGAGAUAGG
hsa-miR-9	UCUUUGGUUAUCUAGCUGUAUGA
hsa-miR-9#	UAAAGCUAGAUAACCGAAAGU
hsa-miR-128b	UCACAGUGAACCGGUCUCUUUC

hsa-miR-129	CUUUUUGCGGUCUGGGCUUGC
hsa-miR-133b	UUGGUCCCCUUCAACCAGCUA
hsa-miR-136	ACUCCAUUUGUUUUGAUGAUGGA
hsa-miR-137	UAUUGCUUAAGAAUACGCGUAG
hsa-miR-138	AGCUGGUGUUGUGAAUC
hsa-miR-151	ACUAGACUGAAGCUCCUUGAGG
hsa-miR-182	UUUGGCAAUGGUAGAACUCACA
hsa-miR-185	UGGAGAGAAAGGCAGUUC
hsa-miR-224	CAAGUCACUAGUGGUUCCGUUUA
hsa-miR-299-5p	UGGUUUACCGUCCCACAUACAU
hsa-miR-30b	UGUAAACAUCCUACACUCAGCU
hsa-miR-422a	CUGGACUUAGGGUCAGAAGGCC
hsa-miR-424	CAGCAGCAAUUCAUGUUUUGAA
RNU24	AUUUGCUAUCUGAGAGAUGGUGAUGACAUUUUAAACCACCAAGAUCGCUGAUGCA
RNU66	GUAACUGUGGUGAUGGAAAUGUGUUAGCCUCAGACACUACUGAGGUGGUUCUUUCUAUCCUAGUACAGUC
RNU19	UUGCACCUCUGAGAGUGGAAUGACUCCUGUGGAGUUGAUCCUAGUCUGGGUGCAAACAAUU
RNU38B	CCAGUUCUGCUACUGACAGUAAGUGAAGAUAAAGUGUGUCUGAGGAGA
RNU49	CACUAAUAGGAAGUGCCGUCAGAAGCGAUAACUGACGAAGACUACUCCUGUCUGAUU
RNU48	GAUGACCCCAGGUAACUCUGAGUGUGUCGCUGAUGCCAUCACCGCAGCGCUCUGACC
hsa-miR-188	CAUCCCUUGCAUGGUGGAGGGU
hsa-miR-18b	UAAGGUGCAUCUAGUGCAGUUA
hsa-miR-193b	AACUGGCCCUCAAAGUCCCGCUUU
hsa-miR-200a#	CAUCUUACCGGACAGUGCUGGA
hsa-miR-202	AGAGGUAUAGGGCAUGGGAAAA
hsa-miR-202#	UUUCCUAUGCAUAUACUUCUUU
hsa-miR-20b	CAAAGUGCUCAUAGUGCAGGUAG
hsa-miR-299-3p	UAUGUGGGAUGGUAAACCGCUU
hsa-miR-365	UAAUGCCCCUAAAAAUCCUUAU
hsa-miR-369-5p	AGAUCGACCGUGUUAUAUUCGC
hsa-miR-409-5p	AGGUUACCCGAGCAACUUUGCA
hsa-miR-412	ACUUCACCUGGUCCACUAGCCGU
hsa-miR-429	UAAUACUGUCUGGUAAAACCGU
hsa-miR-432	UCUUGGAGUAGGUCAUUGGGUGG
hsa-miR-432#	CUGGAUGGCUCCUCCAUGUCU
hsa-miR-433	AUCAUGAUGGGCUCCUCGGUGU
hsa-miR-448	UUGCAUAUGUAGGAUGUCCCAU
hsa-miR-449	UGGCAGUGUAUUGUUAGCUGGU
hsa-miR-450	UUUUUGCGAUGUGUUCCUAAUA
hsa-miR-452	UGUUUGCAGAGGAAACUGAGAC
hsa-miR-452#	UCAGUCUCAUCUGCAAAGAAG
hsa-miR-453	GAGGUUGUCCGUGGUGAGUUCG
hsa-miR-485-5p	AGAGGCUGGCCGUGAUGAAUUC
hsa-miR-490	CAACCUGGAGGACUCCAUGCUG
hsa-miR-491	AGUGGGGAACCCUUCCAUGAGGA
hsa-miR-492	AGGACCUGCGGGACAAGAUUCUU
hsa-miR-493	UUGUACAUGGUAGGCUUUCAUU
hsa-miR-494	UGAAACAUACACGGGAAACCUCUU
hsa-miR-496	AUUACAUGGCCAAUCUC

hsa-miR-497	CAGCAGCACACUGUGGUUUGU
hsa-miR-498	UUUCAAGCCAGGGGGCGUUUUUC
hsa-miR-499	UUAAGACUUGCAGUGAUGUUUAA
hsa-miR-500	AUGCACCUGGGCAAGGAUUCUG
hsa-miR-501	AAUCCUUUGUCCCUGGGUGAGA
hsa-miR-503	UAGCAGCGGGAACAGUUCUGCAG
hsa-miR-505	GUCAACACUUGCUGGUUUCCUC
hsa-miR-506	UAAGGCACCCUUCUGAGUAGA
hsa-miR-507	UUUUGCACCUUUUGGAGUGAA
hsa-miR-508	UGAUUGUAGCCUUUUGGAGUAGA
hsa-miR-509	UGAUUGGUACGUCUGUGGGUAGA
Z30	UGGUAUUGCCAUUGCUUCACUGUUGGCUUUGACCAGGGUAUGAUCUCUUAAUCUUCUCUCUGAGCUG
RNU6B	CGCAAGGAUGACACGCAAAUUCGUGAAGCGUUCCAUAUUUUU
RNU44	CCUGGAUGAUGAUAGCAAAUGCUGACUGAACAUGAAGGUCUUAAUUAGCUCUAACUGACU
RNU43	GAACUUAUUGACGGGCGGACAGAAACUGUGUGCUGAUUGUCACGUUCUGAUU
hsa-miR-139	UCUACAGUGCACGUGUCU
hsa-miR-146b	UGAGAACUGAAUUCCAUAGGCU
hsa-miR-181b	AACAUUCAUUGCUGUCGGUGGG
hsa-miR-181d	AACAUUCAUUGUUGUCGGUGGGUU
hsa-miR-31	GGCAAGAUGCUGGCAUAGCUG
hsa-miR-329	AACACACCUGGUUAACCUCUUU
hsa-miR-376b	AUCAUAGAGGAAAAUCCAUGUU
hsa-miR-425	AUCGGGAAUGUCGUGUCCGCC
hsa-miR-451	AAACCGUUACCAUUACUGAGUUU
hsa-miR-488	CCCAGAUAAUGGCACUCUCAA
hsa-miR-489	AGUGACAUCACAUAUACGGCAGC
hsa-miR-495	AAACAAACAUGGUGCACUUCUUU
hsa-miR-502	AUCCUUGCUAUCUGGGUGCUA
hsa-miR-504	AGACCCUGGUCUGCACUCUAU
hsa-miR-511	GUGUCUUUUGCUCUGCAGUCA
hsa-miR-515-5p	UUCUCCAAAAGAAAGCACUUUCUG
hsa-miR-517#	CCUCUAGAUGGAAGCACUGUCU
hsa-miR-519b	AAAGUGCAUCCUUUUAGAGGUUU
hsa-miR-520b	AAAGUGCUUCCUUUUAGAGGG
hsa-miR-520c	AAAGUGCUUCCUUUUAGAGGGUU
hsa-miR-520d	AAAGUGCUUCUCUUUGGUGGGUU
hsa-miR-520e	AAAGUGCUUCCUUUUUGAGGG
hsa-miR-520f	AAGUGCUUCCUUUUAGAGGGUU
hsa-miR-520g	ACAAAGUGCUUCCCUUUAGAGUGU
hsa-miR-521	AACGCACUUCCCUUUAGAGUGU
hsa-miR-525#	GAAGGCGCUUCCCUUUAGAGC
hsa-miR-526a	CUCUAGAGGGAAGCACUUUCU
hsa-miR-526b#	AAAGUGCUUCCUUUUAGAGGC
hsa-miR-510	UACUCAGGAGAGUGGCAAUCACA
hsa-miR-512-5p	CACUCAGCCUUGAGGGCACUUUC
hsa-miR-513	UUCACAGGGAGGUGUCAUUUAU
hsa-miR-514	AUUGACACUUCUGUGAGUAG
hsa-miR-515-3p	GAGUGCCUUCUUUUGGAGCGU

hsa-miR-516-3p	UGCUUCCUUUCAGAGGGU
hsa-miR-517a	AUCGUGCAUCCCUUUAGAGUGUU
hsa-miR-517b	UCGUGCAUCCCUUUAGAGUGUU
hsa-miR-517c	AUCGUGCAUCCUUUUAGAGUGU
hsa-miR-518a	AAAGCGCUUCCCUUUGCUGGA
hsa-miR-518b	CAAAGCGCUCCCCUUUAGAGGU
hsa-miR-518c	CAAAGCGCUUCUCUUUAGAGUG
hsa-miR-518c#	UCUCUGGAGGGAAGCACUUUCUG
hsa-miR-518d	CAAAGCGCUUCCCUUUGGAGC
hsa-miR-518e	AAAGCGCUUCCCUUCAGAGUGU
hsa-miR-518f	AAAGCGCUUCUCUUUAGAGGA
hsa-miR-519a	AAAGUGCAUCCUUUUAGAGUGUUAC
hsa-miR-519c	AAAGUGCAUCUUUUUAGAGGAU
hsa-miR-519d	CAAAGUGCCUCCCUUUAGAGUGU
hsa-miR-519e	AAAGUGCCUCCUUUUAGAGUGU
hsa-miR-519e#	UUCUCCAAAAGGGAGCACUUUC
hsa-miR-520a	AAAGUGCUUCCCUUUGGACUGU
hsa-miR-520a#	CUCCAGAGGGAAGUACUUUCU
hsa-miR-520d#	UCUACAAAGGGAAGCCCUUUCUG
hsa-miR-520h	ACAAAGUGCUUCCCUUUAGAGU
hsa-miR-522	AAAAUGGUUCCCUUUAGAGUGUU
hsa-miR-523	AACGCGCUUCCCUAUAGAGGG
hsa-miR-524	GAAGGCGCUUCCCUUUGGAGU
hsa-miR-525	CUCCAGAGGGAUGCACUUUCU
hsa-miR-526b	CUCUUGAGGGAAGCACUUUCUGUU
hsa-miR-526c	CUCUAGAGGGAAGCGCUUUCUGUU
hsa-miR-527	CUGCAAAGGGAAGCCCUUUCU
RNU58B	CUGCGAUGAUGGCAUUUCUUAGGACACCUUUGGAUUAAUAAUGAAAACAACUACUCUCUGAGCAGC
RNU58A	CUGCAGUGAUGACUUUCUUGGGACACCUUUGGAUUUACCGUGAAAAUUAAUAAAUUCUGAGCAGC
RPL21	CUUAAUGAUGACUGUUUUUUUUGAUUGCUUGAAGCAAUGUGAAAAACACAUUUCACCGGCUCUGAAAGCU
U54	UGGCGAUGAGGAGGUACCUAUUGUGUUGAGUAACGGUGAUAAUUUUAUACGCUAUUCUGAGCC
HY3	CCAGUCACAGAUUUCUUUGUUCCUUCUCCACUCCCACUGCAUCACUUAACUAGCCUU
U75	AGCCUGUGAUGCUUUAAGAGUAGUGGACAGAAGGGAUUUCUGAAAUUCUAUUCUGAGGCU
U47	UAAUGAUUCUGCCAAAUGAAAUAUAAUGAUAUCACUGUAAAACCGUUCCAUUUUGAUUCUGAGGU
hsa-miR-363#	CGGGUGGAUCACGAUGCAAUUU
hsa-miR-545	AUCAGCAAACAUUUAUUGUGUG
hsa-miR-544	AUUCUGCAUUUUUAGCAAGU
hsa-miR-656	AAUAUUAUACAGUCAACCUCU
hsa-miR-549	UGACAACUAUGGAUGAGCUCU
hsa-miR-657	GGCAGGUUCUCACCCUCUCUAGG
hsa-miR-363	AAUUGCACGGUAUCCAUCUGUA
hsa-miR-18a#	ACUGCCCUAAGUGCUCCUUCU
hsa-miR-362	AAUCCUUGGAACCUAGGUGUGAGU
hsa-miR-410	AAUAUAACACAGAUGGCCUGU
hsa-miR-483	UCACUCCUCUCCUCCCGUCUUCU
hsa-miR-485-3p	GUCAUACACGGCUCUCCUCUCU
hsa-miR-486	UCCUGUACUGAGCUGCCCCGAG
hsa-miR-487a	AAUCAUACAGGGACAUCCAGUU

hsa-miR-455	UAUGUGCCUUUGGACUACAUCG
hsa-miR-516-5p	CAUCUGGAGGUAAGAAGCACUUU
hsa-miR-493-3p	UGAAGGUCUACUGUGUGCCAG
hsa-miR-658	GGCGGAGGGAAGUAGGUCCGUUGGU
hsa-miR-542-3p	UGUGACAGAUUGAUAACUGAAA
hsa-miR-487b	AAUCGUACAGGGUCAUCCACUU
hsa-miR-539	GGAGAAAUUAUCCUUGGUGUGU
hsa-miR-376a#	GGUAGAUUCUCCUUCUAUGAG
hsa-miR-542-5p	UCGGGGAUCAUCAUGUCACGAG
hsa-miR-659	CUUGGUUCAGGGAGGGUCCCCA
hsa-miR-660	UACCCAUUGCAUAUCGGAGUUG
hsa-miR-425-5p	AAUGACACGAUCACUCCCGUUGA
hsa-miR-652	AAUGGCGCCACUAGGGUUGUGCA
hsa-miR-532	CAUGCCUUGAGUGUAGGACCGU
hsa-miR-551a	GCGACCCACUCUUGGUUUCCA
hsa-miR-552	AACAGGUGACUGGUUAGACAA
hsa-miR-553	AAAACGGUGAGAUUUUGUUUU
hsa-miR-554	GCUAGUCCUGACUCAGCCAGU
hsa-miR-555	AGGGUAAGCUGAACCUCUGAU
hsa-miR-556	GAUGAGCUCAUUGUAAUAUG
hsa-miR-557	GUUUGCACGGGUGGGCCUUGUCU
hsa-miR-558	UGAGCUGCUGUACCAAAAU
hsa-miR-559	UAAAGUAAAUAUGCACCAAAA
hsa-miR-561	CAAAGUUUAAGAUCCUUGAAGU
hsa-miR-562	AAAGUAGCUGUACCAUUUGC
hsa-miR-563	AGGUUGACAUACGUUUCCC
hsa-miR-564	AGGCACGGUGUCAGCAGGC
hsa-miR-565	GGCUGGCUCGCGAUGUCUGUUU
hsa-miR-566	GGGCGCCUGUGAUCCCAAC
hsa-miR-567	AGUAUGUUCUUCCAGGACAGAAC
hsa-miR-551b	GCGACCCAUACUUGGUUUCAG
hsa-miR-569	AGUUAAUGAAUCCUGGAAAGU
hsa-miR-570	GAAAACAGCAAUUACCUUUGCA
hsa-miR-548a	CAAAACUGGCAAUUACUUUUGC
hsa-miR-586	UAUGCAUUGUAUUUUUAGGUCC
hsa-miR-587	UUUCCAUAGGUGAUGAGUCAC
hsa-miR-548b	CAAGAACCUCAGUUGCUUUUGU
hsa-miR-588	UUGGCCACAAUGGGUUAGAAC
hsa-miR-589	UCAGAACAAAUGCCGGUUCCCAGA
hsa-miR-550	UGUCUUACUCCCUCAGGCACAU
hsa-miR-591	AGACCAUGGGUUCUCAUUGU
hsa-miR-592	UUGUGUCAAUAUGCGAUGAUGU
hsa-miR-593	AGGCACCAGCCAGGCAUUGCUCAGC
hsa-miR-594	CCCAUCUGGGGUGGCCUGUGACUUU
hsa-miR-596	AAGCCUGCCCGGCUCCUCGGG
hsa-miR-597	UGUGUCACUCGAUGACCACUGU
hsa-miR-622	ACAGUCUGCUGAGGUUGGAGC
hsa-miR-599	GUUGUGUCAGUUUAUCAAAC

hsa-miR-600	ACUUACAGACAAGAGCCUUGCUC
hsa-miR-624	UAGUACCAGUACCUUGUGUUCA
hsa-miR-601	UGGUCUAGGAUUGUUGGAGGAG
hsa-miR-626	AGCUGUCUGAAAAUGUCUU
hsa-miR-627	GUGAGUCUCUAAGAAAAGAGGA
hsa-miR-628	UCUAGUAAGAGUGGCAGUCG
hsa-miR-629	GUUCUCCCAACGUAAGCCCAGC
hsa-miR-630	AGUAUUCUGUACCAGGGAAGGU
hsa-miR-631	AGACCUGGCCCAGACCUCAGC
hsa-miR-603	CACACACUGCAAUUACUUUUGC
hsa-miR-604	AGGCUGCGGAAUUCAGGAC
hsa-miR-606	AAACUACUGAAAAUCAAAGAU
hsa-miR-607	GUUCAAAUCCAGAUCUAUAAC
hsa-miR-608	AGGGGUGGUGUUGGGACAGCUCCGU
hsa-miR-632	GUGUCUGCUUCCUGUGGGA
hsa-miR-609	AGGGUGUUUCUCUCAUCUCU
hsa-miR-633	CUAAUAGUAUCUACCACAAUAAA
hsa-miR-610	UGAGCUAAAUGUGUGCUGGGA
hsa-miR-634	AACCAGCACCCCAACUUUGGAC
hsa-miR-635	ACUUGGGCACUGAAACAAUGUCC
hsa-miR-612	GCUGGGCAGGGCUUCUGAGCUCCUU
hsa-miR-636	UGUGCUUGCUCGUCCCGCCCGCAG
hsa-miR-637	ACUGGGGGCUUUCGGGCUCUGCGU
hsa-miR-638	AGGGAUCGCGGGCGGGUGGCGGCCU
hsa-miR-639	AUCGCUGCGGUUGCGAGCGCUGU
hsa-miR-641	AAAGACAUAGGAUAGAGUCACCUC
hsa-miR-613	AGGAAUGUUCCUUCUUUGCC
hsa-miR-614	GAACGCCUGUUCUUGCCAGGUGG
hsa-miR-615	UCCGAGCCUGGGUCUCCCUCU
hsa-miR-616	ACUCAAAACCCUUCAGUGACUU
hsa-miR-548c	CAAAAAUCUCAAUUACUUUUGC
hsa-miR-617	AGACUUCCCAUUUGAAGGUGGC
hsa-miR-642	GUCCCUCUCCAAAUGUGUCUUG
hsa-miR-618	AAACUCUACUUGUCCUUCUGAGU
hsa-miR-643	ACUUGUAUGCUAGCUCAGGUAG
hsa-miR-619	GACCUGGACAUGUUUGUGCCCAGU
hsa-miR-644	AGUGUGGCUUUCUUAGAGC
hsa-miR-645	UCUAGGCUGGUACUGCUGA
hsa-miR-621	GGCUAGCAACAGCGCUUACCU
hsa-miR-646	AAGCAGCUGCCUCUGAGGC
hsa-miR-647	GUGGCUGCACUCACUUCCUUC
hsa-miR-648	AAGUGUGCAGGGCACUGGU
hsa-miR-649	AAACCUGUGUUGUUCAAGAGUC
hsa-miR-650	AGGAGGCAGCGCUCUCAGGAC
hsa-miR-651	UUUAGGAUAAGCUUGACUUUUG
hsa-miR-548d	CAAAAACCACAGUUUCUUUUGC
hsa-miR-661	UGCCUGGGUCUCUGGCCUGCGCGU
hsa-miR-662	UCCCACGUUGUGGCCCAGCAG

hsa-miR-449b	AGGCAGUGUAUUGUUAGCUGGC
hsa-miR-653	UUGAAACAAUCUCUACUGAAC
hsa-miR-411	UAGUAGACCGUAUAGCGUACG
hsa-miR-654	UGGUGGGCCGCAGAACAUGUGC
hsa-miR-655	AUAAUACAUGGUUAACCUCUUU
hsa-miR-571	UGAGUUGGCCAUCUGAGUGAG
hsa-miR-572	GUCCGCUCGGCGGUGGCCCA
hsa-miR-573	CUGAAGUGAUGUGUAACUGAUCAG
hsa-miR-575	GAGCCAGUUGGACAGGAGC
hsa-miR-576	AUUCUAAUUUCUCCACGUCUUUG
hsa-miR-578	CUUCUUGUGCUCUAGGAUUGU
hsa-miR-579	AUUCAUUUGGUAUAAACCGCGAU
hsa-miR-580	UUGAGAAUGAUGAAUCAUUAGG
hsa-miR-583	CAAAGAGGAAGGUCCCAUUAC
hsa-miR-584	UUAUGGUUUGCCUGGGACUGAG
hsa-miR-585	UGGGCGUAUCUGUAUGCUA
hsa-miR-200b	UAAUACUGCCUGGUAAUGAUGAC
hsa-miR-484	UCAGGCUCAGUCCCCUCCCGAU
hsa-miR-512-3p	AAGUGCUGUCAUAGCUGAGGUC

APPENDIX 5

Oligonucleotide sequences for polymorphic microRNA target site study (Chapter 6)

Primers and probes for data presented in Table 6.1	
Primer	Sequence
rs10117507-F	TGGTAACGTGTGATTGTTTTCA
rs10117507-R	GGCTATTTAATCAAGAAAAGTACCT
rs10122902-F	CGGATCTCATGTATCTACGC
rs10122902-R	TTCATATCGTTTGGCATGTAAGA
rs1043293-F	TCCAGCAAACCTATCGAGATAA
rs1043293-R	CTGCAGGAACCGGTAACT
rs1060120-F	ATCACCGTAGCCAGGTTT
rs1060120-R	TCTCAAAAGTTTGGGTTAGTTTCA
rs10898931-F	AAGCACATGTGAAAGAGCC
rs10898931-R	CTGTAGGCTACGGACCAA
rs10898932-F	AGGTGAGAAAAGCAAGGAGA
rs10898932-R	TCGTGGAGATGATCTATTAGCTT
rs10923444-F	GCCCAGATGAACAAAGAGC
rs10923444-R	ACTTAATTGTTGCTGTCACCAT
rs11184430-F	AGACTGGTTGATGACCGTAAT
rs11184430-R	TGATTCTCCCATCTCGGAC
rs1128687-F	TTCCGTTAAGGGGTCCCT
rs1128687-R	TCAAACTGGAGGTGGGTG
rs11688303-F	CCCACTTCCTCCAGAGAG
rs11688303-R	TGTACCACCACTTCACCAT
rs11768-F	CAAAGCCAGAGACGGTTTC
rs11768-R	AACGCTTCTTTTGTTCCAGA
rs11895-F	CTCCACTGTGCAAAGCAT
rs11895-R	ATGTCCCTAAGTGCCAGC
rs12311-F	TGTTCTATTATCTTTCATCTGCCAA
rs12311-R	TGTGCAGATATCAGACAAGATTT
rs12402294-F	CCCTGCCTATGTTGAGCTT
rs12402294-R	TAACGCCACACCTCCTTC
rs1271-F	CCCCTCTCTTCCAGAACTG
rs1271-R	TTCATTGTTTCCAAATACCATAGC
rs12920360-F	TCCCTTCAGGGTTTACTGTG
rs12920360-R	CAACAGTTTGTAAGCCTCCA
rs1415793-F	CTAGGCATCCTCCGAGAG
rs1415793-R	CTACTCTCTTCCTCCACTTCA
rs164149-F	TGTTAACAGATTTTCAAATGCCTG
rs164149-R	GACCCTCCAATAACACTGC
rs1663196-F	CAGTTCCCTTCGTGTACCA
rs1663196-R	TGGAAAGGCATCTGCCATA
rs16837530-F	TGTCATCCTAGGTCAAACAAGA
rs16837530-R	TGCCTAATTTCTTTCTCCAGC
rs17034228-F	CCTCAGTCCACTGTACCTT
rs17034228-R	CCAATGAACTCTCACCCCA
rs17132305-F	ACCAGACCTCATTTGCTATAGA
rs17132305-R	ACACTAGTCTTTAGAGCCCTG
rs17411988-F	TCATCCGTTATTCTTTAGTGACTT
rs17411988-R	GCCGACACCAGAATTTAAGA

rs17575427-F	AGAATCAGCTAGGTCCAGC
rs17575427-R	TCCAGATAGGCTAATTCCCTG
rs1953550-F	CAATCCAGCTATGAATGACCT
rs1953550-R	CCCTGCTTTCCAATTTTGATTT
rs2050892-F	CCTTGAAGGTAAACTAACTCCA
rs2050892-R	AACTTTGTCACAAGGACCATC
rs2070703-F	CAAAGGAAGTGAGGTAGTGC
rs2070703-R	CTAAGAGGACCCCTAACCAA
rs2272916-F	GCTCCTTTACTCTTACTGCAT
rs2272916-R	AGTTTTATGAGCTACCTTAACCAA
rs2279974-F	CCCCAAGCACATTATCTACC
rs2279974-R	TTGGTTGGCAATCCCAGA
rs2282136-F	CTTTGTCAGCAACATACTGC
rs2282136-R	CCATCTCTAAATGATCCCACTATAC
rs2798566-F	ATGGAGCTGGTAAAGGAGAG
rs2798566-R	AGCACTTGACTCTAGGCAA
rs3736147-F	CCCATCTGTGACTTCCTAGA
rs3736147-R	CCTCCAGAAATCAGATAAGTGAG
rs3825003-F	AGGCTTTTCCAGTTTTATGTCAA
rs3825003-R	TACCCATAAATAGAGCTTGTACCT
rs4289885-F	AAAGCAGACACAGGGATAAGA
rs4289885-R	CTATATCATGTCTATGGTCTCTACC
rs4624663-F	ATATTGGCCATGATACACTAGAAC
rs4624663-R	AAAATATATACCTTCGGGTCGC
rs480104-F	CATGGTTGTTAGACATCATTTTCA
rs480104-R	CAGCATCTGCTTTGGGAAT
rs4969391-F	CATCCAGCACTGGGGAAT
rs4969391-R	TGATGACAGAACAGGCTACA
rs4977494-F	CCAAGATGATGTGCCTACCTA
rs4977494-R	CAGTCATCAACCAGAAGCAT
rs572262-F	CATCCACACAGCCAATACAA
rs572262-R	TCACCTTGAAACAATCACTTTTAAT
rs575797-F	CACAGGATCAGAATTCTGCAT
rs575797-R	CAGTCATTACCGCCCCTA
rs7211218-F	CCTCTTCCTCCTGGTGTTT
rs7211218-R	TGCTCACGTTTGTACTGTTT
rs7368202-F	TGGGTCCCTGTTTCCTTTAAT
rs7368202-R	CATTATATCACAGTGCACACAAC
rs7418910-F	TTCTGGCCTAAGGACTTTCA
rs7418910-R	CTCACTCCCAGATCCTGC
rs7539-F	GTTACACCCTATGCGCCA
rs7539-R	ACAGAGGAGGGAAGGCAA
rs7843128-F	TGAGGCAGGTGTCAAGAG
rs7843128-R	GGGGACACGACCTTTTCA
rs835575-F	CAAAGGCTGCTATATAGTTCCT
rs835575-R	TAAAGGCCTGCTCACCAAT
rs924834-F	CTGAAGGTTGCTGAGTGC
rs924834-R	TTTGTGACCTCAAGCTATTTACT
rs9857007-F	CTGAGGATTCCCTTTCCAGA
rs9857007-R	GAAACCAAGGCCAGGAGA

Probe	Sequence (tags in red)	Bead
rs10117507-A	TCAACAATCTTTTACAATCAAATCGTCTAAGAATGTCAGGGCAAAAA	6
rs10117507-G	TCAATTACCTTTTCAATACAATACGTCTAAGAATGTCAGGGCAAAAG	24
rs10117507-com	TATGGGCATTTTTCTTGCTATGTCTATCTTTAAACTACAAATCTAAC	
rs10122902-A	TATACTATCAACTCAACAACATATCGGAAAGGCAGCACAAAA	89
rs10122902-G	AATCTTACCAATTCATAATCTTCACGGAAAGGCAGCACAAAG	61
rs10122902-com	CTTCCAGTTGAATCCTGTCAAAACTATCTTTAAACTACAAATCTAAC	
rs1043293-C	CTATAAACATATTACATTCACATCCGATAAACTTCCTAATGGCAGC	69
rs1043293-G	TCATTCATATACATACCAATTCATCGATAAACTTCCTAATGGCAGG	34
rs1043293-com	ATATTCACTCTCAATCCTGAAGTTACCTATCTTTAAACTACAAATCTAAC	
rs1060120-C	TACACATCTTACAAACTAATTTCAAAGCGGGTCATTATATTGCATC	74
rs1060120-T	ATACAATCTAACTTCACTATTACAAAGCGGGTCATTATATTGCATT	83
rs1060120-com	CTTTCATAGGAGCTCATTATCACGCTATCTTTAAACTACAAATCTAAC	
rs10898931-A	TCAAAATCTCAAATACTCAAATCAGACCTCAAAGAAGACCGTAATTTA	18
rs10898931-T	CTACTTCATATACTTTATACTACAGACCTCAAAGAAGACCGTAATTTT	63
rs10898931-com	TATCAGTGCTCAAGAATAATTTTGGACTATCTTTAAACTACAAATCTAAC	
rs10898932-C	AATCCTTTTACATTCATTACTTACGAGATAAAGTAGGCTGTGAACATAC	8
rs10898932-G	CTTTCAATTACAATACTCATTACAGAGATAAAGTAGGCTGTGAACATAG	43
rs10898932-com	CGCTCGTTAACCAAGCCCTATCTTTAAACTACAAATCTAAC	
rs10923444-A	CAATTTCATCATTCATTCATTTCAGTTGTATGTGACTCCAGCA	35
rs10923444-G	CAATTCATTTACCAATTTACCAATGTTGTATGTGACTCCAGCG	7
rs10923444-com	CCTTTGTGGGCAACCCTCTATCTTTAAACTACAAATCTAAC	
rs11184430-A	TCAATCAATTACTTACTCAAATACGCCACTGCACCCTTTTAA	19
rs11184430-G	TTCAATCATTCAAATCTCAACTTTGCCACTGCACCCTTTTAG	23
rs11184430-com	AATTAGTATTTAAGTTCCAGATCACTGCCTATCTTTAAACTACAAATCTAAC	
rs1128687-C	TCATCAATCAATCTTTTTCACTTTGCATGTGCTGAACCTCTCC	59
rs1128687-T	TTACCTTTATACCTTTCTTTTTACGCATGTGCTGAACCTCTCT	30
rs1128687-com	GTGCCTCTGCCTCCGCTATCTTTAAACTACAAATCTAAC	
rs11688303-A	CAATATACCAATATCATCATTTACTCAGAGAAGTTCTGGGAAACA	50
rs11688303-G	AATCTAACAAACTCATCTAAATACTCAGAGAAGTTCTGGGAAACG	76
rs11688303-com	CTTCATGTTGACCAAACATAACAACCTATCTTTAAACTACAAATCTAAC	
rs11768-G	CTTTTCATCTTTTCATCTTTCAATGGGTAATTTAAGTGCCCGATG	37
rs11768-T	AATCTTACTACAAATCCTTTCTTTGGGTAATTTAAGTGCCCGATT	29
rs11768-com	GTAGAGGTCTGGCTTCCCCTATCTTTAAACTACAAATCTAAC	
rs11895-A	ATCATTACAATCCAATCAATTCATCAAAGTGGACTGAACATGGA	71
rs11895-G	CTTTTCAAATCAATACTCAACTTTCAAAGTGGACTGAACATGGG	27
rs11895-com	AAGACTTTTATTATAGAAATGACAAGATGCCTATCTTTAAACTACAAATCTAAC	
rs12311-C	CTTTTCAATTACTTCAAATCTTCAAGAATAACCACAGGCAAACAC	25
rs12311-T	CTTTATCAATACATACTACAATCAAGAATAACCACAGGCAAACAT	2
rs12311-com	CAAAACAATACGCATAAGTTAGACAACTATCTTTAAACTACAAATCTAAC	
rs12402294-C	CAATTCAAATCACAATAATCAATCTCTTTCCGGTGGAAGTTACC	5
rs12402294-T	TACATTACCAATAATCTTCAAATCTCTTTCCGGTGGAAGTTACT	4
rs12402294-com	GCCTTCTAACAAACTACATAATTGACCTATCTTTAAACTACAAATCTAAC	
rs1271-C	CTTTAATCCTTTATCACTTTATCATGAATGGTGGAAGTCAGAGAC	17
rs1271-G	TCAATCATCTTTATACTTCACAATTGAATGGTGGAAGTCAGAGAG	52
rs1271-com	CAACCCTGGGGATTGGGCTATCTTTAAACTACAAATCTAAC	
rs12920360-A	CTACTATACATCTTACTATACTTTTCCCCAAAATGCTCTCATCA	14
rs12920360-T	AATCCTTTTTACTCAATTCAATCATCCCCAAAATGCTCTCATCT	22
rs12920360-com	CTTCTGGATGGCTACATAAACAGCTATCTTTAAACTACAAATCTAAC	
rs1415793-C	TAATTATACATCTCATCTTCTACAGACTTACTGACAAAAGGCTCC	53
rs1415793-T	AATCTCATAATCTACATACACTATGACTTACTGACAAAAGGCTCT	97

rs1415793-com	AGTTGGGCTGAACATGTGTCTATCTTTAAACTACAAATCTAAC	
rs164149-C	CTTTCTATTCATCTAAATACAAACCTGAGACCTGCTAGAGTCATAC	93
rs164149-T	ATACTAACTCAACTAACTTTAAACCTGAGACCTGCTAGAGTCATAT	96
rs164149-com	GTTCGGGGAATTAAGTCTTTATCCCTATCTTTAAACTACAAATCTAAC	
rs1663196-C	CTACAAACAAACAAACATTATCAAAAGCCTGACTGCTCTTCC	28
rs1663196-T	CTAACTAACAATAATCTAACTAACAAGCCTGACTGCTCTTCT	80
rs1663196-com	GCCTCTCTATCCCCACATCCTATCTTTAAACTACAAATCTAAC	
rs16837530-C	AATCATACCTTTCAATCTTTTACACCCAGTGACATGATGACATTTAC	75
rs16837530-T	TATATACACTTCTCAATAACTAACCCCAGTGACATGATGACATTTAT	55
rs16837530-com	GTTTTAGAGAGAACACTGGATGCCTATCTTTAAACTACAAATCTAAC	
rs17034228-C	TTACTTCACTTTCTATTTACAATCTTCTGGATGTTGAGGAAGGAC	88
rs17034228-T	AAACAAACTTCACATCTCAATAATTTCTGGATGTTGAGGAAGGAT	48
rs17034228-com	CTAGAGACACATCCTTGAACTAGACTATCTTTAAACTACAAATCTAAC	
rs17132305-C	TACACTTTAAACTTACTACACTAACTTGCTTGGCTAAAGAATATTGC	95
rs17132305-T	TCATTTCACAATTCAATTACTCAACTTGCTTGGCTAAAGAATATTGT	45
rs17132305-com	GCCATTGCCTTTTACAACCACTATCTTTAAACTACAAATCTAAC	
rs17411988-C	CTTTTACAATACTTCAATACAATCTGGATTTTGCTCTTAGGAATTGC	20
rs17411988-G	CTTCTCATTAACTTACTTCATAATTGGATTTTGCTCTTAGGAATTGG	47
rs17411988-com	TTTGCTTAGAAAGTATCAACTTGAATTGCTATCTTTAAACTACAAATCTAAC	
rs17575427-C	AATCTACACTAACAATTTCATAACCATCCTTCTATCGTGAAGTGC	99
rs17575427-G	CTATCTTCATATTTCACTATAAACCATCCTTCTATCGTGAAGTGG	42
rs17575427-com	GCCCATGTACCACGTCTCTATCTTTAAACTACAAATCTAAC	
rs1953550-A	CTTTCTACATTATTCACAACATTAAGTGTGATGGGTGCTAGAATAA	40
rs1953550-G	TACACTTTATCAAATCTTACAATCAGTGTGATGGGTGCTAGAATAG	3
rs1953550-com	CTTTTCCCTTGTGCTGAATTCACTATCTTTAAACTACAAATCTAAC	
rs2050892-A	CTAAATACTTCACAATTCATCTAAAATTCAAATTGCACAGAGACTTTAAATA	90
rs2050892-T	AAACTAACATCAATACTTACATCAAATTCAAATTGCACAGAGACTTTAAATT	87
rs2050892-com	GGGAGCCTCTTTCCCAGCTATCTTTAAACTACAAATCTAAC	
rs2070703-C	ATCAAATCTCATCAATTCAACAATCAGCAGAACAAACTCAGATCTC	73
rs2070703-T	ATACTACATCATAATCAAACATCACAGCAGAACAAACTCAGATCTT	85
rs2070703-com	ATCAGGGTAGCAGCAGAGCTATCTTTAAACTACAAATCTAAC	
rs2272916-C	AATCAATCTTCATTCAAATCATCAAGTAAGAGTCCCAGAGGATCC	16
rs2272916-T	TACACAATCTTTTCATTACATCATAGTAAGAGTCCCAGAGGATCT	39
rs2272916-com	TCAAAGGTGATAAACTCATGATTCCCTATCTTTAAACTACAAATCTAAC	
rs2279974-C	TCATAATCTCAACAATCTTTCTTTGATGTGGCAGCAGCTTC	68
rs2279974-T	TAACATTACAACTATACTATCTACGATGTGGCAGCAGCTTT	66
rs2279974-com	GTTTGGGCTGGCATTTCCCTATCTTTAAACTACAAATCTAAC	
rs2282136-C	CTTTAATCTCAATCAATACAAATCCATTGGCTGTTAAATGAGTCCC	1
rs2282136-T	CTACATATTCAAATTACTACTTACCATTGGCTGTTAAATGAGTCCT	64
rs2282136-com	TTTGCATACTCACTGGAGAGACTATCTTTAAACTACAAATCTAAC	
rs2798566-C	CAATTAACTACATACAATACATACAGAGAGGGCAGCATTGATAC	77
rs2798566-T	TACACTTTCTTTCTTTCTTTCTTTAGAGAGGGCAGCATTGATAT	12
rs2798566-com	CCTATGGTGATTCCAGCTAAACCTATCTTTAAACTACAAATCTAAC	
rs3736147-A	ATACCAATAATCCAATTCATATCATGACCCCGCTTATAGTTCA	70
rs3736147-G	CTTTTCATCAATAATCTTACCTTTTGACCCCGCTTATAGTTCG	65
rs3736147-com	AAGGTAAGCTGACAGGCGCTATCTTTAAACTACAAATCTAAC	
rs3825003-A	TTCATAACATCAATCATAACTTACGCTATGTAGAAAATAGTGAGTGTGTAA	91
rs3825003-G	CTTTTTCAATCACTTTCAATTCATGCTATGTAGAAAATAGTGAGTGTGTAG	54
rs3825003-com	GCTCTGAAGACAGATAGGAATATAAGCTATCTTTAAACTACAAATCTAAC	
rs4289885-C	AATCCTTTCTTTAATCTCAAATCAGTTGCCCAAAAAATGTGATGC	21
rs4289885-T	CTTTCTATCTTTCTACTCAATAATGTTGCCCAAAAAATGTGATGT	94
rs4289885-com	GCTTCATGTTTTCTCTGACTCATCTATCTTTAAACTACAAATCTAAC	

rs4624663-A	AATCTACAAATCCAATAATCTCATCTTTGATTTAAACAGTTCTGACACATAA	60
rs4624663-G	TCATCAATCTTTCAATTTACTTACCTTTGATTTAAACAGTTCTGACACATAG	49
rs4624663-com	GGGATCCACTTGTTTCTTTGCCTATCTTTAAACTACAAATCTAAC	
rs480104-C	CTACTAATTCATTAACATTACTACCATATCCTCTCCAGACTAGGAAC	58
rs480104-G	CAATATCATCATCTTTATCATTACCATATCCTCTCCAGACTAGGAAG	57
rs480104-com	TGTTCTATAGAGACTCCTGTGCCTATCTTTAAACTACAAATCTAAC	
rs4969391-C	TACATACACTAATAACATACTCATACTGTCGGCTTCAGCC	82
rs4969391-T	TCATTTCAATCAATCATCAACAATACTGTCGGCTTCAGCT	51
rs4969391-com	GGACGTGGGCAAAGGGCTATCTTTAAACTACAAATCTAAC	
rs4977494-C	TCAATCATAATCTCATAATCCAATGCGGAGGTCTTTACCCC	62
rs4977494-T	AATCATACTCAACTAATCATTCAAGCGGAGGTCTTTACCCT	98
rs4977494-com	TCCCAAATGAGTCAAACTGCCTATCTTTAAACTACAAATCTAAC	
rs572262-C	CAATAAACTATACTTCTTCACTAAAACAGATGTAGCAACATGAGAAAC	13
rs572262-T	TCAATCATTACACTTTTCAACAATAACAGATGTAGCAACATGAGAAAT	38
rs572262-com	GCTTATGTTACAGGTTACATGAGAGCTATCTTTAAACTACAAATCTAAC	
rs575797-C	CAATTTACTCATATACATCACTTTGTAAGGTAGGACAGCTTAACAAC	56
rs575797-G	TCATTTACCTTTAATCCAATAATCGTAAGGTAGGACAGCTTAACAAG	72
rs575797-com	GATTCTGGTCCTATAAGTGTCGCTATCTTTAAACTACAAATCTAAC	
rs7211218-A	CAATTCATTTCATTCACAATCAATCATTGTGCCAATTTGTCCTTAA	36
rs7211218-C	TTCACTTTTCAATCAACTTTAATCCATTGTGCCAATTTGTCCTTAC	31
rs7211218-com	GTAAATCACTTGTGCTGTGTGCTATCTTTAAACTACAAATCTAAC	
rs7368202-C	TACAAATCATCAATCACTTTAATCTTGTCAATTGGTCTGAAACAAATTC	11
rs7368202-T	ATTATTCACTTCAAACTAATCTACTTGTCAATTGGTCTGAAACAAATTT	32
rs7368202-com	GCTAGGGAATCTATTTGTGTAGAACCTATCTTTAAACTACAAATCTAAC	
rs7418910-C	TTACTCAAAATCTACACTTTTTCAATGGTTGAGATGGGCACC	26
rs7418910-T	TCAATTACTTCACTTTAATCCTTTATGGTTGAGATGGGCACT	33
rs7418910-com	GTTTTGCAGGAAACACCATATTAATCTATCTTTAAACTACAAATCTAAC	
rs7539-C	TCATTTACTCAACAATTACAAATCGAAGTTGTCAAGATGGAACCTC	67
rs7539-G	TTACTACACAATATACTCATCAATGAAGTTGTCAAGATGGAACCTG	41
rs7539-com	AAGATGCTACAGAGGAAATCAGTCTATCTTTAAACTACAAATCTAAC	
rs7843128-C	TCAACTAACTAATCATCTATCAATGCTGTGGGCTGGGATC	84
rs7843128-T	CTATTACACTTTAAACATCAATACGCTGTGGGCTGGGATT	92
rs7843128-com	TGTGGGCCTGAAGCAGCTATCTTTAAACTACAAATCTAAC	
rs835575-G	CTTTAATCTACACTTTCTAACAATCAATTCCTGCACTTGAACATATAAAG	81
rs835575-T	TAATCTTCTATATCAACATCTTACCAATTCCTGCACTTGAACATATAAAT	9
rs835575-com	TCCATGTCTTCAGTGAGAACATACTATCTTTAAACTACAAATCTAAC	
rs924834-C	TTCATAACTACAATACATCATCATCTGCAGGCTATAGTTGCAC	79
rs924834-T	CTAATTACTAACATCACTAACAATCTGCAGGCTATAGTTGCAT	86
rs924834-com	CATTTTGTCTAACCCTCCCAGCTATCTTTAAACTACAAATCTAAC	
rs9857007-A	ATACTTCATTCATTCATCAATTCACATTTATCCTCACACATGCTGA	15
rs9857007-G	TCATTTACCAATCTTTCTTTATACCATTTATCCTCACACATGCTGG	44
rs9857007-com	CTCCATTTCATTCTGATACCTTAAAATGCTATCTTTAAACTACAAATCTAAC	

APPENDIX 6

Supplementary methods for miRSNiPer (Chapter 6)

Introduction

To predict miRNA targets in the 3' UTRs of human genes that overlap with validated SNPs, we require: (1) a source of accurately annotated mRNAs and their splice variants, (2) a database of SNPs with accurate positional and validation information and, (3) a high-throughput algorithm to predict miRNA targets that does not rely on interspecies conservation.

We describe our approach which is greatly influenced by the Rna22 algorithm of Miranda et al, 2006 (A pattern-based method for the identification of microRNA-target sites and their corresponding RNA/RNA complexes T. Huynh, K. Miranda, Y. Tay, Y.-S. Ang, W.-L. Tam, A. M. Thomson, B. Lim, I. Rigoutsos Cell, Vol 126, 1203-1217, 22 September 2006), but which differs in many significant respects. Our procedure consists of two parallel tracks: (1) acquisition of significant sequence motifs from the training set of mature miRNA sequences and (2) isolation and assembly of 3'UTR sequences and insertion of validated SNP markers.

Pattern Acquisition

692 mature human miRNA sequences were obtained from Release 12.0 of Mirbase (ftp://ftp.sanger.ac.uk/pub/mirbase/sequences/12.0/mature.fa.gz) and were filtered with BLAST to remove identical or near-duplicate entries. A reduced set of 624 mature miRNAs in which no two sequences shared greater than 90% identity were subjected to pattern extraction with Teiresias (Rigoutsos, I. and A. Floratos, Combinatorial Pattern Discovery in Biological Sequences: the TEIRESIAS Algorithm. *Bioinformatics,* 14(1),

January 1998) as described below. An additional set of input sequences were obtained from this reduced set by extracting the 5'-terminal 12 nts (which contain the "seed" region) of each entry. The patterns derived from the former will be referred to as the "full-length" patterns and those derived from the latter as "seed" patterns.

Pattern Discovery with Teiresias

Teiresias is a efficient algorithm that is able to rapidly enumerate all conserved non-contiguous patterns that are present within a set of sequences, as long as the density of gaps within a given pattern does not exceed a user-specified threshold. The threshold is specified by two parameters: L, which designates the minimum number of positions that must be explicitly specified by a base within an elementary pattern and W, which designates the maximum width that an elementary pattern may span. Furthermore, K specifies the minimum number of distinct input sequences that must harbor a given pattern.

For example, given a set of input sequences and parameters set to L=4, W=12 and K=2, Teiresias scans for all elementary patterns that contain exactly 4 specified bases and contain no more than 12-4=8 wildcards (i.e., the token "N" which represents any base) and are present in at least 2 input sequences. It then executes a convolution phase in which the elementary patterns are progressively combined into compositional-maximal and length-maximal patterns.

Statistical Significance of Patterns

To determine which patterns are enriched within the full-length and seed miRNA sets we cannot simply enumerate their frequency by scanning the totality of the human chromosome for each instance. Instead we estimate the background frequency of each

convolved pattern by enumerating elementary triplet patterns from a random subset of the human genome and by using these empirical values and Bayes' rule to compute their conditional probability.

To this end we isolated a random set of 927916 non-overlapping sequences from the hg18 build of the human genome (http://hgdownload.cse.ucsc.edu/goldenPath/hg18/chromosomes/). The length distribution of this random background set matched the size distribution of the full-length miRNAs. We compared the observed frequency of each derived pattern with its inferred frequency in the human genomic background and kept only those patterns that were enriched >= 5-fold.

A Teiresias pattern scan of the 624 full-length miRNAs with parameters L=4, W=12 and K=10 yielded 191184 convolved patterns. Of these, 12184 were deemed statistically significant according to the procedure described above and the remainder was discarded.

A Teiresias pattern scan of the 624 seed miRNAs with parameters L=5, W=12, and K=5 yielded 22475 convolved patterns. Of these, 3904 were determined to be statistically significant and the remainder was discarded.

Preparation of 3'UTRs

Our 3'UTR sequences were derived from the Human Apr07 release of AceView (http://www.ncbi.nlm.nih.gov/IEB/Research/Acembly/downloads.v67.html). As stated on the homepage, "AceView provides a curated, comprehensive and non-redundant sequence representation of all public mRNA sequences from GenBank, RefSeq, and single-pass cDNA sequences from dbEST and Trace" (http://www.ncbi.nlm.nih.gov/IEB/Research/Acembly/index.html). In particular, they

provide an exhaustive listing of known splice variants for each gene in which the intronic boundaries are claimed to be "especially reliable". Although the 3'UTR moieties of each gene may be viewed through AceView's online summary pages, they are not indicated in the datasets that are made available for bulk download, and therefore must be reconstructed.

The AceView transcripts are available for bulk download in two different representations: a set of fasta files (AceView.ncbi_36.good_mrnas_fasta.tar.gz) that list the entire sequence of each gene and a set of tabular gff files (AceView.ncbi_36.genes_gff.tar.gz) that denote the relevant landmarks within each gene. These data were analyzed in parallel, logically inconsistent records were discarded and the remainder were converted into distinct fasta records for each exonic component of each deduced 3'UTR. Some 3'UTRs are represented by a single fasta record if entirely contained within one exon and others by several records if divided across multiple exons. It is necessary to maintain the 3'UTR components in their positionally-independent unspliced form during the SNP mapping process.

Insertion of Valid SNPs

SNP position and genotyping data was obtained from build 129 of dbSNP (ftp://ftp.ncbi.nih.gov/snp/organisms/human_9606/XML/). SNPs that fell within the bounds of a 3'UTR fragment were inserted into the sequence if they had a minor allele frequency of at least 0.03 within a relevant Caucasian population and if the reported upstream and downstream flanks matched their corresponding regions in the UTR template. The Caucasian populations that were considered are described by the following triples which designate their NCBI popID, handle and name, respectively: (760, TSC-

CSHL, CEL_caucasian), (761, TSC-CSHL, CEL_caucasian_CEPH), (902, AFFY, Caucasian), (904, AFFY, CEPH), (1303, SEQUENOM, CEPH), (1371, PERLEGEN, AFD_EUR_PANEL), (1409, CSHL-HAPMAP, HapMap_CEU), (1639, ABI, Caucasian), (4401, HB_BONN_CNS_SNPS, EUROPE).

Splicing of Haplotypes and Resolution of SNP Codes

Since the 3'UTRs are scanned with conserved sequence patterns derived from applying the Teiresias algorithm either to full-length miRNAs or to shorter segments containing the seed region, then the longest possible motif that may be discovered will be no longer than the longest input mature miRNA which, in this release (12.0), is 27 nts. Therefore at a given SNP position, the two possible alleles will influence pattern alignment no more than 27-1=26 nts upstream or downstream. So, any two SNPs that are less than 2*26=52 nt apart may have overlapping influences on pattern support. To account for all potentially overlapping influences by neighboring SNPs we must expand the substrate 3'UTRs into all representative "haplotypes". Thus all degenerate 3'UTRs are resolved into the minimum number of haplotypes that represent all possible combinations of neighboring SNPs that may have a compound effect on pattern matching.

Determination of Pattern Support

The statistically significant sets of full-length and seed patterns were translated into their reverse complements and were scanned for every matching occurrence in all of the 3'UTR templates. Each base in each 3'UTR was assigned a single vote for each pattern that matched and, furthermore, was located opposite a specified base within the pattern (i.e., a non wildcard character). The density of votes in the vicinity of each SNP was

compared between different alleles. If the ratio of support density exceeded 2 for any pair of 3'UTR haplotypes at a given SNP locus, then that SNP was flagged as having the potential to disrupt a possible miRNA target.

References

1. Birney, E., J.A. Stamatoyannopoulos, A. Dutta, R. Guigo, T.R. Gingeras, E.H. Margulies, Z. Weng, M. Snyder, E.T. Dermitzakis, R.E. Thurman, M.S. Kuehn, C.M. Taylor, S. Neph, C.M. Koch, S. Asthana, A. Malhotra, I. Adzhubei, J.A. Greenbaum, R.M. Andrews, P. Flicek, P.J. Boyle, H. Cao, N.P. Carter, G.K. Clelland, S. Davis, N. Day, P. Dhami, S.C. Dillon, M.O. Dorschner, H. Fiegler, P.G. Giresi, J. Goldy, M. Hawrylycz, A. Haydock, R. Humbert, K.D. James, B.E. Johnson, E.M. Johnson, T.T. Frum, E.R. Rosenzweig, N. Karnani, K. Lee, G.C. Lefebvre, P.A. Navas, F. Neri, S.C. Parker, P.J. Sabo, R. Sandstrom, A. Shafer, D. Vetrie, M. Weaver, S. Wilcox, M. Yu, F.S. Collins, J. Dekker, J.D. Lieb, T.D. Tullius, G.E. Crawford, S. Sunyaev, W.S. Noble, I. Dunham, F. Denoeud, A. Reymond, P. Kapranov, J. Rozowsky, D. Zheng, R. Castelo, A. Frankish, J. Harrow, S. Ghosh, A. Sandelin, I.L. Hofacker, R. Baertsch, D. Keefe, S. Dike, J. Cheng, H.A. Hirsch, E.A. Sekinger, J. Lagarde, J.F. Abril, A. Shahab, C. Flamm, C. Fried, J. Hackermuller, J. Hertel, M. Lindemeyer, K. Missal, A. Tanzer, S. Washietl, J. Korbel, O. Emanuelsson, J.S. Pedersen, N. Holroyd, R. Taylor, D. Swarbreck, N. Matthews, M.C. Dickson, D.J. Thomas, M.T. Weirauch, J. Gilbert, J. Drenkow, I. Bell, X. Zhao, K.G. Srinivasan, W.K. Sung, H.S. Ooi, K.P. Chiu, S. Foissac, T. Alioto, M. Brent, L. Pachter, M.L. Tress, A. Valencia, S.W. Choo, C.Y. Choo, C. Ucla, C. Manzano, C. Wyss, E. Cheung, T.G. Clark, J.B. Brown, M. Ganesh, S. Patel, H. Tammana, J. Chrast, C.N. Henrichsen, C. Kai, J. Kawai, U. Nagalakshmi, J. Wu, Z. Lian, J. Lian, P. Newburger, X. Zhang, P. Bickel, J.S. Mattick, P. Carninci, Y. Hayashizaki, S. Weissman, T. Hubbard, R.M. Myers, J. Rogers, P.F. Stadler, T.M. Lowe, C.L. Wei, Y. Ruan, K. Struhl, M. Gerstein, S.E. Antonarakis, Y. Fu, E.D. Green, U. Karaoz, A. Siepel, J. Taylor, L.A. Liefer, K.A. Wetterstrand, P.J. Good, E.A. Feingold, M.S. Guyer, G.M. Cooper, G. Asimenos, C.N. Dewey, M. Hou, S. Nikolaev, J.I. Montoya-Burgos, A. Loytynoja, S. Whelan, F. Pardi, T. Massingham, H. Huang, N.R. Zhang, I. Holmes, J.C. Mullikin, A. Ureta-Vidal, B. Paten, M. Seringhaus, D. Church, K. Rosenbloom, W.J. Kent, E.A. Stone, S. Batzoglou, N. Goldman, R.C. Hardison, D. Haussler, W. Miller, A. Sidow, N.D. Trinklein, Z.D. Zhang, L. Barrera, R. Stuart, D.C. King, A. Ameur, S. Enroth, M.C. Bieda, J. Kim, A.A. Bhinge, N. Jiang, J. Liu, F. Yao, V.B. Vega, C.W. Lee, P. Ng, A. Yang, Z. Moqtaderi, Z. Zhu, X. Xu, S. Squazzo, M.J. Oberley, D. Inman, M.A. Singer, T.A. Richmond, K.J. Munn, A. Rada-Iglesias, O. Wallerman, J. Komorowski, J.C. Fowler, P. Couttet, A.W. Bruce, O.M. Dovey, P.D. Ellis, C.F. Langford, D.A. Nix, G. Euskirchen, S. Hartman, A.E. Urban, P. Kraus, S. Van Calcar, N. Heintzman, T.H. Kim, K. Wang, C. Qu, G. Hon, R. Luna, C.K. Glass, M.G. Rosenfeld, S.F. Aldred, S.J. Cooper, A. Halees, J.M. Lin, H.P. Shulha, M. Xu, J.N. Haidar, Y. Yu, V.R. Iyer, R.D. Green, C. Wadelius, P.J. Farnham, B. Ren, R.A. Harte, A.S. Hinrichs, H. Trumbower, H. Clawson, J. Hillman-Jackson, A.S. Zweig, K. Smith, A. Thakkapallayil, G. Barber, R.M. Kuhn, D. Karolchik, L. Armengol, C.P. Bird, P.I. de Bakker, A.D. Kern, N. Lopez-Bigas, J.D. Martin, B.E. Stranger, A. Woodroffe, E. Davydov, A. Dimas, E. Eyras, I.B. Hallgrimsdottir, J. Huppert, M.C. Zody, G.R. Abecasis, X. Estivill, G.G. Bouffard, X. Guan, N.F. Hansen,

J.R. Idol, V.V. Maduro, B. Maskeri, J.C. McDowell, M. Park, P.J. Thomas, A.C. Young, R.W. Blakesley, D.M. Muzny, E. Sodergren, D.A. Wheeler, K.C. Worley, H. Jiang, G.M. Weinstock, R.A. Gibbs, T. Graves, R. Fulton, E.R. Mardis, R.K. Wilson, M. Clamp, J. Cuff, S. Gnerre, D.B. Jaffe, J.L. Chang, K. Lindblad-Toh, E.S. Lander, M. Koriabine, M. Nefedov, K. Osoegawa, Y. Yoshinaga, B. Zhu and P.J. de Jong, *Identification and analysis of functional elements in 1% of the human genome by the ENCODE pilot project.* Nature, 2007. **447**(7146): p. 799-816.

2. Miranda, K.C., T. Huynh, Y. Tay, Y.S. Ang, W.L. Tam, A.M. Thomson, B. Lim, and I. Rigoutsos, *A pattern-based method for the identification of MicroRNA binding sites and their corresponding heteroduplexes.* Cell, 2006. **126**(6): p. 1203-17.
3. Fire, A., S. Xu, M.K. Montgomery, S.A. Kostas, S.E. Driver, and C.C. Mello, *Potent and specific genetic interference by double-stranded RNA in Caenorhabditis elegans.* Nature, 1998. **391**(6669): p. 806-11.
4. Lee, R.C., R.L. Feinbaum, and V. Ambros, *The C. elegans heterochronic gene lin-4 encodes small RNAs with antisense complementarity to lin-14.* Cell, 1993. **75**(5): p. 843-54.
5. Pasquinelli, A.E., B.J. Reinhart, F. Slack, M.Q. Martindale, M.I. Kuroda, B. Maller, D.C. Hayward, E.E. Ball, B. Degnan, P. Muller, J. Spring, A. Srinivasan, M. Fishman, J. Finnerty, J. Corbo, M. Levine, P. Leahy, E. Davidson, and G. Ruvkun, *Conservation of the sequence and temporal expression of let-7 heterochronic regulatory RNA.* Nature, 2000. **408**(6808): p. 86-9.
6. Cai, X., C.H. Hagedorn, and B.R. Cullen, *Human microRNAs are processed from capped, polyadenylated transcripts that can also function as mRNAs.* RNA, 2004. **10**(12): p. 1957-66.
7. Lee, Y., M. Kim, J. Han, K.H. Yeom, S. Lee, S.H. Baek, and V.N. Kim, *MicroRNA genes are transcribed by RNA polymerase II.* EMBO J, 2004. **23**(20): p. 4051-60.
8. Borchert, G.M., W. Lanier, and B.L. Davidson, *RNA polymerase III transcribes human microRNAs.* Nat Struct Mol Biol, 2006. **13**(12): p. 1097-101.
9. Blow, M.J., R.J. Grocock, S. van Dongen, A.J. Enright, E. Dicks, P.A. Futreal, R. Wooster, and M.R. Stratton, *RNA editing of human microRNAs.* Genome Biol, 2006. **7**(4): p. R27.
10. Lee, Y., C. Ahn, J. Han, H. Choi, J. Kim, J. Yim, J. Lee, P. Provost, O. Radmark, S. Kim, and V.N. Kim, *The nuclear RNase III Drosha initiates microRNA processing.* Nature, 2003. **425**(6956): p. 415-9.
11. Han, J., Y. Lee, K.H. Yeom, J.W. Nam, I. Heo, J.K. Rhee, S.Y. Sohn, Y. Cho, B.T. Zhang, and V.N. Kim, *Molecular basis for the recognition of primary microRNAs by the Drosha-DGCR8 complex.* Cell, 2006. **125**(5): p. 887-901.
12. Zeng, Y. and B.R. Cullen, *Efficient processing of primary microRNA hairpins by Drosha requires flanking nonstructured RNA sequences.* J Biol Chem, 2005. **280**(30): p. 27595-603.
13. Duan, R., C. Pak, and P. Jin, *Single nucleotide polymorphism associated with mature miR-125a alters the processing of pri-miRNA.* Hum Mol Genet, 2007. **16**(9): p. 1124-31.

14. Gregory, R.I., K.P. Yan, G. Amuthan, T. Chendrimada, B. Doratotaj, N. Cooch, and R. Shiekhattar, *The Microprocessor complex mediates the genesis of microRNAs.* Nature, 2004. **432**(7014): p. 235-40.
15. Okamura, K., J.W. Hagen, H. Duan, D.M. Tyler, and E.C. Lai, *The mirtron pathway generates microRNA-class regulatory RNAs in Drosophila.* Cell, 2007. **130**(1): p. 89-100.
16. Han, J., J.S. Pedersen, S.C. Kwon, C.D. Belair, Y.K. Kim, K.H. Yeom, W.Y. Yang, D. Haussler, R. Blelloch, and V.N. Kim, *Posttranscriptional crossregulation between Drosha and DGCR8.* Cell, 2009. **136**(1): p. 75-84.
17. Yi, R., Y. Qin, I.G. Macara, and B.R. Cullen, *Exportin-5 mediates the nuclear export of pre-microRNAs and short hairpin RNAs.* Genes Dev, 2003. **17**(24): p. 3011-6.
18. Gregory, R.I., T.P. Chendrimada, N. Cooch, and R. Shiekhattar, *Human RISC couples microRNA biogenesis and posttranscriptional gene silencing.* Cell, 2005. **123**(4): p. 631-40.
19. Haase, A.D., L. Jaskiewicz, H. Zhang, S. Laine, R. Sack, A. Gatignol, and W. Filipowicz, *TRBP, a regulator of cellular PKR and HIV-1 virus expression, interacts with Dicer and functions in RNA silencing.* EMBO Rep, 2005. **6**(10): p. 961-7.
20. Khvorova, A., A. Reynolds, and S.D. Jayasena, *Functional siRNAs and miRNAs exhibit strand bias.* Cell, 2003. **115**(2): p. 209-16.
21. Diederichs, S. and D.A. Haber, *Dual role for argonautes in microRNA processing and posttranscriptional regulation of microRNA expression.* Cell, 2007. **131**(6): p. 1097-108.
22. Diederichs, S., S. Jung, S.M. Rothenberg, G.A. Smolen, B.G. Mlody, and D.A. Haber, *Coexpression of Argonaute-2 enhances RNA interference toward perfect match binding sites.* Proc Natl Acad Sci U S A, 2008. **105**(27): p. 9284-9.
23. Rodriguez, A., S. Griffiths-Jones, J.L. Ashurst, and A. Bradley, *Identification of mammalian microRNA host genes and transcription units.* Genome Res, 2004. **14**(10A): p. 1902-10.
24. Griffiths-Jones, S., H.K. Saini, S. van Dongen, and A.J. Enright, *miRBase: tools for microRNA genomics.* Nucleic Acids Res, 2008. **36**(Database issue): p. D154-8.
25. Ambros, V. and R.C. Lee, *Identification of microRNAs and other tiny noncoding RNAs by cDNA cloning.* Methods Mol Biol, 2004. **265**: p. 131-58.
26. Lai, E.C., P. Tomancak, R.W. Williams, and G.M. Rubin, *Computational identification of Drosophila microRNA genes.* Genome Biol, 2003. **4**(7): p. R42.
27. Lim, L.P., N.C. Lau, E.G. Weinstein, A. Abdelhakim, S. Yekta, M.W. Rhoades, C.B. Burge, and D.P. Bartel, *The microRNAs of Caenorhabditis elegans.* Genes Dev, 2003. **17**(8): p. 991-1008.
28. Bentwich, I., A. Avniel, Y. Karov, R. Aharonov, S. Gilad, O. Barad, A. Barzilai, P. Einat, U. Einav, E. Meiri, E. Sharon, Y. Spector, and Z. Bentwich, *Identification of hundreds of conserved and nonconserved human microRNAs.* Nat Genet, 2005. **37**(7): p. 766-70.

29. Friedlander, M.R., W. Chen, C. Adamidi, J. Maaskola, R. Einspanier, S. Knespel, and N. Rajewsky, *Discovering microRNAs from deep sequencing data using miRDeep.* Nat Biotechnol, 2008. **26**(4): p. 407-15.
30. Lee, Y., K. Jeon, J.T. Lee, S. Kim, and V.N. Kim, *MicroRNA maturation: stepwise processing and subcellular localization.* EMBO J, 2002. **21**(17): p. 4663-70.
31. Baskerville, S. and D.P. Bartel, *Microarray profiling of microRNAs reveals frequent coexpression with neighboring miRNAs and host genes.* RNA, 2005. **11**(3): p. 241-7.
32. Saini, H.K., S. Griffiths-Jones, and A.J. Enright, *Genomic analysis of human microRNA transcripts.* Proc Natl Acad Sci U S A, 2007. **104**(45): p. 17719-24.
33. Mallory, A.C., B.J. Reinhart, M.W. Jones-Rhoades, G. Tang, P.D. Zamore, M.K. Barton, and D.P. Bartel, *MicroRNA control of PHABULOSA in leaf development: importance of pairing to the microRNA 5' region.* EMBO J, 2004. **23**(16): p. 3356-64.
34. Lewis, B.P., I.H. Shih, M.W. Jones-Rhoades, D.P. Bartel, and C.B. Burge, *Prediction of mammalian microRNA targets.* Cell, 2003. **115**(7): p. 787-98.
35. Brennecke, J., A. Stark, R.B. Russell, and S.M. Cohen, *Principles of microRNA-target recognition.* PLoS Biol, 2005. **3**(3): p. e85.
36. Didiano, D. and O. Hobert, *Perfect seed pairing is not a generally reliable predictor for miRNA-target interactions.* Nat Struct Mol Biol, 2006. **13**(9): p. 849-51.
37. Hon, L.S. and Z. Zhang, *The roles of binding site arrangement and combinatorial targeting in microRNA repression of gene expression.* Genome Biol, 2007. **8**(8): p. R166.
38. Grimson, A., K.K. Farh, W.K. Johnston, P. Garrett-Engele, L.P. Lim, and D.P. Bartel, *MicroRNA targeting specificity in mammals: determinants beyond seed pairing.* Mol Cell, 2007. **27**(1): p. 91-105.
39. Grun, D., Y.L. Wang, D. Langenberger, K.C. Gunsalus, and N. Rajewsky, *microRNA target predictions across seven Drosophila species and comparison to mammalian targets.* PLoS Comput Biol, 2005. **1**(1): p. e13.
40. Anderson, P. and N. Kedersha, *RNA granules.* J Cell Biol, 2006. **172**(6): p. 803-8.
41. Knowles, R.B., J.H. Sabry, M.E. Martone, T.J. Deerinck, M.H. Ellisman, G.J. Bassell, and K.S. Kosik, *Translocation of RNA granules in living neurons.* J Neurosci, 1996. **16**(24): p. 7812-20.
42. Kedersha, N. and P. Anderson, *Stress granules: sites of mRNA triage that regulate mRNA stability and translatability.* Biochem Soc Trans, 2002. **30**(Pt 6): p. 963-9.
43. Bashkirov, V.I., H. Scherthan, J.A. Solinger, J.M. Buerstedde, and W.D. Heyer, *A mouse cytoplasmic exoribonuclease (mXRN1p) with preference for G4 tetraplex substrates.* J Cell Biol, 1997. **136**(4): p. 761-73.
44. Kedersha, N., G. Stoecklin, M. Ayodele, P. Yacono, J. Lykke-Andersen, M.J. Fritzler, D. Scheuner, R.J. Kaufman, D.E. Golan, and P. Anderson, *Stress granules and processing bodies are dynamically linked sites of mRNP remodeling.* J Cell Biol, 2005. **169**(6): p. 871-84.

45. Krichevsky, A.M. and K.S. Kosik, *Neuronal RNA granules: a link between RNA localization and stimulation-dependent translation.* Neuron, 2001. **32**(4): p. 683-96.
46. Brengues, M., D. Teixeira, and R. Parker, *Movement of eukaryotic mRNAs between polysomes and cytoplasmic processing bodies.* Science, 2005. **310**(5747): p. 486-9.
47. Zalfa, F., T. Achsel, and C. Bagni, *mRNPs, polysomes or granules: FMRP in neuronal protein synthesis.* Curr Opin Neurobiol, 2006. **16**(3): p. 265-9.
48. Plante, I., L. Davidovic, D.L. Ouellet, L.A. Gobeil, S. Tremblay, E.W. Khandjian, and P. Provost, *Dicer-Derived MicroRNAs Are Utilized by the Fragile X Mental Retardation Protein for Assembly on Target RNAs.* J Biomed Biotechnol, 2006. **2006**(4): p. 64347.
49. Lagos-Quintana, M., R. Rauhut, A. Yalcin, J. Meyer, W. Lendeckel, and T. Tuschl, *Identification of tissue-specific microRNAs from mouse.* Curr Biol, 2002. **12**(9): p. 735-9.
50. Babak, T., W. Zhang, Q. Morris, B.J. Blencowe, and T.R. Hughes, *Probing microRNAs with microarrays: tissue specificity and functional inference.* RNA, 2004. **10**(11): p. 1813-9.
51. Krichevsky, A.M., K.S. King, C.P. Donahue, K. Khrapko, and K.S. Kosik, *A microRNA array reveals extensive regulation of microRNAs during brain development.* Rna, 2003. **9**(10): p. 1274-81.
52. Sempere, L.F., S. Freemantle, I. Pitha-Rowe, E. Moss, E. Dmitrovsky, and V. Ambros, *Expression profiling of mammalian microRNAs uncovers a subset of brain-expressed microRNAs with possible roles in murine and human neuronal differentiation.* Genome Biol, 2004. **5**(3): p. R13.
53. Houbaviy, H.B., M.F. Murray, and P.A. Sharp, *Embryonic stem cell-specific MicroRNAs.* Dev Cell, 2003. **5**(2): p. 351-8.
54. Miska, E.A., E. Alvarez-Saavedra, M. Townsend, A. Yoshii, N. Sestan, P. Rakic, M. Constantine-Paton, and H.R. Horvitz, *Microarray analysis of microRNA expression in the developing mammalian brain.* Genome Biol, 2004. **5**(9): p. R68.
55. Bernstein, E., S.Y. Kim, M.A. Carmell, E.P. Murchison, H. Alcorn, M.Z. Li, A.A. Mills, S.J. Elledge, K.V. Anderson, and G.J. Hannon, *Dicer is essential for mouse development.* Nat Genet, 2003. **35**(3): p. 215-7.
56. Harfe, B.D., M.T. McManus, J.H. Mansfield, E. Hornstein, and C.J. Tabin, *The RNaseIII enzyme Dicer is required for morphogenesis but not patterning of the vertebrate limb.* Proc Natl Acad Sci U S A, 2005. **102**(31): p. 10898-903.
57. Giraldez, A.J., R.M. Cinalli, M.E. Glasner, A.J. Enright, J.M. Thomson, S. Baskerville, S.M. Hammond, D.P. Bartel, and A.F. Schier, *MicroRNAs regulate brain morphogenesis in zebrafish.* Science, 2005. **308**(5723): p. 833-8.
58. Krichevsky, A.M., K.C. Sonntag, O. Isacson, and K.S. Kosik, *Specific microRNAs modulate embryonic stem cell-derived neurogenesis.* Stem Cells, 2006. **24**(4): p. 857-64.
59. Smirnova, L., A. Grafe, A. Seiler, S. Schumacher, R. Nitsch, and F.G. Wulczyn, *Regulation of miRNA expression during neural cell specification.* Eur J Neurosci, 2005. **21**(6): p. 1469-77.

60. Wu, K.Y., U. Hengst, L.J. Cox, E.Z. Macosko, A. Jeromin, E.R. Urquhart, and S.R. Jaffrey, *Local translation of RhoA regulates growth cone collapse.* Nature, 2005. **436**(7053): p. 1020-4.
61. Hengst, U., L.J. Cox, E.Z. Macosko, and S.R. Jaffrey, *Functional and selective RNA interference in developing axons and growth cones.* J Neurosci, 2006. **26**(21): p. 5727-32.
62. Kong, W., H. Yang, L. He, J.J. Zhao, D. Coppola, W.S. Dalton, and J.Q. Cheng, *MicroRNA-155 is regulated by the transforming growth factor beta/Smad pathway and contributes to epithelial cell plasticity by targeting RhoA.* Mol Cell Biol, 2008. **28**(22): p. 6773-84.
63. Leaman, D., P.Y. Chen, J. Fak, A. Yalcin, M. Pearce, U. Unnerstall, D.S. Marks, C. Sander, T. Tuschl, and U. Gaul, *Antisense-mediated depletion reveals essential and specific functions of microRNAs in Drosophila development.* Cell, 2005. **121**(7): p. 1097-108.
64. Frey, U. and R.G. Morris, *Synaptic tagging and long-term potentiation.* Nature, 1997. **385**(6616): p. 533-6.
65. Nguyen, P.V. and E.R. Kandel, *Brief theta-burst stimulation induces a transcription-dependent late phase of LTP requiring cAMP in area CA1 of the mouse hippocampus.* Learn Mem, 1997. **4**(2): p. 230-43.
66. Ashraf, S.I. and S. Kunes, *A trace of silence: memory and microRNA at the synapse.* Curr Opin Neurobiol, 2006. **16**(5): p. 535-9.
67. Park, C.S. and S.J. Tang, *Regulation of microRNA Expression by Induction of Bidirectional Synaptic Plasticity.* J Mol Neurosci, 2009. **38**(1): p. 50-6.
68. Kim, J., K. Inoue, J. Ishii, W.B. Vanti, S.V. Voronov, E. Murchison, G. Hannon, and A. Abeliovich, *A MicroRNA feedback circuit in midbrain dopamine neurons.* Science, 2007. **317**(5842): p. 1220-4.
69. Wang, W.X., B.W. Rajeev, A.J. Stromberg, N. Ren, G. Tang, Q. Huang, I. Rigoutsos, and P.T. Nelson, *The expression of microRNA miR-107 decreases early in Alzheimer's disease and may accelerate disease progression through regulation of beta-site amyloid precursor protein-cleaving enzyme 1.* J Neurosci, 2008. **28**(5): p. 1213-23.
70. Beveridge, N.J., P.A. Tooney, A.P. Carroll, E. Gardiner, N. Bowden, R.J. Scott, N. Tran, I. Dedova, and M.J. Cairns, *Dysregulation of miRNA 181b in the temporal cortex in schizophrenia.* Hum Mol Genet, 2008. **17**(8): p. 1156-68.
71. Perkins, D.O., C.D. Jeffries, L.F. Jarskog, J.M. Thomson, K. Woods, M.A. Newman, J.S. Parker, J. Jin, and S.M. Hammond, *microRNA expression in the prefrontal cortex of individuals with schizophrenia and schizoaffective disorder.* Genome Biol, 2007. **8**(2): p. R27.
72. Jablensky, A., *The 100-year epidemiology of schizophrenia.* Schizophr Res, 1997. **28**(2-3): p. 111-25.
73. Mueser, K.T. and S.R. McGurk, *Schizophrenia.* Lancet, 2004. **363**(9426): p. 2063-72.
74. Castle, D., S. Wessely, G. Der, and R.M. Murray, *The incidence of operationally defined schizophrenia in Camberwell, 1965-84.* Br J Psychiatry, 1991. **159**: p. 790-4.

75. Cardno, A.G. and Gottesman, II, *Twin studies of schizophrenia: from bow-and-arrow concordances to star wars Mx and functional genomics.* Am J Med Genet, 2000. **97**(1): p. 12-7.
76. McGuffin, P., *Nature and nurture interplay: schizophrenia.* Psychiatr Prax, 2004. **31 Suppl 2**: p. S189-93.
77. Toulopoulou, T., A. Grech, R.G. Morris, K. Schulze, C. McDonald, B. Chapple, S. Rabe-Hesketh, and R.M. Murray, *The relationship between volumetric brain changes and cognitive function: a family study on schizophrenia.* Biol Psychiatry, 2004. **56**(6): p. 447-53.
78. Mallard, E.C., A. Rehn, S. Rees, M. Tolcos, and D. Copolov, *Ventriculomegaly and reduced hippocampal volume following intrauterine growth-restriction: implications for the aetiology of schizophrenia.* Schizophr Res, 1999. **40**(1): p. 11-21.
79. Javitt, D.C. and S.R. Zukin, *Recent advances in the phencyclidine model of schizophrenia.* Am J Psychiatry, 1991. **148**(10): p. 1301-8.
80. Kegeles, L.S., D. Martinez, L.D. Kochan, D.R. Hwang, Y. Huang, O. Mawlawi, R.F. Suckow, R.L. Van Heertum, and M. Laruelle, *NMDA antagonist effects on striatal dopamine release: positron emission tomography studies in humans.* Synapse, 2002. **43**(1): p. 19-29.
81. Blouin, J.L., B.A. Dombroski, S.K. Nath, V.K. Lasseter, P.S. Wolyniec, G. Nestadt, M. Thornquist, G. Ullrich, J. McGrath, L. Kasch, M. Lamacz, M.G. Thomas, C. Gehrig, U. Radhakrishna, S.E. Snyder, K.G. Balk, K. Neufeld, K.L. Swartz, N. DeMarchi, G.N. Papadimitriou, D.G. Dikeos, C.N. Stefanis, A. Chakravarti, B. Childs, D.E. Housman, H.H. Kazazian, S. Antonarakis, and A.E. Pulver, *Schizophrenia susceptibility loci on chromosomes 13q32 and 8p21.* Nat Genet, 1998. **20**(1): p. 70-3.
82. Brzustowicz, L.M., K.A. Hodgkinson, E.W. Chow, W.G. Honer, and A.S. Bassett, *Location of a major susceptibility locus for familial schizophrenia on chromosome 1q21-q22.* Science, 2000. **288**(5466): p. 678-82.
83. Coon, H., S. Jensen, J. Holik, M. Hoff, M. Myles-Worsley, F. Reimherr, P. Wender, M. Waldo, R. Freedman, M. Leppert, and et al., *Genomic scan for genes predisposing to schizophrenia.* Am J Med Genet, 1994. **54**(1): p. 59-71.
84. Coon, H., M. Myles-Worsley, J. Tiobech, M. Hoff, J. Rosenthal, P. Bennett, F. Reimherr, P. Wender, P. Dale, A. Polloi, and W. Byerley, *Evidence for a chromosome 2p13-14 schizophrenia susceptibility locus in families from Palau, Micronesia.* Mol Psychiatry, 1998. **3**(6): p. 521-7.
85. DeLisi, L.E., A. Mesen, C. Rodriguez, A. Bertheau, B. LaPrade, M. Llach, S. Riondet, K. Razi, M. Relja, W. Byerley, and R. Sherrington, *Genome-wide scan for linkage to schizophrenia in a Spanish-origin cohort from Costa Rica.* Am J Med Genet, 2002. **114**(5): p. 497-508.
86. DeLisi, L.E., S.H. Shaw, T.J. Crow, G. Shields, A.B. Smith, V.W. Larach, N. Wellman, J. Loftus, B. Nanthakumar, K. Razi, J. Stewart, M. Comazzi, A. Vita, T. Heffner, and R. Sherrington, *A genome-wide scan for linkage to chromosomal regions in 382 sibling pairs with schizophrenia or schizoaffective disorder.* Am J Psychiatry, 2002. **159**(5): p. 803-12.

87. Garver, D.L., J. Holcomb, F.M. Mapua, R. Wilson, and B. Barnes, *Schizophrenia spectrum disorders: an autosomal-wide scan in multiplex pedigrees.* Schizophr Res, 2001. **52**(3): p. 145-60.
88. Gurling, H.M., G. Kalsi, J. Brynjolfson, T. Sigmundsson, R. Sherrington, B.S. Mankoo, T. Read, P. Murphy, E. Blaveri, A. McQuillin, H. Petursson, and D. Curtis, *Genomewide genetic linkage analysis confirms the presence of susceptibility loci for schizophrenia, on chromosomes 1q32.2, 5q33.2, and 8p21-22 and provides support for linkage to schizophrenia, on chromosomes 11q23.3-24 and 20q12.1-11.23.* Am J Hum Genet, 2001. **68**(3): p. 661-73.
89. Levinson, D.F., M.D. Levinson, R. Segurado, and C.M. Lewis, *Genome scan meta-analysis of schizophrenia and bipolar disorder, part I: Methods and power analysis.* Am J Hum Genet, 2003. **73**(1): p. 17-33.
90. Lindholm, E., B. Ekholm, S. Shaw, P. Jalonen, G. Johansson, U. Pettersson, R. Sherrington, R. Adolfsson, and E. Jazin, *A schizophrenia-susceptibility locus at 6q25, in one of the world's largest reported pedigrees.* Am J Hum Genet, 2001. **69**(1): p. 96-105.
91. Paunio, T., J. Ekelund, T. Varilo, A. Parker, I. Hovatta, J.A. Turunen, K. Rinard, A. Foti, J.D. Terwilliger, H. Juvonen, J. Suvisaari, R. Arajarvi, J. Suokas, T. Partonen, J. Lonnqvist, J. Meyer, and L. Peltonen, *Genome-wide scan in a nationwide study sample of schizophrenia families in Finland reveals susceptibility loci on chromosomes 2q and 5q.* Hum Mol Genet, 2001. **10**(26): p. 3037-48.
92. Schwab, S.G., J. Hallmayer, M. Albus, B. Lerer, G.N. Eckstein, M. Borrmann, R.H. Segman, C. Hanses, J. Freymann, A. Yakir, M. Trixler, P. Falkai, M. Rietschel, W. Maier, and D.B. Wildenauer, *A genome-wide autosomal screen for schizophrenia susceptibility loci in 71 families with affected siblings: support for loci on chromosome 10p and 6.* Mol Psychiatry, 2000. **5**(6): p. 638-49.
93. Straub, R.E., C.J. MacLean, Y. Ma, B.T. Webb, M.V. Myakishev, C. Harris-Kerr, B. Wormley, H. Sadek, B. Kadambi, F.A. O'Neill, D. Walsh, and K.S. Kendler, *Genome-wide scans of three independent sets of 90 Irish multiplex schizophrenia families and follow-up of selected regions in all families provides evidence for multiple susceptibility genes.* Mol Psychiatry, 2002. **7**(6): p. 542-59.
94. Ng, M.Y., D.F. Levinson, S.V. Faraone, B.K. Suarez, L.E. DeLisi, T. Arinami, B. Riley, T. Paunio, A.E. Pulver, Irmansyah, P.A. Holmans, M. Escamilla, D.B. Wildenauer, N.M. Williams, C. Laurent, B.J. Mowry, L.M. Brzustowicz, M. Maziade, P. Sklar, D.L. Garver, G.R. Abecasis, B. Lerer, M.D. Fallin, H.M. Gurling, P.V. Gejman, E. Lindholm, H.W. Moises, W. Byerley, E.M. Wijsman, P. Forabosco, M.T. Tsuang, H.G. Hwu, Y. Okazaki, K.S. Kendler, B. Wormley, A. Fanous, D. Walsh, F.A. O'Neill, L. Peltonen, G. Nestadt, V.K. Lasseter, K.Y. Liang, G.M. Papadimitriou, D.G. Dikeos, S.G. Schwab, M.J. Owen, M.C. O'Donovan, N. Norton, E. Hare, H. Raventos, H. Nicolini, M. Albus, W. Maier, V.L. Nimgaonkar, L. Terenius, J. Mallet, M. Jay, S. Godard, D. Nertney, M. Alexander, R.R. Crowe, J.M. Silverman, A.S. Bassett, M.A. Roy, C. Merette, C.N. Pato, M.T. Pato, J.L. Roos, Y. Kohn, D. Amann-Zalcenstein, G. Kalsi, A. McQuillin, D. Curtis, J. Brynjolfson, T. Sigmundsson, H. Petursson, A.R. Sanders, J. Duan, E. Jazin, M. Myles-Worsley, M. Karayiorgou, and C.M. Lewis,

Meta-analysis of 32 genome-wide linkage studies of schizophrenia. Mol Psychiatry, 2009. **14**(8): p. 774-85.
95. Hornstein, E. and N. Shomron, *Canalization of development by microRNAs.* Nat Genet, 2006. **38 Suppl**: p. S20-4.
96. Glinsky, G.V., *Phenotype-defining functions of multiple non-coding RNA pathways.* Cell Cycle, 2008. **7**(11): p. 1630-9.
97. Glinsky, G.V., *An SNP-guided microRNA map of fifteen common human disorders identifies a consensus disease phenocode aiming at principal components of the nuclear import pathway.* Cell Cycle, 2008. **7**(16): p. 2570-83.
98. Martinez, N.J. and A.J. Walhout, *The interplay between transcription factors and microRNAs in genome-scale regulatory networks.* Bioessays, 2009.
99. Makeyev, E.V., J. Zhang, M.A. Carrasco, and T. Maniatis, *The MicroRNA miR-124 promotes neuronal differentiation by triggering brain-specific alternative pre-mRNA splicing.* Mol Cell, 2007. **27**(3): p. 435-48.
100. Schratt, G.M., F. Tuebing, E.A. Nigh, C.G. Kane, M.E. Sabatini, M. Kiebler, and M.E. Greenberg, *A brain-specific microRNA regulates dendritic spine development.* Nature, 2006. **439**(7074): p. 283-9.
101. Davis, T.H., T.L. Cuellar, S.M. Koch, A.J. Barker, B.D. Harfe, M.T. McManus, and E.M. Ullian, *Conditional loss of Dicer disrupts cellular and tissue morphogenesis in the cortex and hippocampus.* J Neurosci, 2008. **28**(17): p. 4322-30.
102. De Pietri Tonelli, D., J.N. Pulvers, C. Haffner, E.P. Murchison, G.J. Hannon, and W.B. Huttner, *miRNAs are essential for survival and differentiation of newborn neurons but not for expansion of neural progenitors during early neurogenesis in the mouse embryonic neocortex.* Development, 2008. **135**(23): p. 3911-21.
103. Hansen, T., L. Olsen, M. Lindow, K.D. Jakobsen, H. Ullum, E. Jonsson, O.A. Andreassen, S. Djurovic, I. Melle, I. Agartz, H. Hall, S. Timm, A.G. Wang, and T. Werge, *Brain expressed microRNAs implicated in schizophrenia etiology.* PLoS ONE, 2007. **2**(9): p. e873.
104. Kocerha, J., M.A. Faghihi, M.A. Lopez-Toledano, J. Huang, A.J. Ramsey, M.G. Caron, N. Sales, D. Willoughby, J. Elmen, H.F. Hansen, H. Orum, S. Kauppinen, P.J. Kenny, and C. Wahlestedt, *MicroRNA-219 modulates NMDA receptor-mediated neurobehavioral dysfunction.* Proc Natl Acad Sci U S A, 2009. **106**(9): p. 3507-12.
105. Beveridge, N.J., P.A. Tooney, A.P. Carroll, E. Gardiner, N. Bowden, R.J. Scott, N. Tran, I. Dedova, and M.J. Cairns, *Dysregulation of miRNA 181b in the temporal cortex in schizophrenia.* Hum Mol Genet, 2008.
106. Hebert, S.S. and B. De Strooper, *Alterations of the microRNA network cause neurodegenerative disease.* Trends Neurosci, 2009.
107. Lukiw, W.J., *Micro-RNA speciation in fetal, adult and Alzheimer's disease hippocampus.* Neuroreport, 2007. **18**(3): p. 297-300.
108. Schaefer, A., D. O'Carroll, C.L. Tan, D. Hillman, M. Sugimori, R. Llinas, and P. Greengard, *Cerebellar neurodegeneration in the absence of microRNAs.* J Exp Med, 2007. **204**(7): p. 1553-8.

109. Livak, K.J. and T.D. Schmittgen, *Analysis of relative gene expression data using real-time quantitative PCR and the 2(-Delta Delta C(T)) Method.* Methods, 2001. **25**(4): p. 402-8.
110. Berezikov, E., F. Thuemmler, L.W. van Laake, I. Kondova, R. Bontrop, E. Cuppen, and R.H. Plasterk, *Diversity of microRNAs in human and chimpanzee brain.* Nat Genet, 2006. **38**(12): p. 1375-7.
111. Galau, G.A., W.H. Klein, M.M. Davis, B.J. Wold, R.J. Britten, and E.H. Davidson, *Structural gene sets active in embryos and adult tissues of the sea urchin.* Cell, 1976. **7**(4): p. 487-505.
112. Ramalho-Santos, M., S. Yoon, Y. Matsuzaki, R.C. Mulligan, and D.A. Melton, *"Stemness": transcriptional profiling of embryonic and adult stem cells.* Science, 2002. **298**(5593): p. 597-600.
113. Strauss, W.M., C. Chen, C.T. Lee, and D. Ridzon, *Nonrestrictive developmental regulation of microRNA gene expression.* Mamm Genome, 2006. **17**(8): p. 833-40.
114. Wang, Y., R. Medvid, C. Melton, R. Jaenisch, and R. Blelloch, *DGCR8 is essential for microRNA biogenesis and silencing of embryonic stem cell self-renewal.* Nat Genet, 2007. **39**(3): p. 380-5.
115. Peter, M.E., *Let-7 and miR-200 microRNAs: guardians against pluripotency and cancer progression.* Cell Cycle, 2009. **8**(6): p. 843-52.
116. Roush, S. and F.J. Slack, *The let-7 family of microRNAs.* Trends Cell Biol, 2008. **18**(10): p. 505-16.
117. Johnson, C.D., A. Esquela-Kerscher, G. Stefani, M. Byrom, K. Kelnar, D. Ovcharenko, M. Wilson, X. Wang, J. Shelton, J. Shingara, L. Chin, D. Brown, and F.J. Slack, *The let-7 microRNA represses cell proliferation pathways in human cells.* Cancer Res, 2007. **67**(16): p. 7713-22.
118. Landgraf, P., M. Rusu, R. Sheridan, A. Sewer, N. Iovino, A. Aravin, S. Pfeffer, A. Rice, A.O. Kamphorst, M. Landthaler, C. Lin, N.D. Socci, L. Hermida, V. Fulci, S. Chiaretti, R. Foa, J. Schliwka, U. Fuchs, A. Novosel, R.U. Muller, B. Schermer, U. Bissels, J. Inman, Q. Phan, M. Chien, D.B. Weir, R. Choksi, G. De Vita, D. Frezzetti, H.I. Trompeter, V. Hornung, G. Teng, G. Hartmann, M. Palkovits, R. Di Lauro, P. Wernet, G. Macino, C.E. Rogler, J.W. Nagle, J. Ju, F.N. Papavasiliou, T. Benzing, P. Lichter, W. Tam, M.J. Brownstein, A. Bosio, A. Borkhardt, J.J. Russo, C. Sander, M. Zavolan, and T. Tuschl, *A mammalian microRNA expression atlas based on small RNA library sequencing.* Cell, 2007. **129**(7): p. 1401-14.
119. Balu, D.T. and I. Lucki, *Adult hippocampal neurogenesis: regulation, functional implications, and contribution to disease pathology.* Neurosci Biobehav Rev, 2009. **33**(3): p. 232-52.
120. Fiore, R. and G. Schratt, *MicroRNAs in vertebrate synapse development.* ScientificWorldJournal, 2007. **7**: p. 167-77.
121. Carninci, P., T. Kasukawa, S. Katayama, J. Gough, M.C. Frith, N. Maeda, R. Oyama, T. Ravasi, B. Lenhard, C. Wells, R. Kodzius, K. Shimokawa, V.B. Bajic, S.E. Brenner, S. Batalov, A.R. Forrest, M. Zavolan, M.J. Davis, L.G. Wilming, V. Aidinis, J.E. Allen, A. Ambesi-Impiombato, R. Apweiler, R.N. Aturaliya, T.L. Bailey, M. Bansal, L. Baxter, K.W. Beisel, T. Bersano, H. Bono, A.M. Chalk,

K.P. Chiu, V. Choudhary, A. Christoffels, D.R. Clutterbuck, M.L. Crowe, E. Dalla, B.P. Dalrymple, B. de Bono, G. Della Gatta, D. di Bernardo, T. Down, P. Engstrom, M. Fagiolini, G. Faulkner, C.F. Fletcher, T. Fukushima, M. Furuno, S. Futaki, M. Gariboldi, P. Georgii-Hemming, T.R. Gingeras, T. Gojobori, R.E. Green, S. Gustincich, M. Harbers, Y. Hayashi, T.K. Hensch, N. Hirokawa, D. Hill, L. Huminiecki, M. Iacono, K. Ikeo, A. Iwama, T. Ishikawa, M. Jakt, A. Kanapin, M. Katoh, Y. Kawasawa, J. Kelso, H. Kitamura, H. Kitano, G. Kollias, S.P. Krishnan, A. Kruger, S.K. Kummerfeld, I.V. Kurochkin, L.F. Lareau, D. Lazarevic, L. Lipovich, J. Liu, S. Liuni, S. McWilliam, M. Madan Babu, M. Madera, L. Marchionni, H. Matsuda, S. Matsuzawa, H. Miki, F. Mignone, S. Miyake, K. Morris, S. Mottagui-Tabar, N. Mulder, N. Nakano, H. Nakauchi, P. Ng, R. Nilsson, S. Nishiguchi, S. Nishikawa, F. Nori, O. Ohara, Y. Okazaki, V. Orlando, K.C. Pang, W.J. Pavan, G. Pavesi, G. Pesole, N. Petrovsky, S. Piazza, J. Reed, J.F. Reid, B.Z. Ring, M. Ringwald, B. Rost, Y. Ruan, S.L. Salzberg, A. Sandelin, C. Schneider, C. Schonbach, K. Sekiguchi, C.A. Semple, S. Seno, L. Sessa, Y. Sheng, Y. Shibata, H. Shimada, K. Shimada, D. Silva, B. Sinclair, S. Sperling, E. Stupka, K. Sugiura, R. Sultana, Y. Takenaka, K. Taki, K. Tammoja, S.L. Tan, S. Tang, M.S. Taylor, J. Tegner, S.A. Teichmann, H.R. Ueda, E. van Nimwegen, R. Verardo, C.L. Wei, K. Yagi, H. Yamanishi, E. Zabarovsky, S. Zhu, A. Zimmer, W. Hide, C. Bult, S.M. Grimmond, R.D. Teasdale, E.T. Liu, V. Brusic, J. Quackenbush, C. Wahlestedt, J.S. Mattick, D.A. Hume, C. Kai, D. Sasaki, Y. Tomaru, S. Fukuda, M. Kanamori-Katayama, M. Suzuki, J. Aoki, T. Arakawa, J. Iida, K. Imamura, M. Itoh, T. Kato, H. Kawaji, N. Kawagashira, T. Kawashima, M. Kojima, S. Kondo, H. Konno, K. Nakano, N. Ninomiya, T. Nishio, M. Okada, C. Plessy, K. Shibata, T. Shiraki, S. Suzuki, M. Tagami, K. Waki, A. Watahiki, Y. Okamura-Oho, H. Suzuki, J. Kawai and Y. Hayashizaki, *The transcriptional landscape of the mammalian genome.* Science, 2005. **309**(5740): p. 1559-63.

122. Amaral, P.P. and J.S. Mattick, *Noncoding RNA in development.* Mamm Genome, 2008. **19**(7-8): p. 454-92.

123. Giacomini, K.M., C.M. Brett, R.B. Altman, N.L. Benowitz, M.E. Dolan, D.A. Flockhart, J.A. Johnson, D.F. Hayes, T. Klein, R.M. Krauss, D.L. Kroetz, H.L. McLeod, A.T. Nguyen, M.J. Ratain, M.V. Relling, V. Reus, D.M. Roden, C.A. Schaefer, A.R. Shuldiner, T. Skaar, K. Tantisira, R.F. Tyndale, L. Wang, R.M. Weinshilboum, S.T. Weiss, and I. Zineh, *The pharmacogenetics research network: from SNP discovery to clinical drug response.* Clin Pharmacol Ther, 2007. **81**(3): p. 328-45.

124. Thomas, F.J., H.L. McLeod, and J.W. Watters, *Pharmacogenomics: the influence of genomic variation on drug response.* Curr Top Med Chem, 2004. **4**(13): p. 1399-409.

125. Gunderson, K.L., F.J. Steemers, H. Ren, P. Ng, L. Zhou, C. Tsan, W. Chang, D. Bullis, J. Musmacker, C. King, L.L. Lebruska, D. Barker, A. Oliphant, K.M. Kuhn, and R. Shen, *Whole-genome genotyping.* Methods Enzymol, 2006. **410**: p. 359-76.

126. Kennedy, G.C., H. Matsuzaki, S. Dong, W.M. Liu, J. Huang, G. Liu, X. Su, M. Cao, W. Chen, J. Zhang, W. Liu, G. Yang, X. Di, T. Ryder, Z. He, U. Surti, M.S.

Phillips, M.T. Boyce-Jacino, S.P. Fodor, and K.W. Jones, *Large-scale genotyping of complex DNA.* Nat Biotechnol, 2003. **21**(10): p. 1233-7.

127. Alderborn, A., A. Kristofferson, and U. Hammerling, *Determination of single-nucleotide polymorphisms by real-time pyrophosphate DNA sequencing.* Genome Res, 2000. **10**(8): p. 1249-58.
128. Lyamichev, V., A.L. Mast, J.G. Hall, J.R. Prudent, M.W. Kaiser, T. Takova, R.W. Kwiatkowski, T.J. Sander, M. de Arruda, D.A. Arco, B.P. Neri, and M.A. Brow, *Polymorphism identification and quantitative detection of genomic DNA by invasive cleavage of oligonucleotide probes.* Nat Biotechnol, 1999. **17**(3): p. 292-6.
129. Livak, K.J., *Allelic discrimination using fluorogenic probes and the 5' nuclease assay.* Genet Anal, 1999. **14**(5-6): p. 143-9.
130. Tobler, A.R., S. Short, M.R. Andersen, T.M. Paner, J.C. Briggs, S.M. Lambert, P.P. Wu, Y. Wang, A.Y. Spoonde, R.T. Koehler, N. Peyret, C. Chen, A.J. Broomer, D.A. Ridzon, H. Zhou, B.S. Hoo, K.C. Hayashibara, L.N. Leong, C.N. Ma, B.B. Rosenblum, J.P. Day, J.S. Ziegle, F.M. De La Vega, M.D. Rhodes, K.M. Hennessy, and H.M. Wenz, *The SNPlex genotyping system: a flexible and scalable platform for SNP genotyping.* J Biomol Tech, 2005. **16**(4): p. 398-406.
131. Lu, J., G. Getz, E.A. Miska, E. Alvarez-Saavedra, J. Lamb, D. Peck, A. Sweet-Cordero, B.L. Ebert, R.H. Mak, A.A. Ferrando, J.R. Downing, T. Jacks, H.R. Horvitz, and T.R. Golub, *MicroRNA expression profiles classify human cancers.* Nature, 2005. **435**(7043): p. 834-8.
132. Dunbar, S.A., C.A. Vander Zee, K.G. Oliver, K.L. Karem, and J.W. Jacobson, *Quantitative, multiplexed detection of bacterial pathogens: DNA and protein applications of the Luminex LabMAP system.* J Microbiol Methods, 2003. **53**(2): p. 245-52.
133. Flagella, M., S. Bui, Z. Zheng, C.T. Nguyen, A. Zhang, L. Pastor, Y. Ma, W. Yang, K.L. Crawford, G.K. McMaster, F. Witney, and Y. Luo, *A multiplex branched DNA assay for parallel quantitative gene expression profiling.* Anal Biochem, 2006. **352**(1): p. 50-60.
134. Zhang, A., L. Pastor, Q. Nguyen, Y. Luo, W. Yang, M. Flagella, R. Chavli, S. Bui, C.T. Nguyen, Z. Zheng, W. He, G. McMaster, and F. Witney, *Small interfering RNA and gene expression analysis using a multiplex branched DNA assay without RNA purification.* J Biomol Screen, 2005. **10**(6): p. 549-56.
135. Landegren, U., R. Kaiser, J. Sanders, and L. Hood, *A ligase-mediated gene detection technique.* Science, 1988. **241**(4869): p. 1077-80.
136. Iannone, M.A., J.D. Taylor, J. Chen, M.S. Li, P. Rivers, K.A. Slentz-Kesler, and M.P. Weiner, *Multiplexed single nucleotide polymorphism genotyping by oligonucleotide ligation and flow cytometry.* Cytometry, 2000. **39**(2): p. 131-40.
137. McNamara, D.T., L.J. Kasehagen, B.T. Grimberg, J. Cole-Tobian, W.E. Collins, and P.A. Zimmerman, *Diagnosing infection levels of four human malaria parasite species by a polymerase chain reaction/ligase detection reaction fluorescent microsphere-based assay.* Am J Trop Med Hyg, 2006. **74**(3): p. 413-21.
138. Mehlotra, R.K., M.N. Ziats, M.J. Bockarie, and P.A. Zimmerman, *Prevalence of CYP2B6 alleles in malaria-endemic populations of West Africa and Papua New Guinea.* Eur J Clin Pharmacol, 2006. **62**(4): p. 267-75.

139. Macdonald, S.J., T. Pastinen, A. Genissel, T.W. Cornforth, and A.D. Long, *A low-cost open-source SNP genotyping platform for association mapping applications.* Genome Biol, 2005. **6**(12): p. R105.
140. Dunbar, S.A., *Applications of Luminex xMAP technology for rapid, high-throughput multiplexed nucleic acid detection.* Clin Chim Acta, 2006. **363**(1-2): p. 71-82.
141. Bortolin, S., M. Black, H. Modi, I. Boszko, D. Kobler, D. Fieldhouse, E. Lopes, J.M. Lacroix, R. Grimwood, P. Wells, R. Janeczko, and R. Zastawny, *Analytical validation of the tag-it high-throughput microsphere-based universal array genotyping platform: application to the multiplex detection of a panel of thrombophilia-associated single-nucleotide polymorphisms.* Clin Chem, 2004. **50**(11): p. 2028-36.
142. Pickering, J.W., G.A. McMillin, F. Gedge, H.R. Hill, and E. Lyon, *Flow cytometric assay for genotyping cytochrome p450 2C9 and 2C19: comparison with a microelectronic DNA array.* Am J Pharmacogenomics, 2004. **4**(3): p. 199-207.
143. Taylor, J.D., D. Briley, Q. Nguyen, K. Long, M.A. Iannone, M.S. Li, F. Ye, A. Afshari, E. Lai, M. Wagner, J. Chen, and M.P. Weiner, *Flow cytometric platform for high-throughput single nucleotide polymorphism analysis.* Biotechniques, 2001. **30**(3): p. 661-6, 668-9.
144. Ye, F., M.S. Li, J.D. Taylor, Q. Nguyen, H.M. Colton, W.M. Casey, M. Wagner, M.P. Weiner, and J. Chen, *Fluorescent microsphere-based readout technology for multiplexed human single nucleotide polymorphism analysis and bacterial identification.* Hum Mutat, 2001. **17**(4): p. 305-16.
145. Wang, H.Y., M. Luo, I.V. Tereshchenko, D.M. Frikker, X. Cui, J.Y. Li, G. Hu, Y. Chu, M.A. Azaro, Y. Lin, L. Shen, Q. Yang, M.E. Kambouris, R. Gao, W. Shih, and H. Li, *A genotyping system capable of simultaneously analyzing >1000 single nucleotide polymorphisms in a haploid genome.* Genome Res, 2005. **15**(2): p. 276-83.
146. Brzustowicz, L.M., J. Simone, P. Mohseni, J.E. Hayter, K.A. Hodgkinson, E.W. Chow, and A.S. Bassett, *Linkage disequilibrium mapping of schizophrenia susceptibility to the CAPON region of chromosome 1q22.* Am J Hum Genet, 2004. **74**(5): p. 1057-63. Epub 2004 Apr 2.
147. Saviouk, V., M.P. Moreau, I.V. Tereshchenko, and L.M. Brzustowicz, *Association of synapsin 2 with schizophrenia in families of Northern European ancestry.* Schizophrenia Research, 2007. **96**(1-3): p. 100-111.
148. Ahmadian, A., B. Gharizadeh, A.C. Gustafsson, F. Sterky, P. Nyren, M. Uhlen, and J. Lundeberg, *Single-nucleotide polymorphism analysis by pyrosequencing.* Anal Biochem, 2000. **280**(1): p. 103-10.
149. Ronaghi, M., M. Uhlen, and P. Nyren, *A sequencing method based on real-time pyrophosphate.* Science, 1998. **281**(5375): p. 363, 365.
150. Eisen, M.B., P.T. Spellman, P.O. Brown, and D. Botstein, *Cluster analysis and display of genome-wide expression patterns.* Proc Natl Acad Sci U S A, 1998. **95**(25): p. 14863-8.
151. Lovmar, L., A. Ahlford, M. Jonsson, and A.C. Syvanen, *Silhouette scores for assessment of SNP genotype clusters.* BMC Genomics, 2005. **6**(1): p. 35.

152. Huentelman, M.J., D.W. Craig, A.D. Shieh, J.J. Corneveaux, D. Hu-Lince, J.V. Pearson, and D.A. Stephan, *SNiPer: improved SNP genotype calling for Affymetrix 10K GeneChip microarray data.* BMC Genomics, 2005. **6**: p. 149.
153. Arthur, D. and S. Vassilvitskii, *k-means++ The Advantages of Careful Seeding.* 2007 Symposium on Discrete Algorithms 2007.
154. Jacobson, J.W., K.G. Oliver, C. Weiss, and J. Kettman, *Analysis of individual data from bead-based assays ("bead arrays").* Cytometry A, 2006. **69**(5): p. 384-90.
155. Jablensky, A., N. Sartorius, G. Ernberg, M. Anker, A. Korten, J.E. Cooper, R. Day, and A. Bertelsen, *Schizophrenia: manifestations, incidence and course in different cultures. A World Health Organization ten-country study.* Psychol Med Monogr Suppl, 1992. **20**: p. 1-97.
156. Cardno, A.G. and Gottesman, II, *Twin studies of schizophrenia: from bow-and-arrow concordances to star wars Mx and functional genomics.* Am J Med Genet, 2000. **97**(1): p. 12-7.
157. Lewis, C.M., D.F. Levinson, L.H. Wise, L.E. DeLisi, R.E. Straub, I. Hovatta, N.M. Williams, S.G. Schwab, A.E. Pulver, S.V. Faraone, L.M. Brzustowicz, C.A. Kaufmann, D.L. Garver, H.M. Gurling, E. Lindholm, H. Coon, H.W. Moises, W. Byerley, S.H. Shaw, A. Mesen, R. Sherrington, F.A. O'Neill, D. Walsh, K.S. Kendler, J. Ekelund, T. Paunio, J. Lonnqvist, L. Peltonen, M.C. O'Donovan, M.J. Owen, D.B. Wildenauer, W. Maier, G. Nestadt, J.L. Blouin, S.E. Antonarakis, B.J. Mowry, J.M. Silverman, R.R. Crowe, C.R. Cloninger, M.T. Tsuang, D. Malaspina, J.M. Harkavy-Friedman, D.M. Svrakic, A.S. Bassett, J. Holcomb, G. Kalsi, A. McQuillin, J. Brynjolfson, T. Sigmundsson, H. Petursson, E. Jazin, T. Zoega, and T. Helgason, *Genome scan meta-analysis of schizophrenia and bipolar disorder, part II: Schizophrenia.* Am J Hum Genet, 2003. **73**(1): p. 34-48.
158. Lewis, C.M., D.F. Levinson, L.H. Wise, L.E. DeLisi, R.E. Straub, I. Hovatta, N.M. Williams, S.G. Schwab, A.E. Pulver, S.V. Faraone, L.M. Brzustowicz, C.A. Kaufmann, D.L. Garver, H.M. Gurling, E. Lindholm, H. Coon, H.W. Moises, W. Byerley, S.H. Shaw, A. Mesen, R. Sherrington, F.A. O'Neill, D. Walsh, K.S. Kendler, J. Ekelund, T. Paunio, J. Lonnqvist, L. Peltonen, M.C. O'Donovan, M.J. Owen, D.B. Wildenauer, W. Maier, G. Nestadt, J.L. Blouin, S.E. Antonarakis, B.J. Mowry, J.M. Silverman, R.R. Crowe, C.R. Cloninger, M.T. Tsuang, D. Malaspina, J.M. Harkavy-Friedman, D.M. Svrakic, A.S. Bassett, J. Holcomb, G. Kalsi, A. McQuillin, J. Brynjolfson, T. Sigmundsson, H. Petursson, E. Jazin, T. Zoega, and T. Helgason, *Genome scan meta-analysis of schizophrenia and bipolar disorder, part II: Schizophrenia.* Am J Hum Genet, 2003. **73**(1): p. 34-48.
159. Ross, C.A., R.L. Margolis, S.A. Reading, M. Pletnikov, and J.T. Coyle, *Neurobiology of schizophrenia.* Neuron, 2006. **52**(1): p. 139-53.
160. Gogos, J.A. and D.J. Gerber, *Schizophrenia susceptibility genes: emergence of positional candidates and future directions.* Trends Pharmacol Sci, 2006. **27**(4): p. 226-33.
161. Harrison, P.J. and D.R. Weinberger, *Schizophrenia genes, gene expression, and neuropathology: on the matter of their convergence.* Mol Psychiatry, 2005. **10**(1): p. 40-68; image 5.

162. Brzustowicz, L.M., J. Simone, P. Mohseni, J.E. Hayter, K.A. Hodgkinson, E.W. Chow, and A.S. Bassett, *Linkage disequilibrium mapping of schizophrenia susceptibility to the CAPON region of chromosome 1q22.* Am J Hum Genet, 2004. **74**(5): p. 1057-63.
163. Bulayeva, K.B., S.J. Glatt, O.A. Bulayev, T.A. Pavlova, and M.T. Tsuang, *Genome-wide linkage scan of schizophrenia: a cross-isolate study.* Genomics, 2007. **89**(2): p. 167-77.
164. Hamshere, M.L., P. Bennett, N. Williams, R. Segurado, A. Cardno, N. Norton, D. Lambert, H. Williams, G. Kirov, A. Corvin, P. Holmans, L. Jones, I. Jones, M. Gill, M.C. O'Donovan, M.J. Owen, and N. Craddock, *Genomewide linkage scan in schizoaffective disorder: significant evidence for linkage at 1q42 close to DISC1, and suggestive evidence at 22q11 and 19p13.* Arch Gen Psychiatry, 2005. **62**(10): p. 1081-8.
165. Williams, N.M., N. Norton, H. Williams, B. Ekholm, M.L. Hamshere, Y. Lindblom, K.V. Chowdari, A.G. Cardno, S. Zammit, L.A. Jones, K.C. Murphy, R.D. Sanders, G. McCarthy, M.Y. Gray, G. Jones, P. Holmans, V. Nimgaonkar, R. Adolfson, U. Osby, L. Terenius, G. Sedvall, M.C. O'Donovan, and M.J. Owen, *A systematic genomewide linkage study in 353 sib pairs with schizophrenia.* Am J Hum Genet, 2003. **73**(6): p. 1355-67.
166. O'Donovan, M.C., N.M. Williams, and M.J. Owen, *Recent advances in the genetics of schizophrenia.* Hum Mol Genet, 2003. **12 Spec No 2**: p. R125-33.
167. Murphy, K.C., L.A. Jones, and M.J. Owen, *High rates of schizophrenia in adults with velo-cardio-facial syndrome.* Arch Gen Psychiatry, 1999. **56**(10): p. 940-5.
168. Hoogendoorn, M.L., J.A. Vorstman, G.R. Jalali, J.P. Selten, R.J. Sinke, B.S. Emanuel, and R.S. Kahn, *Prevalence of 22q11.2 deletions in 311 Dutch patients with schizophrenia.* Schizophr Res, 2008. **98**(1-3): p. 84-8.
169. Weksberg, R., A.C. Stachon, J.A. Squire, L. Moldovan, J. Bayani, S. Meyn, E. Chow, and A.S. Bassett, *Molecular characterization of deletion breakpoints in adults with 22q11 deletion syndrome.* Hum Genet, 2007. **120**(6): p. 837-45.
170. Arinami, T., *Analyses of the associations between the genes of 22q11 deletion syndrome and schizophrenia.* J Hum Genet, 2006. **51**(12): p. 1037-45.
171. Bassett, A.S. and E.W. Chow, *Schizophrenia and 22q11.2 deletion syndrome.* Curr Psychiatry Rep, 2008. **10**(2): p. 148-57.
172. Liu, H., G.R. Abecasis, S.C. Heath, A. Knowles, S. Demars, Y.J. Chen, J.L. Roos, J.L. Rapoport, J.A. Gogos, and M. Karayiorgou, *Genetic variation in the 22q11 locus and susceptibility to schizophrenia.* Proc Natl Acad Sci U S A, 2002. **99**(26): p. 16859-64.
173. Stark, K.L., B. Xu, A. Bagchi, W.S. Lai, H. Liu, R. Hsu, X. Wan, P. Pavlidis, A.A. Mills, M. Karayiorgou, and J.A. Gogos, *Altered brain microRNA biogenesis contributes to phenotypic deficits in a 22q11-deletion mouse model.* Nat Genet, 2008.
174. Zhao, Y., J.F. Ransom, A. Li, V. Vedantham, M. von Drehle, A.N. Muth, T. Tsuchihashi, M.T. McManus, R.J. Schwartz, and D. Srivastava, *Dysregulation of cardiogenesis, cardiac conduction, and cell cycle in mice lacking miRNA-1-2.* Cell, 2007. **129**(2): p. 303-17.

175. Moreau, M.P., S.E. Bruse, R. David-Rus, S. Buyske, and L.M. Brzustowicz, *Altered Expression of microRNAs in Post-mortem Brain Samples from Individuals with Major Psychosis.* 2008, Presented at the annual meeting of the American Society of Human Genetics, Philadelphia, Pennsylvania, Novermber 13, 2008, Available from http://www.ashg.org/2008meeting/abstracts/fulltext/.
176. Cloninger, C.R., C.A. Kaufmann, S.V. Faraone, D. Malaspina, D.M. Svrakic, J. Harkavy-Friedman, B.K. Suarez, T.C. Matise, D. Shore, H. Lee, C.L. Hampe, D. Wynne, C. Drain, P.D. Markel, C.T. Zambuto, K. Schmitt, and M.T. Tsuang, *Genome-wide search for schizophrenia susceptibility loci: the NIMH Genetics Initiative and Millennium Consortium.* Am J Med Genet, 1998. **81**(4): p. 275-81.
177. Suarez, B.K., J. Duan, A.R. Sanders, A.L. Hinrichs, C.H. Jin, C. Hou, N.G. Buccola, N. Hale, A.N. Weilbaecher, D.A. Nertney, A. Olincy, S. Green, A.W. Schaffer, C.J. Smith, D.E. Hannah, J.P. Rice, N.J. Cox, M. Martinez, B.J. Mowry, F. Amin, J.M. Silverman, D.W. Black, W.F. Byerley, R.R. Crowe, R. Freedman, C.R. Cloninger, D.F. Levinson, and P.V. Gejman, *Genomewide linkage scan of 409 European-ancestry and African American families with schizophrenia: Suggestive evidence of linkage at 8p23.3-p21.2 and 11p13.1-q14.1 in the combined sample.* Am J Hum Genet, 2006. **78**(2): p. 315-33.
178. Faraone, S.V., M. Blehar, J. Pepple, S.O. Moldin, J. Norton, J.I. Nurnberger, D. Malaspina, C.A. Kaufmann, T. Reich, C.R. Cloninger, J.R. DePaulo, K. Berg, E.S. Gershon, D.G. Kirch, and M.T. Tsuang, *Diagnostic accuracy and confusability analyses: an application to the Diagnostic Interview for Genetic Studies.* Psychol Med, 1996. **26**(2): p. 401-10.
179. Nurnberger, J.I., Jr., M.C. Blehar, C.A. Kaufmann, C. York-Cooler, S.G. Simpson, J. Harkavy-Friedman, J.B. Severe, D. Malaspina, and T. Reich, *Diagnostic interview for genetic studies. Rationale, unique features, and training. NIMH Genetics Initiative.* Arch Gen Psychiatry, 1994. **51**(11): p. 849-59; discussion 863-4.
180. Brzustowicz, L.M., K.A. Hodgkinson, E.W. Chow, W.G. Honer, and A.S. Bassett, *Location of a major susceptibility locus for familial schizophrenia on chromosome 1q21-q22.* Science, 2000. **288**(5466): p. 678-82.
181. Bassett, A.S., E.J. Collins, S.E. Nuttall, and W.G. Honer, *Positive and negative symptoms in families with schizophrenia.* Schizophr Res, 1993. **11**: p. 9-19.
182. Bassett, A.S. and W.G. Honer, *Evidence for anticipation in schizophrenia.* Am J Hum Genet, 1994. **54**(5): p. 864-70.
183. Wratten, N.S., H. Memoli, Y. Huang, A.M. Dulencin, P.G. Matteson, M.A. Cornacchia, M.A. Azaro, J. Messenger, J.E. Hayter, A.S. Bassett, S. Buyske, J. Millonig, V.J. Vieland, and L.M. Brzustowicz, *Identification of a schizophrenia associated functional non-coding variant in NOS1AP.* Am J Psychiatry, 2009. **166**(4): p. 434-441.
184. Whitty, P., M. Clarke, O. McTigue, S. Browne, M. Kamali, C. Larkin, and E. O'Callaghan, *Diagnostic Stability Four Years After a First Episode of Psychosis.* Psychiatr Serv, 2005. **56**(9): p. 1084-1088.
185. Schwartz, J.E., S. Fennig, M. Tanenberg-Karant, G. Carlson, T. Craig, N. Galambos, J. Lavelle, and E.J. Bromet, *Congruence of diagnoses 2 years after a*

first-admission diagnosis of psychosis. Arch Gen Psychiatry, 2000. **57**(6): p. 593-600.

186. Chen, Y.R., A.C. Swann, and B.A. Johnson, *Stability of diagnosis in bipolar disorder.* J Nerv Ment Dis, 1998. **186**(1): p. 17-23.
187. Brzustowicz, L.M., J.E. Hayter, K.A. Hodgkinson, E.W. Chow, and A.S. Bassett, *Fine mapping of the schizophrenia susceptibility locus on chromosome 1q22.* Hum Hered, 2002. **54**(4): p. 199-209.
188. Mukai, J., H. Liu, R.A. Burt, D.E. Swor, W.S. Lai, M. Karayiorgou, and J.A. Gogos, *Evidence that the gene encoding ZDHHC8 contributes to the risk of schizophrenia.* Nat Genet, 2004. **36**(7): p. 725-31. Epub 2004 Jun 06.
189. Liu, Y.L., C.S. Fann, C.M. Liu, C.C. Chang, W.C. Yang, J.Y. Wu, S.I. Hung, H.Y. Chan, J.J. Chen, M.H. Hsieh, T.J. Hwang, S.V. Faraone, M.T. Tsuang, W.J. Chen, and H.G. Hwu, *HTF9C gene of 22q11.21 region associates with schizophrenia having deficit-sustained attention.* Psychiatr Genet, 2007. **17**(6): p. 333-8.
190. Wang, H.Y., M. Luo, I.V. Tereshchenko, D.M. Frikker, X. Cui, J.Y. Li, G. Hu, Y. Chu, M.A. Azaro, Y. Lin, L. Shen, Q. Yang, M.E. Kambouris, R. Gao, W. Shih, and H. Li, *A genotyping system capable of simultaneously analyzing >1000 single nucleotide polymorphisms in a haploid genome.* Genome Res, 2005. **15**(2): p. 276-83.
191. Bruse, S., M. Moreau, M. Azaro, R. Zimmerman, and L. Brzustowicz, *Improvements to Bead Based Oligonucleotide Ligation SNP Genotyping Assays.* Biotechniques, 2008. **45**(5): p. 559-571.
192. O'Connell, J.R. and D.E. Weeks, *PedCheck: A Program for Identification of Genotype Incompatibilities in Linkage Analysis.* The American Journal of Human Genetics, 1998. **63**(1): p. 259-266.
193. Sobel, E., J.C. Papp, and K. Lange, *Detection and integration of genotyping errors in statistical genetics.* Am J Hum Genet, 2002. **70**(2): p. 496-508.
194. Wigginton, J.E. and G.R. Abecasis, *PEDSTATS: descriptive statistics, graphics and quality assessment for gene mapping data.* Bioinformatics, 2005. **21**(16): p. 3445-7.
195. Lange K, C.R., Horvath S, Perola M, Sabatti C, Sinsheimer J, Sobel E, *Mendel version 4.0: A complete package for the exact genetic analysis of discrete traits in pedigree and population data sets.* Amer J Hum Genetics 2001. **69(supplement):A1886**.
196. Yang, X., J. Huang, M.W. Logue, and V.J. Vieland, *The posterior probability of linkage allowing for linkage disequilibrium and a new estimate of disequilibrium between a trait and a marker.* Hum Hered, 2005. **59**(4): p. 210-9.
197. Huang, Y., A. Segre, J. O'Connell, H. Wang, and V. Vieland, *KELVIN: a 2nd generation distributed multiprocessor linkage and linkage disequilibrium analysis program*. 2006, Presented at the annual meeting of The American Society of Human Genetics, New Orleans, Louisiana, October 10, 2006, Available from http://www.ashg.org/genetics/ashg06s/index.shtml.
198. Vieland, V.J., *Bayesian linkage analysis, or: how I learned to stop worrying and love the posterior probability of linkage.* Am J Hum Genet, 1998. **63**(4): p. 947-54.

199. Vieland, V.J., K. Wang, and J. Huang, *Power to detect linkage based on multiple sets of data in the presence of locus heterogeneity: comparative evaluation of model-based linkage methods for affected sib pair data.* Hum Hered, 2001. **51**(4): p. 199-208.
200. Yang, X., J. Huang, M.W. Logue, and V.J. Vieland, *The posterior probability of linkage allowing for linkage disequilibrium and a new estimate of disequilibrium between a trait and a marker.* Hum Hered, 2005. **59**(4): p. 210-9. Epub 2005 Jul 7.
201. Elston, R.C. and K. Lange, *The prior probability of autosomal linkage.* Ann Hum Genet, 1975. **38**(3): p. 341-50.
202. Papolos, D.F., G.L. Faedda, S. Veit, R. Goldberg, B. Morrow, R. Kucherlapati, and R.J. Shprintzen, *Bipolar spectrum disorders in patients diagnosed with velo-cardio-facial syndrome: does a hemizygous deletion of chromosome 22q11 result in bipolar affective disorder?* Am J Psychiatry, 1996. **153**(12): p. 1541-7.
203. Demily, C., S. Legallic, J. Bou, E. Houy-Durand, T. Van Amelsvoort, J. Zinkstok, S. Manouvrier-Hanue, A. Vogels, V. Drouin-Garraud, N. Philip, A. Philippe, D. Heron, P. Sarda, M. Petit, F. Thibaut, T. Frebourg, and D. Campion, *ZDHHC8 single nucleotide polymorphism rs175174 is not associated with psychiatric features of the 22q11 deletion syndrome or schizophrenia.* Psychiatr Genet, 2007. **17**(5): p. 311-2.
204. Glaser, B., V. Moskvina, G. Kirov, K.C. Murphy, H. Williams, N. Williams, M.J. Owen, and M.C. O'Donovan, *Analysis of ProDH, COMT and ZDHHC8 risk variants does not support individual or interactive effects on schizophrenia susceptibility.* Schizophr Res, 2006. **87**(1-3): p. 21-7.
205. Faul, T., M. Gawlik, M. Bauer, S. Jung, B. Pfuhlmann, B. Jabs, M. Knapp, and G. Stober, *ZDHHC8 as a candidate gene for schizophrenia: analysis of a putative functional intronic marker in case-control and family-based association studies.* BMC Psychiatry, 2005. **5**: p. 35.
206. Otani, K., H. Ujike, Y. Tanaka, Y. Morita, M. Kishimoto, A. Morio, N. Uchida, A. Nomura, and S. Kuroda, *The ZDHHC8 gene did not associate with bipolar disorder or schizophrenia.* Neurosci Lett, 2005. **390**(3): p. 166-70.
207. Glaser, B., J. Schumacher, H.J. Williams, R.A. Jamra, N. Ianakiev, R. Milev, S. Ohlraun, T.G. Schulze, P.M. Czerski, J. Hauser, E.G. Jonsson, G.C. Sedvall, N. Klopp, T. Illig, T. Becker, P. Propping, N.M. Williams, S. Cichon, G. Kirov, M. Rietschel, K.C. Murphy, M.C. O'Donovan, M.M. Nothen, and M.J. Owen, *No association between the putative functional ZDHHC8 single nucleotide polymorphism rs175174 and schizophrenia in large European samples.* Biol Psychiatry, 2005. **58**(1): p. 78-80.
208. Saito, S., M. Ikeda, N. Iwata, T. Suzuki, T. Kitajima, Y. Yamanouchi, Y. Kinoshita, N. Takahashi, T. Inada, and N. Ozaki, *No association was found between a functional SNP in ZDHHC8 and schizophrenia in a Japanese case-control population.* Neurosci Lett, 2005. **374**(1): p. 21-4.
209. Vieland, V.J., *Bayesian linkage analysis, or: how I learned to stop worrying and love the posterior probability of linkage.* Am J Hum Genet, 1998. **63**(4): p. 947-54.

210. Wang, K., V. Vieland, and J. Huang, *A Bayesian approach to replication of linkage findings.* Genet Epidemiol, 1999. **17**(Suppl 1): p. S749-54.
211. Vieland, V.J., *Thermometers: something for statistical geneticists to think about.* Hum Hered, 2006. **61**(3): p. 144-56.
212. Yang, X., J. Huang, M.W. Logue, and V.J. Vieland, *The posterior probability of linkage allowing for linkage disequilibrium and a new estimate of disequilibrium between a trait and a marker.* Hum Hered, 2005. **59**: p. 210-9.
213. Craddock, N., M.C. O'Donovan, and M.J. Owen, *Genes for schizophrenia and bipolar disorder? Implications for psychiatric nosology.* Schizophr Bull, 2006. **32**(1): p. 9-16.
214. Lewis, B.P., C.B. Burge, and D.P. Bartel, *Conserved seed pairing, often flanked by adenosines, indicates that thousands of human genes are microRNA targets.* Cell, 2005. **120**(1): p. 15-20.
215. Xie, X., J. Lu, E.J. Kulbokas, T.R. Golub, V. Mootha, K. Lindblad-Toh, E.S. Lander, and M. Kellis, *Systematic discovery of regulatory motifs in human promoters and 3' UTRs by comparison of several mammals.* Nature, 2005. **434**(7031): p. 338-45.
216. Kim, V.N. and J.W. Nam, *Genomics of microRNA.* Trends Genet, 2006. **22**(3): p. 165-73.
217. Fujita, S. and H. Iba, *Putative promoter regions of miRNA genes involved in evolutionarily conserved regulatory systems among vertebrates.* Bioinformatics, 2008. **24**(3): p. 303-8.
218. Burmistrova, O.A., A.Y. Goltsov, L.I. Abramova, V.G. Kaleda, V.A. Orlova, and E.I. Rogaev, *MicroRNA in schizophrenia: genetic and expression analysis of miR-130b (22q11).* Biochemistry (Mosc), 2007. **72**(5): p. 578-82.
219. Vandesompele, J., K. De Preter, F. Pattyn, B. Poppe, N. Van Roy, A. De Paepe, and F. Speleman, *Accurate normalization of real-time quantitative RT-PCR data by geometric averaging of multiple internal control genes.* Genome Biol, 2002. **3**(7): p. RESEARCH0034.
220. Viallefont, V., A.E. Raftery, and S. Richardson, *Variable selection and Bayesian model averaging in case-control studies.* Stat Med, 2001. **20**(21): p. 3215-30.
221. van Buuren, S., and Groothuis-Oudshoorn, Karin, *Mice: Multivariate Imputation by Chained Equations. R package version 1.21.* 2009.
222. Hoeting, J., Raftery, A.E., Madigan, D., *A Method for Simultaneous Variable Selection and Outlier Identification in Linear Regression.* Computational Statistics and Data Analysis, 1996(22): p. 251-270.
223. Kass, R.E., Raftery, A.E., *Bayes factors.* Journal of the American Statistical Association, 1995(90): p. 773-795.
224. Stark, K.L., B. Xu, A. Bagchi, W.S. Lai, H. Liu, R. Hsu, X. Wan, P. Pavlidis, A.A. Mills, M. Karayiorgou, and J.A. Gogos, *Altered brain microRNA biogenesis contributes to phenotypic deficits in a 22q11-deletion mouse model.* Nat Genet, 2008. **40**(6): p. 751-60.
225. Chen, C., D.A. Ridzon, A.J. Broomer, Z. Zhou, D.H. Lee, J.T. Nguyen, M. Barbisin, N.L. Xu, V.R. Mahuvakar, M.R. Andersen, K.Q. Lao, K.J. Livak, and K.J. Guegler, *Real-time quantification of microRNAs by stem-loop RT-PCR.* Nucleic Acids Res, 2005. **33**(20): p. e179.

226. Harrison, P.J., P.R. Heath, S.L. Eastwood, P.W. Burnet, B. McDonald, and R.C. Pearson, *The relative importance of premortem acidosis and postmortem interval for human brain gene expression studies: selective mRNA vulnerability and comparison with their encoded proteins.* Neurosci Lett, 1995. **200**(3): p. 151-4.
227. Soverchia, L., M. Ubaldi, F. Leonardi-Essmann, R. Ciccocioppo, and G. Hardiman, *Microarrays--the challenge of preparing brain tissue samples.* Addict Biol, 2005. **10**(1): p. 5-13.
228. Chan, J.A., A.M. Krichevsky, and K.S. Kosik, *MicroRNA-21 is an antiapoptotic factor in human glioblastoma cells.* Cancer Res, 2005. **65**(14): p. 6029-33.
229. Bauersachs, J. and T. Thum, *MicroRNAs in the broken heart.* Eur J Clin Invest, 2007. **37**(11): p. 829-33.
230. Jay, C., J. Nemunaitis, P. Chen, P. Fulgham, and A.W. Tong, *miRNA profiling for diagnosis and prognosis of human cancer.* DNA Cell Biol, 2007. **26**(5): p. 293-300.
231. Abelson, J.F., K.Y. Kwan, B.J. O'Roak, D.Y. Baek, A.A. Stillman, T.M. Morgan, C.A. Mathews, D.L. Pauls, M.R. Rasin, M. Gunel, N.R. Davis, A.G. Ercan-Sencicek, D.H. Guez, J.A. Spertus, J.F. Leckman, L.S.t. Dure, R. Kurlan, H.S. Singer, D.L. Gilbert, A. Farhi, A. Louvi, R.P. Lifton, N. Sestan, and M.W. State, *Sequence variants in SLITRK1 are associated with Tourette's syndrome.* Science, 2005. **310**(5746): p. 317-20.
232. Mishra, P.J., D. Banerjee, and J.R. Bertino, *MiRSNPs or MiR-polymorphisms, new players in microRNA mediated regulation of the cell: Introducing microRNA pharmacogenomics.* Cell Cycle, 2008. **7**(7): p. 853-8.
233. Clop, A., F. Marcq, H. Takeda, D. Pirottin, X. Tordoir, B. Bibe, J. Bouix, F. Caiment, J.M. Elsen, F. Eychenne, C. Larzul, E. Laville, F. Meish, D. Milenkovic, J. Tobin, C. Charlier, and M. Georges, *A mutation creating a potential illegitimate microRNA target site in the myostatin gene affects muscularity in sheep.* Nat Genet, 2006. **38**(7): p. 813-8.
234. Doench, J.G. and P.A. Sharp, *Specificity of microRNA target selection in translational repression.* Genes Dev, 2004. **18**(5): p. 504-11.
235. Rigoutsos, I. and A. Floratos, *Combinatorial pattern discovery in biological sequences: The TEIRESIAS algorithm.* Bioinformatics, 1998. **14**(1): p. 55-67.
236. Logue, M.W., L.M. Brzustowicz, A.S. Bassett, E.W. Chow, and V.J. Vieland, *A posterior probability of linkage-based re-analysis of schizophrenia data yields evidence of linkage to chromosomes 1 and 17.* Hum Hered, 2006. **62**(1): p. 47-54.
237. Vieland, V.J., K. Wang, and J. Huang, *Power to detect linkage based on multiple sets of data in the presence of locus heterogeneity: comparative evaluation of model-based linkage methods for affected sib pair data.* Hum Hered, 2001. **51**(4): p. 199-208.
238. Wratten, N.S., H. Memoli, Y. Huang, A.M. Dulencin, P.G. Matteson, M.A. Cornacchia, M.A. Azaro, J. Messenger, J.E. Hayter, A.S. Bassett, S. Buyske, J.H. Millonig, V.J. Vieland, and L.M. Brzustowicz, *Identification of a schizophrenia-associated functional noncoding variant in NOS1AP.* Am J Psychiatry, 2009. **166**(4): p. 434-41.

239. Thierry-Mieg, D. and J. Thierry-Mieg, *AceView: a comprehensive cDNA-supported gene and transcripts annotation.* Genome Biol, 2006. **7 Suppl 1**: p. S12 1-14.
240. Thiele, H. and P. Nurnberg, *HaploPainter: a tool for drawing pedigrees with complex haplotypes.* Bioinformatics, 2005. **21**(8): p. 1730-2.
241. Hofacker, I., W Fontana, PF Stadler, LS Bonhoeffer, M Tacker, and P Schuster, *Fast folding and comparison of RNA secondary structures.* Chemical Monthly, 1994. **125**(2): p. 167-188.
242. Tagami, H., D. Ray-Gallet, G. Almouzni, and Y. Nakatani, *Histone H3.1 and H3.3 complexes mediate nucleosome assembly pathways dependent or independent of DNA synthesis.* Cell, 2004. **116**(1): p. 51-61.
243. Ahmad, K. and S. Henikoff, *The histone variant H3.3 marks active chromatin by replication-independent nucleosome assembly.* Mol Cell, 2002. **9**(6): p. 1191-200.
244. Santenard, A. and M.E. Torres-Padilla, *Epigenetic reprogramming in mammalian reproduction: contribution from histone variants.* Epigenetics, 2009. **4**(2): p. 80-4.

Curriculum Vita

Michael P. Moreau

2006	B.A. Genetics and Microbiology, Rutgers College, Rutgers – the State University of New Jersey
2006 – 2009	Graduate Assistant / Graduate Fellow, Rutgers University Department of Genetics, Laboratory of Dr. Linda Brzustowicz
2007	Article: Saviouk, V., **M.P. Moreau**, I.V. Tereshchenko, and L.M. Brzustowicz. Association of synapsin 2 with schizophrenia in families of Northern European ancestry. *Schizophr Res*, 2007. **96**(1-3): p. 100-11.
2008	Article: Shannon E. Bruse, **Michael P. Moreau**, Marco A. Azaro, Ray Zimmerman, and Linda M. Brzustowicz. Improvements to bead-based oligonucleotide ligation SNP genotyping assays. *BioTechniques* Vol. 45, No. 5: pp 559-571 (Nov 2008)